

University of Alberta

Modeling the Hydrology and Water Resources Management of South Saskatchewan River Basin under the Potential Combined Impacts of Climate Change and Climate Anomalies

by

Md. Zahidul Islam

A thesis submitted to the Faculty of Graduate Studies and Research

in partial fulfillment of the requirements for the degree of

Doctor of Philosophy

in

Water Resources Engineering

Department of Civil and Environmental Engineering

©Md. Zahidul Islam

Spring, 2013

Edmonton, Alberta

Permission is hereby granted to the University of Alberta Libraries to reproduce single copies of this thesis and to lend or sell such copies for private, scholarly or scientific research purposes only. Where the thesis is converted to, or otherwise made available in digital form, the University of Alberta will advise potential users of the thesis of these terms.

The author reserves all other publication and other rights in association with the copyright in the thesis and, except as herein before provided, neither the thesis nor any substantial portion thereof may be printed or otherwise reproduced in any material form whatsoever without the author's prior written permission.

*To my parents, my wife Rifat, and my son Nirzhor,
for the sacrifice you have made for me.
You are the love of my life.*

Abstract

The objective of this research study is to investigate the potential impact of climate change, and the combined impacts of climate change and climate anomalies on the hydrology and water resources management for the South Saskatchewan River Basin (SSRB) of Alberta for the 21st century.

The fully-distributed physically based hydrologic model MISBA was selected to simulate the future streamflow of SSRB under the potential impact of climate change, and the combined impacts of climate change and climate anomalies. Under these climate projections, MISBA simulated significantly less streamflow for SSRB in 2020s, 2050s, and 2080s. While considering the potential combined impact of climate change and climate anomalies, a further decrease (increase) in the streamflow of SSRB by 2050s was simulated if the climate anomaly considered was El Niño (La Niña).

Next, the Irrigation District Model (IDM) of Alberta Agriculture Food and Rural Development was used to assess the future irrigation water demand of the SSRB. Under the impact of climate change, IDM's simulations show that the irrigation water demand are expected to increase over 21st century. A further decrease (increase) in the irrigation demand by 2050s is projected under the potential combined impact of climate change and El Niño (La Niña).

Finally, the Water Resources Management Model (WRMM) of Alberta Environment was used to assess the future outlook of water resources management of SSRB. According to the simulations of WRMM, license holders categorized under district irrigation, junior and future private irrigation, and senior, junior and future non-irrigation consumptive user groups will face water shortages which will progressively get worse in the 21st century. As compared to the impact of climate change alone, the combined effect of climate change with El Niño (La Niña) episodes would lead to even more (less) severe water shortages by 2050s if were considered.

Acknowledgement

I would like to express my gratitude and thanks to my supervisor Dr. Thian Yew Gan for his excellent supervision, motivation, innovative ideas, and continuous encouragement throughout this study. I would also like to thank Dr. Masaki Hayashi, Dr. Gerhard Reuter, Dr. Vivek Bindiganavile, Dr. Faye Hicks, and Dr. Peter Steffler for their valuable comments and suggestions.

I am grateful to the University of Alberta FSChia PhD Scholarship and Graduate Assistantship Program; Alberta Innovates Technology Features PhD Scholarship Program; and Natural Sciences and Engineering Research Council of Canada for providing financial assistance for this study. The dataset used in this study were obtained from different projects authorities and organizations: Distributed Model Inter-comparison Project Phase 2 (DMIP2) of the US National Weather Services (NWS) and Office of Hydrologic Development (OHD); Oklahoma Mesonet; Alberta Environment and Sustainable Resource Development; Alberta Agriculture Food and Rural Development; Canadian Climate Change Scenarios Network; National Water Research Institute (NWRI), Canada; and European Centre for Mid-range Weather Forecasts. I am grateful to those organizations.

I am very much thankful to Mr. Tom Tang and Mr. Kent Berg of Alberta Environment and Sustainable Resource Development, and Mr. Bob Riewe and

Mr. Bob Winter of Alberta Agriculture and Rural Development for their advice and data throughout the study. I would like to express my heartfelt thanks to Dr. Adam Gobena, Dr. Ernst Kerkhoven and Ms. Shoma Tanzeeba for their valuable suggestions. The research support group of Academic Information and Communication Technologies (AICT), University of Alberta, especially Dr. Masao Fujinaga, provided significant amount of technical support in data decoding. Technical helps from Mr. Perry Fedun of Water Resources Engineering group is much appreciated.

I would also like to convey my gratefulness to my parents (Abdul Jalil Mian and Jobeda Begum), my parents in law (Mir Rafique Hossen and Shewly Hossen) for their encouragements. Special thanks to my wife Rifat Jahan and my son Nirzhor Islam for their love and affection which made every moment of my live joyful and enthusiastic.

I also acknowledge the support I have received from the Water Policy Branch of Alberta Environment and Sustainable Resource Development, especially from Mr. Andy Ridge, Mr. John Taggart, and Mr. Michael Seneka.

Above all, I am thankful to Allah, the most Gracious, and most Merciful for giving me this excellent opportunity.

Table of Contents

ABSTRACT

ACKNOWLEDGEMENT

TABLE OF CONTENTS

LIST OF TABLES

LIST OF FIGURES

LIST OF ABBREVIATIONS

LIST OF NOTATIONS

CHAPTER 1 INTRODUCTION AND RESEARCH OBJECTIVES..... 1

1.1 CLIMATE CHANGE IMPACT ASSESSMENT..... 1

1.2 COMBINED IMPACT OF CLIMATE CHANGE AND CLIMATE ANOMALIES..... 3

1.3 HYDROLOGIC MODELING..... 3

1.4 WATER RESOURCES MANAGEMENT 6

1.5 BACKGROUND AND PROBLEM STATEMENTS 8

1.6 RESEARCH OBJECTIVES..... 11

1.7 ORGANIZATION OF THESIS 12

1.8 REFERENCES..... 14

CHAPTER 2 EFFECTS OF BIASES IN NEXRAD PRECIPITATION ESTIMATES AND SUB-BASIN

RESOLUTION IN THE HYDROLOGIC MODELING OF BLUE RIVER BASIN USING A SEMI AND A

FULLY DISTRIBUTED HYDROLOGIC MODEL 23

2.1 INTRODUCTION..... 23

2.2 MODEL DESCRIPTIONS 28

2.2.1	<i>Semi-Distributed Physically based Hydrologic Model using Remote Sensing and GIS (DPHM-RS)</i>	28
2.2.2	<i>Modified Interaction Soil Biosphere Atmosphere (MISBA)</i>	31
2.3	BLUE RIVER BASIN (BRB)	32
2.4	DATA REQUIREMENT	33
2.4.1	<i>DPHM-RS</i>	33
2.4.2	<i>MISBA</i>	34
2.5	RESEARCH METHODOLOGY	34
2.5.1	<i>Semi-distributed Modeling</i>	34
2.5.2	<i>Fully-distributed Modeling</i>	36
2.6	MODIFICATION OF DPHM-RS	37
2.7	MODEL CALIBRATION	37
2.8	DISCUSSIONS OF RESULTS.....	39
2.8.1	<i>DPHM-RS Simulated runoff and soil moisture</i>	39
2.8.2	<i>Biases in NEXRAD precipitation data</i>	41
2.8.3	<i>Comparison with other DMIP studies</i>	43
2.8.4	<i>Effect of sub-basin resolution</i>	44
2.8.5	<i>Comparison of semi versus fully distributed modeling</i>	46
2.9	SUMMARY AND CONCLUSIONS.....	47
2.10	REFERENCES.....	50

CHAPTER 3	PHYSICALLY BASED HYDROLOGICAL MODELING OF FUTURE STREAMFLOW OF SOUTH SASKATCHEWAN RIVER BASIN UNDER COMBINED IMPACT OF CLIMATE CHANGE AND CLIMATE ANOMALIES	68
3.1	INTRODUCTION.....	68
3.2	THE SOUTH SASKATCHEWAN RIVER BASIN (SSRB)	72
3.3	PHYSICALLY BASED HYDROLOGIC MODELING.....	73

3.3.1	<i>Modified Interaction Soil Biosphere Atmosphere (MISBA)</i>	75
3.3.2	<i>Data Requirement of MISBA</i>	77
3.3.3	<i>Calibration and Validation of MISBA</i>	78
3.4	RESEARCH METHODOLOGY	79
3.4.1	<i>Climate Change Scenario</i>	80
3.4.2	<i>Classification of El Niño and La Niña years</i>	82
3.4.3	<i>Climate Subjected to Combined Climate Change and El Niño/ La Niña Impact</i>	84
3.5	DISCUSSIONS OF RESULTS	85
3.5.1	<i>Impact of Climate Change to Sub-basin Streamflow</i>	85
3.5.1.1	Mean Annual Average Streamflow	85
3.5.1.1.1	Changes in Streamflow by 2010-2039 (2020s).....	86
3.5.1.1.2	Changes in Streamflows by 2040-2069 (2050s).....	88
3.5.1.1.3	Changes in Streamflows by 2070-2099 (2080s)	90
3.5.1.2	Mean Seasonal Streamflow.....	91
3.5.1.3	Sensitivity of Changes in Streamflow	95
3.5.2	<i>Combined Impact of Climate Change and Climate Anomalies to Streamflow</i>	96
3.5.2.1	Mean Annual Streamflow	96
3.5.2.1.1	2050s SRES Climate Scenarios Combined with El Niño Episodes	97
3.5.2.1.2	2050s SRES Climate Scenarios Combined with La Niña Episodes	99
3.5.2.2	Mean Seasonal Streamflow.....	101
3.5.2.2.1	2050s SRES Climate Scenarios Combined with El Niño Episodes	101
3.5.2.2.2	2050s Scenario Combined with La Niña Episodes.....	103
3.6	SUMMARY AND CONCLUSIONS.....	105
3.7	REFERENCES.....	109

**CHAPTER 4 FUTURE IRRIGATION DEMAND OF SOUTH SASKATCHEWAN RIVER BASIN
UNDER THE COMBINED IMPACTS OF CLIMATE CHANGE AND CLIMATE ANOMALIES 131**

4.1	INTRODUCTION.....	131
-----	-------------------	-----

4.2	IRRIGATION IN SSRB.....	134
4.3	IRRIGATION DISTRICT MODEL (IDM)	136
4.4	DATA AND METHODOLOGY	141
4.4.1	<i>Base Case Scenario</i>	142
4.4.2	<i>Climate Change Scenario</i>	142
4.4.3	<i>Classification of ENSO years</i>	145
4.4.4	<i>Climate Subjected to Combined Climate Change and ENSO Impact</i>	146
4.5	DISCUSSIONS OF RESULTS	148
4.5.1	<i>Simulated Irrigation Demand under Climate Change</i>	149
4.5.1.1	Irrigation Districts.....	149
4.5.1.2	Private Irrigation Blocks	152
4.5.1.3	Sensitivity of Changes in Irrigation Demand	154
4.5.2	<i>Simulated Irrigation Demand under the Combined Impacts of Climate Change and Climate Anomalies</i>	155
4.5.2.1	Irrigation Districts.....	155
4.5.2.2	Private Irrigation Blocks	158
4.6	SUMMARY AND CONCLUSIONS.....	160
4.7	REFERENCES.....	163

CHAPTER 5 EFFECTS OF CLIMATE CHANGE ON THE SURFACE WATER MANAGEMENT OF SOUTH SASKATCHEWAN RIVER BASIN 180

5.1	INTRODUCTION.....	180
5.2	REVIEW OF WATER RESOURCES MANAGEMENT SUBJECTED TO CLIMATE CHANGE	184
5.2.1	<i>Water Resources Management Modeling</i>	184
5.2.2	<i>Water supply and demand in SSRB</i>	187
5.2.2.1	Instream Flow Requirement.....	188
5.2.2.2	Consumptive Demands	189
5.2.2.3	Apportionment of the South Saskatchewan River Flow.....	189

5.2.3	<i>Allocated Licenses</i>	190
5.2.4	<i>Projection of Future Climate Scenarios</i>	190
5.3	RESEARCH METHODOLOGY	193
5.3.1	<i>Base Case Scenario</i>	194
5.3.2	<i>Climate Change Scenarios</i>	195
5.4	DISCUSSIONS OF RESULTS	201
5.4.1	<i>Projected Changes to Future Water Supply</i>	201
5.4.2	<i>Projected Changes to Future Water Demand</i>	203
5.4.3	<i>Simulated Deficits under Climate Change</i>	204
5.5	CONCLUSIONS	209
5.6	REFERENCES.....	211

**CHAPTER 6 COMBINED EFFECTS OF CLIMATE CHANGE AND CLIMATE ANOMALIES ON
SURFACE WATER MANAGEMENT OF SOUTH SASKATCHEWAN RIVER BASIN..... 224**

6.1	INTRODUCTION.....	224
6.2	MODEL DESCRIPTIONS	229
6.2.1	<i>Modified Interaction Soil Biosphere Atmosphere (MISBA)</i>	229
6.2.2	<i>Irrigation District Model (IDM)</i>	230
6.2.3	<i>Water Resources Management Model (WRMM)</i>	231
6.3	RESEARCH METHODOLOGY	232
6.3.1	<i>Base Case Scenario and Climate Change Scenarios</i>	233
6.3.2	<i>Climate Subjected to Combined Climate Change and ENSO Impact</i>	234
6.4	DISCUSSIONS OF RESULTS	239
6.4.1	<i>Projected Changes to Future Water Supply</i>	239
6.4.2	<i>Projected Changes to Future Water Demand</i>	244
6.4.3	<i>Deficits under Combined Climate Change and Anomaly Impact</i>	246
6.5	SUMMARY AND CONCLUSIONS.....	250

6.6	REFERENCES.....	252
CHAPTER 7	CONCLUSIONS AND RECOMMENDATIONS.....	263
7.1	SUMMARY AND CONCLUSIONS.....	263
7.2	RECOMMENDATIONS	267
7.2.1	<i>Adaptation</i>	267
7.2.2	<i>Future Study</i>	270
7.3	REFERENCES.....	274
APPENDIX A	278
APPENDIX B	279
APPENDIX C	282

List of Tables

Table 2.1 Distributions of major vegetation and soil types of BRB divided into 7 sub-basins	56
Table 2.2 Input data requirements of DPHM-RS.	56
Table 2.3 NEXRAD precipitation statistics for the calibration (1996-2002) and the validation (2002-2006) periods.....	56
Table 2.4 Comparison of Measured and Calibrated Channel Top Width as Varies with Drainage Area	57
Table 2.5 Summary statistics of the calibration and validation results of DPHM-RS applied to BRB.....	57
Table 2.6 Comparing the calibration and validation results based on the original NEXRAD precipitation input of DMIP 2 and the adjusted precipitation input.....	58
Table 2.7 Comparing the calibration and validation results of DMPH-RS with several previous studies of DMIP and DMIP2 using NEXRAD precipitation data.	58
Table 2.8 The effect of sub-basin resolution to the performance of DPHM-RS applied to BRB.....	59
Table 2.9 Comparison of statistics of simulated streamflow by DPHM-RS and MISBA for calibration and validation period	59

Table 3.1 Statistics of calibration and validation runs using Modified Interaction Soil Biosphere Atmosphere (MISBA) for different sub-basins of the South Saskatchewan River Basin (SSRB) considered in this study.....	118
Table 3.2 MISBA simulated percentage changes in mean annual runoff from the climate normal (1961-1990) with respect to climate change scenarios projected by four GCMs (CCSRNIES, CGCM2, ECHAM4, HadCM3) forced by three SRES emissions (A1FI, A21 and B21) of IPCC for the SSRB independently, and when combined with El Niño and La Niña episodes (See Table 3.1 for Basin definitions)	119
Table 3.3 MISBA simulated changes in seasonal streamflow of sub-basins of the SSRB (expressed as a percentage of the mean annual average streamflow) from the climate normal (1961-1990) with respect to climate change scenarios projected by four GCMs (CCSRNIES, CGCM2, ECHAM4, HadCM3) forced by three SRES emissions (A1FI, A21 and B21) of IPCC for the 2020s, 2050s, and 2080s independently, and when 2050s scenario combined with El Niño and La Niña episodes (See Table 3.1 for Basin definitions).....	120
Table 3.4 Percentage Changes in Future Streamflow Per °C Rise in Temperature in the 21st Century for Different sub-basins of the South Saskatchewan River Basin (SSRB) considered in this study	121
Table 4.1 Characteristics of South Saskatchewan River Basin (SSRB) Irrigation Districts (Irrigation Water Management Study Committee 2002a;	

Irrigation Branch, Alberta Agriculture Food and Rural Development, 2000)	
.....	171

Table 4.2 The percentage changes in irrigation demand for the 12 irrigation districts in 2020s, 2050s, 2080s, and combined scenarios (2050s+ El Niño and 2050s+ La Niña) from the base case scenario with respect to climate change scenarios projected by four General Circulations Models (CCSRNIES, CGCM2, ECHAM4, HadCM3) forced by three Special Report on Emissions Scenarios (SRES) emissions (A1FI, A21 and B21) of Intergovernmental Panel on Climate Change (IPCC) for the South Saskatchewan River Basin (SSRB)	172
--	-----

Table 4.3 The percentage changes in irrigation demand for the private irrigation blocks in 2020s, 2050s, 2080s, and combined scenarios (2050s+ El Niño and 2050s+ La Niña) from the base case scenario with respect to climate change scenarios projected by four General Circulations Models (CCSRNIES, CGCM2, ECHAM4, HadCM3) forced by three Special Report on Emissions Scenarios (SRES) emissions (A1FI, A21 and B21) of Intergovernmental Panel on Climate Change (IPCC) for the South Saskatchewan River Basin (SSRB).	172
---	-----

Table 4.4 Percentage Changes in Future Irrigation Demand Per °C Rise in Temperature in the 21st Century for Irrigation districts and Private Irrigation Blocks for Different sub-basins of the South Saskatchewan River Basin (SSRB) considered in this study	173
---	-----

Table 5.1 Statistics of calibration and validation runs using Modified Interaction Soil Biosphere Atmosphere (MISBA), and MISBA simulated percentage changes in mean annual runoff from the climate normal (1961-1990) with respect to climate change scenarios projected by four General Circulations Models (CCSRNIES, CGCM2, ECHAM4, HadCM3) forced by three Special Report on Emissions Scenarios (SRES) emissions (A1FI, A21 and B21) of Intergovernmental Panel on Climate Change (IPCC) for the South Saskatchewan River Basin (SSRB)..... 218

Table 6.1 Modified Interaction Soil Biosphere Atmosphere (MISBA) simulated percentage changes in mean annual runoff from the climate normal (1961-1990) with respect to climate change scenarios projected by four General Circulations Models (CCSRNIES, CGCM2, ECHAM4, HadCM3) forced by three Special Report on Emissions Scenarios (SRES) emissions (A1FI, A21 and B21) of Intergovernmental Panel on Climate Change (IPCC) in 2050s, and 2050s scenario combined with El Niño and La Niña Episodes. 257

List of Figures

Figure 2.1 BRB divided into 7 sub-basins together with meteorological and hydrological grid-points/stations.....	60
Figure 2.2 . Comparing a) Infiltration rate, and b) runoff hydrograph of the original and modified DPHM-RS.	61
Figure 2.3 Observed verses simulated hydrograph for BRB by DPHM-RS driven by NEXRAD precipitation data for the calibration (a and b) and the validation (c and d) periods.	62
Figure 2.4 Averaged cumulative hourly flow (a and b), monthly mean flow, standard deviation and monthly mean precipitation (c and d) for calibration (1996-2002) and validation (2002-2006) periods, respectively.....	63
Figure 2.5 Oklahoma Mesonet soil moisture estimates and simulated top 10 cm volumetric soil moisture of DPHM-RS at sub-basin #3 of BRB divided into 7 sub-basins for calibration (a) and validation (b & c) periods.....	64
Figure 2.6 Comparison of monthly mean precipitation of BRB derived from NEXRAD precipitation and Mesonet rain-gauge data for 1996-1999.	65
Figure 2.7 Comparing summary statistics of model performance of DPHM-RS applied to BRB discretized to different sub-basin resolutions (APB is the	

absolute percent bias, PB is the percent bias, RMSE is the root mean square error, R is the coefficient of correlation, E_f is the Nash-Sutcliffe efficiency)..... 65

Figure 2.8 a) Ratio of simulated over observed runoff volume, b) Average monthly flow, c) Cumulative monthly flow, and d) Average monthly top layer soil moisture of BRB for different sub-basin resolutions over 1996-2002. 66

Figure 2.9 Comparison of DPHM-RS and MISBA simulated streamflow of Blue River Basin for a) calibration period (1996-2002) and b) validation period (2002-2006)..... 67

Figure 3.1 South Saskatchewan River Basin of Alberta. 122

Figure 3.2 Comparison of naturalized and MISBA simulated streamflow for calibration (1961-1980) and validation (1980-1990) periods at selected locations of the SSRB. 123

Figure 3.3 MISBA simulated mean annual average streamflows at different location of the SSRB in comparison to that of the base scenario (black square) with respect to the climate change scenarios projected by four GCMs (CCSRNIES, CGCM2, ECHAM4, and HadCM3) forced by three SRES emissions (A1FI, A21, and B21) of IPCC for 2020s, 2050s, and 2080s (continued)..... 124

Figure 3.4 Boxplots of MISBA simulated percentage changes in mean annual average streamflow ($\% \Delta Q_{\text{mean}}$) for different sub-basins of the SSRB as compared to the climate normal (1960-1991) with respect to the climate change scenarios projected by four GCMs (CCSRNIES, CGCM2, ECHAM4, and HadCM3) forced by three SRES emissions (A1FI, A21, and B21) of IPCC for 2010-2039 (2020s), 2040-2069(2050s), and 2070-2099 (2080s) (Sub-Basin names have been defined in Table 3.1)..... 126

Figure 3.5 MISBA simulated changes in seasonal streamflow of sub-basins of the SSRB (expressed as a percentage of the mean annual average streamflow) from the climate normal (1961-1990) with respect to climate change scenarios projected by four GCMs (CCSRNIES, CGCM2, ECHAM4, HadCM3) forced by three SRES emissions (A1FI, A21 and B21) of IPCC for the 2020s, 2050s, and 2080s (Sub-Basin names have been defined in Table 3.1). 127

Figure 3.6 MISBA simulated percentage changes in mean annual average streamflow at different location of the SSRB for 2050s and for combined scenarios (2050s+El Niño, 2050s+La Niña) in comparison to that of the base scenario with respect to the climate change scenarios projected by four GCMs (CCSRNIES, CGCM2, ECHAM4, and HadCM3) forced by three SRES emissions (A1FI, A21, and B21) of IPCC (continued)..... 128

Figure 3.7 MISBA simulated changes in seasonal streamflow of sub-basins of the SSRB (expressed as a percentage of the mean annual average

streamflow) from the climate normal (1961-1990) with respect to climate change scenarios projected by four GCMs (CCSRNIES, CGCM2, ECHAM4, HadCM3) forced by three SRES emissions (A1FI, A21 and B21) of IPCC for the 2050s independently, and when 2050s scenario combined with El Niño and La Niña episodes (Sub-Basin names have been defined in Table 3.1). 130

Figure 4.1 Irrigation districts and private irrigation in the South Saskatchewan River Basin (SSRB). 174

Figure 4.2 Percentage changes in the mean annual precipitation ($\% \Delta P$) and changes in the mean annual temperature (ΔT) for 2020s, 2050s, and 2080s climate scenario projected by four General Circulations Models (CCSRNIES, CGCM2, ECHAM4, HadCM3) forced by three Special Report on Emissions Scenarios (SRES) emissions (A1FI, A21 and B21) of Intergovernmental Panel on Climate Change (IPCC), and for climate scenarios of 2050s combined with El Niño and La Niña episodes for the South Saskatchewan River Basin (SSRB) as compared to the climate normal (1960-1991). 175

Figure 4.3 Irrigation District Model (IDM) simulated annual average irrigation demand for 12 irrigation districts of SSRB in comparison to that of the base case scenario (black square) with respect to the climate change scenarios projected by four GCMs (CCSRNIES, CGCM2, ECHAM4, and

HadCM3) forced by three SRES emissions (A1FI, A21, and B21) of IPCC for 2020s, 2050s, and 2080s..... 176

Figure 4.4 Irrigation District Model (IDM) simulated annual average irrigation demand for private irrigation blocks in Red Deer (a), Bow (b), Oldman (c), and South Saskatchewan River (d) sub-basins of SSRB in comparison to that of the base scenario (black square) with respect to the climate change scenarios projected by four GCMs (CCSRNIES, CGCM2, ECHAM4, and HadCM3) forced by three SRES emissions (A1FI, A21, and B21) of IPCC for 2020s, 2050s, and 2080s..... 177

Figure 4.5 Irrigation District Model (IDM) simulated percentage changes in average annual irrigation demand for 12 irrigation districts of South Saskatchewan River Basin (SSRB) versus ΔT as compared to the climate scenarios of 2050s with respect to the combined scenarios projected by four General Circulations Models (CCSRNIES, CGCM2, ECHAM4, and HadCM3) forced by three Special Report on Emissions Scenarios (SRES) emissions (A1FI, A21, and B21) of Intergovernmental Panel on Climate Change (IPCC) combined with El Niño and La Niña episodes. 178

Figure 4.6 Irrigation District Model (IDM) simulated percentage changes in average annual irrigation demand for the private irrigation blocks of South Saskatchewan River Basin (SSRB) versus ΔT as compared to the climate scenarios of 2050s with respect to the combined scenarios projected by four General Circulations Models (CCSRNIES, CGCM2,

ECHAM4, and HadCM3) forced by three Special Report on Emissions Scenarios (SRES) emissions (A1FI, A21, and B21) of Intergovernmental Panel on Climate Change (IPCC) combined with El Niño and La Niña episodes. 179

Figure 5.1 The South Saskatchewan River Basin (SSRB) (left) and a part of the SSRB water management node-link network schematic (right). See Appendix C for detail schematic. 219

Figure 5.2 Percentage changes in the mean annual precipitation ($\% \Delta P$) and changes in the mean annual temperature (ΔT) projected by four General Circulations Models (CCSRNIES, CGCM2, ECHAM4, HadCM3) forced by three Special Report on Emissions Scenarios (SRES) emissions (A1FI, A21 and B21) of Intergovernmental Panel on Climate Change (IPCC) for the South Saskatchewan River Basin (SSRB) as compared to the climate normal (1960-1991). 220

Figure 5.3 Modified Interaction Soil Biosphere Atmosphere (MISBA) simulated a) percentage changes in mean annual average streamflow ($\% \Delta Q_{mean}$), and b) percentage changes in mean annual maximum streamflow ($\% \Delta Q_{max}$) for the South Saskatchewan River Basin (SSRB) versus ΔT as compared to the climate normal (1960-1991) with respect to the climate change scenarios projected by four General Circulations Models (CCSRNIES, CGCM2, ECHAM4, and HadCM3) forced by three Special Report on Emissions Scenarios (SRES) emissions (A1FI, A21, and B21) of

Intergovernmental Panel on Climate Change (IPCC) for 2010-2039, 2040-2069, and 2070-2099. 221

Figure 5.4 Irrigation District Model (IDM) simulated percentage changes in average annual irrigation demand for the South Saskatchewan River Basin (SSRB) versus ΔT as compared to the base case scenario with respect to the climate change scenarios projected by four General Circulations Models (CCSRNIES, CGCM2, ECHAM4, and HadCM3) forced by three Special Report on Emissions Scenarios (SRES) emissions (A1FI, A21, and B21) of Intergovernmental Panel on Climate Change (IPCC) for 2010-2039, 2040-2069, and 2070-2099 for Irrigation Districts (a), and Private Irrigation blocks (b)..... 222

Figure 5.5 Water Resources Management Model (WRMM) simulated % Deficit Years versus ΔT for base case scenario and climate change periods with respect to the climate change scenarios projected by four GCMs(CCSRNIES, CGCM2, ECHAM4, and HadCM3) forced by three SRES emissions (A1FI, A21, and B21) of IPCC for 2010-2039, 2040-2069, and 2070-2099 for different water sectors of the SSRB: a) Instream flow requirement b) District irrigation c) Senior private irrigation d) Junior private irrigation e) Future private irrigation f) Senior non-irrigation consumptive uses g) Junior non-irrigation consumptive uses h) Future non-irrigation consumptive uses. 223

Figure 6.1 The South Saskatchewan River Basin (SSRB) (left) and a part of the SSRB water management node-link network schematic (right). See Appendix C for detail schematic. 258

Figure 6.2 Percentage changes in the mean annual precipitation ($\% \Delta P$) and changes in the mean annual temperature (ΔT) for 2050s climate scenario projected by four General Circulations Models (CCSRNIES, CGCM2, ECHAM4, HadCM3) forced by three Special Report on Emissions Scenarios (SRES) emissions (A1FI, A21 and B21) of Intergovernmental Panel on Climate Change (IPCC), and for climate scenarios of 2050s combined with El Niño and La Niña episodes for the South Saskatchewan River Basin (SSRB) as compared to the climate normal (1960-1991)..... 259

Figure 6.3 Modified Interaction Soil Biosphere Atmosphere (MISBA) simulated a) percentage changes in mean annual average streamflow ($\% \Delta Q_{mean}$), and b) percentage changes in mean annual maximum streamflow ($\% \Delta Q_{max}$) for the South Saskatchewan River Basin (SSRB) versus ΔT and $\% \Delta P$ as compared to the climate normal (1960-1991) with respect to the climate change scenarios projected by four General Circulations Models (CCSRNIES, CGCM2, ECHAM4, and HadCM3) forced by three Special Report on Emissions Scenarios (SRES) emissions (A1FI, A21, and B21) of Intergovernmental Panel on Climate Change (IPCC) for 2050s, and for climate scenarios of 2050s combined with El Niño and La Niña episodes. 260

Figure 6.4 Irrigation District Model (IDM) simulated percentage changes in average annual irrigation demand for the South Saskatchewan River Basin (SSRB) versus ΔT as compared to the base case scenario with respect to the climate change scenarios projected by four General Circulations Models (CCSRNIES, CGCM2, ECHAM4, and HadCM3) forced by three Special Report on Emissions Scenarios (SRES) emissions (A1FI, A21, and B21) of Intergovernmental Panel on Climate Change (IPCC) for 2050s, and for climate scenarios of 2050s combined with El Niño and La Niña episodes for Irrigation Districts (a), and Private Irrigation blocks (b).
..... 261

Figure 6.5 Irrigation District Model (IDM) simulated percentage changes in average annual irrigation demand for the South Saskatchewan River Basin (SSRB) versus ΔT as compared to the climate scenarios of 2050s with respect to the combined scenarios projected by four General Circulations Models (CCSRNIES, CGCM2, ECHAM4, and HadCM3) forced by three Special Report on Emissions Scenarios (SRES) emissions (A1FI, A21, and B21) of Intergovernmental Panel on Climate Change (IPCC) combined with El Niño and La Niña episodes for Irrigation Districts (a), and Private Irrigation blocks (b)..... 261

Figure 6.6 Water Resources Management Model (WRMM) simulated % Deficit Years versus ΔT for base case scenario and combined scenarios (2050s+El Niño, 2050s+La Niña) with respect to the climate change scenarios

projected by four GCMs(CCSRNIES, CGCM2, ECHAM4, and HadCM3) forced by three SRES emissions (A1FI, A21, and B21) of IPCC for 2050s combined with El Niño and La Niña episodes for different water sectors of the SSRB: a) Instream flow requirement b) District irrigation c) Senior private irrigation d) Junior private irrigation e) Future private irrigation f) Senior non-irrigation consumptive uses g) Junior non-irrigation consumptive uses h) Future non-irrigation consumptive uses. 262

List of Abbreviations

Acronym	Definition
2020s	2010-2039
2050s	2040-2069
2080s	2070-2099
AAFRD	Alberta Agriculture Food and Rural Development
ACADIA	Acadia Valley Irrigation Project
AID	Aetna Irrigation District
ARBRFC	Arkansas-Red Basin River Forecast Center
AVHRR	Advanced Very High Resolution Radiometer
BLGW	Belly near Glenwood
BLIB	Belly at International Boundary
BLMO	Belly at Mouth
BLMV	Belly near Mountain View
BLWC	Belly at Waterton Confluence
BRB	Blue River Basin
BRID	Bow River Irrigation District
BWCG	Bow at Calgary
CNLB	Crowsnest near Lundbreck
CSBM	Castle near Beaver Mines

CV	Coefficient of Variation
DEM	Digital Elevation Model
DMIP	Distributed Model Intercomparison Project
DMIP2	Distributed Model Intercomparison Project Phase 2
DPHM-RS	Semi-Distributed Physically based Hydrologic Model using Remote Sensing and GIS
EBGD	Elbow below Glenmore Dam
EID	Eastern irrigation District
ENSO	El Niño Southern Oscillation
ERA-40	40-year re-analysis data of the European Centre for Mid- range Weather Forecasts
ET	Evapotranspiration
GCM	General Circulation Model
GRIPCD	Gridded Prairie Climate Database
GWT	Ground Water Table
HBDF	Hydrometeorologic Base Data File
HIDP	Highwood Interim Diversion Project
HRCDHM	Hydrologic Research Center Distributed Hydrologic Model
HWMO	Highwood at Mouth
ID	Irrigation District
IDM	Irrigation District Model
IFN	Instream Flow Needs

IPCC	Intergovernmental Panel on Climate Change
IRM	Irrigation Requirements Module
ISBA	Interaction Soil Biosphere Atmosphere
LDAS	Land Data Assimilation System
LID	Leavitt Irrigation District
LNID	Lethbridge Northern Irrigation District
MAE	Mean Absolute Error
MEI	Multivariate ENSO Index
MID	Magrath Irrigation District
MISBA	Modified Interaction Soil Biosphere Atmosphere
MVID	Mountain View Irrigation District
NARR	North American Regional Reanalysis
NASA	National Aeronautics and Space Administration
NDVI	Normalized Difference Vegetation Index
NEXRAD	Next-Generation Radar
NFP	Network Flow Programming
NMM	Network Management Module
NOAA	National Oceanic and Atmospheric Administration
NWRI	National Water Research Institute
NWS	National Weather Service
OMBR	Oldman near Brocket
OMFM	Oldman near Fort Macleod

OMLB	Oldman near Lethbridge
OMMO	Oldman near Monarch
OMWC	Oldman near Waldron Corner
PB	Percent Bias
PCPC	Pincher at Pincher Creek
PDO	Pacific Decadal Oscillation
PNA	Pacific/North American index
RCID	Ross Creek Irrigation District
RCM	Regional Climate Model
RDBL	Red Deer at Bindloss
RDBV	Red Deer at Big Valley
RDDD	Red Deer at Dickson Dam
RDDH	Red Deer at Drumheller
RDNJ	Red Deer Near Jenner
RDNN	Red Deer Near Nevis
RDRD	Red Deer at Red Deer
RID	Raymond Irrigation District
RMSE	Root Mean Square Error
SAC-SMA	Sacramento Soil Moisture Accounting Model
SAWSP	Special Areas Water Supply Project
SD	Standard Deviation
SLP	Sea Level Pressure

SMIB	St. Mary International Boundary
SMRID	St. Mary River Irrigation District
SMSD	St. Mary at St. Mary Dam
SRES	Special Report on Emissions Scenarios
SSARR	Streamflow Synthesis and Reservoir Regulation
SSR	South Saskatchewan River
SSRB	South Saskatchewan River Basin
SST	Sea Surface Temperature
STRIBS	Southern Tributaries
TAU	Trans Alta Utilities
TID	Taber Irrigation District
TIN	Triangulated Irregular Network
UID	United Irrigation District
USGS	U.S. Geological Survey
WID	Western Irrigation District
WLCL	Willow above Chain Lakes
WLCS	Willow near Claresholm
WLNO	Willow near Nolan
WRMM	Water Resources Management Model
WTRS	Waterton at Waterton Reservoir

List of Notations

Symbol	Definition (Unit)
θ	The stored soil moisture (mm)
θ_{RZ}	Root zone Soil Moisture (mm)
θ_C	Soil Moisture Capacity (mm/mm)
θ_{LZ}	lower zone soil moisture (mm)
A	Total Number of Arcs
c_{ij}	Arbitrary Cost (or penalty) Per Unit Flow Along Arc (i,j)
D	Farm Diversion (mm)
D_{RZ}	Root Depth (mm)
D_S	soil depth (mm)
E	Evaporation Loss through (mm)
E_0	Daily Lake Evaporation (mm/day) of a Particular Month
E_f	Nash-Sutcliffe Efficiency
ET_A	Actual Evapotranspiration (mm)
ET_P	Potential Evapotranspiration (mm)
$ETSF$	The evapotranspiration scaling factor
f	Exponential Decay Parameter of Saturated Hydraulic Conductivity (m^{-1})
G	Ground Heat Flux ($MJ/m^2/day$)

h	Station Elevation (m)
I	Deep Percolation (mm)
K_C	Crop Coefficient
K_{CA}	The Adjusted Crop Coefficient
k_{qr}	return flow factor
L	Latitude (degrees) of the station
I_{ij}	Lower Bound on Flow Along Arc (i,j)
N	Total Nodes
n	Mannings' Roughness Coefficient
O	Outflow Water (mm)
Q_I	inflow to the irrigation field (mm)
Q_R	return flow from the irrigation field (mm)
R	Correlation Coefficient
R^2	Coefficient of Determination
R_{ann}	Difference Between Mean Temperatures of the Hottest and Coldest Months ($^{\circ}$ C)
R_n	Net Radiation (MJ/m^2)
R_o	Runoff (mm)
$T_1(P_1)$	Baseline Observed Temperature (Precipitation) ($^{\circ}$ C)
$T_1'(P_1')$	GCM predicted Mean Temperature (Precipitation) for Climate Normal ($^{\circ}$ C)
$T_2(P_2)$	Future Temperature (Precipitation) (mm)

$T_2' (P_2')$	GCM Simulated Mean Temperature (Precipitation) for Climate Scenario ($^{\circ}$ C)
T_R	Monthly Mean Range of Temperature ($^{\circ}$ C)
u_{ij}	Upper Bound on Flow Along Arc (l,j) (m^3/s)
x_{ij}	Flow Along Arc (l,j) (m^3/s)
α	Priestley-Taylor coefficient
γ	Psychrometric Constant
Δ	Slope of the Saturation Vapor Pressure-Temperature Relationship ($kPa/^{\circ}$ C)
$\Delta P (\Delta T)$	Monthly Precipitation (Temperature) Change ($^{\circ}$ C)
$\Delta Q_{max} (\Delta Q_{mean})$	Changes in Annual Maximum (Mean) Flow (m^3/s)
ϵ_a	the application efficiency
λ	Latent Heat of Vaporization (MJ/kg)
T	Mean Monthly Temperature ($^{\circ}$ C)

CHAPTER 1

Introduction and Research Objectives

1.1 Climate Change Impact Assessment

The potential impact of climate change is of major concern worldwide now-a-days, as we witness hydrologic extremes occurring more frequently and in greater severity, such as semi-arid Canadian Prairies experiencing recurrent droughts. In the Prairies environment, the potential evapotranspiration is in the order of 600 mm or higher per annum (Buttle et.al 2005) while on the average the actual evapotranspiration (other than the foothill areas) is somewhere between 300 to 400 mm. Therefore on the average, out of about 500 mm of annual precipitation, the Prairies provinces' average runoff is only slight over 100 mm/year in an average year (Gan 2000). However, during drought years, the surface runoff could be significantly less. Given that about 88% of the water supply of Canadian municipalities comes from surface sources (Environment Canada 2007), the assessment of impact of climate change to the future availability of water supply and strategies for reducing vulnerability are the national priorities.

Assessment of impacts of climate change to the future (e.g., 21st century) water resources management can generally be done in three steps:

Step 1: Simulation of water supply (e.g., streamflow), water demand (e.g., irrigation demand), and water resources management outlook (e.g., deficits) under present climatic conditions for climate normal period (a 30 years period, usually 1961-1990) by a hydrologic, an irrigation demand, and a water resources management model, respectively, calibrated and validated with historical data;

Step 2: Generation of climate change scenarios for different future periods, usually three 30 years period of 21st century, namely, 2010-2039 (2020s), 2040-2069 (2050s), and 2070-2099 (2080s);

Step 3: Simulation of water supply (e.g., streamflow), water demand (e.g., irrigation demand), and water resources management outlook (e.g., deficits) under the changed climatic conditions for future periods based on the generated climate change scenarios.

The effect of climate change on surface water resources in future is usually demonstrated by comparing the results generated from step 3 and step 1.

1.2 Combined Impact of Climate Change and Climate Anomalies

Other than the potential impact of climate change, climate anomalies as El Niño Southern Oscillation or ENSO lead to significant changes in streamflow. The ENSO-streamflow relationship also appears to be modulated by interdecadal oscillations of the North Pacific called Pacific Decadal Oscillation (PDO). Their interactions are constructive when in phase and destructive otherwise. Therefore the impact of climate change on the streamflow could be quite significantly modified by some climate anomalies individually and collectively, when such anomalies occur. If both ENSO and PDO occur in the same year, their cumulative effect on the climate would be even more complex. The combined impacts of climate change and climate anomalies for future periods can be simulated by driving aforementioned models in Section 1.1 (e.g., hydrologic, irrigation demand, water resources management model) with re-sampled climate data of a river basin observed during El Niño and La Niña years within the base case period and adjusted with various future climate scenarios.

1.3 Hydrologic Modeling

Eventually, a major task in conducting research on climate change effects, and combined impacts of climate change and climate anomalies on the management of water resources involves modeling of basin hydrology, which can be

challenging because it involves highly nonlinear processes, complex interactions and high spatial variabilities at basin scale. Hydrologic models can be classified according to the physical processes involved in modeling as conceptual and physically based (Refsgaard 1997). In conceptual models each of the hydrologic processes, that we read into our observations of the catchment, are represented by simplified mathematical relationships, where as in physically based model the detail physical processes can be represented in a deterministic way by representations of mass, momentum and energy conservation (Refsgaard 1997). According to the spatial description of the watershed process, hydrologic models can be classified as lumped and distributed models. In a lumped model the spatial variability of watershed characteristics are ignored, while in a distributed model the spatial variability of vegetation, soil, topography, etc are taken into account. The conceptual models are usually lumped while the physically based model in practice has to be distributed in manner (Refsgaard 1997). Though conceptual models are among the more popularly used models, as physical laws at microscale are well established (such as Richard's infiltration equation, Penman's potential evaporation model, etc.), many physically-based models are developed from well established scientific laws at micro-scale to water behavior at the meso-scale or regional scale, such as the scale of South Saskatchewan River Basin, and its sub-catchments, through certain parameterization approaches. Therefore in recent decades, there have been various physically-based land surface schemes developed which consider fairly detailed physics of

land surface processes in terms of water, energy and heat fluxes. Such models generally have better physical basis than statistical models, and in theory are capable of providing natural flow forecasts with less uncertainties.

Resolution of horizontal discretization could be an important factor in physically based hydrologic modeling. Various types of discretization schemes are found in literature and they can be broadly classified into three categories (Kite and Pietriniro 1996): orthogonal grid base, irregular grid base, and hydrologic response unit or grouped response unit base. In orthogonal grid base discretization, the river basin is divided into rectangular grids. The resolution of the grids can vary within the basin but must be same for a given row or column in a network array (Abbott et al. 1986b). Wood et al. (1988) proposed a Representative Element Area scale of horizontal discretization at which the spatial variability assumed to be disappeared in watershed runoff. Physically based hydrologic models that fall in this type of discretization are SHE (Abbott et al. 1986a; 1986b), WATBAL (Knudsen et al. 1986), MIKE SHE (Refsgaard and Storm 1995), ISBA (Nolihan and Planton 1989), MISBA (Kerkhoven and Gan 2006), LISTFLOOD (Van der Knijff et al. 2010; De Roo et al. 2000), WATFLOOD/SPL9 (Kouwen 1988; 2000; Kouwen and Mousavi 2002), HydroGeoSphere (Therrien et al. 2010), PAWS (Shen and Phanikumar 2010), CREST (Wang et al. 2011) etc. In irregular grid base discretization, the river basin is divided into irregular elements depending on basin topography and terrain features. Hydrologic modeling elements are generated either based on streamlines and

equipotential lines or by triangulated irregular networks. THALES (Grayson et al. 1992a; 1992b), tRIBS (Ivanov et al. 2004), R.WATER.FEA (Vieux and Gauer 1994) are the examples of terrain based hydrologic model. In hydrological response unit base discretization, the river basin is divided into a number of sub-basins which are drained by a defined drainage network (Biftu and Gan 2004). The hydrologic processes are usually evaluated at a point scale for different land class and then aggregated in sub-basin scale. Wide number of physically based hydrologic model, namely, TOPMODEL (Beven et al 1979; 1995), TOPNET (Bandaragoda et al. 2004), SWAT (Arnold et al. 1998), HRCDHM (Carpenter et al. 2001), DPHM-RS (Biftu and Gan 2001; 2004), IHDM (Beven et al. 1987; Calver and Wood 1995) are based on this concept of basin discretization. In Grouped Response Unit (GRU) Base discretization, a watershed is subdivided into sub units, in which a grid cell or a group of grid cells or a sub-basin may be represented as a GRU (e.g., SLURP of Kite 1995).

1.4 Water Resources Management

Water management involves the development, control, protection, regulation, and beneficial use of water sources by meeting up the water demands in an efficient way. With increasing competition for water use across sectors and regions, a river basin has been recognized as the appropriate unit of analysis for addressing the challenges of water resources management. The essential relations within each component and the interrelations between these

components in the basin can be considered in an integrated modeling framework which can provide essential information for policymakers in their resource allocation decisions.

Simulation and optimization are the two principal approaches to river basin modeling. In simulation, water resources behavior are simulated based on a set of rules governing water allocations and infrastructure operation, and in optimization, the allocations are optimized based on an objective function and accompanying constraints (McKinney et al. 1999). Water resources management involves the identification and development of water resources project investments that are net benefit maximizing or at least cost-minimizing, while considering non monetized impacts, such as potential ecosystem degradation or negative social impacts (Mayer and Muñoz-Hernandez 2009). So there are economic-driven optimization models in which the objective is to allocate water to maximize the accumulated net benefit over the planning period (e.g., Cai et al. 2006; Draper et al. 2003; Letcher et al. 2004; Ward et al. 2006) and priority-driven optimization models in which the objective is to minimize the total penalty or cost (e.g., Draper et al. 2004; Stockholm Environment Institute 2001; Alberta Environment 2002).

1.5 Background and Problem Statements

South Saskatchewan River Basin (SSRB) consisting of Oldman, Bow, Red Deer, and South Saskatchewan River Sub-Basins provides nearly 57% of the water allocated in Alberta. The combined watershed of the basins is 121,095 km², of which 41% is from the Red Deer sub-basin, 22% from the Oldman, 21% from the Bow and 16% from the South Saskatchewan. Occupying about a quarter of the surface area of the province, it contains less than 6% of the province's water resources. Having a sub humid to semiarid continental climate, the summer in the SSRB is short with a mean temperature varying from 14 to 16° C and the winter is long having a mean temperature from -2.5 to -8.0° C (Lac 2004). The mean annual precipitation in the SSRB usually varies between 200 mm to 500 mm (Martz et al. 2007).

In 2003 Government of Alberta established its 'Water for Life' strategic program with the goals of providing safe, secure drinking water; healthy aquatic ecosystems; and reliable, quality water supplies for a sustainable economy. To achieve these goals, the Government of Alberta released the 'Water for Life Action Plan' for managing Alberta's water resources, and it has served as the roadmap for the Albertan government and its partners since 2003. The implementation of this action plan began with the SSRB so that the water of SSRB is used in a sustainable and environmentally responsible way (Alberta Environment 2003b). The Phase 1 of the SSRB management plan ended in June

2002 with a finding that its water resources is under stress because the amount of water supply allocated to its various users has already approached its limit. The report also recommended that any future transfer of water allocation between users within the SSRB would require the approval of Alberta Environment (Alberta Environment 2003c). The Phase 2 started shortly thereafter with a goal of finding the balance between water consumption and environmental protection in the SSRB (Alberta Environment 2003b). In the first part of Phase 2, eight scenario simulations classified under three major groups (Base Case, Potential Development Scenario and Exploratory Scenarios) were carried out. In the second part of Phase 2, attempts were made to conserve water (water conservation objectives) while achieving a balance between water consumption and environmental protection in the SSRB. On the basis of these studies, the water management plan for the SSRB was approved in 2006. This plan recommended the Alberta Environment not to accept any further application for new water licenses for the Bow, Oldman and South Saskatchewan River Sub-basins (Alberta Environment 2006).

In the aforementioned studies on the water management of the SSRB, the effects of future climate change and anomalies were not taken into consideration even though the major water supply for the SSRB comes from natural streamflow, of which snowmelt runoff from the Canadian Rocky constitutes a major component of the overall runoff for the basin, which could be affected by the effects of climate change and anomalies expected over the

21st century. Tanzeeba and Gan (2012) simulated the potential impacts of climate change on three of the four sub-basins of SSRB and their results showed that climate change could significantly affect the future runoff of the three sub-basins of the SSRB. In a separate study undertaken by Golder Associates Ltd., it was also found that climate change could incur significant changes to the future water supply of South Saskatchewan Regional Planning area (Alberta Environment 2010).

Gobena and Gan (2006) showed that El Niño (La Niña) episodes lead to significant negative (positive) streamflow anomalies in south western Canada, and Gan et al. (2007) found statistically significant correlation between winter precipitation of south western Canada and the ENSO index 'Niño3' (about -0.41 to -0.42), Pacific/North American index or PNA (about -0.44 to -0.52) and PDO (about -0.44 to -0.54). In other words, the possible impact of climate change on the natural inflow of the SSRB could be quite significantly modified by these climate anomalies individually and collectively.

About 75% of the licensed water use in the SSRB belongs to irrigation consumptive use (Alberta Environment 2005) which is expected to change because Special Report on Emissions Scenarios (SRES) climate scenarios of Intergovernmental Panel on Climate Change (IPCC) projected changes to the future temperature and precipitation of SSRB. The future instream flow requirement is also expected to change. The other future non-irrigation water

demand (e.g., municipal, industrial, stock watering, flood control, and lake stabilization) with respect to the future population has also been taken into consideration by Alberta Environment (Alberta Environment 2002) in implementing the Phase 2 of the South Saskatchewan River Basin water management plan (Alberta Environment 2003a). However, an investigation on the possible combined effect of climate change and climate anomalies on SSRB has not yet been carried out.

1.6 Research Objectives

The specific objectives of this research study are:

- i) To study the effect of basin discretization in basin-scale hydrologic modeling by comparing fully distributed versus semi distributed hydrologic modeling;
- ii) To investigate possible changes to streamflow of the SSRB on the basis of climate change projected by General Circulation Models (GCMs) forced by selected SRES emission scenarios of IPCC (2001) for 2010-2039(2020s), 2040-2069 (2050s), and 2070-2099 (2080s); and the impact of climate change projected by GCMs forced by selected SRES emissions of IPCC for 2050s, combined with the possible impact of ENSO episodes.

- iii) To investigate possible changes to water demand of irrigation districts and private irrigation blocks of the SSRB on the basis of climate change projected by GCMs forced by selected SRES emission scenarios of IPCC (2001) for 2020s, 2050s, and 2080s; and the impact of climate change projected by GCMs forced by selected SRES emissions of IPCC for 2050s, combined with the possible impacts of ENSO.
- iv) From the results of (ii) and (iii), investigate the potential impact of climate change, and the combined impacts of climate change and ENSO on the water resources management for the SSRB of Alberta for the 21st century.

1.7 Organization of Thesis

The thesis consists of seven chapters. Chapter 1 provides a background of SSRB water resources management initiatives and an overview of effect of climate change and climate anomalies on hydrology and water resources management in general. In Chapter 2, the effect of basin discretization in basin-scale hydrologic modeling has been explored by applying a semi-distributed and a fully-distributed physically based hydrologic model to a small river basin, the Blue River Basin of Oklahoma. Chapter 3 provides the future streamflow of SSRB under the potential impact of climate change, and the combined impacts of climate change and climate anomalies as simulated by a physically based fully

distributed hydrologic model, the Modified Interaction Soil Biosphere Atmosphere (MISBA). The Irrigation District Model (IDM) simulated future irrigation water demand of the SSRB under the potential impact of climate change, and the combined impacts of climate change and climate anomalies are presented in Chapter 4. Chapter 5 and Chapter 6 provide the Water Resources Management Model (WRMM) simulated results on the assessment of the future outlook of surface water resources management of SSRB under the potential impacts of climate change, and the combined impacts of climate change and climate anomalies, respectively. Finally, the overall research outcomes and recommendations for the future research are presented in Chapter 7.

1.8 References

Abbott, M.B., Bathurst, J.C., Cunge, J.A., O'Connell, P.E., Rasmussen, J. (1986a).

“An introduction to the European Hydrological System—Systeme Hydrologique European, ‘SHE’, 1: History and philosophy of a physically-based distributed modelling system.” *J. Hydrol.*, 87, 45–59.

Abbott, M.B., Bathurst, J.C., Cunge, J.A., O'Connell, P.E., Rasmussen, J. (1986b).

“An introduction to the European Hydrological System—Systeme Hydrologique European ‘SHE’. 2: Structure of a physically based, distributed modelling system.” *J. Hydrol.*, 87, 61–77.

Alberta Environment (2002). “Water Resources Management Model Computer Program Description.” *Southern Region, Resource Management Branch*.
Alberta Environment.

Alberta Environment (2003a). “South Saskatchewan River Basin Water Management Plan Phase 2: Scenario Modelling Results Part 1.” *Alberta Environment*.

Alberta Environment (2003b). “South Saskatchewan River Basin Water Management Plan Phase Two: background Studies.” *Alberta Environment*.

- Alberta Environment (2003c). "Terms of Reference: Phase Two Water Management Plan for the South Saskatchewan River Basin." *Alberta Environment*.
- Alberta Environment (2005). "South Saskatchewan River Basin Water Allocation." *Alberta Environment*.
- Alberta Environment (2006). "Approved Water Management Plan for the South Saskatchewan River Basin (Alberta)." *Alberta Environment*.
- Alberta Environment (2010). "South Saskatchewan Regional Plan: Water Quantity and Quality Modeling Results." *Alberta Environment*.
- Arnold, J.G., Srinivasan, R., Muttiah, R.S., Williams, J.R. (1998). "Large area hydrologic modelling and assessment. Part I. Model development." *Journal of American Water Resources Association*, 34(1), 73–89.
- Bandaragoda, C., Tarboton, D.G., and Woods, R. (2004). "Application of TOPNET in the distributed model Intercomparison project." *Journal of Hydrology*, 298(1-4), 178-201.
- Beven, K. J., Calver, A., and Morris, E. M. (1987). "The Institute of Hydrology distributed model." *Institute of Hydrology, Report 98, Wallingford, UK*.
- Beven, K.J., Kirkby, M.J. (1979). "A physically based variable contributing area model of basin hydrology." *Hydrological Sciences Bulletin*, 24 (1), 43–69.

- Beven, K.J., Lamb, R., Quinn, P., Romanowicz, R., Freer, J. (1995). "TOPMODEL and GRIDATB: A User's Guide to the Distribution Versions", *CRES Technical Report TR110 (2nd edn.)*. Lancaster University.
- Biftu, G. F., and Gan, T.Y. (2001). "Semi-distributed, physically based, hydrologic modeling of the Paddle River Basin, Alberta, using remotely sensed data." *Journal of Hydrology* 244, 137-156.
- Biftu, G., and Gan, T. (2004). "Semi-distributed, Hydrologic Modeling of Dry Catchment with Remotely Sensed and Digital Terrain Elevation Data." *International Journal of Remote Sensing*, 25 (20), 4351-4379.
- Buttle, JM, IF Creed, and RD Moore (2005). "Advances in Canadian forest hydrology, 1999-2003." *Hydrological Processes*, 19, 169-200.
- Cai, X., Ringler, C., and Rosegrant, M.W. (2006). "Modeling water resources management at the basin level, methodology and application to the Maipo River Basin." Research report 149, International Food Policy Research Institute, Washington, DC.
- Calver, A., and Wood, W.L. (1995). "The Institute of Hydrology Distributed Model." In: Singh, V.P., (Ed.), *Computer Models of Watershed Hydrology*, 17. *Water Resources Publications, Highlands Ranch, CO, (Chapter 17)*; pp. 595–626.

- Carpenter, T.M., Georgakakos, K.P., Sperflage, J.A. (2001). "On the parametric and NEXRAD-radar sensitivities of a distributed hydrologic model suitable for operational use." *J. Hydrol.*, 254, 169–193.
- De Roo, A.P.J., Wesseling, C.G. and Van Deursen, W.P.A. (2000). "Physically based river basin modelling within a GIS: The LISFLOOD model." *Hydrological Processes*, 14, 1981–1992.
- Draper, A.J., Jenkins, M.W., Kirby, K.W., Lund, J.R., and Howitt, R.E. (2003). "Economic-engineering optimization for California water management." *J. Water Resour. Plann. Manage.*, 129(3), 155–164.
- Draper, A.J., Munévar, A., Arora, S.K., Reyes, E., Parker, N., Chung, F.I., and Peterson, L.E. (2004). "CalSim: generalized model for reservoir system analysis." *J. Water Resour. Plann. Manage.*, 136(6), 480–489.
- Environment Canada (2007). "Municipal Water Use Report, 2004 Statistics." *Environment Canada*.
- Gan, T. Y. (2000). "Reducing vulnerability of water resources of Canadian Prairies to potential droughts and possible climatic warming." *Water Resources Management*, 14(2), 111-135.
- Gan, T. Y., A. K. Gobena, and Q. Wang, Q. (2007). "Precipitation of southwestern Canada - Wavelet, Scaling, Multifractal Analysis, and Teleconnection to Climate Anomalies." *J. of Geophysical Research-Atmosphere*, 112.

- Gobena, A. K., and Gan, T.Y. (2006). "Low-frequency variability in southwestern Canadian streamflow: links to large-scale climate anomalies." *International Journal of Climatology*, 26, 1843-1869.
- Grayson, R.B., More, I.D., and McMahon, T.A. (1992a). "Physically based hydrological modelling 1: A terrain based model for investigative purposes." *Water Resour. Res.*, 28(10), 2639-2658.
- Grayson, R.B., More, I.D., and McMahon, T.A. (1992b). "Physically based hydrological modelling 2: Is the concept realistic?" *Water Resour. Res.*, 28(10), 2659-2666.
- IPCC (2001) "Climate Change 2001: The Scientific Basis. Contribution of Working Group I to the Third Assessment Report of the Intergovernmental Panel on Climate Change. *Cambridge University Press, Cambridge, United Kingdom and New York, NY, USA.*
- Ivanov, V.Y., Vivoni, E. R., Bras, R. L., and Entekhabi, D. (2004). "Preserving high-resolution surface and rainfall data in operational-scale basin hydrology: a fully distributed approach." *Journal of Hydrology*, 298(1-4), 80-111.
- Kerkhoven, E. and Gan, T.Y, (2006). "A modified ISBA surface scheme for modeling the hydrology of Athabasca River Basin with GCM-scale data." *Advanced in Water Resources*, 29.
- Kite, G. W., and Pietroniro, A.(1996). "Remote sensing applications in hydrological modeling". *Hydrological Sciences Journal*, 41, 563–591.

- Kite, G.W. (1995). "The SLURP Model." *In: Singh, V.P., (Ed.), Computer Models of Watershed Hydrology, 17. Water Resources Publications, Highlands Ranch, CO, (Chapter 15); pp. 521-562.*
- Knudsen, A., Thomson, A., and Refsgaard, J.C. (1986). "WATBAL, A semi-distributed, physically based hydrological modelling system." *Nordic Hydrology, 17, 347-362.*
- Kouwen, N. (1988). "WATFLOOD. A micro-computer based flood forecasting system based on real-time weather radar." *Canadian Water Resources Journal, 13, 62-77.*
- Kouwen, N. (2000). "WATFLOOD/SPL9: Hydrological Model and Flood Forecasting System." *Department of Civil Engineering, University of Waterloo, Waterloo, ON.*
- Kouwen, N., Mousavi, S. F. (2002). "WATFLOOD/SPL9 hydrological model & flood forecasting system." *In: Singh, V. P. and Frevert, D.K., (Ed.), Mathematical models of large watershed hydrology, 649-685.*
- Lac, S. (2004). "A Climate Change Adaptation Study for the South Saskatchewan River Basin." *SSHRC MCRI-Institutional Adaptation to Climate Change project, Canadian Plains Research Centre, University of Regina. Regina, Saskatchewan. 2004.*

- Letcher, R.A., Jakeman, A.J., and Croke, B.F.W. (2004). "Model development for integrated assessment of water allocation options." *Water Resour. Res.*, 40, W05502.
- Martz, L., J. Bruneau, and Rolfe, J.T. (2007). "Climate and Water". *SSRB Final Technical Report, 2007.*
- Mayer, A. and Muñoz-Hernandez, A. (2009). "Integrated Water Resources Optimization Models: An Assessment of a Multidisciplinary Tool for Sustainable Water Resources Management Strategies." *Geography Compass*, 3(3), pp. 1176–1195.
- McKinney, D. C., Cai, X., Rosegrant, M. W., Ringler, C. and Scott, C.A. (1999). "Modeling water resources management at the basin level: review and future directions." *SWIM Paper, Colombo, Sri Lanka: International Water Management Institute.*
- Nolihan, J., and Planton, S. (1989). "A simple parameterization of land surface processes for meteorological models." , 17.
- Refsgaard, J. C. (1997). "Parameterization, calibration and validation of distributed hydrological models." *J. Hydrol.*, 198, 69-97.
- Refsgaard, J.C. and Storm, B. (1995). "MIKE SHE." *In: Singh, V.P., (Ed.), Computer Models of Watershed Hydrology, 18. Water Resources Publications, Highlands Ranch, CO, (Chapter 23); pp. 809–846.*

- Shen,C., and Phanikumar, M.S. (2010). "A process-based, distributed hydrologic model based on a large-scale method for surface–subsurface coupling." *Advances in Water Resources*, 33, 1524–1541.
- Stockholm Environment Institute (2001). "WEAP (Water Evaluation and Planning): User Guide for WEAP21". *Stockholm Environment Institute, Boston USA*.
- Tanzeeba, S. and Gan, T.Y. (2012). "Potential impact of climate change on the water availability of South Saskatchewan River Basin." *Climatic Change*, 112, 355-386.
- Therrien, R., McLaren, R.G., Sudicky, E.A. and Panday, S.M. (2010). "HydroGeoSphere: A Three-dimensional Numerical Model Describing Fully-integrated Subsurface and Surface Flow and Solute Transport." *Groundwater Simulations Group, Waterloo, Canada*.
- Van der Knijff, J.M., Younis, J. and De Roo, A.P.J. (2010). "LISFLOOD: a GIS-based distributed model for river basin scale water balance and flood simulation." *International Journal of Geographical Information Science*, 24(2), 189–212.
- Vieux, B.E., Gauer, N. (1994). "Finite element modeling of storm water runoff using GRASS GIS." *Microcomput. Civil Eng.* 9(4), 263–270.
- Wang, J., Yang, H., Li, L., Gourley, J. J., Sadiq, I. K., Yilmaz, K. K., Adler, R. F., Policelli, F. S., Habib, S., Irwn, D., Limaye, A. S., Korme, T. & Okello, L.,

(2011). "The coupled routing and excess storage (CREST) distributed hydrological model." *Hydrol. Sci. J.*, 56(1), 84–98.

Ward, F.A., Booker, J.F., and Michelsen, A.M. (2006). "Integrated economic, hydrologic and institutional analysis of alternative policy responses to mitigate impacts of severe drought in the Rio Grande Basin." *J. Water Resour. Plann. Manage.*, 132(6), 488–502.

Wood, E. F., Sivapalan, M., Beven, K., and Band, L. (1988). "Effects of spatial variability and scale with implications to hydrologic modelling." *Journal of Hydrology*, 102, 29–47.

CHAPTER 2

Effects of Biases in NEXRAD Precipitation Estimates and Sub-Basin Resolution in the Hydrologic Modeling of Blue River Basin using a Semi and a Fully Distributed Hydrologic Model¹

2.1 Introduction

Modeling basin hydrology is a complex task as it involves highly nonlinear rainfall-runoff transforming processes, their interactions and various types of uncertainties. Physically based hydrologic models are based on known scientific principles of energy and water fluxes whereas conceptual models are based on conceptual storages and model parameters that require calibration, or they are moisture accounting models without explicitly considering energy fluxes, and so they mimic physical processes in a simplified manner. Hydrologic models can be fully distributed where a river basin is discretized as a rectangular grid mesh, or

¹ Partial results included in this chapter have been published in *Distributed Model Intercomparison Project Phase 2 (DMIP 2) joint publication*. Smith, M. B., Koren, V., Zhang, Z., ... & DMIP2 Participants (..,Islam, Z., Gan, T.,...). (2012). *Results of the DMIP 2 Oklahoma experiments*. *Journal of Hydrology*, 418, 17-48.

be semi-distributed when the basin is divided into limited number of sub-basins based on the terrain features and the drainage network. From this perspective, as we divide a river basin into more and more sub-basins, we generally can be regarded as moving from semi-distributed to fully distributed modeling.

In general, it requires significant amount of atmospheric, soil and topographical data to drive a fully distributed, physically based hydrologic model while semi-distributed models generally require less data. Basin hydrologic processes can also be modeled using lumped conceptual hydrologic models which require less data but model parameters require extensive model calibration. Furthermore, calibrated model parameters may not be valid when the hydrologic regime of the river basin changes because of anthropogenic impacts or forest fire. Partly to avoid some of the problems of distributed models and partly to exploit the potential of the satellite data in hydrologic modeling, a semi-distributed, physically based hydrologic model DPHM-RS was developed by Biftu and Gan (2001; 2004). DPHM-RS was applied to the semi-arid, Paddle River Basin, Central Alberta and good agreement was found between simulated and observed runoff as well as between simulated surface temperature and net radiation with the observed. However, they only tested DPHM-RS for short-term simulation. DPHM-RS has also been applied to the 1235 km² Blue River Basin (BRB) of Oklahoma, USA for event simulations and again good results were obtained (Kalinga and Gan 2006). This current study investigated the validity of DPHM-RS for long term simulation of runoff and soil moisture using data provided by the

Distributed Model Intercomparison Project Phase 2 (DMIP 2) of National Oceanic and Atmospheric Administration (NOAA) and the effect of biases associated with Next-Generation Radar (NEXRAD) precipitation data.

To model basin hydrology in a fully distributed manner, Kerkhoven and Gan (2006) developed the Modified Interaction Soil Biosphere Atmosphere (MISBA). MISBA has been applied to Athabasca River Basin of Alberta (Kerkhoven and Gan 2006; 2007; 2010), Fraser River Basin of British Columbia (Kerkhoven and Gan 2010), SSRB of Alberta (Tanzeeba and Gan 2012), and Upper Blue Nile River Basin (Elsanabary 2012), and generally a good correlation of simulated and measured runoff were observed. In this study MISBA will also be applied to model BRB in a fully distribute approach.

In the first phase of DMIP, BRB was modeled using several fully distributed models. Carpenter and Georgakakos (2004) formulated a Hydrologic Research Center Distributed Hydrologic Model (HRCDHM) which they refer to as a semi-distributed model and applied it to five different DMIP watersheds including the BRB. However, they divided BRB into 21 sub-basins of an average sub-basin area of 60 km². They obtained good correlation between simulated and observed discharge during the calibration period. Bandaragoda et al. (2004) calibrated a network version of TOPMODEL called TOPNET to BRB by adjusting model parameters with multipliers to minimize the mean square error between observed and simulated hourly streamflow. Ivanov et al. (2004) applied a fully

distributed, triangulated irregular network (TIN) hydrologic model tRIBS to BRB and other DMIP basins. The above studies involved hydrologic modeling which required more parametric input and computational effort than a typical semi-distributed approach.

It is expected that the resolution of sub-basins will affect the model performance given that the data available is of certain given resolution and any hydrologic model has its limitation. No matter how complex a hydrologic model, the hydrologic processes considered still cannot fully account for the complexity of nature. Several past studies were carried out to investigate the effect of basin discretization. Using Sacramento Soil Moisture Accounting Model (SAC-SMA), Ziang et al. (2004) tested the effect of disaggregation by sub-dividing the BRB into 8 sub-basins and found that a semi-distributed approach performs consistently better than a lumped approach for both high and low flood events. Carpenter and Georgakakos (2006) compared a lumped model with their distributed model HRCDHM for BRB and found that the distributed model shows better performance with respect to peak flow magnitude. Andréassian et al. (2004) compared the lumped approach with two types of semi-distributed approaches applied to over 2500 chimera watersheds to assess the relative importance of rainfall distribution versus parameter distribution in rainfall-runoff models. They found that the greatest improvement that can be achieved by spatial distribution comes from accounting for rainfall variability, and secondarily from disaggregating the model parameters. Quinn et al. (1991) studied the effect

of grid size on simulated outflow using TOPMODEL applied to the Booro-Borotou catchment and found that finer grid size gave more accurate results, as similarly found by Kuo et al. (1999).

Liang et al. (2004) studied the effects of spatial resolution on daily water flux by dividing the BRB into rectangular grids having a grid size of 1/32, 1/16, 1/8, 1/4, ½ and 1 degree and on the basis of model performance, and they found that 1/8 degree which represents a grid area of about 133 km² to be the optimum resolution for BRB. However they discretized a river basin using a rectangular grid mesh which is somewhat artificial since nature does not behave in a rectangular framework. Boyle et al. (2001) sub-divided BRB into 3 and 8 sub-basins, applied the conceptual model SAC-SMA for each sub-basin, and compared them with the results of a lumped case. They found that the semi-distributed approach provided significant performance improvement over the lumped approach. By sub-dividing the BRB in 5, 7, 13 and 20 sub-basins, Kalinga and Gan (2006) found 7 sub-basins to be the optimum resolution for BRB, or an average sub-basin area of about 170 km², which is larger than about 133 km² of Liang et al. (2004) probably because the latter used a rectangular modeling framework which is less realistic than sub-dividing a river basin on the basis of terrain features.

Lastly, beyond the aforementioned issues, another key factor in hydrologic modeling is the accuracy of precipitation data which unfortunately are highly

variable spatially. Even though via DMIP 2 we have the luxury of using NEXRAD precipitation which has good spatial coverage as compared to rain gauge data which are point measurements, there are still unresolved problems using such spatially distributed data, particularly in terms of rainfall depth.

In view of the above problems, the objectives of this study are to apply the semi-distributed DPHM-RS and fully distributed MISBA to model the hydrology of BRB using the NEXRAD precipitation and North American Regional Reanalysis (NARR) forcing data to address the following issues:

1. The effect of sub-basin resolution on hydrologic modeling for long-term simulation,
2. Effects of biases of NEXRAD precipitation data on basin-scale hydrologic modeling,
3. Comparison of semi-distributed and fully distributed physical based modeling of basin hydrology.

2.2 Model Descriptions

2.2.1 Semi-Distributed Physically based Hydrologic Model using Remote Sensing and GIS (DPHM-RS)

The semi-distributed DPHM-RS sub-divides a river basin to a number of sub-basins, computes the evapotranspiration, soil moisture and surface runoff using

energy and rainfall forcing data in a sub-basin scale. It consists of six basic components: interception of rainfall, evapotranspiration, soil moisture, saturated subsurface flow, surface flow and channel routing, as described in Biftu and Gan (2001; 2004). A brief summary are presented below:

The interception of precipitation from the atmosphere by the canopy is modeled using the Rutter Interception Model (Rutter et al. 1975). The land surface evaporation and vegetation transpiration are computed separately using the Two Source Model of Shuttleworth and Gurney (1990), which is based on the energy balance above canopy, within canopy and at soil surface. This model solves the non linear equations based on the energy balance for the canopy, surface, and air temperatures at canopy height, evaporation from soil surface and transpiration from vegetation. A soil profile of three homogeneous layers (active, transmission and saturated layers) is used to model the soil moisture on the basis of water balance between layers. The active layer is 15-30 cm thick and it simulates the rapid changes of soil moisture content under high frequency atmospheric forcing. The transmission zone lies between the base of the active layer and the top of the capillary fringe and so it more characterizes the seasonal (instead of transient) changes of soil moisture. In modeling the unsaturated flow component of soil water, the water transport is assumed vertical and non-interactive between sub-basins. The lower boundary of the unsaturated zone is the top of capillary fringe controlled by the local average ground water table derived from the catchment average water table and topographic soil index

which include the spatial variability of the topographic and soil parameters (Sivapalan et al. 1987). Starting with an observed value from the surrounding wells of the modeled basin, the temporal changes in the average ground water depth is based on the water balance analysis for the whole catchment, and the rate of change of the average ground water table is assumed to be the rate of change of local water table (Famiglietti and Wood 1994).

After simulating the soil moisture, the saturation and Hortonian infiltration excess for vegetated and bare soil are computed to generate the surface runoff for each sub-basin. Philip's equation is used to compute the infiltration capacity of soil, and the surface runoff is distributed temporally using a time lag response function obtained from a reference rainfall excess of 1 cm depth applied to each grid cell within the sub-basin for one time step. Then for each grid cell, which has the resolution of the digital elevation model (DEM) used, the flow is routed according to the kinematic wave equation from cell to cell based on eight possible flow directions until the total runoff water for the sub-basin is completely routed. The resulting runoff becomes a lateral inflow to the stream channel within the sub-basin and these flows are routed through the drainage network by the Muskingum-Cunge routing method whose variable parameters are evaluated by an iterative four point approach (Ponce and Yevjevich 1978).

2.2.2 Modified Interaction Soil Biosphere Atmosphere (MISBA)

MISBA (Kerkhoven and Gan 2006) is a modified version of the land surface scheme, the Interaction Soil Biosphere Atmosphere or ISBA (Nolihan and Planton 1989; Nolihan and Mahfouf 1996). MISBA is a soil vegetation atmosphere transfer (SVAT) scheme used to model the hydrologic processes at GCM scale. MISBA is designed to simulate the exchange of heat, mass and momentum between the land or water surface and the overlying atmosphere (Tanzeeba 2009). MSBA requires two basic types of parameters – four primary and 22 secondary parameters. The primary parameters are percentage of sand, percentage of clay, vegetation and land-water ratio that are specified at each grid points. The secondary parameters are determined from the primary parameters. Primary and secondary parameters are listed in **Appendix A**.

MISBA uses the relationship of Deardorff (1978) to model the precipitation interception. MISBA has three soil layers. Evaporation from soil and vegetation is based on energy balance and aerodynamic method. MISBA uses a sub-grid runoff scheme that considers sub-grid variation of soil moisture by the Xinanjiang distribution (Habets et al. 1999). The scheme acts like a multi-bucket model in which the distribution of buckets size is defined by the Xinanjiang distribution (e.g., Zhao 1992) and when a bucket fills its capacity surface runoff occurs (Kerkhoven and Gan 2006). In original ISBA, sub-surface runoff is

represented by a gravity drainage scheme following a linear reservoir. In the modified version of ISBA, namely MISBA, the sub-surface runoff equation is converted from a linear function to a nonlinear function of soil water to account for interflow more accurately.

2.3 Blue River Basin (BRB)

The study site BRB is one of the DMIP 2 basins as shown in Figure 2.1, situated in South Central Oklahoma (USA), and has a total catchment area of 1235 km². Being an unregulated basin of relatively flat topography with an elevation ranging from 158 to 400 m msl, BRB generally has low relief. The gently sloping channel, deeply incised (Ivanov et al. 2004), has a maximum distance of 136 km. The average slope of the main channel and the entire channel network is 1.67 and 5.28 m/km respectively. As shown in Table 2.1, woody savannah is the dominant vegetation occupying about 77 % of the basin (Ivanov et al. 2004). The other vegetations are deciduous forest (about 14%), evergreen needleleaf forest (about 4-5 %), grassland, and cropland (about 4%). The basin has some urbanized areas but they occupy about 0.5 % of the total catchment. The major soil type is clay and loam mixed with sand or silt. The average precipitation is 1000 mm while the mean annual flow is 9.58 m³/s with a standard deviation of 3.28 m³/s.

2.4 Data Requirement

2.4.1 DPHM-RS

The model parameters of DPHM-RS, derived either from remotely sensed or ground observations or model calibration at sub-basin scale (Biftu and Gan 2001), and data such as topographic, landuse, soil, streamflow, and meteorological are summarized in Table 2.2. The DEM data obtained from the USGS National Elevation Dataset is used to derive the mean elevation, flow direction, flow accumulation, and slope of each grid cell of 100 m square resolution. The vegetation type and their coverage are derived from the vegetation data of National Aeronautics and Space Administration (NASA) Land Data Assimilation System (LDAS) of 1 km resolution. The soil types are derived from DMIP's soil texture data of 1 km resolution whereas the soil hydraulic properties are based on that of Rawls and Brakensiek (1985). The hourly streamflow data of BRB are that of United States Geological Survey (USGS), the meteorological forcing data are derived from the 3-hourly, 32 km resolution NARR data. Oklahoma Mesonet soil moisture estimates are used to validate the simulated active layer soil moisture of DPHM-RS. The NEXRAD precipitation data of the National Weather Service (NWS) Arkansas-Red Basin River Forecast Center (ARBRFC) is used as the input precipitation, while the channel properties for routing are taken from the DMIP2 database. However, it was found necessary to

adjust the NEXRAD data with respect to Oklahoma Mesonet precipitation data (see Section 2.8.2).

2.4.2 MISBA

MISBA requires topographic, landuse, meteorological, and hydrometric data to simulate hydrologic processes for a river basin. In this study, a DEM data obtained from the USGS National Elevation Dataset is used to determine the drainage area and drainage network for the BRB. The 30 arc seconds ecoclimap dataset derived from combining landcover maps, climate and Advanced Very High Resolution Radiometer (AVHRR) satellite data (Masson et al. 2003), was chosen as the landuse data and for determining the model parameters of MISBA. The 3-hourly, 32 km resolution NARR data was used as the meteorological dataset to drive MISBA. The NEXRAD precipitation data of the NWS ARBRFC is used as the input precipitation.

2.5 Research methodology

2.5.1 Semi-distributed Modeling

DPHM-RS accounts for the spatial variability of meteorological and hydrological variables by a semi-distributed approach (Biftu and Gan 2001), and it was designed to input the energy forcing and precipitation data from one or more meteorological stations. On the basis of the distance between the sub-basin centre and meteorological stations the input variables were distributed to all

sub-basins with necessary spatial and altitude adjustments. As shown by circular points in Figure 2.1, it was found that among 16 grid points (around the BRB) of NARR energy forcing data of 32 km resolution only 3 directly fall on BRB (S1, S2, and S3 in Figure 2.1) and thus 3-hourly data of these three stations were selected and linearly interpolated to hourly time series. At a particular time, the NEXRAD data at 4 km grid size within each sub-basin of BRB are extracted and averaged to become the input precipitation for the sub-basin. The number of grid-points of NEXRAD used for each sub-basin depends on the resolution of the sub-basins, or more grid-points per sub-basin were used for fewer number of total sub-basins and vice versa. As shown in Figure 2.1 (diamond points), a total of 39 grid point values are considered to generate the rainfall time series for seven sub-basins for 1996 to 2006 (Table 2.3). It was found that during the calibration period the maximum precipitation rate varied from 36 mm per hour at sub-basin 3 to 57 mm per hour at sub-basin 5; however the total and average rainfall is quite uniform over all sub-basins during both calibration and validation periods.

Model parameters of DPHM-RS are classified under three types: vegetation, soil and channel. The vegetation parameters are taken from Kalinga and Gan (2006) for BRB. The depth and initial moisture content of the active soil layer are still set as 20 cm and at 60% respectively. The mean water table depth for the basin was initialized at a depth of 8.0 m.

2.5.2 Fully-distributed Modeling

While modeling the hydrology of BRB in MISBA, cross-referencing between the topographic, landuse, and meteorological dataset was required. Following methodology was applied to link each DEM square to its nearest landuse data square and each landuse data square to its nearest meteorological grid (NARR and NEXRAD) square (Kerkhoven and Gan 2006):

First, from the DEM dataset, the portion of each NARR meteorological square which is within the BRB is determined.

Second, the distribution of land surface parameters in each NARR grid was done by cross-referencing the '32km × 32 km' NARR forcing, '4 km × 4 km' NEXRAD precipitation, '100 m × 100m' DEM and '1 km × 1 km' Ecoclimap landuse datasets.

Third, a mosaic of land cover tiles was generated by group averaging the land surface parameters based on common land cover type in each NARR grid. Then, MISBA was run for each land cover type present in each meteorological grid square.

Finally, the runoff generated by each land cover tile in each grid of the flow network was aggregated and total runoff was routed by a Muskingum-Cunge routing model (Cunge 1969) to obtain the total basin stream flow.

2.6 Modification of DPHM-RS

In the original DPHM-RS model the cumulative infiltration was recomputed at the model time step (1-hour) which resulted in an infiltration rate that increase and decrease in a zigzag manner throughout a continuous rainfall event (Figure 2.2a). Therefore the soil moisture algorithm of DPHM-RS was modified to compute the cumulative infiltration in a continuous manner up to the duration of the rainfall event (without intermediate re-start), which lead to a smoother changes in the simulated infiltration rate throughout each storm. This modification also resulted in a less cumulative infiltration which means more surface runoff, as shown by running DPHM-RS with and without the modified infiltration algorithm from October 1st 1996 to March 31st 1997. This increase in the simulated runoff because of the above modification resulted in a marginally improved R (against observed hydrograph) from 0.87 to 0.90 at the calibration stage (Figure 2.2b).

2.7 Model Calibration

As a physically based model, most model parameters of DPHM-RS were obtained from measurement or field observations, and only four parameters still require calibration which are the exponential decay parameter of saturated hydraulic conductivity (f), Manning's roughness coefficient (n) for soil and vegetation, mean cross sectional top width and n for the channel (Biftu and Gan 2001). Even

though only 4 parameters, they exert significant sensitivity on model results. f directly affects the depth of the local ground water table and the amount of base flow; n for soil and vegetation significantly changes the response function generated by the kinematic wave equation; and the channel top width and channel n also affect the shape of the simulated hydrograph.

The model parameters were calibrated with respect to the observed hydrographs from October 1996 to September 2002 in three steps. f was manually adjusted by a trial and error approach so as to simulate adequate base flows with respect to the observed. Inadequate f values could cause the simulated ground water table (GWT) depth to decrease continuously with time or the reverse throughout the year. More realistic GWT was obtained by setting f to be 1.0 m^{-1} for silty clay loam, 0.7 m^{-1} for sandy clay and 0.4 m^{-1} for clay.

After calibrating f , the response functions for the seven sub-basins were further calibrated by manually adjusting Manning's n values for forest and bare soil, with the objective of matching the simulated with the observed hydrographs, especially the peak flows. The Manning's n derived were 0.08 for forest, 0.07 for bare soil and 0.015 for the channel. Based on the Muskingum-Cunge method for channel routing it was not needed to adjust the mean top width of the channel reaches (Biftu and Gan 2001) and the cross-sectional measurements provided by DMIP 2 were used as an alternative.

Comparing to DPHM-RS, MISBA required less calibration as the later consider more heterogeneity in modeling. In MISBA, channel routing characteristics (e.g., channel top width, Mannings' n) were assumed to be simple power function of drainage area:

$$\text{Eq. 2.1} \quad W = N_1 A^{N_2}$$

$$\text{Eq. 2.2} \quad n = N_3 A^{N_4}$$

where A is the basin area at a point where the channel width is W and Manning's roughness coefficient is n. N_1 , N_2 , N_3 , N_4 were initially determined from the channel characteristics (e.g., width, Mannings' n, drainage area) from the DMIP2 database and then calibrated with respect to the observed hydrographs from October 1996 to September 2002. A comparison of measured and calibrated channel top width and Manning's n are listed in Table 2.4.

2.8 Discussions of results

2.8.1 DPHM-RS Simulated runoff and soil moisture

During calibration the goal was to match the observed and simulated runoff for the wet and dry seasons, the overall water balance and the runoff coefficient. A good match between the simulated and observed runoff during wet seasons resulted in an over simulation of runoff during dry seasons. Therefore the strategy was to optimize the model parameters so as to achieve an overall good

agreement between observed and simulated hydrograph and runoff volume for both high and low flow seasons. Figure 2.3a and Figure 2.3b compares the observed and simulated runoff for 1996-2002. On the basis of the calibration results (Table 2.5), DPHM-RS generally simulated the storm events reasonably well, but the simulated peaks tended to be underestimated during high flows and to some extent over estimated during low flows, resulting in an overall correlation coefficient (R) of 0.70 (see Figure 2.4a and Figure 2.4c). The overall Percent Bias (PB) is -4.54% which indicates a slight underestimation of the simulated runoff for the calibration period. The Nash-Sutcliffe efficiency (E_f) was 0.50 and the runoff coefficient was 0.215.

The validation results plotted in Figure 2.3(c and d) show that simulated and observed runoff generally match well during winter, spring and summer but DPHM-RS overestimated runoff during late summer and fall (see Figure 2.4b and Figure 2.4d). The R value was 0.60, bias was 50.73% and E_f was only -0.16 (see Table 2.5). The problem of gross overestimation of runoff is addressed in Section 2.8.2.

The simulated top layer soil moisture of DPHM-RS was compared with the Oklahoma Mesonet soil moisture estimates derived from the methodology of Arya and Paris (1981) which predicted the moisture characteristic of a soil from its particle-size distribution, bulk density, and particle density parameters. Tishomingo Mesonet station soil moisture data (M2 in Figure 2.1) that was close

to the sub-basin 3 of sub-divided BRB, was used to compare with the simulated soil moisture for calibration and validation periods (Figure 2.5). It was found that DPHM-RS can generally simulate the active layer soil moisture realistically.

2.8.2 Biases in NEXRAD precipitation data

From Section 2.8.1 it is obvious that the simulated runoff generally underestimated the observed during high flow periods and overestimated during low flow periods. As precipitation is the most important and often an uncertain variable in hydrologic modeling, it became obvious that precipitation at least partly contributed to the mismatch between observed and simulated runoff as shown in Figure 2.3. From the plots, it became apparent that (especially in May-September) simulated runoff was high because the input precipitation based on NEXRAD data was high even though the observed runoff was relatively low (highlighted by rectangular boxes in Figure 2.3). This problem of mismatch between simulated and observed runoff might be partly caused by biases of NEXRAD precipitation. However, there could be other sources of errors such as springs and losing/gaining sections of the river, e.g., the largest spring in Oklahoma drains out of the northern part of the basin from a point upstream of the USGS gauge near Connerville, Oklahoma (Michael Smith, NOAA, personal communication).

Even though few model parameters can be adjusted to suppress over-simulated or to increase under-simulated runoff, that approach would not have addressed

the real problem and so it makes more sense to question the validity of NEXRAD precipitation data. To investigate this, average monthly precipitation for the basin derived from the NEXRAD were compared with the corresponding average precipitation collected from three Mesonet gauging stations adjacent to BRB (M1, M2, and M3 in Figure 2.1). The hourly precipitation data from those Mesonet stations (see Kalinga and Gan 2006) for October 1996 to September 1999 were averaged to monthly mean values. With respect to Mesonet ground measurements, it became evident that NEXRAD generally underestimated (overestimated) precipitation during October to April (May- September) (see Figure 2.6).

To validate this conjecture about the biases of NEXRAD data, these data was adjusted on the basis of monthly mean precipitation of the three Mesonet stations and DPHM-RS was driven again using these adjusted precipitation data for the 1996-2006 period without changing the previously calibrated model parameters. By so doing, it was found that R improved from 0.70 to 0.76 (0.60 to 0.71) in the calibration (validation) periods while E_f was marginally improved in the calibration stage (0.50 to 0.53) but significantly improved in the validation stage (-0.16 to 0.46). The percent bias was also reduced during the validation stage (see Table 2.6 for details). Given that the adjustment of NEXRAD precipitation with respect to the Mesonet ground measurements lead to better agreement between simulated and observed runoff especially in the validation stage, it can be concluded that NEXRAD precipitation data might contain biases

which can be partly rectified with good measurements of local climate stations. Looper et al. (2009) discuss similar analyses of radar-based precipitation in which bias correction of the radar based precipitation estimates was found to be justified (Smith et al. 2009).

2.8.3 Comparison with other DMIP studies

In this study calibration periods are chosen to be wetter than validation periods to test if the calibrated DPHM-RS model can accurately simulate events that are beyond its calibration experience. The purpose is to validate whether good model calibration results are achieved with sound physical basis instead of curve-fitting. Model parameters that lack physical basis will more likely lead to poor model performance in the validation stage. Using NEXRAD precipitation data of DMIP 2, R of DPHM-RS was 0.70 and 0.60 for calibration and validation respectively, which means model performance is marginally better in the calibration than the validation stage. These results are comparable with three previous studies of DMIP on BRB, namely that of tRIBS (Ivanov et al., 2004), HRCDHM (Carpenter and Georgakakos, 2004) and TOPNET (Bandaragoda et al., 2004) (Table 2.7). It was found that the calibration results of DPHM-RS in terms of R and E_f is similar to the other three studies. In addition, DPHM-RS and HRCDHM have relatively low biased simulated runoff for the calibration period compared to the other models.

In the validation period the performance of all models was relatively poor, but in terms of percent bias and E_f , DPHM-RS was marginally better than other three cases before adjusting the NEXRAD data, and it became significantly better after adjusting the NEXRAD data with the Mesonet data. It is expected that the performance of these three other models to also improve if they had used the NEXRAD precipitation data that are similarly adjusted.

2.8.4 Effect of sub-basin resolution

Given that the resolution of horizontal discretization could be an important factor in distributed and semi-distributed hydrologic modeling, the effect of sub-basin resolution was investigated by dividing BRB into 1, 5, 7, 13 and 20 sub-basins which lead to an average grid size of 1235, 240, 170, 90, 60 km², respectively. DPHM-RS was separately simulated for a period of six years (1996-2002) for each of the above sub-basin resolutions. In searching for the optimal sub-basin resolution in these experiments, the response function for each sub-basin was re-computed and in channel routing, the Manning's n for the channel network was re-calibrated to account for the change of travel distances associated with different sub-basin resolutions. The spatial variability of NEXRAD precipitation data was also accounted for at different sub-basin scales. The simulated versus observed hourly runoff was compared and statistical measures are shown in Table 2.8 and in Figure 2.7. It was found that simulated runoff for the 7 sub-basin case (a spatial scale of 170 km² per sub-basin) gives the best R

and E_f , and less Percent Bias (PB) and Root Mean Square Error (RMSE). This is partly because increasing the number of sub-basin cause higher simulated runoff in both high and low flow seasons for the same total precipitation input which generally leads to an increase in the correlation during high flow and a decrease in the correlation during low flow. Starting from a low resolution, e.g., 1 sub-basin which means a lumped approach, the correlation increases with an increase in the basin resolution but it plateau at 7 sub-basins and then its performance dropped off (Figure 2.7).

In addition, Figure 2.8a shows that the ratio of simulated verses observed runoff volume is approximately one when BRB discretized into 7 sub-basins, but less or more than one otherwise. With an increasing number of sub-basins, the simulated runoff increases (Figure 2.8b - Figure 2.8c) because the top soil moisture decreases (Figure 2.8d). This occurs because with smaller sub-basin areas, water has to travel a shorter distance via surface runoff to the nearest channel networks. In other words, increasing the number of sub-basins (or decreasing the sub-basin area) causes a quicker drainage of water. Furthermore, higher moisture content at larger sub-basin areas give rise to higher actual evaporation, thus lowering the effective precipitation (the difference between actual precipitation and evaporation) and so the net outflow from the entire basin decreased as number of sub-basins decrease, as similarly shown by Kuo et al.(1999).

It is expected that, the optimal sub-basin resolution to be dependent on the climate, terrain features, and scale of the watersheds which should be the focus of future research in modeling basin hydrology. It should be noted that optimum number of sub-basins also in an agreement with the study of Kalinga and Gan (2006), however they only consider some storm events and never tested it for long-term simulation.

2.8.5 Comparison of semi versus fully distributed modeling

To compare the simulated streamflow of the semi-distributed DPHM-RS versus the fully distributed MISBA, the later was also calibrated and validated for 6 years (1996-2002) and 4 years (2002-2006), respectively, using the bias corrected NEXRAD precipitation (see Section 2.8.2) and NARR forcing datasets. The simulated streamflow of DPHM-RS and MISBA for the calibration and validation periods are shown in Figure 2.9. The goodness-of-fit statistics obtained for the calibration and validation runs of DPHM-RS and MISBA on BRB are also listed in Table 2.9. The R and E_f of DPHM-RS simulated streamflow are 0.76 and 0.53 respectively, for the calibration runs, which improve to 0.93 and 0.82 respectively, when MISBA was used to model. Similarly, R and E_f of MISBA simulated streamflow for the validation runs are 0.90 and 0.83 respectively, which are also better than that of DPHM-RS (0.71 and 0.46). The mean absolute error (MAE) values in the calibration period are 6.57 m³/s for DPHM-RS and 3.15 m³/s for MISBA, and in the validation period, 3.69 m³/s for DPHM-RS and 2.13

m³/s for MISBA respectively. The percent bias in DPHM-RS's simulated streamflow for calibration and validation stages are about -29.20 and -2.01%, respectively, which reduces to -14.06 and -1.43% for MISBA. The Absolute Percent Bias (APB) and the RMSE also improve from about 68.83% and 21.58 m³/s in DPHM-RS for the calibration runs to about 32.86% and 13.38 m³/s respectively, for MISBA; and for the validation runs the APB and RMSE statistics are about 79.61% and 9.91 m³/s for DPHM-RS and about 46.05% and 2.13 m³/s, respectively for MISBA.

These statistics generally demonstrate that the fully distributed MISBA could better model the hydrology of BRB than the semi-distributed DPHM-RS. As discussed in Section 2.8.1, DPHM-RS tends to under-simulate the peak flows and over-simulate the low flows, but the problem seem to be significantly resolved in the fully distributed MISBA model (Figure 2.9). The performance of DPHM-RS is poorer than MISBA because the spatially distributed variability of soil, landuse and precipitation data are partially averaged out in the sub-basin framework of DPHM-RS, but such spatial variability of soil, vegetation and precipitation are retained in the fully distributed framework of MISBA.

2.9 Summary and Conclusions

By applying DPHM-RS and MISBA to the BRB in Oklahoma under the framework of DMIP2 for a 10-years simulation split up into calibration (1996-2002) and

validation (2002-2006) stages, driven by NEXRAD precipitation and other data, the conclusions are as follows:

- 1) Even as a semi-distributed, physically based hydrologic model and using 7 sub-basins, DPHM-RS performed comparably at the calibration stage with three other hydrologic models that are either TIN-based (Ivanov et al. 2004; Bandaragoda et al. 2004), or with 21 sub-basins (Carpenter and Georgakakos 2004), and marginally better in the validation stage;
- 2) Considering there could be other sources of errors, the degradation of model performance at the validation stage for DPHM-RS can partly be attributed to biases associated with NEXRAD precipitation even though it is already merged with rain gauge data, as evident in some cases where high precipitation based on NEXRAD data under reasonable antecedent moisture content resulted in minimal observed runoff;
- 3) By adjusting NEXRAD precipitation data with rainfall measurements from 3 selected Mesonet stations, DPHM-RS's performance improve marginally in the calibration stage and significantly in the validation stage, which supports the suspicion on the biases associated with NEXRAD data. Therefore we suggest that whenever possible, NEXRAD precipitation data should first be compared and adjusted to local conditions (e.g., rain gauge data) before applying the data to simulate basin hydrology.

- 4) For a given climatic regime and river basin characteristics (topography, vegetation and geology), there might be an optimum level of discretization in modeling basin hydrology and for BRB it turned out to be 7 sub-basins (170 km² per sub-basin), which is still the same as that of Kalinga and Gan (2006) even though we used long-term instead of event based simulations.
- 5) With respect to the Mesonet's soil moisture estimates, it seems that DPHM-RS simulated realistic soil moisture, which together with realistic simulated runoff hydrograph, demonstrate the physical basis of the semi-distributed model, which should be subjected to more extensive testing to confirm this observation.
- 6) Comparison of statistics from the DPHM-RS and MISBA simulated streamflow demonstrate generally well performance of MISBA in both calibration and validation stages over DPHM-RS.

2.10 References

- Andréassian, V., Oddos, A., Michel, C., Anctil, F., Perrin, C., Loumagne, C. (2004).
“Impact of spatial aggregation of inputs and parameters on the efficiency
of rainfall-runoff models: A theoretical study using chimera watersheds.”
Water Resources Research, 40, W05209, doi: 10.1029/2003WR002854.
- Arya, L. M., and Paris, J. F. (1981). “A physicoempirical model to predict the soil
moisture characteristic from particle-size distribution and bulk density
data.” *Soil Science Society of America Journal*, 45, 1023-1030.
- Bandaragoda, C., Tarboton, D.G., and Woods, R. (2004). “Application of TOPNET
in the distributed model Intercomparison project.” *Journal of Hydrology*,
298(1-4), 178-201.
- Biftu, G. F., and Gan, T. Y. (2001). “Semi-distributed, physically based, hydrologic
modeling of the Paddle River Basin, Alberta, using remotely sensed data.”
Journal of Hydrology, 244, 137-156.
- Biftu, G. F., and Gan, T. Y. (2004). “Semi-distributed, Hydrologic Modeling of Dry
Catchment with Remotely Sensed and Digital Terrain Elevation Data.”
International Journal of Remote Sensing, 25(20), 4351-4379.
- Boyle, D.P., Gupta, H.V., Sorooshian, S., Koren, V., Zhang, Z., Smith, M. (2001).
“Toward improved streamflow forecast: value of semidistributed
modeling.” *Water Resources Research*, 37(11), 2749–2759.

- Carpenter, T.M., and Georgakakos, K.P. (2004). "Continuous streamflow simulation with the HRCDHM distributed hydrologic model." *Journal of Hydrology*, 298(1-4), 61-79.
- Carpenter, T.M., and Georgakakos, K.P. (2006). "Intercomparison of lumped versus distributed hydrologic model ensemble simulations on operational forecast scales." *Journal of Hydrology*, 329, 174-185.
- Cunge, J. A. (1969). "On the Subject of a Flood Propagation Method (Muskingum Method)." *Journal of Hydraulic Research*, 7 (2), 205-230.
- Deardorff, J. W. (1978). "Prediction of Ground Surface Temperature and Moisture, With Inclusion of a Layer of Vegetation." *Journal of Geophysical Research*, 83 (C4), 1889-1903.
- Elsanabary, M. (2012). "Teleconnection, Modeling, Climate Annomalies Impact and Forecasting of Rainfall and Streamflow of the Upper Blue Nile River Basin." *PhD Thesis, University of Alberta*.
- Famiglietti, J.S., and Wood, E.F. (1994). "Multi-scale modeling of spatially-variable water and energy balance process." *Water Resources Research*, 30(11), 3061-3078.
- Habets, F, J Nolihan, C Golaz, J. P. Goutorbe, P. Lacarrère, and E Leblois (1999). "The ISBA surface scheme in a macroscale hydrological model applied to the Hapex–Mobilhy area. Part 1. Model and database." *Journal of Hydrology*, 75-96.

- Ivanov, V.Y., Vivoni, E. R., Bras, R. L., and Entekhabi, D. (2004). "Preserving high-resolution surface and rainfall data in operational-scale basin hydrology: a fully distributed approach." *Journal of Hydrology*, 298(1-4), 80-111.
- Kalinga, O.A., and Gan, T.Y. (2006). "Semi-distributed modeling of basin hydrology with radar and gauged precipitation." *Hydrologic Processes*, 20, 3725-3746.
- Kerkhoven, E. and Gan, T.Y. (2006). "A modified ISBA surface scheme for modeling the hydrology of Athabasca River Basin with GCM-scale data." *Advanced in Water Resour.*, 29(6), 808-826.
- Kerkhoven, E. and Gan, T.Y. (2010). "Differences and sensitivities in potential hydrologic impact of climate change to regional-scale Athabasca and Fraser River basins of the leeward and windward sides of the Canadian Rocky Mountains respectively." *Climatic Change*, 106(4), 583-607.
- Kerkhoven, E., and Gan, T.Y. (2007). "Development of a hydrologic scheme for use in land surface models and its application to climate change in the Athabasca River Basin." *Cold Region Atmospheric and Hydrologic Studies. The Mackenzie GEWEX Experience, Volume 2: Hydrologic Processes.*
- Kuo, W. L., Steenhuis, T. S., McCulloch, C. E., Mohler, C. L., Weinstein, D.A., DeGloria, S. D., and Swaney, D.P. (1999). "Effect of grid size on runoff and soil moisture for a variable-source-area hydrology model." *Water Resources Research*, 35 (11), 3419-3428.

- Liang, X., and Guo, J. and Leung, L.R. (2004). "Assessment of the effects of spatial resolutions on daily water flux simulations." *Journal of Hydrology*, 298, 287-310.
- Looper, J., Vieux, B., and Moreno, M.A. (2009). "Evaluating precipitation uncertainties using the Vflo hydrologic model." *23rd Conference on Hydrology, American Meteorological Society 2009 Annual Meeting, Paper 4.5*, Phoenix, Arizona, Jan 11-16.
- Masson, V., Champeaux, J.-L., Chauvin, F., Meriguet, C. and Lacaze, R. (2003) "A Global Database of Land Surface Parameters at 1 km Resolution in Meteorological and Climate Models." *Journal of Climate*, 16, 1261-1282.
- Nolihan, J, and Mahfouf, J. (1996). "ISBA land surface parameterization scheme." *Global and Planetary Change*, 13, 145-159.
- Nolihan, J, and Planton, S. (1989). "A simple parameterization of land surface processes for meteorological models." *Monthly Weather Review*, 17.
- Ponce, V.M., and Yevjevich, V. (1978). "Muskingum-Cunge method for variable parameters." *Proc. ASCE 104(HY12)*.
- Quinn, P., Beven, K., Chevallier, P., and Planchon, O. (1991). "The prediction of hillslope flow paths for distributed hydrological modeling using digital terrain models." *Hydrological Processes*, 5, 59-79.

- Rawls, W.J., and Brakensiek, D.L. (1985). "Prediction of soil water properties for hydrologic modeling." *Watershed Management in the Eighties*, ASCE, 293-299.
- Rutter, A.J., Morton, A.J., and Robins, P.C. (1975). "A predictive model of rain interception in forests, 1.Generalization of the model and comparison with observation in some coniferous and hardwood stands." *Journal of Applied Ecology*, 12, 364-380.
- Shuttleworth, J.W., and Gurney, R.J. (1990). "The theoretical relationship between foliage temperature and canopy resistance in sparse crop." *Quarterly Journal of Royal Meteorology Society*, 116, 497-519.
- Sivapalan, M., Wood, E.F., and Beven, K.J. (1987). "On hydrologic similarity, 2 a scaled model of storm runoff prediction." *Water Resources Research*, 23(12), 2266-2278.
- Smith, M., Koren, V., Zhang, Z., & Cui, Z. (2009). "Distributed hydrologic modeling: From research to operational forecasting." *ASCE World Environmental and Water Resources Congress*.
- Tanzeeba, S. (2009) Potential Impact of Climate Change on the Water Availability in the South Saskatchewan River Basin. *Msc Thesis, University of Alberta*.
- Tanzeeba, S. and Gan, T.Y. (2012). "Potential impact of climate change on the water availability of South Saskatchewan River Basin." *Climatic Change*, 112, 355-386.

Zhang, Z., Koren, V., Smith, M., Reed, S., and Wang, D., (2004). "Use of next generation weather radar data and basin disaggregation to improve continuous hydrograph simulation." *J. Hydrologic Engineering*, 9(2), 103-115.

Zhao, R.J. (1992). "The Xinanjiang model applied in China." *J Hydrol*, 135, 371–381.

Table 2.1 Distributions of major vegetation and soil types of BRB divided into 7 sub-basins

Sub-basin	Area (km ²)	Land Use Classes (%)						Dominant Soil Type
		Water Body	Woody Savannah	Mixed Forest	Agricultural Land	Grass land	Impervious land	
1	170.57	0.01	91.57	2.45	1.42	3.74	0.81	Silty Clay Loam
2	150.34	0.01	88.73	0.01	0.01	11.24	0.01	
3	169.68	0.01	86.43	10.53	1.67	1.36	0.01	
4	221.51	0.00	68.72	28.03	3.23	0.00	0.00	Sandy Clay
5	188.41	0.01	83.46	16.28	0.25	0.01	0.01	Clay
6	204.25	0.00	78.35	16.72	1.50	0.33	3.10	
7	130.37	0.01	48.00	51.97	0.01	0.01	0.01	

Table 2.2 Input data requirements of DPHM-RS.

Data Type	Parameters	Source
Topographic	Mean Altitude, Aspects, Flow direction, Surface slope, Drainage network, Topographic soil index	DEM of USGS National Elevation Dataset
Land use	Spatial distribution of land use, classes, Surface Albedo, Surface emissivity, Leaf Area Index	NASA LDAS, NOAA-AVHRR Satellite data
Soil Properties	Spatial distribution of soil types, Antecedent moisture content, Soil hydraulic properties	STATSGO and Soil Properties of Rawls and Brakensiek (1985)
Hydrological	Hourly streamflow data, Channel cross section	USGS
Meteorological	Shortwave radiation, Wind speed, Air temperature, Ground temperature, Relative humidity, Net radiation, Ground heat flux	North American Regional Reanalysis (NARR)
	Hourly Precipitation	Multisensor (NEXRAD and gauge) Precipitation Data

Table 2.3 NEXRAD precipitation statistics for the calibration (1996-2002) and the validation (2002-2006) periods.

Sub-Basin ID	Hourly Precipitation (mm)					
	Maximum		Average		Standard Deviation	
	1996-2002	2002-2006	1996-2002	2002-2006	1996-2002	2002-2006
1	40.63	35.93	0.1170	0.0975	0.9110	0.8021
2	42.54	32.90	0.1207	0.0948	0.9470	0.7768
3	36.52	39.91	0.1214	0.0956	0.9216	0.8101
4	42.99	37.20	0.1250	0.1024	0.9399	0.8987
5	56.86	40.53	0.1268	0.1016	0.9532	0.8642
6	47.74	41.78	0.1274	0.0992	0.9559	0.8727
7	50.14	38.80	0.1247	0.0955	0.9680	0.8598

Table 2.4 Comparison of Measured and Calibrated Channel Top Width as Varies with Drainage Area

Drainage Area (km ²)	Measured Top Width (m)	Calibrated Top Width (m)	Measured Manning's n	Calibrated Manning's n
1204	30.49	26.98	0.015	0.014
1089	31.10	26.47		0.014
964	27.44	25.85		0.015
961	21.34	25.84		0.015
931	18.29	25.68		0.015
793	25.91	24.90		0.016
512	20.12	22.88	0.020	0.019
473	18.29	22.53		0.019
393	42.68	21.74		0.021
358	21.04	21.36		0.021
291	26.83	20.52		0.023
127	13.11	17.49		0.030
84	11.89	16.15		0.035
9	12.20	10.50	0.070	0.075

Table 2.5 Summary statistics of the calibration and validation results of DPHM-RS applied to BRB.

Statistical Measures	Calibration Period (1996-2002)	Validation Period (2002-2006)
Coefficient of Correlation, R	0.70	0.60
Percent Bias (% PB)	-4.54	50.73
Absolute Percent Bias (% APB)	81.67	115.41
Mean Observed Flow (Q_o mean) (m ³ /s)	9.58	4.64
Mean Simulated Flow (Q_s mean) (m ³ /s)	9.14	6.99
CVfor Observed Streamflow(CV_o) (m ³ /s)	3.28	2.92
CVfor Simulated Streamflow (CV_s) (m ³ /s)	2.34	2.52
Root Mean Square Error (RMSE) (m ³ /s)	22.28	14.58
Nash-Sutcliffe Coefficient (E_f)	0.50	-0.16

Table 2.6 Comparing the calibration and validation results based on the original NEXRAD precipitation input of DMIP 2 and the adjusted precipitation input.

Index	Calibration Period (1996-2002)		Validation Period (2002-2006)	
	NEXRAD	Adjusted NEXRAD	NEXRAD	Adjusted NEXRAD
R	0.70	0.76	0.60	0.71
% PB	-4.54	-29.20	50.73	-2.01
% APB	81.67	68.83	115.41	79.61
Q_o mean (m ³ /s)	9.58	9.58	4.64	4.64
Q_s mean (m ³ /s)	9.14	6.78	6.99	4.54
CV_o (m ³ /s)	3.28	3.28	2.92	2.92
CV_s (m ³ /s)	2.34	2.58	2.52	2.72
$RMSE$ (m ³ /s)	22.28	21.58	14.58	9.91
E_f	0.50	0.53	-0.16	0.46

Table 2.7 Comparing the calibration and validation results of DPHM-RS with several previous studies of DMIP and DMIP2 using NEXRAD precipitation data.

Index	Studies						
	Current Study		Ivanov et al. (2004)	Carpenter and Georgakakos, 2004	Bandaragoda et al. (2004)		
Model	DPHM-RS		tRIBS	HRCDHM	TOPNET		
Discretization	Semi- Distributed		Distributed	Distributed	Distributed		
Duration	6 years	6 years	6 years	6 years	1 year	6 years	1 year
Period	Calibration	Validation	Calibration	Calibration	Validation	Calibration	Validation
	10/1996-09/2002	10/2002-09/2006	04/1994-07/2000	06/1993-05/1999	06/1999-7/2000	06/1993-05/1999	06/1999-7/2000
R	0.70	0.60	0.73	0.83	0.76	-238.50	-381.56
% PB	-4.54	50.73	8.41	1.00	92.20		
% APB	81.67	115.41	66.08				
Q_o mean (m ³ /s)	9.58	4.64	8.93	9.80	2.30	9.83	2.25
Q_s mean (m ³ /s)	9.14	6.99	9.68	9.90	4.30	15.21	9.04
CV_o (m ³ /s)	3.28	2.92	2.69	2.57	1.13		
CV_s (m ³ /s)	2.34	2.52	1.69	2.42	1.28		
$RMSE$ (m ³ /s)	22.28	14.58	16.41				
E_f	0.50	-0.16	0.53	0.68	-1.9	0.53	-13.64

Table 2.8 The effect of sub-basin resolution to the performance of DPHM-RS applied to BRB.

Number of Sub-Basins	R	% PB	% APB	Q_o mean (m ³ /s)	Q_s mean (m ³ /s)	CV_o (m ³ /s)	CV_s (m ³ /s)	$RMSE$ (m ³ /s)	E_f
1	0.46	-14.03	97.42	9.58	8.24	3.28	1.55	27.97	0.21
5	0.68	-10.12	83.09	9.58	8.61	3.28	2.24	23.00	0.46
7	0.70	-4.54	81.67	9.58	9.14	3.28	2.34	22.28	0.50
13	0.65	5.62	85.71	9.58	10.12	3.28	2.46	24.34	0.40
20	0.59	3.63	89.99	9.58	9.93	3.28	2.84	27.09	0.25

Table 2.9 Comparison of statistics of simulated streamflow by DPHM-RS and MISBA for calibration and validation period

Index	Calibration Period (1996-2002)		Validation Period (2002-2006)	
	DPHM-RS	MISBA	DPHM-RS	MISBA
R	0.76	0.93	0.71	0.90
E_f	0.53	0.82	0.46	0.83
% PB	-29.20	-14.06	-2.01	-1.43
% APB	68.83	32.86	79.61	46.05
CV (m ³ /s)	2.58	2.74	2.72	2.61
$RMSE$ (m ³ /s)	21.58	13.38	9.91	5.93
MAE (m ³ /s)	6.57	3.15	3.69	2.13

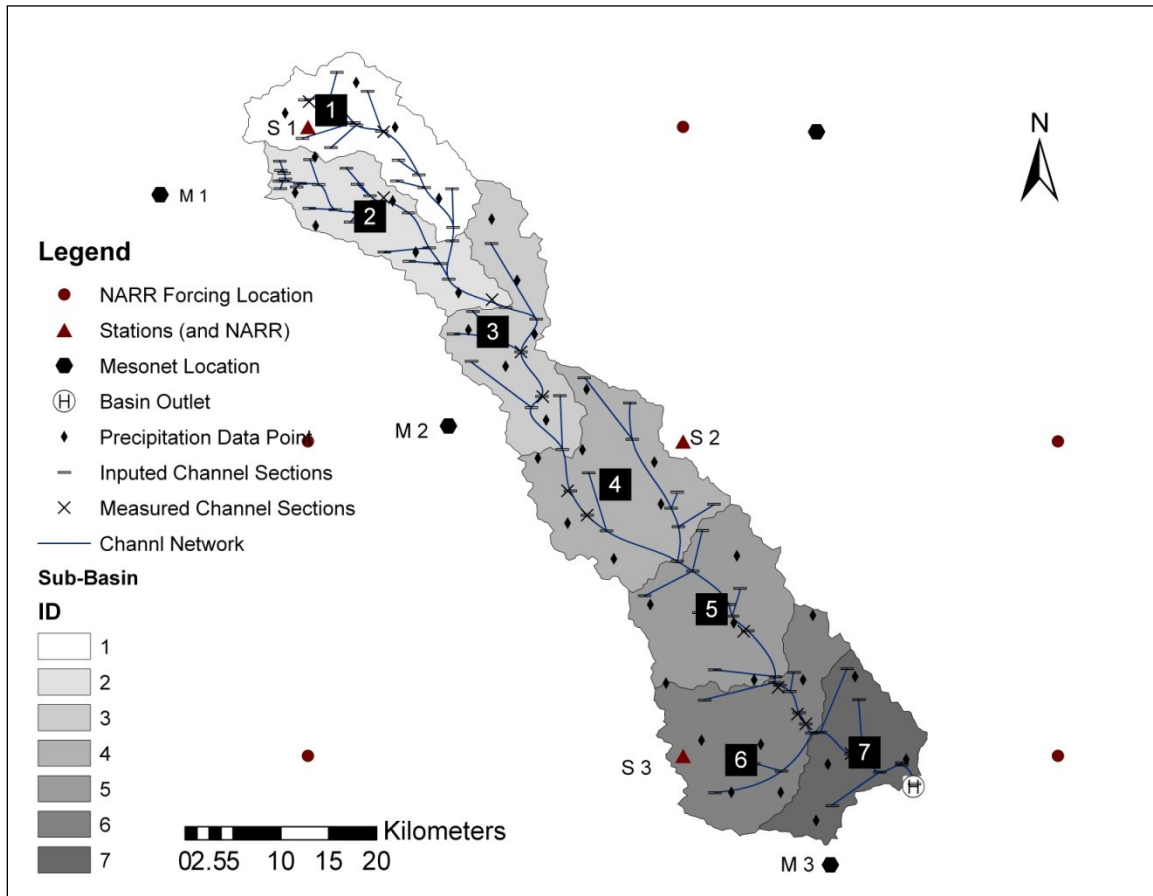
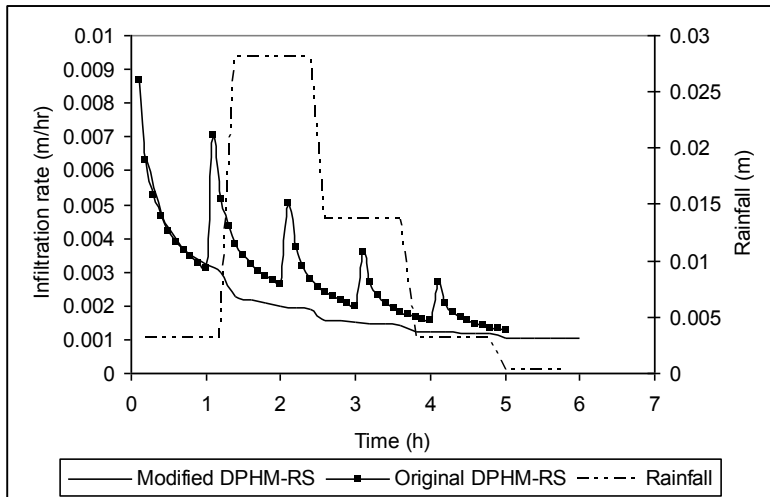
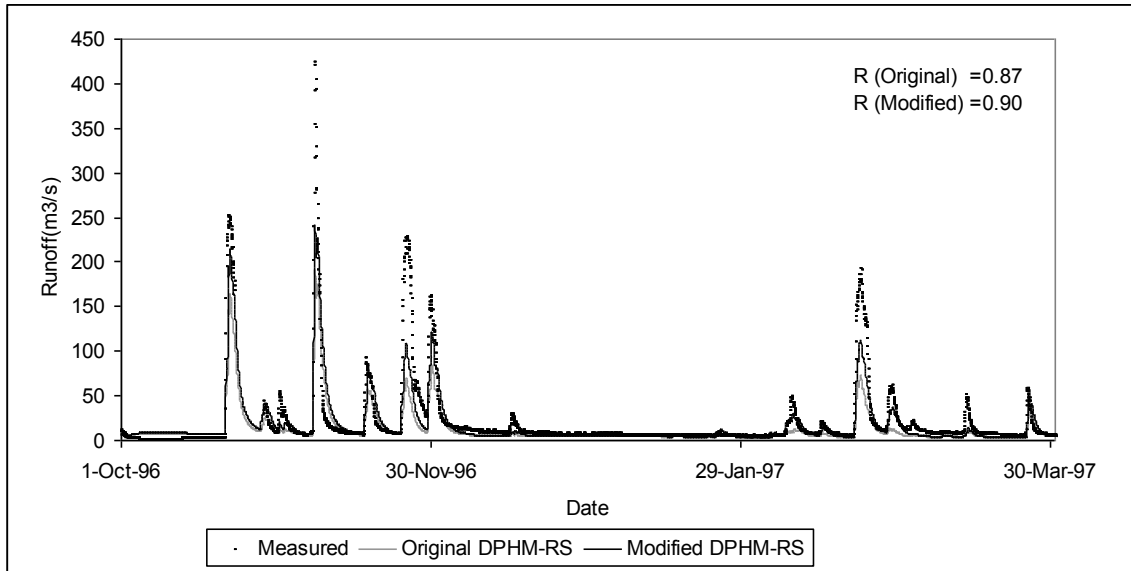


Figure 2.1 BRB divided into 7 sub-basins together with meteorological and hydrological grid-points/stations.

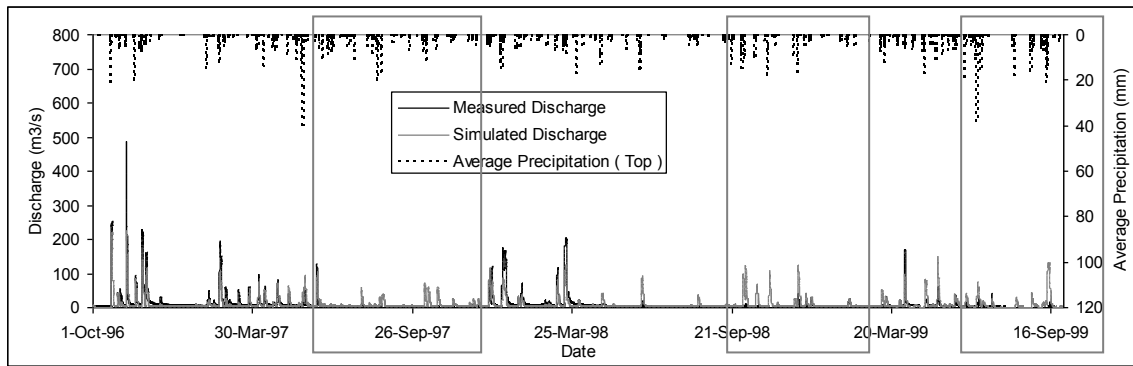


a)

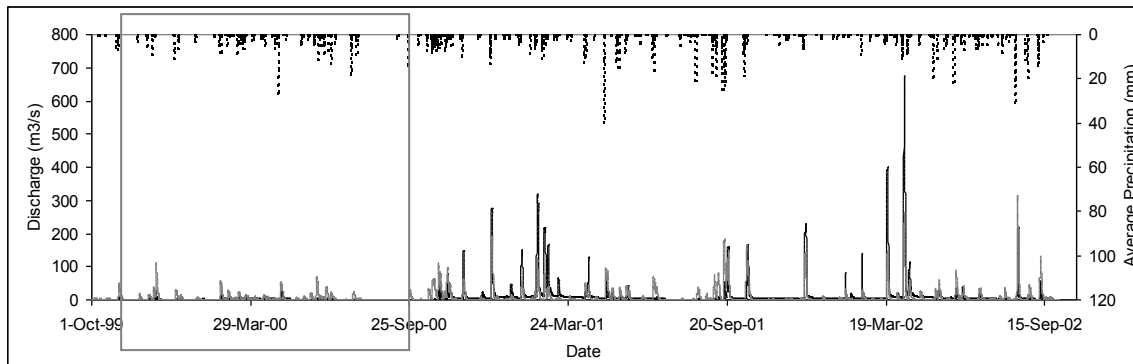


b)

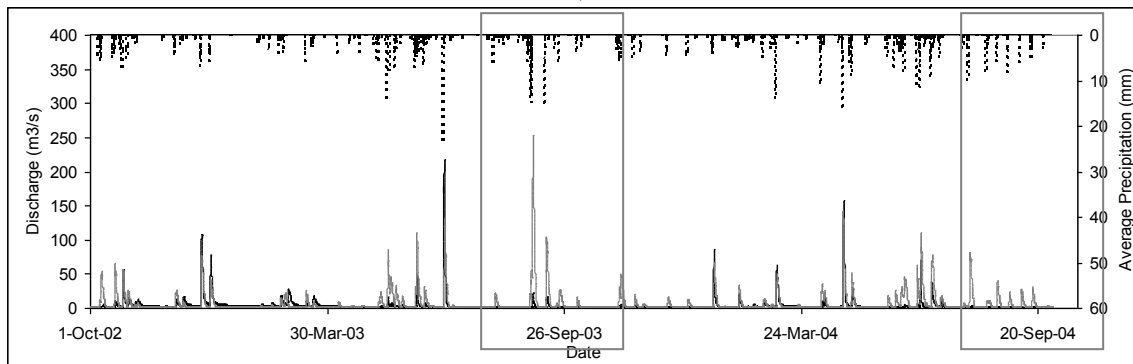
Figure 2.2 . Comparing a) Infiltration rate, and b) runoff hydrograph of the original and modified DPHM-RS.



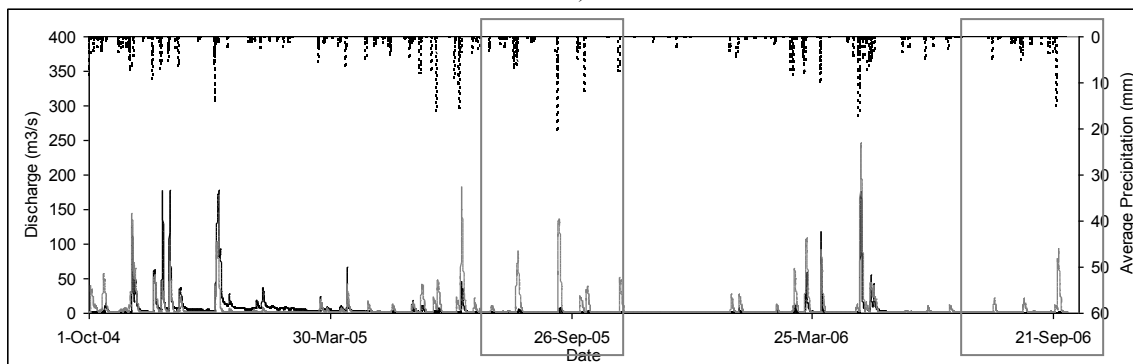
a)



b)

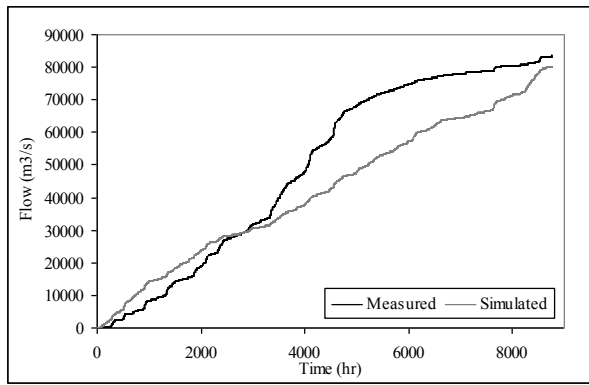


c)

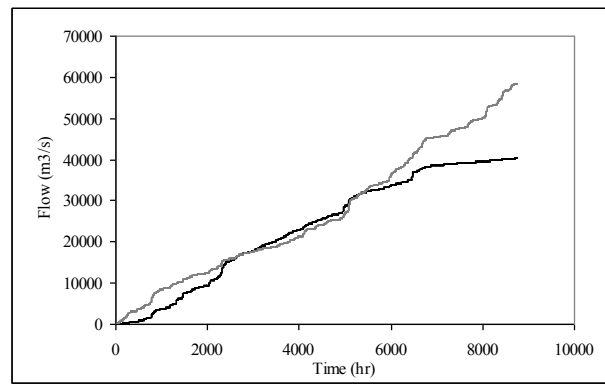


d)

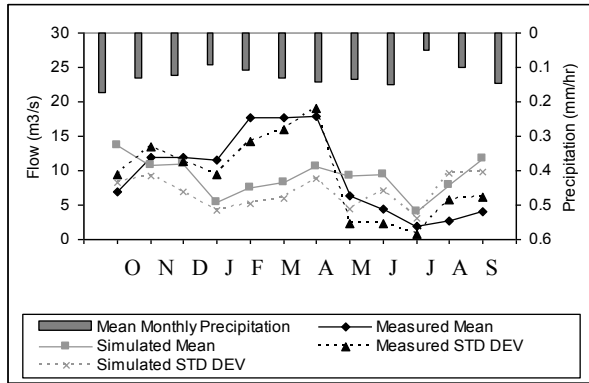
Figure 2.3 Observed versus simulated hydrograph for BRB by DPHM-RS driven by NEXRAD precipitation data for the calibration (a and b) and the validation (c and d) periods.



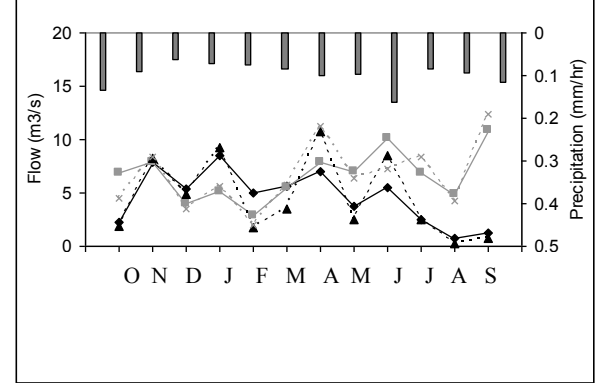
a)



b)

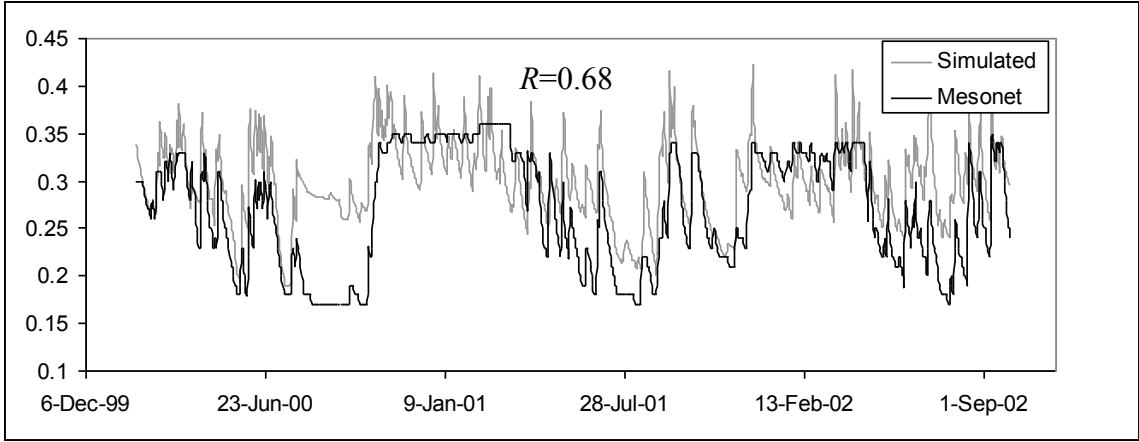


c)

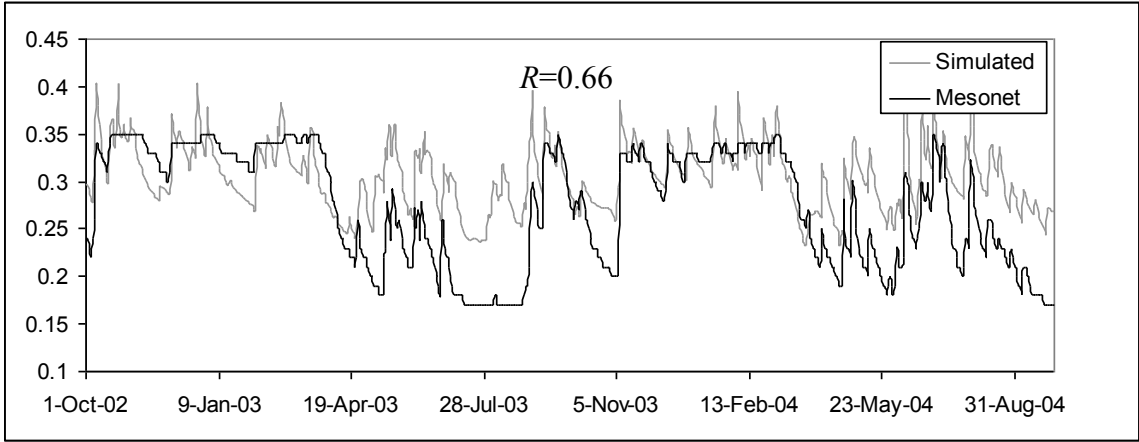


d)

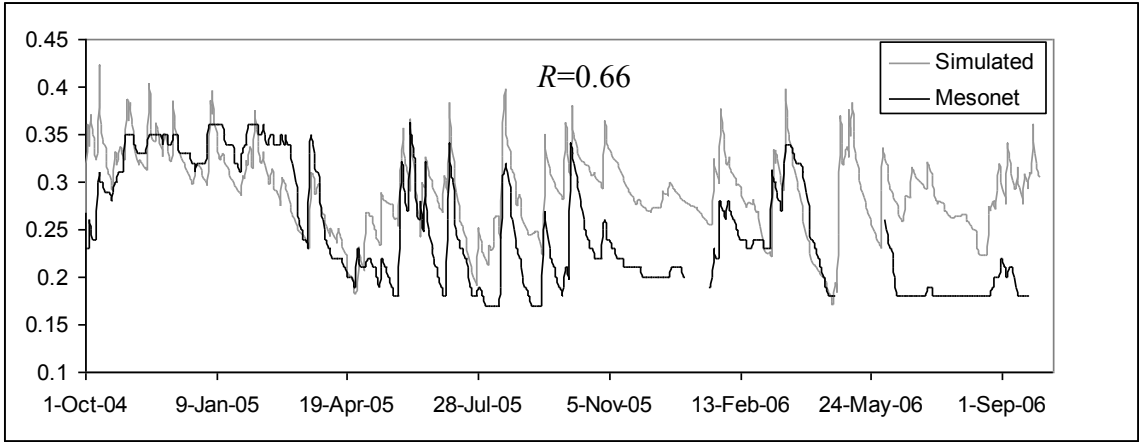
Figure 2.4 Averaged cumulative hourly flow (a and b), monthly mean flow, standard deviation and monthly mean precipitation (c and d) for calibration (1996-2002) and validation (2002-2006) periods, respectively.



a)



b)



c)

Figure 2.5 Oklahoma Mesonet soil moisture estimates and simulated top 10 cm volumetric soil moisture of DPHM-RS at sub-basin #3 of BRB divided into 7 sub-basins for calibration (a) and validation (b & c) periods.

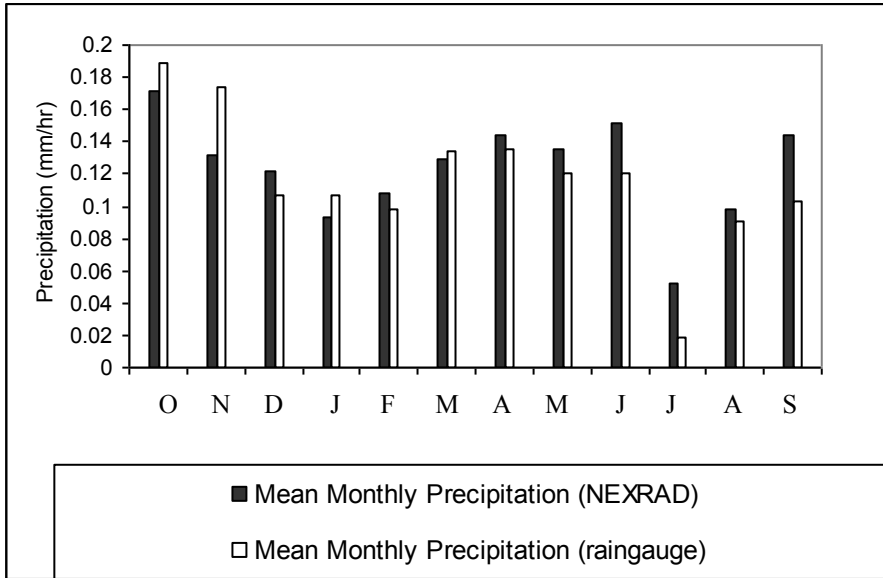


Figure 2.6 Comparison of monthly mean precipitation of BRB derived from NEXRAD precipitation and Mesonet rain-gauge data for 1996-1999.

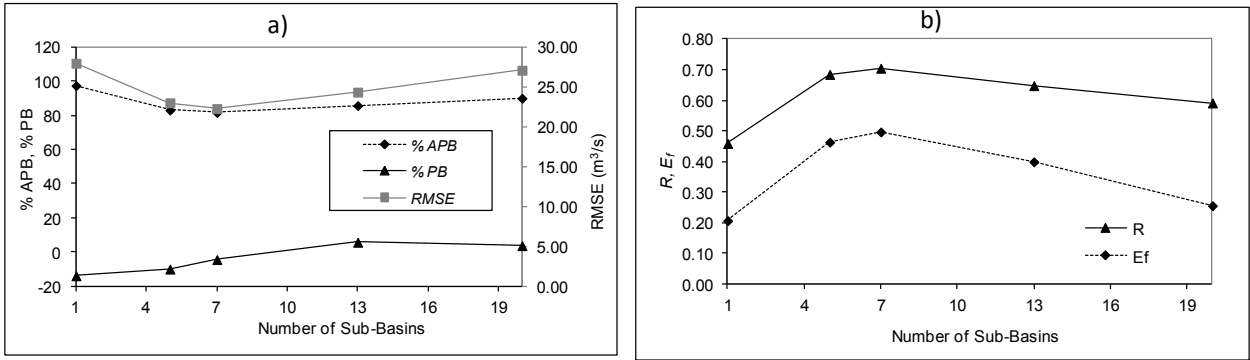


Figure 2.7 Comparing summary statistics of model performance of DPHM-RS applied to BRB discretized to different sub-basin resolutions (APB is the absolute percent bias, PB is the percent bias, RMSE is the root mean square error, R is the coefficient of correlation, E_f is the Nash-Sutcliffe efficiency).

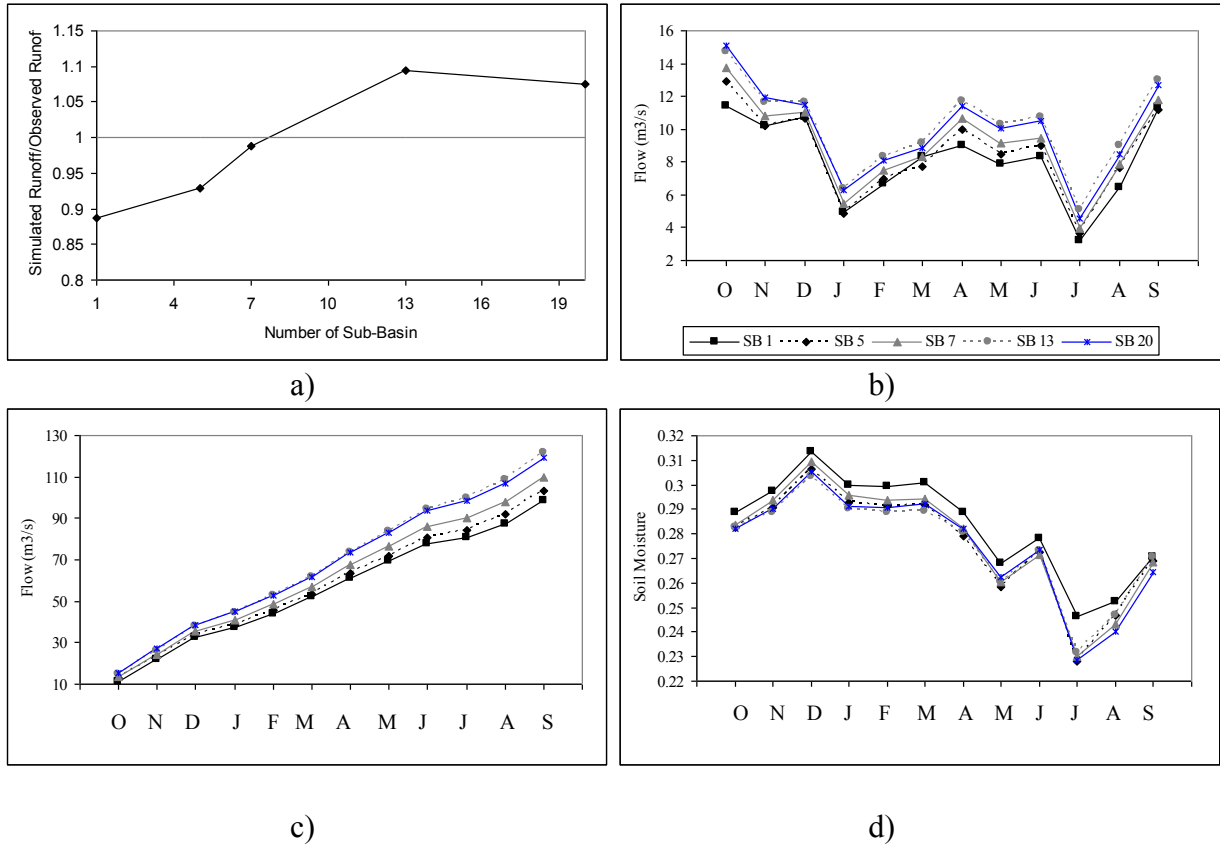
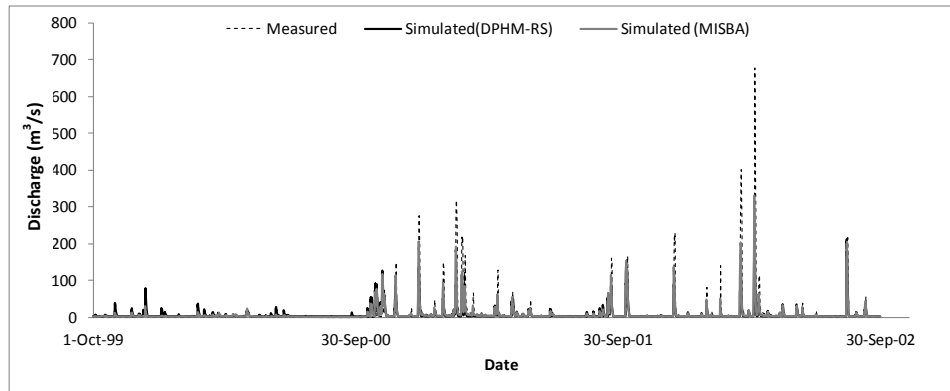
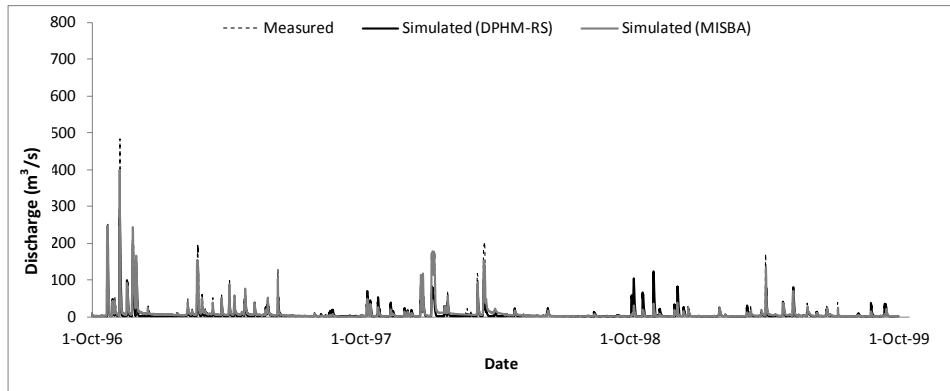
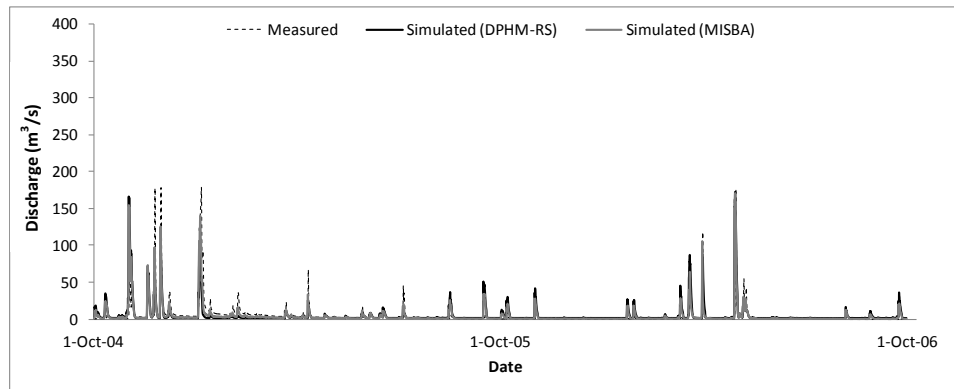
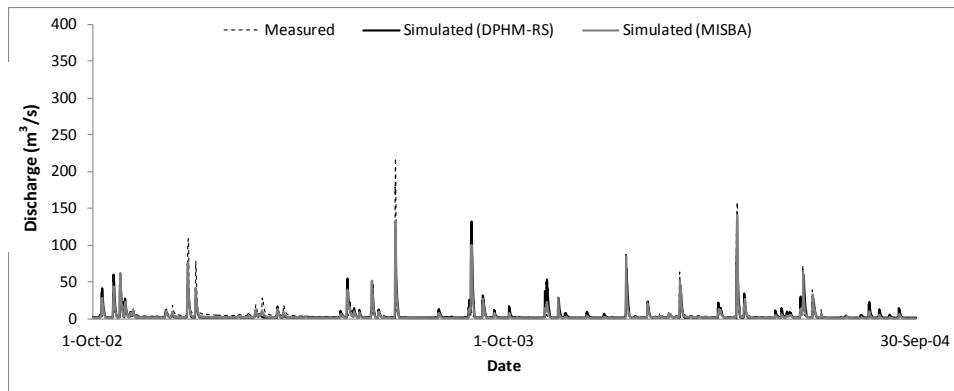


Figure 2.8 a) Ratio of simulated over observed runoff volume, b) Average monthly flow, c) Cumulative monthly flow, and d) Average monthly top layer soil moisture of BRB for different sub-basin resolutions over 1996-2002.



a) Calibration Period (1996-2002)



b) Validation Period (2002-2006)

Figure 2.9 Comparison of DPHM-RS and MISBA simulated streamflow of Blue River Basin for a) calibration period (1996-2002) and b) validation period (2002-2006).

CHAPTER 3

Physically Based Hydrological Modeling of Future Streamflow of South Saskatchewan River Basin under Combined Impact of Climate Change and Climate Anomalies

3.1 Introduction

In recent years, the potential impact of climate change has been of major concern worldwide, as there are more and more observations supporting the evidence of climate change, such as observed increase in globally averaged temperatures, increasing occurrences of climatic extremes, melting of glaciers and arctic sea ice, rising sea levels, and diminishing snowpacks. Relative to the 1906-1970 level, major General Circulation Models (GCM) project a drastic increase in the surface temperature of North America in the 21st Century (IPCC 2007). For the South Saskatchewan River Basin (SSRB), several GCMs (e.g., CCSRNIES, CGCM2, ECHAM4, and HadCM3) forced by different Special Report on Emissions Scenarios (SRES) of Intergovernmental Panel on Climate Change (IPCC) project that for the 21st century, compared to the climate normal, the

temperature of SSRB is expected to increase by 1.3°C, 3.1°C and 5.0 °C in 2010-2039 (2020s), 2040-2069 (2050s) and 2070-2099 (2080s), respectively while precipitation is expected to change between -4.25% to 3.5 % by 2020s, 1% to 8.0% by 2050s and -2.5% to 13.5 % by 2080s (Islam and Gan 2012). However, GCMs projections involve much uncertainty.

These projected changes in temperature likely mean less snowpacks, and more rainfall at the expense of snowfall. For watersheds dominated by spring snowmelt such as those in the Canadian Prairies, climate change will lead to an earlier onset of snowmelt and increasing risk of lower water supply during summer. Recent studies regarding major river basins of Alberta show potential decline in streamflow. Schindler and Donohue (2006) found that yield of the Athabasca River has declined in the past 30 years. Kerkhoven and Gan (2011) in their study on the potential hydrologic impact of climate change to the Athabasca River basin, they projected that the shortened snowfall season and increased sublimation together could lead to a decline in the spring snowpack, and mean annual flows, such that the runoff coefficient could drop by about 8% per °C rise in temperature. On the basis of climate projections of 7 GCMs of IPCC, Kerkhoven and Gan (2011) found that by the end of the 21st century, the annual runoff, mean maximum annual flow and mean minimum annual flow of Athabasca River Basin could decline by -21%, -4.4%, and -41%, respectively. Tanzeeba and Gan (2012) simulated the potential impacts of climate change on three of the four sub-basins of SSRB and their results also showed that SSRB will

generally experience a decrease in the mean annual maximum flow in the 21st century, an approximately 2 weeks earlier onset of the spring snow melt at the expense of summer flow. Further, climate change could lead to changes to the streamflows of SSRB from +5% to -30% in the 2040-2069, and climate variability would further decrease its streamflows by 25% or more during dry years (Alberta Environment 2010).

Other than the potential impact of climate change, climate anomalies as El Niño, La Niña episodes could impact the streamflow of Alberta. The El Niño Southern Oscillation (ENSO)-streamflow relationship also appears to be modulated by interdecadal oscillations of the North Pacific called Pacific Decadal Oscillation (PDO) such that their interactions are constructive when in phase and destructive otherwise. For example, the El Niño (La Niña) signals are likely to be stronger and stable when the PDO is highly positive (negative); in contrast, signals tend to be weak, spatially incoherent, and unstable during the El Niño–Negative PDO and La Niña–Positive PDO phase combinations (Gershunov and Barnett 1998). By superimposing the climate projections of GCMs on historical temperature and precipitation dataset of the SSRB resampled for the El Niño and La Niña episodes, there could be more drastic future changes to precipitation and temperature of SSRB. For the 2050s, when considering potential combined impact of both climate change and climate anomalies such as El Niño, it seems on the average that precipitation could decrease by 5.15% while temperature could marginally increase by about 0.3°C than that of the SRES climate scenarios

of 2050s. In contrast, for La Niña years, on the average precipitation could increase by about 9% while temperature decreases by about 0.3° C than that of SRES climate scenarios of 2050s. These possible changes to the precipitation and temperature expected from the possible combined impact of climatic change and climate anomalies may further aggravate the reliability of water supply for SSRB. For example, if we have a La Niña year, the drying effect of climate change on the SSRB should be somewhat reduced by La Niña but the drying effect of climate change could get worse in El Niño years. These results agree with the findings of Gobena and Gan (2006) who showed that El Niño and La Niña episodes lead to significant negative and positive streamflow anomalies in south western Canada, respectively. Gan et al. (2007) found statistically significant correlation between winter precipitation of south western Canada and the ENSO index 'Nino3' (about -0.41 to -0.42), Pacific/North American index or PNA (about -0.44 to -0.52) and PDO (about -0.44 to -0.54). Therefore the potential impact of climate change on the streamflow of SSRB could be quite significantly modified by some climate anomalies individually and collectively, when such anomalies occur. Given that about 88% of the water supply of Canadian municipalities comes from surface sources (Environment Canada 2007), an assessment of the combined impact of climate change and climate anomalies to the future water supply of Canada and strategies for reducing such vulnerability will be of national priority.

Based on the above statements of problems, the objectives of this research study is to investigate possible changes to streamflow of the sub-basins of SSRB (a) on the basis of climate change projected by GCMs forced by selected SRES emissions of IPCC (2001) for 2020s, 2050s, and 2080s; and (b) the impact of climate change projected by GCMs forced by selected SRES emissions of IPCC for 2050s, combined with the possible impact of El Niño and La Niña episodes.

3.2 The South Saskatchewan River Basin (SSRB)

The SSRB, part of the Nelson River Basin of Canada, has a watershed area of 121,095 km², of which 41% is from the Red Deer, 22% from the Oldman, 21% from the Bow and 16% from the South Saskatchewan River sub-basin (Figure 3.1). After originating in the Rocky Mountains, the SSRB extends eastward through southern Alberta and south-central Saskatchewan. Therefore, SSRB encompasses diversified landscapes varying from the front range of the Rocky Mountains to the rolling parkland around the Red Deer city and then to relatively flat grasslands adjacent to the South Saskatchewan border (Tanzeeba 2009). About 70% of the annual runoff of the SSRB comes from the snowmelt of Rocky Mountains and the foothills (Ashmore and Church, 2001). Even though it occupies only about a quarter of the land area of Alberta, it provides nearly 57% of the water allocated in Alberta, even though it only possesses less than 6% of Alberta's total water resources because southern Alberta has a semi-arid climate. Having a sub humid to semiarid continental climate, summer in SSRB is

short with a mean temperature varying from 14 to 16° C while winter is long having a mean temperature from -2.5 to -8.0° C (Lac 2004). The mean annual precipitation of SSRB varies between 200 mm and 500 mm (Martz et al. 2007).

3.3 Physically Based Hydrologic Modeling

A physically based hydrologic model uses known scientific principles to mimic basin scale hydrologic processes as well as interactions between them. In a mathematical hydrologic model, inter-relationships between soil, water, climate, and landuse are considered and represented through mathematical abstraction (Gosain et al. 2009). This can be challenging because it involves highly nonlinear processes with complex interactions and high spatial variability in precipitation, soil properties and vegetative covers. Starting from the mid of the twentieth century, hydrologic modelling has made great progress in the understanding of physical processes, computational power, speed and data retrieving facilities. Deterministic hydrologic models can be broadly classified as conceptual and physically based (Refsgaard 1996). In conceptual models, hydrologic processes that are observable or not directly observable in the field are represented by conceptual, mathematical relationships, while in physically based models detailed physical processes can be represented in a deterministic way by representations of mass, momentum and energy conservation (Refsgaard 1996).

In terms of spatial descriptions of the watershed process, hydrologic models can be classified as lump, semi-distributed and fully distributed models. In a lumped model the spatial variability of watershed characteristics are ignored, while in a semi- or fully distributed model, the spatial variability of vegetation, soil, topography, etc are partially or fully taken into account. Conceptual models are usually lumped while physically based models are generally semi- or fully distributed (Refsgaard 1996). In the latter a river basin is either divided into limited number of sub-basins of uneven shapes and sizes (semi-distributed), or discretized as a rectangular or square grid mesh of constant sizes (fully distributed). The hydrologic process of water movement are then modeled either by the finite difference approximation of the partial differential equation representing the mass, momentum and energy balance, or, by empirical equations (Abbott et al. 1986). Typically the primary components of hydrologic cycle related to the land phase (e.g., interception, snowmelt, evapotranspiration, sub-surface runoff, groundwater flow, surface runoff and channel routing) are taken into consideration.

A number of physically based semi-distributed (e.g., TOPMODEL of Beven et al. 1995; SLURP of Kite 1995; SWAT of Arnold et al. 1998; DPHM-RS of Biftu and Gan 2001) and fully distributed (e.g., ISBA of Nolihan and Mahfouf 1996; WATFLOOD of Kouwen 2000; tRIBS of Ivanov et al. 2004) hydrologic models have been reviewed for this study and a modified version of ISBA, namely Modified Interaction Soil Biosphere Atmosphere or MISBA of Kerkhoven and Gan

(2006) has been selected to model the basin hydrology at selected outlet points of the SSRB as, it has been developed from well established scientific laws at micro-scale to water behavior at the meso-scale or regional scale, its parameters are physically based, it consider the spatial heterogeneities of landuse, soil, and input variables, it require less calibration, and it has been applied for the river basins of Alberta in previous studies (Kerkhoven and Gan, 2006; Tanzeeba and Gan 2012).

3.3.1 Modified Interaction Soil Biosphere Atmosphere (MISBA)

The land surface scheme, ISBA (Nolihan and Planton 1989; Nolihan and Mahfouf 1996) is a soil vegetation atmosphere transfer (SVAT) scheme used to model the hydrologic processes at GCM scale. ISBA is designed to simulate the exchange of heat, mass and momentum between the land or water surface and the overlying atmosphere (Tanzeeba 2009). ISBA requires two basic types of parameters – 4 primary and 22 secondary parameters. The primary parameters are percentage of sand, percentage of clay, vegetation, and land-water ratio that are specified at each grid points. The secondary parameters are determined from the primary parameters. The primary and secondary parameters are listed in **Appendix A**.

ISBA uses the relationship of Deardorff (1978) to model the precipitation interception. ISBA has three soil layers. Evaporation from soil and vegetation is based on energy balance and aerodynamic method. ISBA uses a sub-grid runoff

scheme that considers sub-grid variation of soil moisture by the Xinanjiang distribution (Habets et al. 1999). The scheme acts like a multi-bucket model in which the distribution of buckets size is defined by the Xinanjiang distribution (e.g., Zhao 1992) and when a bucket fills its capacity surface runoff occurs (Kerkhoven and Gan 2006). Sub-surface runoff is represented by a gravity drainage scheme following a linear reservoir. In the modified version of ISBA, namely MISBA (Kerkhoven and Gan 2006), the sub-surface runoff equation is converted from a linear function to a nonlinear function of soil water to account for interflow more accurately.

MISBA has three-layer snow model where the upper snow layer serves as the interface between snow pack and atmosphere and the lower layer acts as an interface between snow pack and soil surface. Melting in the snow pack occurs when additional heat is available at or above the freezing point of water and liquid water produced from melting snow or rainfall infiltrates through snow layers to the soil surface (Tanzeeba 2009). The simulated runoff of MISBA was routed by a Muskingum-Cunge routing model (Cunge 1969) to obtain the total basin stream flow.

MISBA has been applied to Athabasca River Basin of Alberta (Kerkhoven and Gan 2006; 2010), Fraser River Basin of British Columbia (Kerkhoven and Gan 2010), SSRB of Alberta (Tanzeeba and Gan 2012), and Upper Blue Nile River Basin

(Elsanabary 2012), and generally a good correlation of simulated and measured runoff were observed.

3.3.2 Data Requirement of MISBA

MISBA requires topographic, landuse, meteorological, and hydrometric data to simulate hydrologic processes for a river basin. In this study, a 9 arc seconds Digital Elevation Model (DEM) data from the National Water Research Institute (NWRI), Canada was used to determine the drainage area and drainage network for the sub-basins of SSRB listed in Table 3.1. The 30 arc seconds ecoclimap dataset derived from combining landcover maps, climate and Advanced Very High Resolution Radiometer (AVHRR) satellite data (Masson et al. 2003), was chosen as the landuse data and for determining the model parameters of MISBA. The 6-hourly, 40-year re-analysis data of the European Centre for Mid-range Weather Forecasts (ERA-40) data was used as the meteorological dataset to drive MISBA.

The hydrometric data for SSRB, naturalized flow data generated by Alberta Environment (Alberta Environment 1998), were used for the calibration and validation purposes at stations listed in Table 3.1. Alberta Environment's naturalized flow is an estimate of the natural flow at a site by adjusting the historical flow record to remove the effects of regulation, and it also includes estimated discharges to fill missing historical data. The effects of regulation include that of major reservoirs, irrigation withdrawals and return flows for

irrigation districts, municipal withdrawals and return flows at major urban centers. Much of the naturalization were carried out using computerized procedures in which daily flows were adjusted using the U.S. Army Corps of Engineers Streamflow Synthesis and Reservoir Regulation (SSARR) routing model (Alberta Environment 1998).

3.3.3 Calibration and Validation of MISBA

MISBA was calibrated for simulating the streamflow of all sub-basins of SSRB listed in Table 3.1 separately. Calibration was performed using 20 years (1961-1980) of ERA-40 re-analysis data. MISBA's simulated streamflow were compared with the historical naturalized streamflow data of Alberta Environment for those sub-basins of the SSRB. In calibration stage, a simple procedure discussed in Skaugen et al. (2003) was adopted to adjust the monthly ERA-40 precipitation data (Tanzeeba and Gan 2012). First, the ratio between the ERA-40 mean monthly precipitation data and the observed mean monthly precipitation data for the climate normal (1961-1990) for each month were computed, and then, the 6 hourly precipitation data from ERA-40 dataset was adjusted with these monthly adjustment factors.

After calibration, keeping all the calibrated model parameters unchanged, MISBA was validated against 10 years (1981-1990) of data independent of the calibration experience. The goodness-of-fit statistics obtained for the calibration and validation runs of MISBA on these sub-basins of SSRB are listed in Table 3.1.

In general, coefficient of determination (R^2) and Nash-Sutcliffe coefficient of efficiency (E_f) range from 0.63 to 0.89 and 0.46 to 0.82, respectively, in calibration runs, and 0.62 to 0.86 and 0.34 to 0.88, respectively, in validation runs. For most of the sub-basins, the mean absolute error (MAE) values in calibration and validation periods are less than half the standard deviation of the naturalized streamflow data and hence MISBA is considered well calibrated for the sub-basins of SSRB (Singh et al. 2004). The Percent Bias (PB) for calibration and validation stages was within $\pm 15\%$ for most of sub-basins, and was within $\pm 20\%$ for several sub-basins. These statistics demonstrate generally well performance of MISBA in both calibration and validation stages based on historical naturalized data for all the sub-basins listed in Table 3.1 (Moriasi et al. 2007), which establishes the basis for conducting climate change studies based on the simulations of MISBA, assuming the basins' physical conditions remain basically unchanged to the end of the 21st century (Tanzeeba and Gan 2012). The comparison between the naturalized and MISBA simulated streamflow for the calibration and validation periods at some of the selected sub-basins of the SSRB are shown in Figure 3.2a to Figure 3.2f. These plots show that MISBA's simulated flow agrees reasonably well with naturalized flow.

3.4 Research Methodology

To assess the impact of climate change and combined effects of climate change and climate anomalies on the streamflow of sub-basins of SSRB, MISBA has been

driven by three sets of input data: the first is the ERA-40 reanalysis dataset for the climate normal period (1961-1990); the second is the climate normal ERA-40 dataset adjusted for the SRES climate projections of four GCMs for the 2020s, 2050s, and 2080s; and the third dataset represents selected years of the ERA-40 dataset within the climate normal period (1961-1990) affected by El Niño and La Niña episodes, resampled and adjusted for the SRES climate projections of 2050s.

3.4.1 Climate Change Scenario

To account for uncertainties associated with GCMs' projected climate scenarios, climate scenarios based on four GCMs forced by multiple SRES emission scenarios for the SSRB are considered. Among the four GCMs selected are Japan's CCSRNIES which projected the warmest climate, Germany's ECHAM4 which projected the driest climate, UK's HadCM3 which projected the wettest climate, and Canada's CGCM2 projected changes that are in between the other three GCMs' projections for SSRB. The three SRES emission scenarios selected are the fossil fuel intensive, A1FI, and the mid-range emission, A21 and B21 scenarios (IPCC 2000).

After calibration and validation, MISBA was set to simulate streamflow of the sub-basins of SSRB for the 2020s, 2050s and 2080s based on the climate normal (1961-1990) ERA-40 reanalysis data adjusted for the impact of climate change in the three respective era. A two-step process was adopted to downscale climate

projections at GCM to local scale data for MISBA to simulate the streamflow of the sub-basins. First, using the Adaptive Gaussian Window Interpolation method (Agüi and Jiménez 1987), the change fields of mean monthly precipitation and mean monthly temperature at selected grids of the four GCMs for 2020s, 2050s and 2080s were interpolated to the ERA-40 grids selected for the sub-basins of SSRB. In this study the change fields of monthly mean precipitation and temperature are calculated as,

$$\text{Eq. 3.1} \quad T_2 = T_1 + (T_2' - T_1')$$

$$\text{Eq. 3.2} \quad P_2 = P_1 \times \frac{P_2'}{P_1'}$$

where T_1 and P_1 are the baseline observed temperature and precipitation; T_2 and P_2 are the future temperature and precipitation; T_1' and P_1' are the GCM's simulated mean temperature and precipitation for climate normal period (1961-1990); and T_2' and P_2' are the GCM's projected mean temperature and precipitation for future climate scenarios, respectively. Second, these interpolated change fields of GCMs were used to adjust the 1961-1990 climate normal of ERA-40 at grids selected for the sub-basins of SSRB for 2020s, 2050s, and 2080s. The above adjusted ERA-40 data was then used to drive MISBA for each sub-basin to generate the future streamflow under the impact of climate change.

This Delta Change approach has been used in many past climate change studies on water resources (e.g. Lettenmaier and Gan 1990; Wood et al. 2002; Miller et al. 2003; Ryu et al. 2009; Boyer et al. 2010; Kerkhoven and Gan 2010; Tanzeeba and Gan 2012). The Delta change approach incorporates projected changes of GCMs forced by SRES emission scenarios to key climate variables such as temperature and precipitation by a simple calculation. Partly because it avoids tedious computation, and partly it is a stable and robust method (Fowler et al. 2007; Graham et al. 2007), it has been a popular approach in many climate change studies. However, there are disadvantages to this simplistic approach: it assumes a constant bias, accounts for changes to the mean, maxima or minima of climate variables and it ignores possible changes to the variance of these climate variables; and in the case of precipitation, properties such as the temporal sequence of wet days or dry days are assumed to remain unchanged (Fowler et al. 2007; Wilby et al. 2009; Boyer et al. 2010).

3.4.2 Classification of El Niño and La Niña years

El Niño and La Niña years can be classified by year of occurrence, strength, duration, or timing (Hanley et al. 2003). Different authors and agencies have provided methods for identifying the occurrence of an ENSO warm or cold phase based on different ENSO indexes. In this study, we classified El Niño and La Niña years based on the Extended Multivariate ENSO Index (MEI.ext) which uses more than one variable to monitor ENSO. MEI is robust against a variety of changes in

its computation and composition (Wolter and Timlin 2011; Royce et al. 2011). The original MEI is based on six observed variables: Sea Level Pressure (SLP), zonal and meridional components of the surface wind, Sea Surface Temperature (SST), surface air temperature, and total cloudiness fraction of the sky over the tropical Pacific (Wolter 2011a; Wolter and Timlin 1993; 1998; 2008).

Wolter and Timlin (2011) presented a simplified version of MEI based on reconstructed SLP and SST fields. Similar to the original MEI, the extended MEI is computed for each of twelve sliding bi-monthly seasons (Wolter 2011b). The extended MEI values are also computed for four overlapping 4-month seasons, Nov–Feb (NDJF), Feb–May (FMAM), May–Aug (MJJJ), and Aug–Nov (ASON), from Dec1870/Jan1871 through Nov/Dec 2005 (135 full years). The extended MEI values are ranked from the lowest number (e.g., 1), which denote the strongest La Niña case for that four-month season, to the highest number (e.g., 135), which denote the strongest El Niño case. Using pre-defined percentiles, the ranked, seasonal indices are then classified to indicate warm (W), cold (C), or neutral (N) conditions, e.g., the top 25 percentiles (ranks 102 or above) as warm episodes, the bottom 25 percentile (ranks 34 or lower) as cold episodes and in between (ranks 35-101) as neutral episodes. A year is classified to be an El Niño or a La Niña year if out of four overlapping 4-month seasons at least three indicates warm or cold episodes, respectively (please see **Appendix B** for details). It was found that out of 135 years, 21 years (16%) are classified as El Niño year, 21 years are classified as La Niña year (16%) and 93 years (69%) are

classified as neutral year. This classification leads to 5 El Niño years (1969, 1977, 1980, 1983, and 1987) and 4 La Niña years (1971, 1974, 1975, and 1989) in the climate normal (1961-1990) period.

3.4.3 Climate Subjected to Combined Climate Change and El Niño/ La Niña Impact

First, from the ERA-40 dataset, data that correspond to El Niño (e.g., 1969, 1977, 1980, 1983, 1987) and La Niña (1971, 1974, 1975, 1989) years were re-sampled using the standard bootstrap method with replacement to replace the 30-year (1961-1990) climate normal data. The bootstrap resampling process is equivalent to writing each of the El Niño or La Niña years on separate slips of paper and putting them in a box (Wilks 2011). Then, 30 slips of paper are drawn from the box and their data values recorded, but each slip is put back in the box and mixed before the next slip is drawn.

The temperature (T_1) and precipitation (P_1) data of re-sampled ERA-40 dataset were then adjusted (as T_2 and P_2) for SRES climate change scenarios for 2050s. T_2 for each SRES scenario will be estimated as $T_2 = T_1 + \Delta T$, where ΔT or $(T_2' - T_1')$ of Eq. 3.1 is the monthly temperature change from that of the climate normal projected for the SRES scenario, while P_2 will be estimated as $P_2 = P_1 \times \Delta P$, where ΔP or (P_2'/P_1') of Eq. 3.2 is a ratio of the monthly precipitation projected for that SRES scenario to that of the climate normal.

MISBA was then driven by these re-sampled and adjusted ERA-40 data to simulate the streamflow of SSRB that reflect the combined effects of climate change and El Niño and La Niña episodes for each sub-basins listed in Table 3.1.

3.5 Discussions of Results

3.5.1 Impact of Climate Change to Sub-basin Streamflow

3.5.1.1 Mean Annual Average Streamflow

Compared to the climate normal, the average annual temperature of the SSRB is projected to increase by 1.3°C, 3.1°C, and 5.0 °C in 2020s, 2050s, and 2080s, respectively while precipitation is projected to change between -4.25% to 3.5 % by 2020s, 1% to 8.0% by 2050s, and -2.5% to 13.5 % by 2080s, respectively. In response to these projected changes to the primary climatic factors, MISBA simulated the mean annual streamflow at different sub-basins of SSRB for various climate change scenarios projected by four GCMs (CCSRNIES, CGCM2, ECHAM4, and HadCM3) forced by three SRES emissions (A1FI, A21, and B21) of IPCC for 2020s, 2050s, and 2080s, with respect to that of the climate normal (black square shown in Figure 3.3). It was found that even though precipitation is generally projected to increase by up to 13.5% over the 21st century, except for a few cases, most of the scenario runs show a decrease in the mean annual streamflow for most of the sub-basins located in SSRB. The mean annual flow is

projected to decrease because the enhanced evaporation caused by rising temperature offsets the increase in precipitation (Tanzeeba and Gan 2012).

MISBA's simulated percentage changes in the mean annual streamflow from the climate normal (1961-1990) with respect to climate change scenarios are listed in Table 3.2. Figure 3.4 shows boxplots of differences in the mean annual average streamflow simulated by MISBA for A1FI, A21, and B21 scenarios of CCSRNIES, CGCM2, ECHAM4, and HadCM3 GCMs with respect to the climate normal. According to MISBA's simulations, a gradual decreasing trend is observed in the mean annual streamflow over the 21st century. However, projected changes to streamflow from the climate normal are sensitive to the selected CGMs and SRES emission scenarios, and the range of uncertainty associated with climate projections grow as we project into to the distant future.

3.5.1.1.1 Changes in Streamflow by 2010-2039 (2020s)

In 2020s, all of the seven sub-basins of the Red Deer River (from Dickson Dam to Bindloss) considered in this study show a general decrease in the mean annual streamflow (Figure 3.3a to Figure 3.3g). Based on the climate change projected by the A1FI scenario of CCSRNIES, about 6% decrease in the mean annual streamflow will be expected for the Dickson Dam location at the Red Deer River, which increase to about 15% at Bindloss of Red Deer River. Compared to the A1FI climate scenario, the B21 scenario of CCSRNIES leads to a smaller projected decrease in the mean annual streamflow (e.g., 10% at Bindloss). Similar changes

to the Red Deer River at Bindloss were projected for other climate scenarios, e.g., for climate scenarios of CGCM2-A21, ECHAM4-A21, and HadCM3-A1FI, the mean annual streamflow will decrease by about 10%, 24%, and 8%, respectively, while for climate scenarios of CGCM2-B21, ECHAM4-B21, and HadCM3-B21, the mean annual streamflow will decrease by about 8%, 21%, and 2%, respectively. The climate scenarios of ECHAM4-A21 and HadCM3-B21 lead to the maximum and the minimum projected decrease in the mean annual streamflow for all the sub-basins of the Red Deer River, respectively.

On an average, the maximum projected % decrease in the mean annual streamflow are 3%, 5%, 6%, 6%, 8%, 12%, and 12% at Dickson Dam, Red Deer, Nevis, Big Valley, Drumheller, Jenner, and Bindloss, of the Red Deer River, respectively. The mean annual streamflow of Bow River and two of its tributaries (e.g., Elbow River and Highwood River) is also projected to decrease (Figure 3.3h to Figure 3.3j). The maximum projected decrease in the mean annual streamflow for the Bow River at Calgary, Elbow River below Glenmore Dam, and Highwood River at Mouth are about 11.5%, 12%, and 23%, respectively.

Except for a few cases (CGCM2-B21 and HadCM3-B21), most of the climate scenario runs show an overall decrease in streamflow for sub-basins located in the mainstem (from Waldron Corner to Lethbridge) of Oldman River (Figure 3.3k to Figure 3.3o). Maximum projected decrease in the mean annual streamflow for the Oldman River at Waldron Corner, Brocket, Fort Macleod, Monarch and

Lethbridge are about 23%, 14%, 14%, 17%, and 13%, respectively. The A1FI and B21 scenarios of CCSRNIES, A21 and B21 scenarios of ECHAM4, and A1FI scenario of HadCM3 lead to significant projected decrease in streamflow for the upstream tributaries (e.g., Crowsnest River, Castle River, Pincher Creek, and Willow Creek) and southern tributaries (e.g., Belly River, St. Mary River, and Waterton River) of the Oldman River, while other climate scenario runs show either marginal decrease (e.g., CGCM A21 and HadCM3 B21), or, marginal increase (e.g., CGCM2 B21) in streamflow (Figure 3.3p to Figure 3.3ac). The maximum projected decrease in the mean annual streamflow for the Crowsnest River near Lundbreck, Castle River near Beaver Mines, Pincher Creek at Pincher Creek, and Willow Creek near Nolan are about 18%, 16%, 15%, and 20%, respectively. Among the southern tributaries, maximum decrease in the mean annual streamflows projected for the Belly River at Mouth, St. Mary River at St. Mary Dam and Waterton River at Waterton Reservoir are 17%, 16%, and 18%, respectively.

3.5.1.1.2 Changes in Streamflows by 2040-2069 (2050s)

In 2050s, except for the CCSRNIES-B21 and CGCM2-B21, all other climate change scenarios lead to significant decrease in the projected streamflow for all sub-basins of the Red Deer River. Going downstream from the Dickson Dam, the projected decrease in streamflow for the Red Deer River gets worse, e.g., the maximum projected % decrease in the mean annual streamflow are 9%, 10%,

12%, 12%, 15%, 26%, and 27% for the Red Deer River at Dickson Dam, Red Deer, Nevis, Big Valley, Drumheller, Jenner, and at Bindloss, respectively. Similar to the Red Deer River, except for the climate scenarios of CCSRNIES-B21 and CGCM2-B21, all other climate change scenarios also lead to a projected decrease in the streamflow of the Bow River and its tributaries. The maximum % decrease in the mean annual streamflow is projected for the Highwood River at Mouth (31%) while for the Bow River at Calgary and Elbow River below Glenmore Dam, the mean annual streamflow is projected to decrease up to 15% and 12%, respectively.

The maximum projected % decrease in the mean annual streamflow for the Oldman river at Waldron Corner, Bocket, Fort Macleod, Monarth and Lethbridge are about 22%, 16%, 15%, 20%, and 10%, respectively. Similar to the Red Deer River and Bow River, the CCSRNIES-B21 climate scenario leads to a projected increase in streamflow for the mainstem, upper tributaries, and southern tributaries of the Oldman River. The maximum projected decrease in the mean annual streamflow for the Crowsnest River near Lundbreck, Castle River near Beaver Mines, Pincher Creek at Pincher Creek, and Willow Creek near Nolan are about 19%, 15%, 13%, and 20%, respectively. Among the southern tributaries, the maximum projected decrease in the mean annual streamflow for the Belly River at Mouth, St. Mary River at St. Mary Dam, and Waterton River at Waterton Reservoir are 17%, 19%, and 17%, respectively.

3.5.1.1.3 Changes in Streamflows by 2070-2099 (2080s)

Given the uncertainty associated with climate projections grow as we project to the distant future, it seems that the CCSRNIES-A1FI and CCSRNIES-B21 scenarios for the 2080s lead to significant projected increase in streamflow in all the sub-basins of Red Deer River, about 24% and 16%, respectively; but CGCM2-A21 and HadCM3-B21 lead to marginal projected increase (on average, about 5% and 2%, respectively) in the streamflow of Red Deer River from Dickson Dam to Drumheller. In contrast, other climate scenarios lead to a significant decrease in the projected streamflow for the Red Deer River. The maximum projected % decrease in the mean annual streamflow for all climate scenarios considered are 9%, 13%, 17%, 17%, 22%, 42%, and 43% for the Red Deer River at Dickson Dam, Red Deer, Nevis, Big Valley, Drumheller, Jenner, and Bindloss, respectively.

The A1FI and B21 emissions of CCSRNIES also lead to a projected increase in the streamflow of Bow River and its tributaries while other climate scenarios lead to projected decrease in streamflow. The maximum projected % decrease in the mean annual streamflow for the Bow River at Calgary, Elbow River below Glenmore Dam, and Highwood River at Mouth are about 21%, 22%, and 44%, respectively. Similar to the Red Deer River and Bow River, an increase in the streamflow is projected for the CCSRNIES-A1FI (about 29% on the average) and CCSRNIES-B21 (about 13% on the average) scenarios for the mainstem and the tributaries of the Oldman River, while all other scenarios generally lead to a

projected decrease in streamflows for the Oldman River. The maximum projected % decrease in the mean annual streamflow for the Oldman River at Waldron Corner, Brocket, Fort Macleod, Monarch and Lethbridge are about 32%, 23%, 24%, 33%, and 19%, respectively. Among upstream tributaries of the Oldman River, Crowsnest River near Lundbreck, Castle River near Beaver Mines, Pincher Creek at Pincher Creek, and Willow Creek near Nolan, the mean annual streamflow are project up to decrease by about 23%, 24%, 23%, and 39%, respectively. Among the southern tributaries, the maximum projected decrease in the mean annual streamflow for the Belly River at Mouth, St. Mary River at St. Mary Dam, and Waterton River at Waterton Reservoir are about 28%, 31%, and 26%, respectively.

3.5.1.2 Mean Seasonal Streamflow

Possible changes to seasonal streamflow are important for climate change impact studies. For the SSRB, the mean winter (December-February), spring (March-May), summer (Jun-August), and autumn (September-November) streamflow constitutes about 2.3%, 37.4%, 50.8%, and 9.6%, of the total annual runoff, respectively. In terms of seasonal variation of streamflow, most of the climate scenario runs project an increase in winter and spring streamflow at the expense of summer and autumn streamflow. With reference to mean seasonal streamflow simulated for sub-basins of SSRB for the climate normal (1961-1990), Figure 3.5 and Table 3.3 show average changes to seasonal streamflow (winter,

spring, summer and autumn) simulated by MISBA for climate change scenarios projected by four GCMs (CCSRNIES, CGCM2, ECHAM4, HadCM3) forced by three SRES emissions (A1FI, A21 and B21) of IPCC for the 2020s, 2050s, and 2080s.

The projected % changes in seasonal streamflow, averaged over all climate change scenarios considered in this study, have been expressed as a percentage of the mean annual average streamflow. The winter runoff is projected to increase gradually over the 21st century for all of the sub-basins of the SSRB (Figure 3.5a). On the average, in 2020s, a minor (about 2% of the mean annual average streamflow) increase or no change to the mean winter streamflow are projected for most of the sub-basins of SSRB. However, by 2050s and 2080s, the mean winter streamflow are projected to increase up to 8% and 19% of the mean annual streamflow for the sub-basins of SSRB, respectively.

Other than some sub-basins, e.g., Highwood River at Mouth, Oldman River (near Waldron Corner, Brocket, and Monarch), Crowsnest River near Lundbreck, Pincher Creek at Pincher Creek, Willow Creek above Chain Lakes and near Nolan, the spring streamflow is projected to increase significantly over the 21st century (Figure 3.5b). Overall, the mean spring streamflow is predicted to increase by 2%, 9%, and 9% of the mean annual streamflow for the Red Deer River sub-basins in 2020s, 2050s, and 2080s, respectively, while that of the Bow River at Calgary is projected to increase by 6%, 16%, and 23% of its mean annual streamflow in 2020s, 2050s, and 2080s, respectively. Even though a decrease in

spring streamflow is projected for the Oldman River from Waldron Corner to Brocket, at further downstream (e.g., Oldman River at Lethbridge), the mean spring streamflow is projected to increase up to 9%, 22%, and 29% of its mean annual streamflow by 2020s, 2050s, and 2080s, respectively. Among the upstream and southern tributaries of Oldman River, the spring streamflow is projected to increase by about 69% for the Castle River near Beaver Mines, about 38% for the Belly River at Mountain View, about 42% for the Willow Creek above Chain Lake, and about 8% for the Waterton River at Waterton Reservoir by 2080s. On a whole, by 2020s, 2050s, and 2080s, the mean spring streamflow is projected to increase up to 4%, 9%, and 10% of the mean annual streamflow for the sub-basins of SSRB, respectively.

In contrast, because the enhanced evaporation attributed to rising temperature offsets the increase in precipitation (Tanzeeba and Gan 2012), the summer streamflow is projected to decrease significantly for all sub-basins of SSRB over the 21st century (Figure 3.5c). The projected decrease in the mean summer streamflow for the Red Deer River at Bindloss are about 37%, 44%, and 47% of the mean annual streamflow in 2020s, 2050s, and 2080s, respectively. On a whole, the mean summer streamflow of Bow River and its tributaries (Elbow River and Highwood River) are projected to decrease by 25%, 26% and 28% in 2020s, 2050s, and 2080s, respectively. The mean summer streamflows of Oldman River and its tributaries are projected to decrease by 31% and 30% of their mean annual streamflow, by 34% and 35%, and by 34% and 36%, in 2020s,

2050s, and 2080s, respectively. On a whole, by 2020s, 2050s, and 2080s, the mean summer average streamflow are projected to decrease by 29%, 31%, and 31% of the mean annual streamflow for the sub-basins of the SSRB, respectively.

The autumn runoff is projected to decrease for majority of sub-basins of SSRB in 2020s, 2050s and 2080s, but to increase for Red Deer River at Dickson Dam and at Red Deer, Bow River at Calgary, Oldman River at Brouck, Castle River near Beaver Mines, Corwsnest River near Lundbreck, Pincher Creek at Pincher Creek, Belly River from International Boundary to Waterton Confluence, and Waterton River in 2080s (Figure 3.5d). The mean autumn streamflow of Red Deer River at Bindloss is projected to decrease by 9%, 22%, and 25% of the mean annual streamflow in 2020s, 2050s, and 2080s, respectively. The mean autumn streamflow for Bow River at Calgary is projected to decrease by 2% and 7% in 2020s and 2050s, respectively, but to increase by 4% in 2080s. However, the mean autumn streamflow for the tributaries of Bow River (Elbow River below Glenmore Dam and Highwood River at Mouth) are projected to decrease by 2.5%, 9% and 7% in 2020s, 2050s, and 2080s, respectively. The mean autumn average streamflow of Oldman River at Lethbridge is expected to decrease by 7%, 21%, and 19% in 2020s, 2050s, and 2080s, respectively. Comparatively less decrease, or even increase in mean autumn streamflow in 2080s than that of in 2020s and in 2050s may be attributed by the fact that on average, mean autumn precipitation for SSRB is expected to increase more in 2080s (-0.3% to 10.24%) than in 2020s (-1.34% to 2.79%) and in 2050s (-7.69% to 3.77%). On a whole, the

mean autumn streamflow of tributaries of the Oldman River are projected to decrease by 2% and 6% of their mean annual streamflow in 2020s and 2050s, respectively, but to increase by 4% in 2080s.

3.5.1.3 Sensitivity of Changes in Streamflow

Since compare to climate normal most of the climate change scenario runs show a decrease in the mean annual streamflow for most of the sub-basins located in SSRB, an analysis has been done to assess the amount of decrease in streamflow per °C rise of temperature in the 21st century, and are listed in Table 3.4. Even though a few scenarios projected increase in streamflows for some of the sub-basins, those are not included in this analysis.

On an average, the % decrease in the mean annual streamflow per °C rise in temperature are expected to 3.68%, 4.5%, 4.34%, 4.34%, 5.77%, 7.6%, and 7.87% at Dickson Dam, Red Deer, Nevis, Big Valley, Drumheller, Jenner, and Bindloss, of the Red Deer River, respectively. In Bow River sub-basin, Bow River at Calgary, Elbow River below Glenmore Dam, and Highwood River at Mouth shows about 4.34%, 3.25%, and 8.26% decrease in streamflow per °C rise of temperature in 21st century, respectively. Projected decrease in the mean annual streamflow per °C rise in temperature for the Oldman River at Waldron Corner, Brocket, Fort Macleod, Monarch and Lethbridge are about 8.71%, 5.47%, 4.92%, 5.72%, and 3.91%, respectively. Among the upstream tributaries of Oldman River, the Crowsnest River near Lundbreck, Castle River near Beaver

Mines, Pincher Creek at Pincher Creek, and Willow Creek near Nolan project about 6.33%, 5.62%, 4.52%, and 6.84% decrease in streamflow per C rise in temperature, respectively. Among the southern tributaries, decrease in the mean annual streamflows per °C rise in temperature projected for the Belly River at Mouth, St. Mary River at St. Mary Dam and Waterton River at Waterton Reservoir are 5.74%, 5.78%, and 6.04%, respectively.

3.5.2 Combined Impact of Climate Change and Climate Anomalies to Streamflow

3.5.2.1 Mean Annual Streamflow

From the re-sampled, selected years of ERA-40 meteorological data of SSRB affected by ENSO episodes, it seems that in El Niño years, on the average precipitation will be less by about 5% but temperature higher by about 0.3°C while in La Niña years, precipitation will be more by about 9% but temperature lower by about 0.3°C. Based on MISBA's simulated streamflow for the sub-basins of SSRB, driven by these re-sampled ERA-40 dataset, the mean annual streamflow for all of sub-basins will decrease in years affected by El Niño, but the mean annual streamflow will increase for most sub-basins in years affected by La Niña. When MISBA was forced by these re-sampled ERA-40 dataset that reflect the influence of El Niño (La Niña) episodes and adjusted for climate projection of several GCMs forced by SRES emission scenarios of 2050s for SSRB, MISBA projects a further decrease (increase) in the mean annual streamflows of

SSRB than if ERA-40 dataset was only adjusted for climate projections of GCMs. Percent changes in the mean annual streamflows of the sub-basins of SSRB simulated by MISBA for the SRES climate scenarios of 2050s and climate scenarios combined with ENSO ('2050s+El Niño' and '2050s+La Niña') are shown in Table 3.2 and Figure 3.6.

3.5.2.1.1 2050s SRES Climate Scenarios Combined with El Niño Episodes

When compared to MISBA's simulated streamflow for the SRES climate scenarios of 2050s, the combined '2050s+El Niño' cases project further decrease in streamflow of Red Deer River, e.g., the maximum decrease in the mean annual streamflow of Red Deer River at Dickson Dam (Figure 3.6a), Big Valley (Figure 3.6d), near Jenner (Figure 3.6f), and at Bindloss (Figure 3.6g) would be about 9%, 12%, 26%, and 27%, respectively for climate scenarios of 2050s, to about 15%, 19%, 30%, and 33%, respectively for climate scenarios of 2050s combined with El Niño episodes. Similar results are also found for the Bow River and its tributaries. The mean annual streamflow of Bow River at Calgary (Figure 3.6i), Elbow River below Glenmore Dam (Figure 3.6h), and Highwood River at Mouth (Figure 3.6j), which are projected to decrease up to 15%, 12%, and 31%, respectively under the SRES climate scenarios of 2050s, are projected to decrease up to 24%, 26%, and 51%, respectively under the SRES scenarios of 2050s combined with El Niño episodes.

The maximum % decrease in the mean annual streamflow for the Oldman River at Waldron Corner (Figure 3.6k), Oldman River at Brocket (Figure 3.6l), Oldman River at Fort Macleod (Figure 3.6m), Oldman River at Monarch (Figure 3.6n), and Oldman River at Lethbridge (Figure 3.6o) are projected to further decrease from about 22%, 16%, 15%, 20%, and 10%, respectively, under the SRES climate scenarios of 2050s, to about 37%, 30%, 28%, 43%, and 26%, respectively, under the SRES scenarios of 2050s combined with El Niño episodes. As expected, the upstream and southern tributaries of Oldman River show similar further decrease in streamflow under the combined effect of climate change and El Niño: the maximum decrease in the mean annual streamflow of Crowsnest River near Lundbreck (Figure 3.6p), Castle River near Beaver Mines (Figure 3.6q), Pincher Creek at Pincher Creek (Figure 3.6r), Belly River at Mouth (Figure 3.6w), St. Mary River at St. Mary Dam (Figure 3.6y), Willow Creek near Nolan (Figure 3.6ab), and Waterton River at Waterton Reservoir (Figure 3.6ac) are projected to about 19%, 15%, 13%, 17%, 19%, 20%, and 17%, respectively, under the SRES scenarios of 2050s, to become 32%, 29%, 26%, 28%, 25%, 60%, and 29%, respectively, under the SRES scenarios of 2050s combined with El Niño episodes.

Overall drying effect on SSRB streamflows in El Niño affected years can be explained from composites of 500-hPa geopotential height anomalies associated with El Niño. In an El Niño event there is a deeper than normal Aleutian low, an amplification, and eastward displacement of the western Canadian ridge. This upper-atmospheric flow pattern is likely associated with a split in the jet stream

over North America: a weaker branch diverted northward and a lower subtropical branch shifted southward. The southern Canadian region as the SSRB lies in between the two jets and receive lower than normal precipitation resulting overall drying impacts (Shabbar et al. 1996; Shabbar and Khandekar 1996; Gan et al. 2007).

3.5.2.1.2 2050s SRES Climate Scenarios Combined with La Niña Episodes

Under the SRES climate scenarios of 2050s, the maximum decrease in the mean annual streamflow of Red Deer River near Jenner and at Bindloss simulated by MISBA were about 26% and 27%, respectively. However, under the SRES scenarios of 2050s combined with La Niña episodes, MISBA projected a more modest decrease in the streamflow of these two locations of Red Deer River, e.g., 13% and 19%, respectively. For other sub-basins of the Red Deer River, e.g., at Red Deer, near Nevis, and at Drumheller, a more modest decrease, or at Dickson Dam and Big Valley, no significant changes, are projected for the SRES climate scenarios of 2050s combined with La Niña episodes.

Similarly, for the Bow River at Calgary, Elbow River below Glenmore Dam, and Highwood River at Mouth, the mean annual streamflow which are projected to decrease up to 15%, 12%, and 31%, respectively under the SRES climate scenarios of 2050s, are projected to decrease up to 12%, 6%, and 27%, respectively under the SRES climate scenario of 2050s combined with La Niña episodes.

For the Oldman River and its tributaries, with respect to the climate normal, the maximum % changes in the mean annual streamflow of the Oldman River at Brocket, Oldman River at Fort Macleod, Oldman River at Monarch, and Oldman River at Lethbridge, are projected to change by about -16%, -15%, -20%, and -10%, respectively, under the SRES climate scenarios of 2050s. The corresponding changes to the mean annual streamflow of the Oldman River at the above locations are projected to about -3%, -3%, -11%, and 6%, respectively, under the SRES climate scenario of 2050s combined with La Niña episodes. For the upstream and southern tributaries of Oldman River, the corresponding % changes in the mean annual streamflow of Crowsnest River near Lundbreck, Castle River near Beaver Mines, Pincher Creek at Pincher Creek, Belly River at Mouth, St. Mary River at St. Mary Dam, Willow Creek near Nolan, and Waterton River at Waterton Reservoir, are projected to about -19%, -15%, -13%, -17%, -19%, -20%, and -17%, respectively, under the SRES climate scenarios of 2050s; and are projected to about -4%, -7%, -3%, -7%, 4%, -3%, and -8%, respectively, under the SRES climate scenarios combined with La Niña episodes.

In general wetting effect of La Niña events on SSRB can be explained from composites of 500-hPa geopotential height anomalies associated with La Niña. In a La Niña event there is a weaker than normal Aleutian low, an erosion, and westward displacement of the western Canadian ridge. The upper-atmospheric flow associated with this circulation pattern includes stronger westerlies moving across the eastern Pacific and into southern Canada. As a result, the moist air

originating from the Pacific result in positive precipitation anomalies over southern Canada (Shabbar et al. 1996; Shabbar and Khandekar 1996; Gan et al. 2007).

3.5.2.2 Mean Seasonal Streamflow

With respect to the climate normal (1961-1990), Figure 3.7 and Table 3.3 show MISBA simulated seasonal changes (as a % of the mean annual streamflow) for winter (December-February), spring (March-May), summer (Jun-August), and autumn (September-November) for the sub-basins of SSRB under the SRES climate scenarios of 2050s combined with El Niño and La Niña episodes.

3.5.2.2.1 2050s SRES Climate Scenarios Combined with El Niño Episodes

Winter streamflow is projected to increase under most SRES climate scenarios of 2050s, and a further increase in the winter streamflow is projected under SRES climate scenarios of 2050s combined with El Niño episodes. In 2050s, the average projected % increase in the mean winter streamflow are about 2%, 3%, and 4% of the mean annual streamflow for the Red Deer, Bow, and Oldman rivers, respectively. The corresponding increase in the winter streamflow under SRES climate scenarios of 2050s combined with El Niño episodes are projected to about 3%, 4%, and 7%, respectively (Figure 3.7a).

Similarly, most spring streamflow is projected to increase under the impact of climate change by 2050s, but it is projected to decrease under the combined

impact of climate change by 2050s and El Niño episodes. Under the SRES climate scenarios of 2050s, the percent changes of the mean spring streamflow of Red Deer River at Bindloss, Elbow River below Glenmore Dam, Bow River at Calgary, Highwood River at Mouth, Oldman River at Lethbridge, Crowsnest River near Lundbreck, Castle River near Beaver Mines, Pincher Creek at Pincher Creek, Belly River at Mouth, St. Mary River at St. Mary Dam, Willow Creek Near Nolan, and Waterton River at Waterton Reservoir from the 1961-1990 climate normal are projected to about 4%, 7%, 16%, -22%, 22%, -15%, 54%, -3%, 1%, 0%, -9%, and 8%, respectively. Under the SRES climate scenarios of 2050s combined with El Niño episodes, the projected changes for the above locations are about -5%, 6%, -1%, -63%, -5%, -34%, 59%, -29%, -26%, -55%, -94%, and -11%, respectively (Figure 3.7b).

Except for the Red Deer River, further decrease in the summer streamflow is projected under the SRES climate scenarios of 2050s combined with El Niño episodes. Under the SRES scenarios of 2050s, the average % decrease in the mean summer streamflow are projected to about 25%, 26%, and 34% of the mean annual streamflow for the Red Deer, Bow, and Oldman River basin, respectively, while under the SRES scenarios of 2050s combined with El Niño episodes, the projected changes are about 16%, 47%, and 66%, respectively (Figure 3.7c).

For the Red Deer River, the Bow River and the Oldman River, either a further decrease or no further change to the autumn streamflow are projected under the combined impact of SRES climate scenarios of 2050s with El Niño episodes than those only under the impact of SRES climate scenarios of 2050s, e.g., 17%, 7% and 7%, respectively for the combined climate change and El Niño cases as against 9%, 6% and 7%, respectively for the climate change cases (Figure 3.7d).

3.5.2.2.2 2050s Scenario Combined with La Niña Episodes

As shown in Figure 3.7a, under the combined impact of SRES climate scenarios of 2050s with La Niña episodes, the mean winter streamflow is projected to increase more than that of SRES scenarios of 2050s for some sub-basins (e.g., Elbow River below Glenmore Dam, Oldman River near Borcket, Oldman River near Monarch, Crowsnest River near Lundbreck, Castle River near Beaver Mines, Pincher Creek at Pincher Creek, Belly River at Waterton Confluence, Belly River at Mouth, Willow Creek from Chian Lakes to Nolan, and Waterton River at Waterton Reservoir), or minor or no difference for other sub-basins (e.g., Red Deer River at Dickson Dam, Red Deer River near Jenner, and Highwood River at Mouth). Under the combined impact of SRES scenarios of 2050s with La Niña episodes, the spring streamflow is mostly projected to increase more significantly than under the SRES scenarios of 2050s alone. For example, when combined climate change and La Niña impact are considered, the average projected % increase in the mean spring streamflow for the Red Deer, Bow, and

Oldman rivers for 2050s are 45%, 20%, and 56%, respectively, as against about 9%, 1%, and 10%, respectively, when only climate change impact is considered (Figure 3.7b).

On the other hand, in 2050s, except for Red Deer River, the summer streamflow is projected to decrease less under the potential combined impact of climate change and La Niña, than under the potential impact of climate change only. For example, the projected changes of the mean summer streamflow for Red Deer, Bow, and Oldman River basin for the combined impact cases by 2050s are -47%, -22%, and -27%, respectively, compared to about -25%, -26%, and -34%, respectively, for the climate change impact cases (Figure 3.7c).

Under the combined climate change and La Niña impact cases, the autumn streamflow of the Red Deer River is projected to experience larger decrease than the climate change impact cases, e.g., the average change in the mean autumn streamflow of Red Deer River at Dickson Dam, Red Deer, near Nevis, Big Valley, Drumheller, near Jenner, and Bindloss are projected to decrease by about 15%, 17%, 16%, 16%, 26%, 18%, and 23%, respectively, in 2050s under the combined impact of climate change and La Niña as against about -2%, 4%, 6%, 6%, 9%, 17%, and 22% in 2050s under the impact of climate change only. In contrast, for Bow and Oldman rivers, the projected decrease in the autumn streamflow for the combined impact cases by 2050s is less (5% and 4%, respectively) than for the climate change impact cases (6% and 7%, respectively).

3.6 Summary and Conclusions

In this study, potential impacts of climate change on the future streamflow of SSRB are simulated by MISBA on the basis of climate change scenarios projected by four GCMs forced by three SRES emissions of IPCC (2001) for 2020s, 2050s, and 2080s of the 21st century. Furthermore, the combined impacts of climate change and climate anomalies (ENSO) for the 2050s are simulated by driving MISBA with a meteorological dataset re-sampled from selected years of the ERA-40 dataset within the climate normal period (1961-1990) affected by El Niño and La Niña episodes.

In general, sub-basins of Red Deer, Bow, and Oldman rivers are projected to decrease in the mean annual streamflow over the 21st century under the climate projections of 4 GCMs and 3 SRES emission scenarios of IPCC (2001) considered in this study. However, under the climate projection of CCSRNIES-B21 and CGCM2-B21, some sub-basins are projected to experience marginal increase in streamflow by 2050s; and by 2080s, most sub-basins are projected to experience significant increase in streamflow under the climate projections of CCSRNIES-A1FI and CCSRNIES-B21. The maximum projected % decrease in the mean annual streamflow of Red Deer River at Bindloss, Bow River at Calgary, and Oldman River at Lethbridge are 12%, 11.5%, and 13%, in 2020s; 27%, 15%, and 10%, in 2050s; and 43% , 21%, and 19%, in 2080s, respectively. Similar decreasing trends in streamflow are also projected for the sub-basins of the tributaries of Bow and

Oldman River. Even though the future precipitation is projected to increase, the sub-basins of SSRB are projected to become drier in the 21st century because enhanced evaporation caused by rising temperature could offset the increase in precipitation (Tanzeeba and Gan 2012). In addition, under a warmer climate, an earlier onset of the spring snowmelt and an increase in the rainfall over snowfall ratio for the SSRB would result in increased streamflow in winter and spring, at the expense of decreased streamflow in the summer and autumn. On average, at the end of 21st century, the mean winter and spring streamflow of sub-basins of SSRB are projected to increase by about 8% and 10% of their mean annual streamflow, respectively. In contrast, the mean summer and autumn streamflow of the sub-basins of the SSRB are projected to decrease by 31% and 7% of their mean annual streamflow, respectively. Since winter, spring, summer, and autumn streamflow of SSRB constitute about 2.3%, 37.4%, 50.8%, and 9.6% of the total annual runoff, respectively, a significant decrease in summer and autumn streamflow can be expected over the increase in winter and spring streamflow would result in an overall decrease in streamflow in the 21st century. On average, the streamflow of SSRB is projected to decrease about 6% per °C rise of temperature in the 21st century.

While considering the potential combined impact of climate change and climate anomalies, a further decrease in streamflow by 2050s is projected if the climate anomaly considered is El Niño since El Niño tends to associate with drier climate in Alberta (Gan et al., 2007). In contrast, if the climate anomaly considered is La

Niña, then considering the combined impact of climate change and La Niña would lead to a higher projected streamflow in SSRB by 2050s, than only if the impact of climate change is considered. With reference to the 1961-1990 climate normal, the maximum % decrease in the mean annual streamflow of Red Deer River at Bindloss, Bow River at Calgary, and Oldman River at Lethbridge under the potential combined impact of climate change and El Niño are projected as 33%, 24% and 26%, respectively, as compared to 27%, 15%, and 10%, respectively, by 2050s, if only climate change impact is considered. On the other hand, if the potential combined impact of climate change and La Niña is considered, the corresponding projected % decrease in the mean annual streamflow by 2050s will be 19%, 12%, and 6%, respectively.

For seasonal streamflow, most of the climate scenarios of 2050s considered lead to a projected increase in winter streamflow, an increase in spring streamflow, a significant decrease in summer streamflow, and a decrease in the autumn streamflow. These seasonal changes are projected to be more severe in winter, summer and autumn; and modest in spring when the combined impact of climate change and El Niño are considered. In contrast, if the climate anomaly considered is La Niña, the projected change to the winter streamflow by 2050s is either severe or similar to only if climate change impact is considered.

Under the SRES climate scenarios of 2050s, the spring streamflow of most sub-basins are projected to increase while the summer streamflow is projected to

decrease significantly because of the earlier onset of spring snowmelt. However, under the potential combined impact of climate change and La Niña, the projected increase in spring streamflow by 2050s is generally more severe and decrease in the summer streamflow by 2050s is generally more modest than if La Niña is not considered. For the autumn streamflow, if besides SRES scenarios of 2050s, La Niña is also considered, then the projected decrease in the mean streamflow is more for the Red Deer River but less for Bow and Oldman River than if La Niña is not considered.

3.7 References

- Abbott, M.B., Bathurst, J.C., Cunge, J.A., O'Connell, P.E., Rasmussen, J. (1986). "An introduction to the European Hydrological System—Systeme Hydrologique Europeen 'SHE'. 2: Structure of a physically based, distributed modelling system." *J. Hydrol.* 87, 61–77.
- Agüí, J.C., and Jiménez, J. (1987). "On the performance of particle tracking." *J. Fluid. Mech.*, 185, 447-468.
- Alberta Environment (1998). "South Saskatchewan River Basin, Historical Weekly Natural Flows, 1912 to 1995", *Main Report*.
- Alberta Environment (2010). "South Saskatchewan Regional Plan: Water Quantity and Quality Modeling Results." *Alberta Environment*.
- Arnold, J.G., Srinivasan, R., Muttiah, R.S., Williams, J.R. (1998). "Large area hydrologic modelling and assessment. Part I. Model development." *Journal of American Water Resources Association*, 34(1), 73–89.
- Ashmore, P. and Church, M. (2001) "The Impact of Climate Change on Rivers and River Processes in Canada." *Geological Survey of Canada*, Bulletin 555.
- Beven, K., Lamb, R., Quinn, P., Romanowicz, R., Freer, J. (1995). "TOPMODEL." In: Singh, V.P., (Ed.), *Computer Models of Watershed Hydrology*. Water Resources Publications, Highlands Ranch, CO, (Chapter 18), 627–668.

- Biftu, G.F., and Gan, T.Y. (2001). "Semi-distributed, physically based, hydrologic modelling of the Paddle River Basin, Alberta, using remotely sensed data." *Journal of Hydrology*, 244, 137-156.
- Boyer, C., Chaumont, D., Chartier, I., and Roy, A.G. (2010). "Impact of climate change on the hydrology of St. Lawrence tributaries." *J. Hydrol.*, 384 (1-2), 65–83.
- Cunge, J. A. (1969). "On the Subject of a Flood Propagation Method (Muskingum Method)." *Journal of Hydraulic Research*, 7 (2), 205-230.
- Deardorff, J. W. (1978). "Prediction of Ground Surface Temperature and Moisture, With Inclusion of a Layer of Vegetation." *Journal of Geophysical Research*, 83 (C4), 1889-1903.
- Elsanabary, M. (2012). "Teleconnection, Modeling, Climate Annomalies Impact and Forecasting of Rainfall and Streamflow of the Upper Blue Nile River Basin." *PhD Thesis, University of Alberta*.
- Environment Canada (2007). "Municipal Water Use Report, 2004 Statistics." *Environment Canada*.
- Fowler, H. J., Blenkinsop, S., and Tebaldi, C. (2007). "Linking climate change modelling to impacts studies: Recent advances in downscaling techniques for hydrological modelling." *Int. J. Climatol.*, 27(12), 1547-1578.

- Gan, T. Y., Gobena, A. K., and Wang, Q. (2007). "Precipitation of southwestern Canada - Wavelet, Scaling, Multifractal Analysis, and Teleconnection to Climate Anomalies." *J. of Geophysical Research*, 112, D10110.
- Gershunov, A. and Barnett, T. P. (1998). "Interdecadal Modulation of ENSO Teleconnections." *Bulletin of the American Meteorological Society*, 79(12), 2715-2725.
- Gobena, A. K., and Gan, T. Y. (2006). "Low-frequency variability in southwestern Canadian streamflow: links to large-scale climate anomalies." *Int. J. Climatol.*, 26 (13), 1843-1869.
- Gosain, A.K., Mani, A., Dwivedi, C. (2009). "Hydrological modelling literature review", *Report No.1. Indo-Norwegian Institutional Cooperation Program 2009-2011*.
- Graham, L.P., Hagemann, S., Jaun, S., and Beniston, M. (2007). "On interpreting hydrological change from regional climate models." *Climatic Change*, 81, 97–122.
- Habets, F, J Nolihan, C Golaz, J. P. Goutorbe, P. Lacarrère, and E Leblois (1999). "The ISBA surface scheme in a macroscale hydrological model applied to the Hapex–Mobilhy area. Part 1. Model and database." *Journal of Hydrology*, 75-96.

- Hanley, D.E., Bourassa, M.A, O'brien, J.J., Smith, S.R. and Spade, E.R. (2003). "A Quantitative Evaluation of ENSO Indices, Notes and Correspondence." *J.Climate*, 16, 1249-1258.
- IPCC (2000). "Summary for Policymakers: Emissions Scenarios, A Special Report of Working Group III of the Intergovernmental Panel on Climate Change." *Cambridge University Press, UK*.
- IPCC (2001) "Climate Change 2001: The Scientific Basis. Contribution of Working Group I to the Third Assessment Report of the Intergovernmental Panel on Climate Change." *Cambridge University Press, Cambridge, United Kingdom and New York, NY, USA*.
- IPCC (2007). "Climate Change 2007, Intergovernmental Panel on Climate Change Fourth Assessment Report."
- Islam, Z. and Gan, T. (2012). "Effects of Climate Change on the Surface Water Management of South Saskatchewan River Basin." *J. Water Resour. Plann. Manage.* doi: 10.1061/(ASCE)WR.1943-5452.0000326 .
- Ivanov, V.Y., Vivoni, E. R., Bras, R. L., and Entekhabi, D. (2004). "Preserving high-resolution surface and rainfall data in operational-scale basin hydrology: a fully distributed approach." *Journal of Hydrology*, 298(1-4), 80-111.
- Kerkhoven, E. and Gan, T.Y. (2006). "A modified ISBA surface scheme for modeling the hydrology of Athabasca River Basin with GCM-scale data." *Advanced in Water Resour.*, 29(6), 808-826.

Kerkhoven, E. and Gan, T.Y. (2010). "Differences and sensitivities in potential hydrologic impact of climate change to regional-scale Athabasca and Fraser River basins of the leeward and windward sides of the Canadian Rocky Mountains respectively." *Climatic Change*, 106(4), 583-607.

Kerkhoven, E. and Gan, T.Y. (2011). "Differences and sensitivities in potential hydrologic impact of climate change to regional-scale Athabasca and Fraser River basins of the leeward and windward sides of the Canadian Rocky Mountains respectively." *Earth and Environmental Science*. 106 (4), 583-607.

Kite, G.W. (1995). "The SLURP Model. In: Singh, V.P., (Ed.), *Computer Models of Watershed Hydrology*." *Water Resources Publications, Highlands Ranch, CO, (Chapter 15); pp. 521-562*.

Kouwen, N. (2000). "WATFLOOD/SPL9: Hydrological Model and Flood Forecasting System." *Department of Civil Engineering, University of Waterloo, Waterloo, ON*.

Lac, S. (2004). "A Climate Change Adaptation Study for the South Saskatchewan River Basin." *SSHRC MCRI-Institutional Adaptation to Climate Change project, Canadian Plains Research Centre, University of Regina. Regina, Saskatchewan*.

- Lettenmaier, D.P. and Gan, T.Y. (1990). "Hydrologic sensitivity of the Sacramento-San Joaquin River Basin, California, to global warming." *Water Resour. Res.*, 26(1), 69–86.
- Martz, L., J. Bruneau, and J.T. Rolfe. (2007). "Climate and Water". *SSRB Final Technical Report*.
- Masson, V., Champeaux, J.-L., Chauvin, F., Meriguet, C. and Lacaze, R. (2003) "A Global Database of Land Surface Parameters at 1 km Resolution in Meteorological and Climate Models." *Journal of Climate*, 16, 1261-1282.
- Miller, N.L., Bashford, K.E., and Strem, E. (2003). "Potential impacts of climate change on California hydrology." *J. American Water Resour. Assoc.*, 39(4), 771–784.
- Moriasi, D. N. , Arnold, J. G. , Van Liew, M. W. , Bingner, R. L. , Harmel, R. D. , and Veith, T. L. (2007). "Model evaluation guidelines for systematic quantification of accuracy in watershed simulations." *Transactions of American Society of Agricultural and Biological Engineers*. 50(3): 885–900.
- Nolihan, J, and Mahfouf, J. (1996). "ISBA land surface parameterization scheme." *Global and Planetary Change*, 13, 145-159.
- Nolihan, J, and Planton, S. (1989). "A simple parameterization of land surface processes for meteorological models." *Monthly Weather Review*, 17.

- Refsgaard, J.C. (1996). "Terminology, modelling protocol and classification of hydrologic model codes." *Distributed Hydrologic Modelling, edited by Michael B. Abbott and Jens C. Refsgaard*, 41-54.
- Royce, F.S., Fraisse, C.W., and Baigorria, G.A. (2011). "ENSO classification indices and summer crop yields in the Southeastern USA." *Agricultural and Forest Meteorology*, 151, 817–826.
- Ryu, J. H., Palmer, R. N., Wiley, M. W., and Jeong, S. (2009). "Mid-Range Streamflow Forecasts Based on Climate Modeling-Statistical Correction and Evaluation." *J American Water Resour Assoc.*, 45(2), 355-368.
- Schindler D.W. and Donahue, W.F. (2006). "An Impending Water Crisis in Canada's Western Prairie Provinces." *Proceedings of National Academy of Sciences, USA*.
- Shabbar, A. and Khandekar, M. (1996). "The impact of El Nino-Southern Oscillation on the temperature field over Canada." *Atmosphere-Ocean*, 34, 401–416.
- Shabbar, A., Bonsal, B. and Khandekar, M. (1997). "Canadian precipitation patterns associated with the Southern Oscillation." *Journal of Climate*, 10, 3016–3027.
- Skaugen, T., Beldring, S., Udnaes, H. C. (2003) "Dynamical properties of the spatial distribution of snow." *Hydrology and Earth System Sciences*, 7(5), 744-753.

Singh, J., H. V. Knapp, and M. Demissie (2004). "Hydrologic modeling of the Iroquois River watershed using HSPF and SWAT." *ISWS CR 2004-08. Champaign, Ill.: Illinois State Water Survey. Available at: www.sws.uiuc.edu/pubdoc/CR/ISWSCR2004-08.pdf. Accessed 15 July 2012.*

Tanzeeba, S. (2009) Potential Impact of Climate Change on the Water Availability in the South Saskatchewan River Basin. *Msc Thesis, University of Alberta.*

Tanzeeba, S. and Gan, T.Y. (2012). "Potential impact of climate change on the water availability of South Saskatchewan River Basin." *Climatic Change*, 112, 355-386.

Wilby, R. L., Troni, J., Biot, Y., Tedd, L., Hewitson, B. C., Smithe, D. M. and Sutton, R. T. (2009). "A review of climate risk information for adaptation and development planning." *Int. J. Climatol.*, 29, 1193–1215.

Wilks, D. S. (2011). "Statistical methods in the atmospheric sciences (Vol. 100)". Academic press.

Wolter, K. (Klaus.Wolter@noaa.gov) (2011a). "Multivariate ENSO Index (MEI)." (<http://www.esrl.noaa.gov/psd/enso/mei/>). *National Oceanic and Atmospheric Administration, Earth System Research Laboratory, Physical Sciences Division.*

Wolter, K. (Klaus.Wolter@noaa.gov) (2011b). "Extended Multivariate ENSO Index (MEI.ext)." (<http://www.esrl.noaa.gov/psd/enso/mei.ext/>). *National*

Oceanic and Atmospheric Administration, Earth System Research Laboratory, Physical Sciences Division.

Wolter, K. and Timlin, M. (1993). "Monitoring ENSO in COADS with a seasonally adjusted principal component index." *In: Proceedings of the 17th Climate Diagnostics Workshop, Univ. of Oklahoma, Norman, OK, 52–57.*

Wolter, K. and Timlin, M. (1998). "Measuring the strength of ENSO—how does 1997/98 rank?" *Weather, 53 (9), 315–324.*

Wolter, K. and Timlin, M. (2008). "An improved multivariate ENSO index (MEI)—a progress report." *In: Session 11: Technical Issues. Climate Prediction Applications Science Workshop, Chapel Hill, North Carolina (March 4–7).*

Wolter, K. and Timlin, M. (2011). "El Niño/Southern Oscillation behaviour since 1871 as diagnosed in an extended multivariate ENSO index (MEI.ext)." *Int. J. Climatol. 31, 1074–1087.*

Wood, A. W., Maurer, E. P., Kumar, A., and Lettenmaier, D. P. (2002). "Long-range experimental hydrologic forecasting for the eastern United States." *J Geophysical Res, 107(D20), ACL 6-1-ACL 6-15.*

Zhao, R.J. (1992). "The Xinanjiang model applied in China." *J Hydrol, 135, 371–381.*

Table 3.1 Statistics of calibration and validation runs using Modified Interaction Soil Biosphere Atmosphere (MISBA) for different sub-basins of the South Saskatchewan River Basin (SSRB) considered in this study.

Sub-Basin	Area (Km ²)	Calibration (1961-1980)						Validation (1981-1990)					
		R ²	E _f	SD (m ³ /s)	RMSE (m ³ /s)	MAE (m ³ /s)	PB	R ²	E _f	SD (m ³ /s)	RMSE (m ³ /s)	MAE (m ³ /s)	PB
Red Deer at Dickson Dam (RDDD)	5951	0.68	0.58	30.18	19.54	13.53	-14.71	0.69	0.44	32.64	24.41	15.81	5.28
Red Deer at Red Deer (RDRD)	12,502	0.67	0.64	43.13	25.81	15.95	-6.78	0.67	0.47	45.12	32.64	20.65	13.66
Red Deer Near Nevis (RDNN)	20,340	0.72	0.67	47.80	27.61	16.56	4.84	0.70	0.52	50.11	34.40	21.59	16.59
Red Deer at Big Valley (RDBV)	20,710	0.73	0.68	48.40	27.49	16.26	14.03	0.75	0.63	50.43	30.59	17.99	9.92
Red Deer at Drumheller (RDDH)	28,388	0.74	0.72	55.28	29.26	16.18	3.68	0.78	0.64	52.38	31.29	18.15	18.06
Red Deer Near Jenner (RDNJ)	45,614	0.63	0.57	59.43	38.81	23.83	4.51	0.82	0.74	52.82	27.01	17.19	21.00
Red Deer at Bindloss (RDBL)	49,437	0.70	0.67	61.15	35.00	22.56	15.65	0.77	0.69	53.73	30.00	21.01	27.76
Elbow below Glenmore Dam (EBGD)	1,298	0.71	0.57	8.13	5.35	3.72	-15.08	0.63	0.36	6.57	5.25	3.87	-7.42
Bow at Calgary (BWCG)	8,332	0.70	0.50	90.46	63.66	43.91	-9.97	0.69	0.34	80.08	64.66	44.23	1.59
Highwood at Mouth (HWMO)	4,166	0.74	0.71	28.56	15.45	8.73	-9.10	0.75	0.51	20.37	14.16	8.33	21.67
Oldman near Waldron Corner (OMWC)	1,501	0.80	0.76	18.71	9.20	5.47	-19.23	0.63	0.53	13.67	9.30	5.44	-10.58
Oldman near Brocket (OMBR)	4,560	0.68	0.63	56.26	34.13	18.46	-12.93	0.77	0.69	39.53	21.92	12.20	1.15
Oldman near Fort Macleod (OMFM)	6,039	0.74	0.74	58.54	29.95	15.50	0.80	0.70	0.62	40.99	25.11	16.18	21.68
Oldman near Monarch (OMMO)	9,240	0.82	0.79	61.81	27.97	15.98	-8.29	0.91	0.88	42.90	15.11	11.58	4.18
Oldman near Lethbridge (OMLB)	17,677	0.80	0.79	139.35	63.04	35.59	-3.67	0.74	0.68	94.89	53.09	33.47	10.69
Crowsnest near Lundbreck (CNLB)	700	0.69	0.46	6.95	5.12	3.38	-19.81	0.62	0.36	4.99	3.97	2.90	-23.63
Castle near Beaver Mines (CSBM)	855	0.78	0.69	23.23	12.90	7.22	-12.12	0.68	0.56	16.39	10.78	6.71	-20.78
Pincher at Pincher Creek (PCPC)	168	0.77	0.76	1.62	0.80	0.45	-1.08	0.70	0.66	1.21	0.70	0.41	9.02
Belly at International Boundary (BLIB)	201	0.85	0.74	8.11	4.10	2.96	-33.55	0.79	0.55	5.41	3.62	2.58	-15.37
Belly near Mountain View (BLMV)	331	0.89	0.82	11.30	4.73	3.47	-26.71	0.86	0.73	7.74	4.02	2.99	-12.54
Belly near Glenwood (BLGW)	740	0.81	0.77	11.31	5.38	3.76	-16.46	0.76	0.60	7.68	4.87	3.61	-2.20
Belly at Waterton Confluence (BLWC)	3,553	0.73	0.71	44.48	23.85	14.65	-13.84	0.69	0.58	30.31	19.62	12.91	0.97
Belly at Mouth (BLMO)	3,874	0.78	0.74	44.73	22.71	14.27	-7.62	0.74	0.54	30.00	20.17	12.52	6.79
St. Mary International Boundary (SMIB)	1,272	0.74	0.64	31.45	18.93	12.85	-28.31	0.65	0.53	23.28	15.91	11.18	-19.60
St. Mary at St. Mary Dam (SMSD)	2,180	0.72	0.64	34.32	20.64	13.76	-24.11	0.63	0.54	24.49	16.63	11.05	-15.50
Willow above Chain Lakes (WLCL)	174	0.72	0.69	1.58	0.89	0.44	-17.58	0.74	0.73	1.24	0.64	0.32	-2.68
Willow near Claresholm (WLCS)	983	0.77	0.76	4.73	2.32	1.25	-11.45	0.81	0.66	2.75	1.59	0.99	48.86
Willow near Nolan (WLNO)	2,380	0.76	0.75	6.27	3.11	1.66	0.33	0.77	0.44	3.12	2.34	1.25	58.44
Waterton at Waterton Reservoir (WTRS)	1,289	0.76	0.74	30.84	15.74	9.40	-14.96	0.76	0.69	21.32	11.81	8.04	-6.06

R² - coefficient of determination, E_f - Nash-Sutcliffe coefficient of efficiency, SD- Standard Deviation of naturalized streamflow, RMSE- Root Mean Square Error, MAE- Mean Absolute Error, and PB-Percent Bias are given by,

$$R^2 = \left[\frac{\sum_{i=1}^N (O_i - \bar{O})(S_i - \bar{S})}{\sqrt{\sum_{i=1}^N (O_i - \bar{O})^2} \sqrt{\sum_{i=1}^N (S_i - \bar{S})^2}} \right]^2, \quad E_f = 1 - \frac{\sum_{i=1}^N (O_i - S_i)^2}{\sum_{i=1}^N (O_i - \bar{O})^2}, \quad SD = \frac{\sum_{i=1}^N (O_i - \bar{O})^2}{N}, \quad RMSE = \sqrt{\frac{\sum_{i=1}^N (O_i - S_i)^2}{N}}, \quad MAE = \frac{\sum_{i=1}^N |O_i - S_i|}{N}, \quad PB = \frac{\sum_{i=1}^N (O_i - S_i)}{\sum_{i=1}^N O_i} \times 100\%$$

where, O_i and S_i are the naturalized and simulated monthly streamflows at timestep i and N is the number of observation.

Table 3.2 MISBA simulated percentage changes in mean annual runoff from the climate normal (1961-1990) with respect to climate change scenarios projected by four GCMs (CCSRNIES, CGCM2, ECHAM4, HadCM3) forced by three SRES emissions (A1FI, A21 and B21) of IPCC for the SSRB independently, and when combined with El Niño and La Niña episodes (See Table 3.1 for Basin definitions)

Basin	% Change in Mean Annual Runoff from Climate Normal (1961-1990)														
	2010-2039 (2020s)			2040-2069 (2050s)			2070-2099 (2080s)			2050s+ El Niño			2050s+ La Niña		
	Min	Max	Ave	Min	Max	Ave	Min	Max	Ave	Min	Max	Ave	Min	Max	Ave
RDDD	-10	3	-3	-9	20	2	-9	38	8	-15	17	-4	-12	19	0
RDRD	-15	1	-5	-10	19	0	-13	38	6	-12	21	-1	-19	7	-10
RDNN	-14	2	-6	-12	12	-3	-17	21	2	-3	25	9	-16	9	-6
RDBV	-14	1	-6	-12	12	-3	-17	21	1	-19	10	-8	-15	10	-5
RDDH	-16	1	-8	-15	10	-4	-22	20	-2	-12	16	0	-21	-1	-12
RDNJ	-24	0	-12	-26	9	-12	-42	17	-13	-30	7	-16	-13	20	2
RDBL	-24	-2	-12	-27	7	-13	-43	12	-14	-33	0	-20	-19	13	-5
EBGD	-12	1	-4	-12	10	-3	-22	14	-4	-26	3	-14	-6	20	4
BWCG	-12	1	-6	-15	12	-3	-21	24	-1	-24	12	-10	-12	17	0
HWMO	-23	-3	-12	-31	12	-12	-44	41	-11	-51	-5	-30	-27	20	-7
OMWC	-23	-2	-14	-22	0	-14	-32	21	-12	-37	-17	-30	-30	3	-20
OMBR	-14	2	-7	-16	8	-6	-23	28	-3	-30	-5	-19	-3	24	8
OMFM	-14	4	-5	-15	13	-3	-24	33	1	-28	0	-17	-3	28	10
OMMO	-17	4	-6	-20	16	-5	-33	38	-1	-43	-6	-28	-11	26	6
OMLB	-13	3	-5	-10	-1	-5	-19	6	-4	-26	-18	-21	6	20	13
CNLB	-18	-3	-11	-19	4	-10	-23	22	-8	-32	-9	-21	-4	26	8
CSBM	-16	7	-6	-15	2	-7	-24	7	-7	-29	-10	-22	-7	21	4
PCPC	-15	5	-4	-13	10	-3	-23	28	-2	-26	-3	-17	-3	25	8
BLIB	-14	9	-2	-13	17	-1	-27	29	0	-31	5	-17	-1	36	15
BLMV	-17	1	-8	-19	12	-6	-35	31	-5	-36	8	-19	-7	22	6
BLGW	-18	5	-6	-20	18	-4	-31	44	0	-31	10	-15	-11	27	7
BLWC	-16	9	-3	-15	15	-2	-25	41	2	-29	1	-16	-4	26	10
BLMO	-17	9	-5	-17	16	-3	-28	46	1	-28	5	-14	-7	26	8
SMIB	-68	4	-16	-21	-1	-11	-33	14	-9	-26	4	-10	1	23	10
SMSD	-16	2	-7	-19	-2	-9	-31	8	-7	-25	-4	-14	4	23	13
WLCL	-18	3	-7	-25	28	-6	-33	60	0	-38	4	-24	-17	52	5
WLCS	-16	7	-5	-14	4	-4	-29	23	-2	-48	-32	-40	0	21	10
WLNO	-20	6	-7	-20	2	-8	-39	21	-6	-60	-42	-51	-3	23	9
WTRS	-18	10	-5	-17	23	-1	-26	56	5	-29	11	-14	-8	37	11

Table 3.3 MISBA simulated changes in seasonal streamflow of sub-basins of the SSRB (expressed as a percentage of the mean annual average streamflow) from the climate normal (1961-1990) with respect to climate change scenarios projected by four GCMs (CCSRNIES, CGCM2, ECHAM4, HadCM3) forced by three SRES emissions (A1FI, A21 and B21) of IPCC for the 2020s, 2050s, and 2080s independently, and when 2050s scenario combined with El Niño and La Niña episodes (See Table 3.1 for Basin definitions).

Basin	% Change in Mean Annual Runoff from Climate Normal (1961-1990)																			
	2010-2039 (2020s)				2040-2069(2050s)				2070-2099 (2080s)				2050s+El Niño				2050s+La Niña			
	Winter	Spring	Summer	Autumn	Winter	Spring	Summer	Autumn	Winter	Spring	Summer	Autumn	Winter	Spring	Summer	Autumn	Winter	Spring	Summer	Autumn
RDDD	0	5	-18	0	1	13	-6	2	4	17	6	9	0	2	-1	-10	1	25	-10	-15
RDRD	1	2	-21	-2	5	8	-9	-4	14	8	2	3	7	3	-6	-15	3	23	-53	-17
RDNN	1	3	-26	-1	5	10	-23	-6	19	10	-16	-1	7	31	11	-16	3	34	-44	-16
RDBV	1	3	-26	-2	5	11	-23	-6	18	10	-17	-2	7	3	-24	-17	3	39	-46	-16
RDDH	0	3	-30	-4	3	11	-24	-9	10	12	-22	-10	3	21	-3	-20	-1	49	-66	-26
RDNJ	-1	-3	-37	-7	-2	5	-43	-17	-1	5	-44	-19	-2	-13	-38	-15	-2	84	-56	-18
RDBL	-1	-2	-37	-9	1	4	-44	-22	10	2	-47	-25	1	-5	-49	-24	-1	58	-56	-23
EBGD	0	3	-18	-2	3	7	-19	-7	3	5	-27	-8	3	6	-51	-8	4	24	-9	-3
BWCG	0	6	-30	-1	1	16	-31	-2	11	23	-32	4	1	-1	-33	-7	2	43	-37	-7
HWMO	0	-17	-28	-3	4	-22	-28	-11	6	-24	-26	-6	8	-63	-58	-7	4	-8	-21	-4
OMWC	-1	-18	-33	-2	0	-15	-41	2	1	-16	-42	17	0	-34	-78	-6	1	-19	-55	-3
OMBR	0	-9	-18	-1	4	-10	-19	3	13	-13	-19	15	5	-37	-37	-8	8	43	-17	1
OMFM	-6	58	-59	-14	1	57	-58	-26	13	52	-53	-14	5	27	-80	-20	3	108	-57	-12
OMMO	1	-1	-24	-2	6	-3	-20	-11	14	-3	-13	-3	8	-69	-47	-5	7	42	-22	-5
OMLB	-1	9	-22	-7	1	22	-33	-21	13	29	-40	-19	1	-5	-68	-14	3	89	-21	-13
CNLB	0	-15	-27	-1	3	-15	-29	5	4	-17	-31	13	3	-34	-45	-8	6	52	-28	0
CSBM	0	36	-57	-2	2	54	-88	8	3	69	-112	25	1	59	-149	-3	6	68	-58	1
PCPC	1	-1	-15	-1	7	-3	-17	-2	5	-9	-16	6	10	-29	-47	-7	9	41	-18	-1
BLIB	0	27	-35	1	1	41	-45	-1	1	59	-65	14	2	57	-116	-5	1	52	9	-5
BLMV	0	15	-45	-1	1	28	-54	-4	1	38	-65	11	2	21	-95	-5	1	46	-15	-5
BLGW	2	3	-27	-2	7	8	-28	-7	7	10	-25	3	13	-17	-43	-8	5	42	-8	-8
BLWC	2	1	-15	-1	8	3	-16	-6	15	1	-10	5	15	-25	-40	-8	9	49	-16	-6
BLMO	2	0	-20	-2	7	1	-17	-9	14	0	-9	-1	12	-26	-41	-8	9	42	-16	-7
SMIB	1	-11	-51	-2	4	-1	-44	-16	6	1	-42	-10	10	-28	-19	-2	2	81	-36	-3
SMSD	1	1	-28	-3	5	0	-35	-22	8	2	-37	-15	13	-55	-9	-5	3	94	-42	-6
WLCL	1	21	-47	-4	2	30	-57	-1	0	42	-54	13	1	21	-113	-8	9	50	-44	5
WLCS	0	-3	-15	-2	5	-4	-16	-15	4	-6	-11	-13	11	-91	-77	-4	7	67	-30	-4
WLNO	0	-5	-19	-4	5	-9	-23	-18	4	-12	-21	-18	12	-94	-111	-9	8	60	-25	-8
WTRS	1	2	-22	0	4	8	-16	4	8	8	-6	20	5	-11	-42	-6	6	50	-13	0

Table 3.4 Percentage Changes in Future Streamflow Per °C Rise in Temperature in the 21st Century for Different sub-basins of the South Saskatchewan River Basin (SSRB) considered in this study

Sub-Basin	% Decrease in Per °C Rise in Temperature	
	Mean Annual Average Streamflow (ΔQ_{Mean})	Mean Annual Maximum Streamflow (ΔQ_{Max})
Red Deer at Dickson Dam	3.68	6.25
Red Deer at Red Deer	4.50	6.13
Red Deer Near Nevis	4.34	6.87
Red Deer at Big Valley	4.34	6.41
Red Deer at Drumheller	5.77	8.75
Red Deer Near Jenner	7.60	11.84
Red Deer at Bindloss	7.87	10.75
Elbow below Glenmore Dam	3.25	6.40
Bow at Calgary	4.34	7.37
Highwood at Mouth	8.26	9.26
Oldman near Waldron Corner	8.71	6.34
Oldman near Brocket	5.47	8.64
Oldman near Fort Macleod	4.92	5.99
Oldman near Monarch	5.72	8.67
Oldman near Lethbridge	3.91	7.18
Crowsnest near Lundbreck	6.33	9.84
Castle near Beaver Mines	5.62	6.26
Pincher at Pincher Creek	4.52	6.60
Belly at International Boundary	3.48	7.29
Belly near Mountain View	5.73	11.42
Belly near Glenwood	5.48	9.82
Belly at Waterton Confluence	4.73	8.86
Belly at Mouth	5.74	8.99
St. Mary International Boundary	8.58	12.16
St. Mary at St. Mary Dam	5.78	9.02
Willow above Chain Lakes	7.38	5.28
Willow near Claresholm	6.84	8.40
Willow near Nolan	6.84	9.93
Waterton at Waterton Reservoir	6.04	8.06

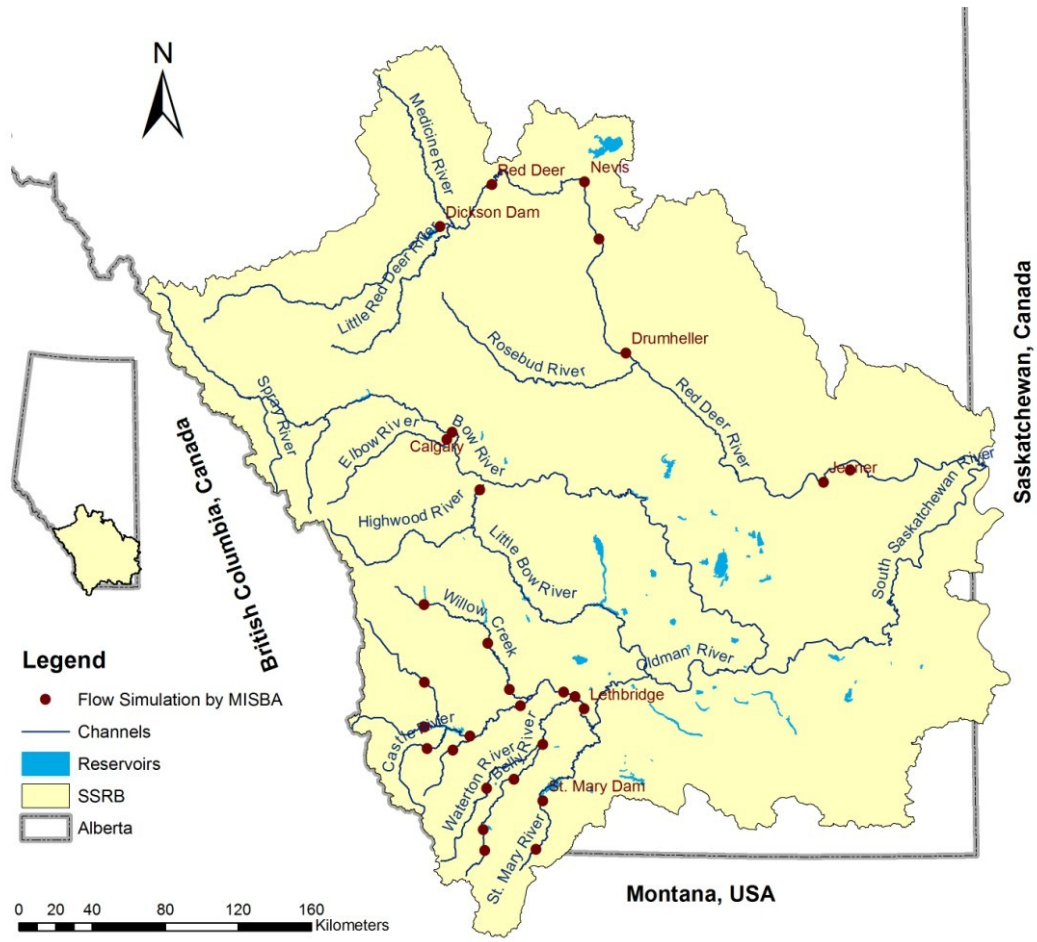


Figure 3.1 South Saskatchewan River Basin of Alberta.

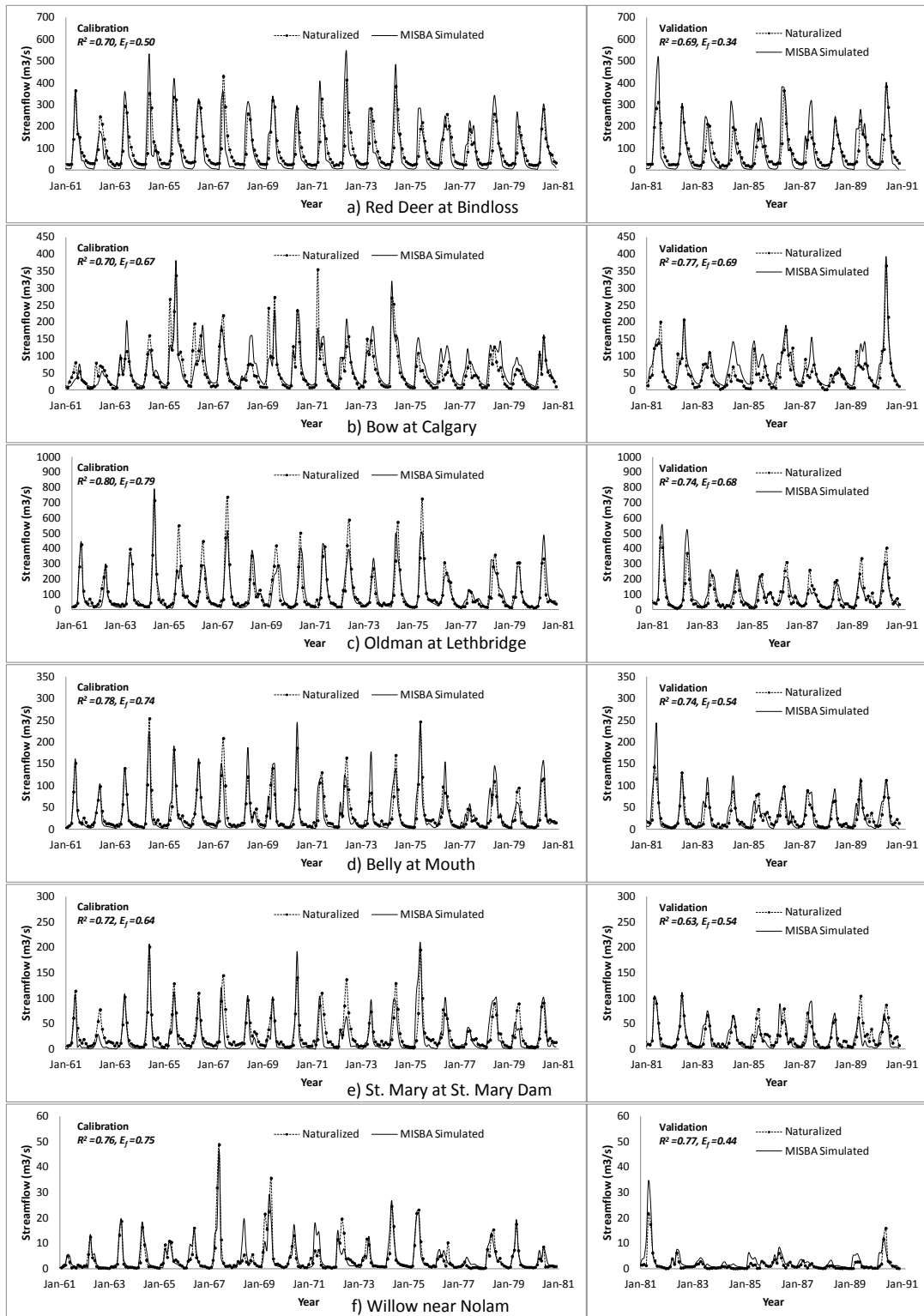


Figure 3.2 Comparison of naturalized and MISBA simulated streamflow for calibration (1961-1980) and validation (1980-1990) periods at selected locations of the SSRB.

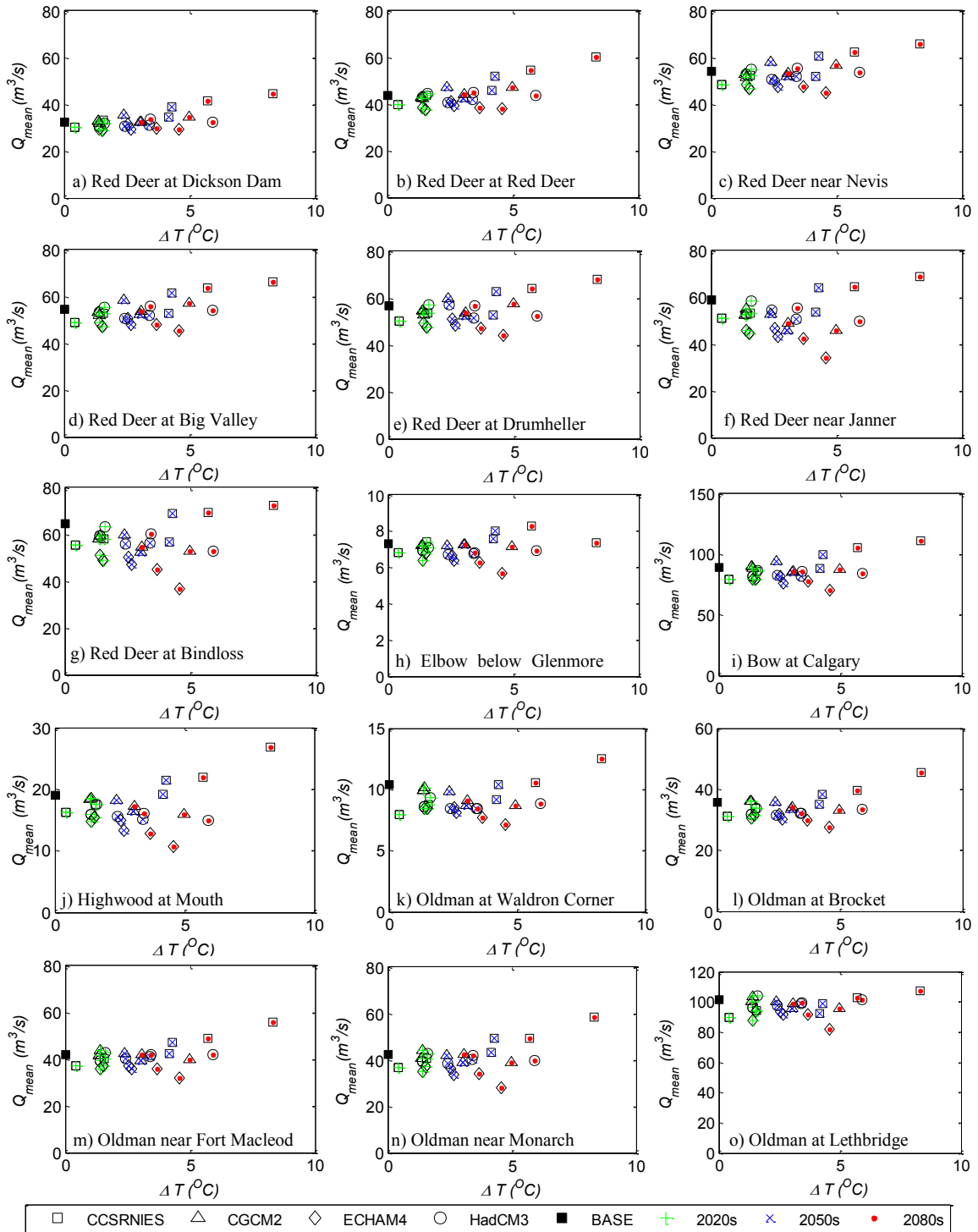


Figure 3.3 MISBA simulated mean annual average streamflows at different location of the SSRB in comparison to that of the base scenario (black square) with respect to the climate change scenarios projected by four GCMs (CCSRNIES, CGCM2, ECHAM4, and HadCM3) forced by three SRES emissions (A1FI, A21, and B21) of IPCC for 2020s, 2050s, and 2080s (continued).

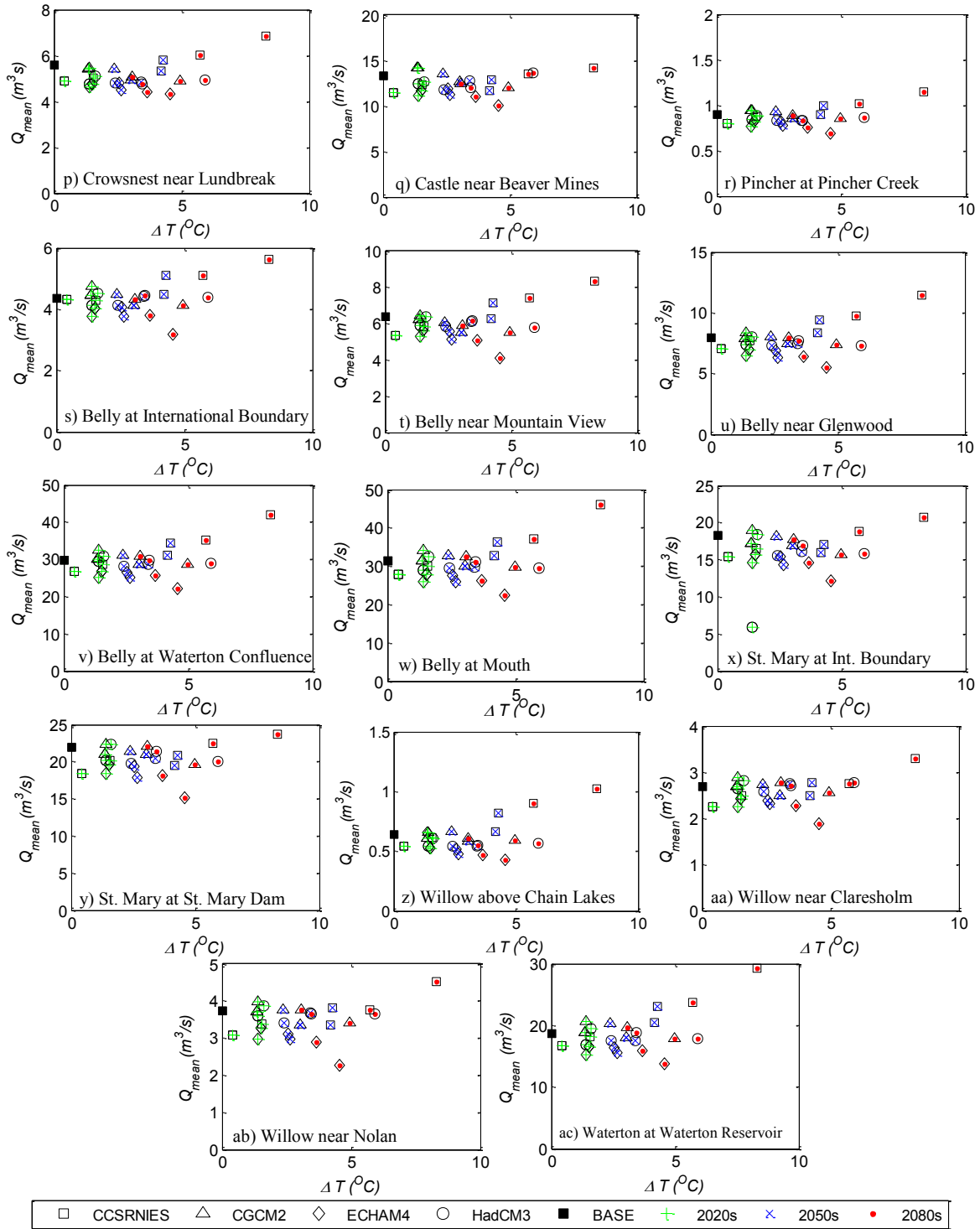


Figure 3.3 MISBA simulated mean annual average streamflows at different location of the SSRB in comparison to that of the base scenario (black square) with respect to the climate change scenarios projected by four GCMs (CCSRNIES, CGCM2, ECHAM4, and HadCM3) forced by three SRES emissions (A1FI, A21, and B21) of IPCC for 2020s, 2050s, and 2080s.

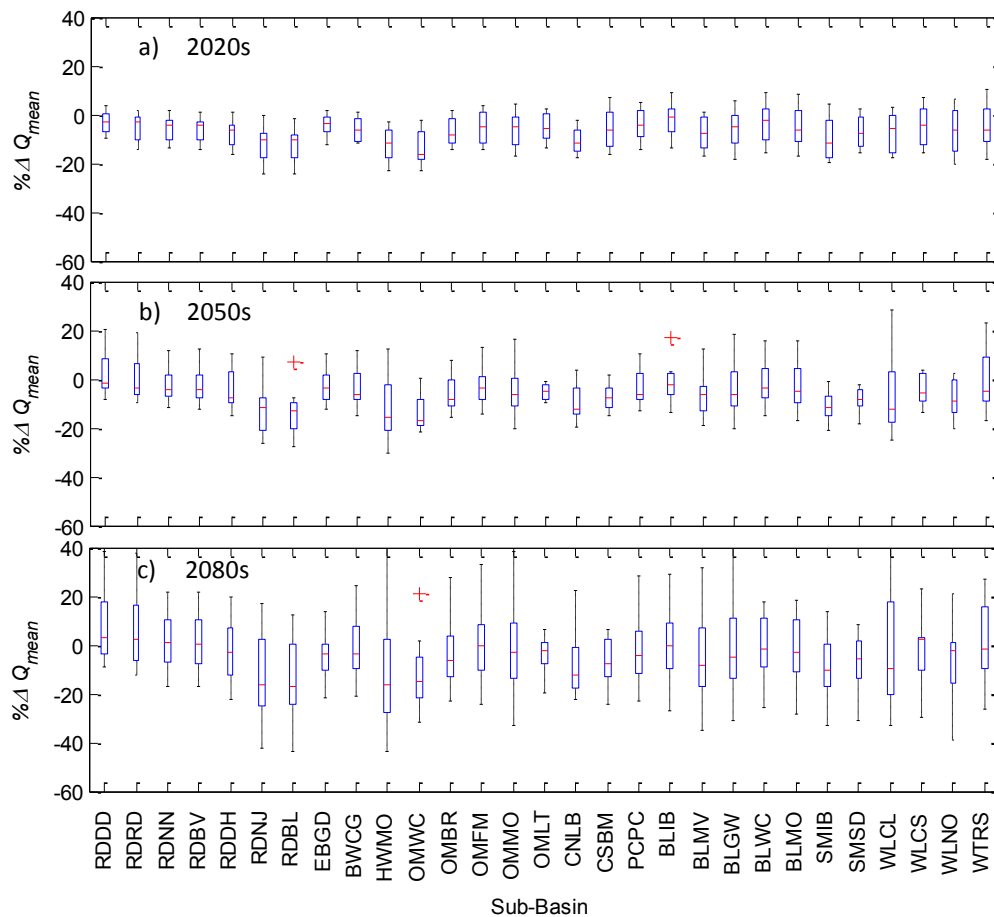


Figure 3.4 Boxplots of MISBA simulated percentage changes in mean annual average streamflow ($\% \Delta Q_{\text{mean}}$) for different sub-basins of the SSRB as compared to the climate normal (1960-1991) with respect to the climate change scenarios projected by four GCMs (CCSRNIES, CGCM2, ECHAM4, and HadCM3) forced by three SRES emissions (A1FI, A21, and B21) of IPCC for 2010-2039 (2020s), 2040-2069(2050s), and 2070-2099 (2080s) (Sub-Basin names have been defined in Table 3.1).

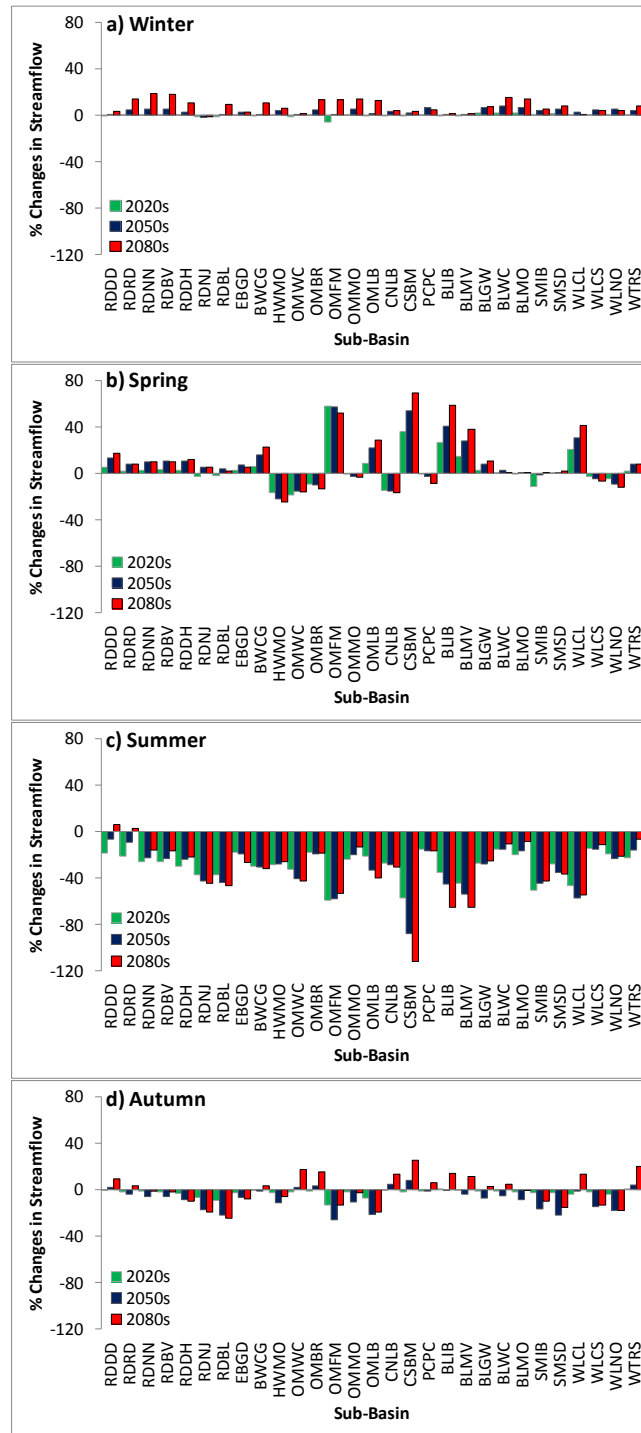


Figure 3.5 MISBA simulated changes in seasonal streamflow of sub-basins of the SSRB (expressed as a percentage of the mean annual average streamflow) from the climate normal (1961-1990) with respect to climate change scenarios projected by four GCMs (CCSRNIES, CGCM2, ECHAM4, HadCM3) forced by three SRES emissions (A1FI, A21 and B21) of IPCC for the 2020s, 2050s, and 2080s (Sub-Basin names have been defined in Table 3.1).

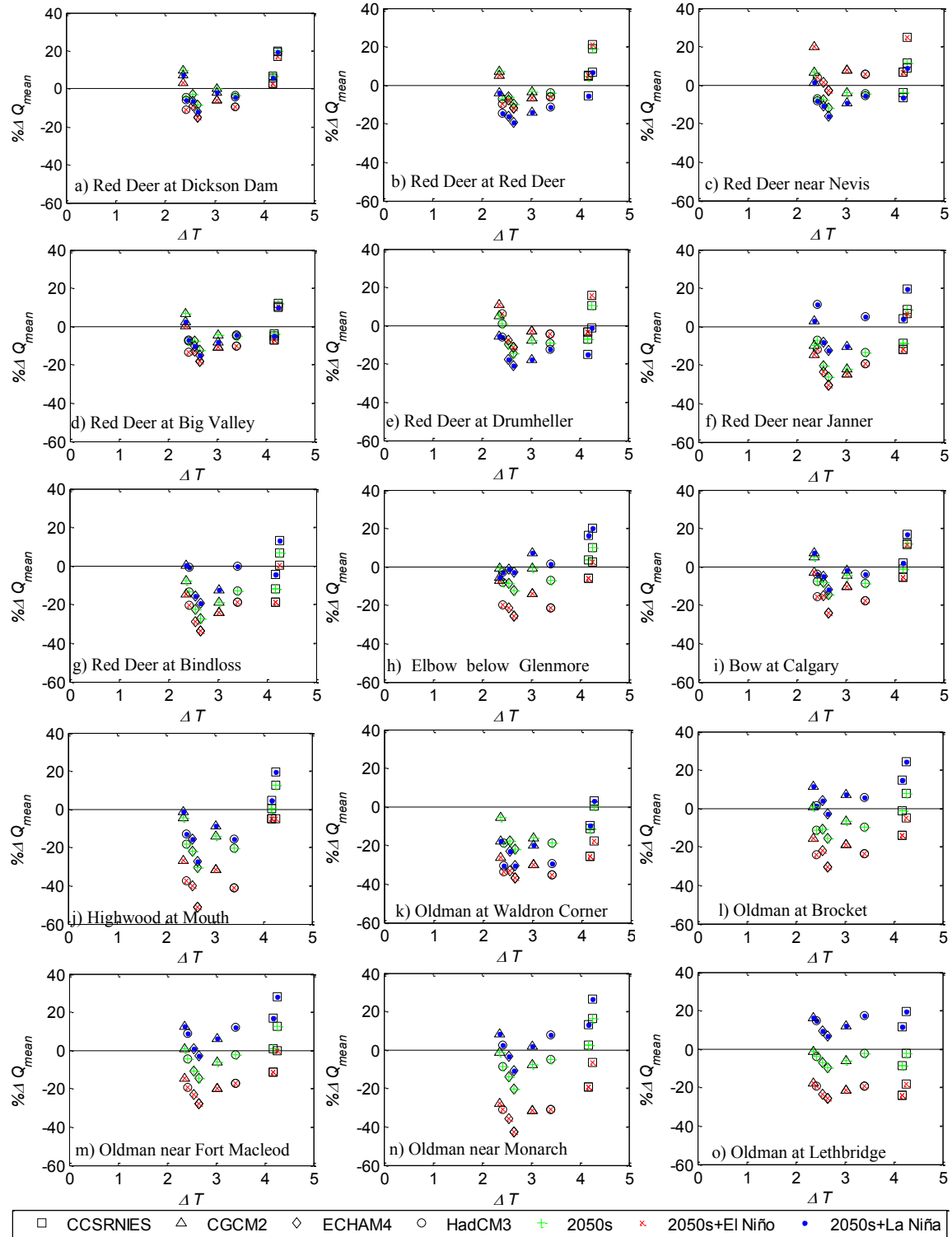


Figure 3.6 MISBA simulated percentage changes in mean annual average streamflow at different location of the SSRB for 2050s and for combined scenarios (2050s+El Niño, 2050s+La Niña) in comparison to that of the base scenario with respect to the climate change scenarios projected by four GCMs (CCSRNIES, CGCM2, ECHAM4, and HadCM3) forced by three SRES emissions (A1FI, A21, and B21) of IPCC (continued).

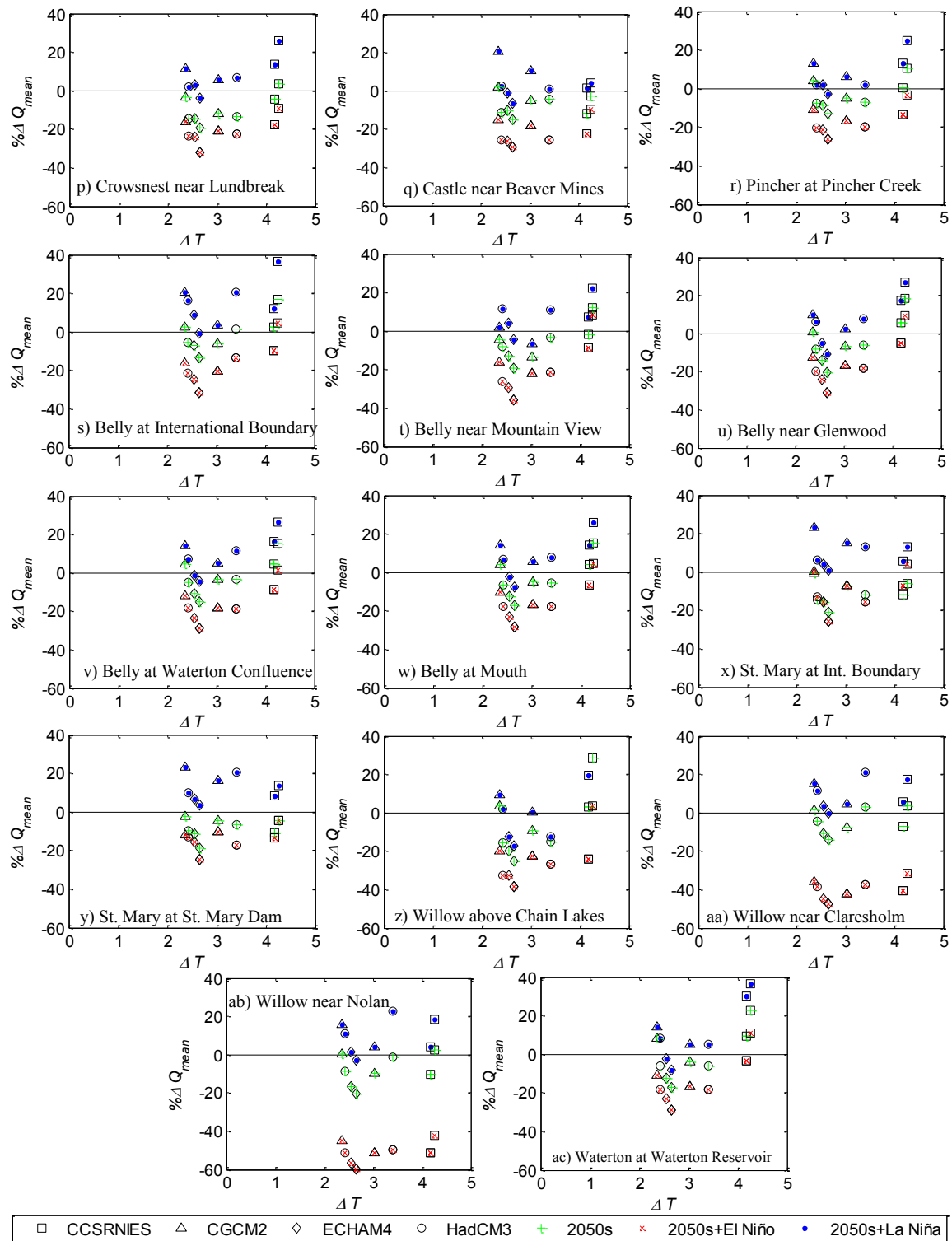


Figure 3.6 MISBA simulated percentage changes in mean annual average streamflow at different location of the SSRB for 2050s and for combined scenarios (2050s+El Niño, 2050s+La Niña) in comparison to that of the base scenario with respect to the climate change scenarios projected by four GCMs (CCSRNIES, CGCM2, ECHAM4, and HadCM3) forced by three SRES emissions (A1FI, A21, and B21) of IPCC.

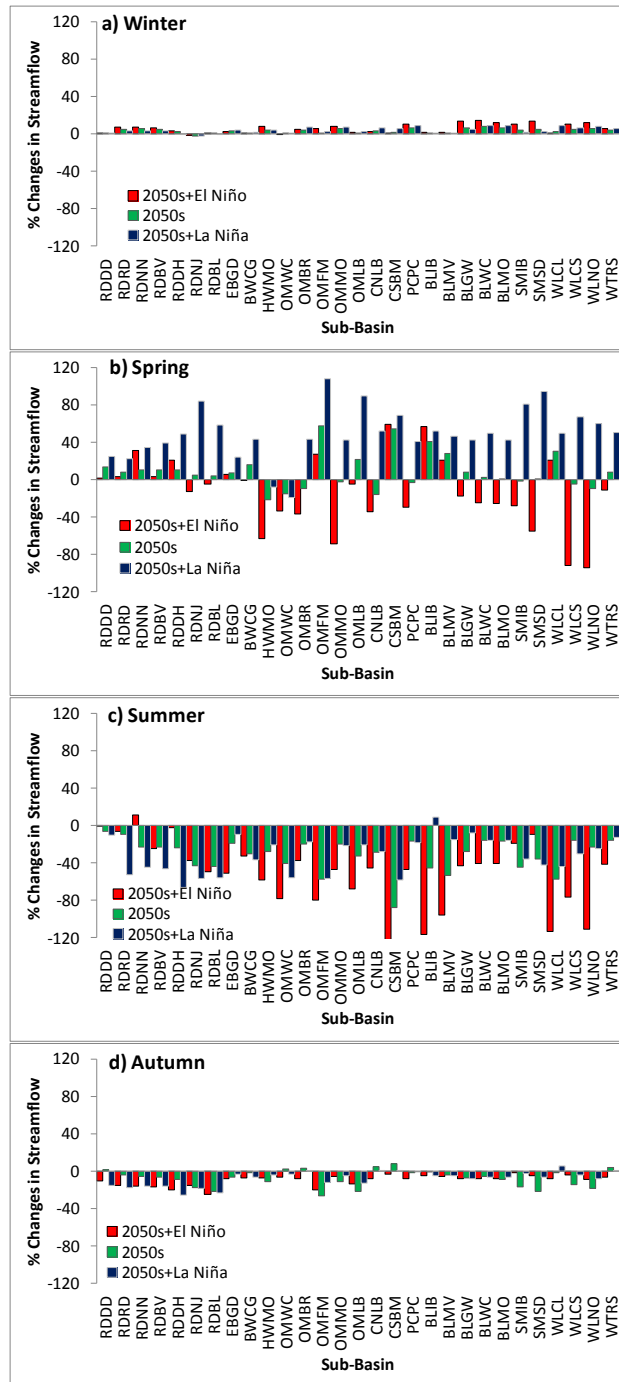


Figure 3.7 MISBA simulated changes in seasonal streamflow of sub-basins of the SSRB (expressed as a percentage of the mean annual average streamflow) from the climate normal (1961-1990) with respect to climate change scenarios projected by four GCMs (CCSRNIES, CGCM2, ECHAM4, HadCM3) forced by three SRES emissions (A1FI, A21 and B21) of IPCC for the 2050s independently, and when 2050s scenario combined with El Niño and La Niña episodes (Sub-Basin names have been defined in Table 3.1).

CHAPTER 4

Future Irrigation Demand of South Saskatchewan River Basin under the Combined Impacts of Climate Change and Climate Anomalies

4.1 Introduction

Alberta is known as the capital of irrigation in Canada as about 65% of the total irrigation area in Canada is located in this province. Therefore irrigation plays an important role in Alberta's economy (Irrigation Branch, Alberta Agriculture, Food and Rural Development 2000). History of irrigation in Alberta started more than a century ago, and by the beginning of the 21st century it has about 600,000 hectares of irrigated land, most of which are located in southern part of the province where most of the water comes from the South Saskatchewan River Basin (SSRB).

Alberta's irrigated land located in irrigation districts and private irrigation projects has been increasing steadily especially during an unprecedented growth in the 1970-1980 decade (Irrigation Branch, Alberta Agriculture, Food and Rural

Development 2000). Because of increasing irrigated land area, which resulted in a high demand for water from southern Alberta which unfortunately has limited water resources, in 1990 the province began to limit the amount of water to be allocated for irrigation purpose in the SSRB, which was followed by the SSRB Water Allocation regulation in 1991 (Alberta Environment 1990; 1991). In 1996, Alberta Irrigation Projects Association, Alberta Agriculture Food and Rural Development (AAFRD), and the Prairie Farm Rehabilitation Administration of Agriculture and Agri-Food Canada jointly initiated a study in irrigation district water requirements in the SSRB. This study provided a comprehensive analysis of current and future water management within the irrigation districts with the objectives of identifying and quantifying current irrigation water requirements and possible future irrigation water use by assessing the risks, impacts and possibilities of irrigation area expansion (Irrigation Water Management Study Committee 2002a, b, c, d, and e). However, in this study the potential impacts of climate change on SSRB's future irrigation demand have not been considered, even though a longer growing season and a warmer annual surface temperature are predicted in the SSRB as results of the potential impact of climate change (Barrow and Yu 2005). The long-term temporal trends in the agro-climate of Alberta reveal that the May through August precipitation has increased by 14% from 1901 to 2002, and this increase in precipitation is highest in the north and the northwest of Alberta, then diminishes in central and southern Alberta, and finally becomes relatively higher again in the southeast corner of the province

(Shen et al. 2005). Besides, in recent decades there have been unequivocal, observational evidences of global warming such as increases in the global average air and ocean temperatures (Bates et al. 2008). These changes in the global climate can affect the hydrological cycle such as precipitation, snowmelt, evaporation, soil moisture, and runoff. Such climatic changes in the hydrologic system will affect the irrigation requirement and agricultural productivity of Alberta (Xu and Singh 2004; Zhou et al. 2010; Thomas 2008; Fischer et al. 2007).

Other than the potential impacts of climate change, climate anomalies such as El Niño and La Niña may also have significant impact in agricultural production (Hansen et al. 1998; Gan 2000; Meza 2005; Jacob et al. 2006). Conversely, the impact of climate change on the irrigation water demand could be quite significantly modified by some climate anomalies individually and collectively, when such anomalies occur. It is anticipated that irrigation demand of southern Alberta, which takes up about 75% of the licensed water use in SSRB (Alberta Environment 2005), is expected to change because of the possible impact of climatic changes in SSRB based on projected, Special Report on Emissions Scenarios (SRES) climate scenarios of the Intergovernmental Panel on Climate Change (IPCC), and also because of the possible impact of climate variability on SSRB. Therefore, an assessment of the combined impacts of climate change and climate anomalies on the future irrigation water demand of SSRB and strategies for reducing such vulnerability will be of national priority.

With these statements of problems, the key objective of this research study is to investigate possible changes to irrigation demand of the irrigation districts and private irrigation blocks of SSRB (a) on the basis of climate change projected by General Circulation Models (GCMs) forced by selected SRES emissions of IPCC (2001) for 2010-2039(2020s), 2040-2069 (2050s), and 2070-2099 (2080s); and (b) the possible impact of climate change projected by GCMs forced by selected SRES emissions of IPCC for 2050s, combined with the possible impact of El Niño and La Niña episodes when either of these anomalies are active.

4.2 Irrigation in SSRB

The SSRB has a watershed area of 121,095 km², of which 41% is from the Red Deer, 22% from the Oldman, 21% from the Bow and 16% from the South Saskatchewan River sub-basin (Figure 4.1). Even though it only occupies about a quarter of the land area of Alberta, it provides nearly 57% of the water allocated in Alberta. However, ironically it possesses less than 6% of Alberta's total water resources because southern Alberta has a semi-arid climate. Most of the soils in SSRB are ideally suited for irrigation because of its medium-to-fine textured glacial tills which have good water-holding capacities and slow movement through the lower root zone (Irrigation Branch, Alberta Agriculture, Food and Rural Development 2000). SSRB has 13 irrigation districts and among them, Bow River (BRID), Eastern (EID), and Western (WID) irrigation districts are in the Bow River sub-basin; Aetna (AID), Leavitt (LID), Lethbridge Northern (LNID), Magrath

(MID), Mountain View (MVID), Raymond (RID), St.Mary River (SMRID), Taber (TID), and United (UID) irrigation districts are in the Oldman River sub-basin; and Ross Creek (RCID) irrigation district is in the South Saskatchewan River sub-basin (Figure 4.1). Table 4.1 shows some of the characteristics (e.g. total area, irrigation area, length of distribution system, license water volume, and crop mix proportion) of these irrigation districts. Beside these irrigation districts, there are more than 2,500 private irrigation projects in Alberta of which about 80% are in SSRB (Irrigation Water Management Study Committee 2002a). Figure 4.1 also shows the location of private irrigation projects in the SSRB.

Precipitation in Alberta has high spatial variability, with the southern part receiving only 300-450 mm of annual precipitation of which less than half it occurs from May to August. In SSRB, the growing season precipitation or the moisture needed to support plant growth, decreases from the west to east. In contrast, the potential evapotranspiration of SSRB increases from west to east. As a result, the net growing season moisture deficit, which is the difference between evapotranspiration and growing season precipitation, increases from west to east (Irrigation Water Management Study Committee 2002a). Therefore, on an average, there will be a net annual water deficit of about 380 mm in the southeast region of SSRB resulted from a combination of abundant sunshine, warm temperatures and a long growing season (Irrigation Branch, Alberta Agriculture, Food and Rural Development 2000). Irrigation allows water that is stored in the spring to be used in mid-summer to help balance these net water

deficits. However, irrigation demands depend on the climatic condition and thus it varies year to year (Alberta Environment 2003).

4.3 Irrigation District Model (IDM)

The IDM of AAFRD has been selected in this study to generate the irrigation consumptive demands for irrigation districts and private irrigation blocks. IDM comprises of two major integrated modules: the Irrigation Requirements Module (IRM) and the Network Management Module (NMM). Details information on IDM can be found in the Irrigation Water Management Study Committee (2002d), and only a summary will be discussed in the following paragraphs.

IRM contains meteorological and field-based data needed to determine farm delivery requirements. IRM has four level of components, viz. as, Model, Block, Field and Band components. The model component is the highest level object that encapsulates all other objects used to model the water demands of irrigated lands; the Block component consists of a collection of field, and typically used to represent the organization units of an irrigation system; the Field component consists of a collection of band objects, an irrigation object, and a crop objects. The Band is the lowest level component which represents the portion of a field irrigated in one day.

IRM is used to determine the on-farm irrigation water demand by modeling the crop water use, irrigation system and irrigation method. The current version of

IRM includes crop parameters and crop coefficient curves for about 58 different crops and 21 different irrigation methods. The crop, weather and soil data are used to simulate the evapotranspiration (ET) from a crop followed by a water balance calculation to determine the change in soil moisture resulting from the ET (Irrigation Water Management Study Committee 2002e).

Gross On-Farm Demand is the volume of water delivered through the irrigation project conveyance works to meet specific on-farm system demand:

$$\text{Eq. 4.1} \quad \textit{Gross On-Farm Demand} = D + \textit{Down Time Loss}$$

where, *Down Time Loss* is the volume of water not diverted to the farm due to on-farm system shut-down and/or temporary suspension of irrigation; and *D* is the farm diversion, which is equal to the net amount of water that is actually diverted and delivered into the on-farm, infield irrigation system, and is given by,

$$\text{Eq. 4.2} \quad D = \theta + I + O + E$$

where θ is the stored soil moisture, *I* the deep percolation, *O* the outflow water (i.e., the amount of applied water that flows off an irrigated land), and *E* is the evaporation loss through aerial application, the crop canopy, soil, and surface irrigation systems. The actual evapotranspiration is calculated as,

$$\text{Eq. 4.3} \quad ET_A = ETSF \times K_{CA} \times ET_P$$

where, ET_{SF} is the ET scaling factor, ET_A and ET_P are the actual and potential ET, respectively, and K_{CA} is the adjusted crop coefficient. K_{CA} is obtained from the crop coefficient table in the IRM database, based on the crop type and the Julian Day, and is adjusted to take into account the available soil moisture as follows,

Eq. 4.4

$$K_{CA} = K_C \times \left[\frac{\ln\left(\frac{\theta_{RZ}}{D_{RZ} * \theta_C} \times 100 + 1\right)}{\ln(101)} \right]$$

where, K_C , θ_{RZ} , θ_C , and D_{RZ} are the crop coefficient, root zone soil moisture, soil moisture capacity, and root depth, respectively. The potential ET (ET_P) used in Eq. 4.3 is calculated from the Priestley-Taylor (Jansen et al. 1990) equation,

Eq. 4.5

$$ET_P = \alpha \left(\frac{\Delta}{\Delta + \gamma} \right) \left(\frac{R_n - G}{\lambda} \right)$$

where, α , Δ , γ , R_n , G , and λ are the Priestley-Taylor coefficient, slope of the saturation vapor pressure-temperature relationship, psychrometric constant, net radiation, ground heat flux and latent heat of vaporization, respectively. Due to the semi-arid condition of southern Alberta, α was assumed to be 1.7 (Jansen et al. 1990). The calculated actual ET (ET_A) is then subtracted from the root zone soil moisture (θ_{RZ}) to update the soil moisture in the root zone and it is constrained in such a way that it can never be negative.

The runoff (R_o) is based on the precipitation in a single day (P) and is calculated as,

$$\text{Eq. 4.6} \quad R_o = \theta_{RZ} + \theta_{LZ} + P - 1.1 * (D_s \times \theta_C) \quad ; P < 25 \text{ mm}$$

$$\text{Eq. 4.7} \quad R_o = P - \left[0.9177 + 1.811 \times \ln(P) - 0.0097 \times \ln(P) \times \left(\frac{\theta_{RZ} + \theta_{LZ}}{D_s \times \theta_C} \right) \times 100 \right] \quad ; P > 25 \text{ mm}$$

where, θ_{RZ} , θ_{LZ} are the root zone and lower zone soil moisture; D_s is the soil depth; and θ_C is the soil moisture capacity.

The root zone soil moisture is then updated as,

$$\text{Eq. 4.8} \quad \theta_{RZ} = \theta_{RZ} + P - R_o$$

Percolation is calculated in two phase. In the first phase, the amount of soil moisture in the root zone which exceeds the soil moisture capacity is calculated and added to the lower zone soil moisture. In the second phase, the amount of soil moisture which exceeds the soil moisture capacity is calculated and considered as the percolation loss.

The amount of water not absorbed by the soil moisture is removed from the irrigation network and returns to the irrigation system as the return flow (Q_R),

Eq. 4.9

$$Q_R = Q_I \times \left(\frac{1 - \varepsilon_A}{100} \right) \times k_{qr}$$

where, Q_R and Q_I are the return flow from the irrigation field and inflow to the irrigation field, respectively; ε_A is the application efficiency; and k_{qr} is the return flow factor.

NMM represents the physical characteristics of each district or non-district irrigation blocks, which includes pipelines, canals, reservoirs and return flow channels, and their respective operating characteristics and losses. NMM simulates the irrigation water distribution network by via a number of simulation components, viz. as, canal segment, closed pipe segment, diversion, junction, control gate, reservoir, irrigation demand, runoff collector, base flow, system source, and system sink.

IDM and its modules (e.g. IRM, NMM) were first calibrated and then validated to ensure a good match between modeling results and actual recorded water demand and consumption data (Irrigation Water Management Study Committee 2002a). Parameters considered in the calibration process are total seasonal consumptive use for each crop type, timing of crop water use, harvesting dates and "water on and off" dates, carry-over and net residual soil moisture conditions (fall, winter and early spring), on-farm irrigation efficiencies, on-farm irrigation management by crop-type and method, return flow volumes, and canal seepage rates. In the validation stage, model output are compared with water

diversions through conveyance systems, return flow quantities, seasonal profiles of daily water demands, and reservoir levels throughout the irrigation season. In general, modeling results in the validation stage are within 1% to 2% of the actual recorded data (Irrigation Water Management Study Committee 2002a).

4.4 Data and Methodology

To assess the effects of climate change and combined effects of climate change and climate anomalies on the water demand of 12 irrigation districts and licensed private irrigation blocks of the SSRB, IDM has been driven by three types of input data: the first is the SSRB 68 years agro-climatic dataset for the base case period (1928-1995); the second is the base case agro-climatic dataset adjusted for the SRES climate projections of four GCMs for the 2020s, 2050s, and 2080s; and the third dataset represents selected years of the agro-climatic dataset within the base case period (1928-1995) affected by El Niño and La Niña episodes, re-sampled and adjusted for the SRES climate projections of 2050s.

As surface runoff is the primary source of water for the Ross Creek Irrigation District (RCID) and not from any of the main stem river water sources, it was not included in the approved water management plan for the SSRB (Alberta Environment 2006), and so it will not be considered in this study (Bob Riewe, Irrigation Modelling Specialist, Basin Water Management Branch, AAFRD, personal communication).

4.4.1 Base Case Scenario

The historical on-farm irrigation demand based on 68 years (1928-1995) of agro-climatic dataset, commonly known as the Gridded Prairie Climate Database or GRIPCD (McGinn et al. 1994), is considered as the base case scenario in the current study. The 50 km × 50 km gridded dataset provides a basis for daily, crop-specific ET computations for the irrigated area of southern Alberta. In the base case scenario, provisions have been made to expand irrigation water to irrigation districts in the Bow River basins by 20% and that of the Oldman River Basin water by 10%, respectively. However, private irrigation areas are limited to their current areas without expansion. The same dataset has been used in the study of the approved water management plan for the South Saskatchewan River Basin of Alberta (Alberta Environment 2006)

4.4.2 Climate Change Scenario

Primarily climate scenarios based on the projections of GCMs have been used in climatic change impact studies. To account for uncertainties associated with GCMs' projected climate scenarios, climate scenarios based on four GCMs forced by multiple SRES emission scenarios for the SSRB are considered. Among the four GCMs selected are Japan's CCSRNIES which projected the warmest climate for the SSRB, Germany's ECHAM4 which projected the driest climate, UK's HadCM3 which projected the wettest climate, and Canada's CGCM2 which projected changes that are in between the other three GCMs' projections. The three SRES

emission scenarios selected are the fossil fuel intensive, A1FI, and the mid-range emission, A21 and B21 scenarios (IPCC 2000).

Because of GCM's relatively coarse spatial and temporal resolutions, climatic variables (e.g., precipitation, temperature) obtained from GCMs should be downscaled to subgrid scales before they are adequate for basin scale climate change modeling. Downscaling of GCM output can either be done statistically, in which empirical relationships are established between GCM-scale climate variables (predictors) and local-scale meteorological variables (predictands) using statistical methods, or it can be done dynamically, where a Regional Climate Model is used to produce higher resolution outputs. In this study, climate change scenarios are statistically downscaled from GCM outputs using a delta change approach, as

$$\text{Eq. 4.10} \quad T_2 = T_1 + (T_2' - T_1')$$

$$\text{Eq. 4.11} \quad P_2 = P_1 \times \frac{P_2'}{P_1'}$$

where T_1 and P_1 are the baseline observed temperature and precipitation; T_2 and P_2 are the future temperature and precipitation; T_1' and P_1' are the GCM simulated mean temperature and precipitation for climate normal period (1961-1990); and T_2' and P_2' are GCM simulated mean temperature and precipitation for future climate scenarios, respectively.

Even though the Delta change approach incorporates projected changes of GCMs forced by SRES emission scenarios to key climate variables such as temperature and precipitation by a simple calculation, there are disadvantages to this simplistic approach: it assumes a constant bias; it only accounts for changes to the mean, maxima or minima of climate variables but it ignores possible changes to the variance of these climate variables. In the case of precipitation, properties such as temporal sequences of wet days or dry days are assumed to remain unchanged (Fowler et al. 2007, Wilby et al. 2009; Boyer et al. 2010). However, partly because it avoids tedious computation, the Delta change is a popular approach and has been used in many climate change studies on water resources (e.g. Lettenmaier and Gan 1990; Wood et al. 2002; Miller et al. 2003; Ryu et al. 2009; Boyer et al. 2010; Kerkhoven and Gan 2010; Islam and Gan 2012). It is considered a stable and robust method (Fowler et al. 2007; Graham et al. 2007).

The change fields of the mean monthly precipitation (% change) and the mean monthly temperature (absolute change) centered on the 2020s, 2050s and 2080s are collected from the Canadian Climate Change Scenarios Network. For each IPCC's SRES climate scenarios, 68 years (1928-1995) of temperature (T_1) and precipitation (P_1) data used to compute irrigation demand were adjusted as T_2 and P_2 to represent three future periods of the 21st century: 2020s, 2050s and 2080s. T_2 for each SRES scenario is estimated as $T_2 = T_1 + \Delta T$, where ΔT or $(T_2' - T_1')$ of Eq. 4.10, is the monthly temperature change projected for the SRES

scenario from that of the climate normal, while P_2 is estimated as $P_2 = P_1 \times \Delta P$, where ΔP or $(P_2') / (P_1')$ of Eq. 4.11 is a ratio of the monthly precipitation projected for that SRES scenario to that of the climate normal. Finally, the IDM was driven by these adjusted data to generate the irrigation consumptive demands for all irrigation blocks of SSRB subjected to the effects of climate change.

4.4.3 Classification of ENSO years

Different indices are used to represent the occurrence of an El Niño Southern Oscillation (ENSO) warm or cold phases: Sea Surface Temperature (SST) based indices (e.g., Niño-1+2, Niño-3, Niño-4, Niño-3.4, Japan Meteorological Agency index, Oceanic Niño Index, trans- Niño index); surface atmospheric pressure–based Southern Oscillation index; multivariate ENSO index (MEI); and Extended MEI. In this study, El Niño and La Niña years have been classified in terms of the Extended MEI which uses more than one variable to monitor ENSO. MEI is robust against a variety of changes in its computation and composition (Wolter and Timlin 2011; Royce et al. 2011). The original MEI is based on six observed variables: sea level pressure (SLP), zonal and meridional components of the surface wind, SST, surface air temperature, and total cloudiness fraction of the sky over the tropical Pacific (Wolter 2011a; Wolter and Timlin 1993; 1998; 2008). However, Wolter and Timlin (2011) presented a simplified version of MEI, namely, Extended MEI based on reconstructed SLP and SST fields. Similar to the

original MEI, the Extended MEI is computed for each of twelve sliding bi-monthly seasons (Wolter 2011b). The extended MEI values are also computed for four overlapping 4-month seasons, Nov–Feb, Feb–May, May–Aug, and Aug–Nov, from Dec1870/Jan1871 through Nov/Dec 2005 (135 full years). The extended MEI values are ranked from the lowest number (e.g., 1), which denote the strongest La Niña case for that four-month season, to the highest number (e.g., 135), which denote the strongest El Niño case. Using pre-defined percentiles, the ranked seasonal indices are then classified to indicate warm, cold, or neutral conditions, e.g., the top 25 percentiles (ranks 102 or above) represents warm episodes, the bottom 25 percentile (ranks 34 or lower) as cold episodes and in between (ranks 35-101) as neutral episodes. A year is classified to be an El Niño or a La Niña year if out of four overlapping 4-month seasons at least three indicates warm or cold episodes, respectively (please see **Appendix B** for details). This classification leads to 14 El Nino years between 1928 and 1995 (1930, 1940, 1941, 1958, 1959, 1969, 1977, 1980, 1983, 1987, 1991, 1992, 1993, and 1994) and 7 La Niña years (1950, 1955, 1956, 1971, 1974, 1975, 1989).

4.4.4 Climate Subjected to Combined Climate Change and ENSO Impact

A two step method was adopted to generate the agro-climatic dataset affected by the combined impacts of climate change and climate anomalies (e.g., El Niño, La Niña). First, from the base case agro-climatic dataset of SSRB, data that

correspond to El Niño and La Niña years were re-sampled using the standard bootstrap method with replacement to replace the 68-year (1928-1995) data. The bootstrap resampling process is equivalent to writing each of the El Niño or La Niña years on separate slips of paper and putting them in a box (Wilks 2011). Then, 30 slips of paper are drawn from the box and their data values recorded, but each slip is put back in the box and mixed before the next slip is drawn. Second, for each IPCC SRES climate scenarios of 2050s, the re-sampled agro-climatic dataset (e.g., maximum/minimum temperature, precipitation, and the potential evaporation) were adjusted.

IDM was then driven by these re-sampled adjusted data to generate the irrigation consumptive demands for all irrigation blocks of irrigation districts and private irrigation blocks of SSRB that reflect the combined effects of climate change and El Niño or La Niña episodes for 2050s. For each irrigation districts, the average annual irrigation demands from each irrigation block are estimated as the total areally weighted demand divided by the total area of that irrigation district. For private irrigation water uses, the average annual water demands for Red Deer, Bow, Oldman, and South Saskatchewan River sub-basin are estimated by dividing the total areally weighted demand for each sub-basin by the total area of that sub-basin.

4.5 Discussions of Results

As irrigation demands depend on the climatic condition, projected irrigation demands are primarily dependant on future precipitation and temperature changes in the SSRB predicted for some assumed climate change scenarios. Figure 4.2 shows percentage changes from climate normal of 1961-1990 in the mean annual precipitation ($\% \Delta P$) and changes in the mean annual temperature (ΔT) predicted by four GCMs forced by three SRES emission scenarios of IPCC for the study periods (2020s, 2050s, and 2080s), and climate scenarios of 2050s combined with ENSO (2050s+El Niño and 2050s+La Niña) episodes in the SSRB. Even though predicted changes in temperature and precipitation vary between GCMs and the selected SRES scenarios, in general, for SSRB, most GCMs project an increase in the precipitation while all GCMs project an increase in temperature with respect to the climate normal of 1961-1990. Compared to the climate normal, the temperature of the SSRB is projected to increase by 0.5-1.5 °C by 2020s, 2.5-4.25 °C by 2050s and 3-8°C by 2080s. On the average, temperature is expected to increase by 1.3°C, 3.1°C and 5.0 °C in 2020s, 2050s and 2080s, respectively while precipitation is projected to change between -4.25% and 3.5 % by 2020s, 1% and 8.0% by 2050s and -2.5% and 13.5 % by 2080s. When considering the potential combined impacts of climate change and climate anomalies such as El Niño, it seems on the average that precipitation could decrease by 5.15% while temperature could marginally increase by about

0.3°C than that of the SRES climate scenarios of 2050s alone. In contrast, for La Niña years, on the average precipitation could increase by about 9% while temperature decreases by about 0.3° C than that of SRES climate scenarios of 2050s. The effects of these changes in meteorological variables on irrigation demand under the impact of climate change, and combined impact of climate change and climate anomalies for the SSRB will be discussed below.

4.5.1 Simulated Irrigation Demand under Climate Change

4.5.1.1 Irrigation Districts

The IDM simulated water demand for the 12 irrigation districts for SSRB in response to the climate scenarios projected by the four GCMs forced by SRES emissions of IPCC considered, in comparison to that of the base case scenario (black square), are plotted with respect to projected temperature change (ΔT °C) in Figure 4.3.

Water demands simulated for irrigation districts under the base case scenario vary between the irrigations districts partly because of variations in the net growing season moisture deficit over SSRB. In SSRB, the growing season precipitation decreases from the west to east but the potential ET increases from west to east. As a result, the net growing season moisture deficit of SSRB also increases from west to east (Irrigation Water Management Study Committee 2002a). Eventually, irrigation districts located in the western region of SSRB (e.g.,

AID, LID, LNID, MID, MVID, and UID) has relatively lower water demand in the base case scenario than those located in the eastern region (e.g., BRID, EID, RID, SMRID, TID). The crop mix categories within the irrigation districts, as shown in Table 4.1, are also partially responsible for these variations in irrigation demand. In general, irrigation districts located on the western part of SSRB are cooler and have more moisture, and are dominated by cereal and forage crops. In contrast, irrigation districts located farther east, where temperature is higher and the growing season is longer, crop types are markedly more diverse (Irrigation Water Management Study Committee 2002a). The maximum (388 mm) and minimum (208 mm) annual average irrigation water demand for the base scenario were estimated for the EID and MVID, respectively. While considering the river basin, irrigation districts that located in the Bow River basin have a higher average annual water demand (358 mm) than that located in the Oldman River basin (293 mm).

The projected irrigation demands for future periods are found to be strongly related to temperature changes, and are dependent on the selected GCMs and SRES emission scenarios of IPCC. In general, all the irrigation districts will experience a projected increase in the irrigation demand for the 21st century (Figure 4.3). Table 4.2 shows percentage changes in irrigation demands for the 12 irrigation districts in 2020s, 2050s, and in 2080s with reference to the base case scenario. In general, the SRES scenarios of ECHAM4 and HadCM3 lead to the highest projected increase in the future water demands of SSRB, while that

of CGCM2 lead to a minimal projected increase in the water demand and that of CCSRNIES falls in between.

It was found that except for the MVID; most of the irrigation districts projected an average increase in an irrigation demand of about 7 % in 2020s, 12% in 2050s, and 13.5% in 2080s. Water demands for the AID (Figure 4.3a), EID (Figure 4.3c), LID (Figure 4.3d), LNID (Figure 4.3e), RID (Figure 4.3h), SMRID (Figure 4.3i), TID (Figure 4.3j), and WID (Figure 4.3l) are expected to increase by 7% in 2020s, but they could range over 0%-15%, 3%-12%, 0%-17%, 2%-13%, 2%-13%, 2%-12%, 3%-12%, and 3%-13%, respectively. Similarly, average water demands for the AID, EID, LID, LNID, RID, SMRID, TID, and WID will be 13% (4%-18%), 11%(3%-15%), 14%(3%-22%), 12% (4%-17%), 11% (3%-15%), 11% (4%-15%), 12% (5%-16%), and 12% (5%-17%), respectively, in 2050s; and 14% (3% -29%), 13% (4%-24%), 16% (4%-32%), 13% (4%-26%), 12% (3%-23%), 12% (4%-23%), 13% (5%-26%), and 14% (5%-28%), respectively in 2080s.

Future water demands for BRID (Figure 4.3b), MID (Figure 4.3f), and UID (Figure 4.3k) are expected to increase by 6%, 9%, and 8% in 2020s, but they could range over 3%-12%, 3%-16%, and 0%-17%, respectively. Similarly, average water demands for the BRID, MID, and UID were 11% (3%-16%), 12% (4%-17%), and 14% (2%-21%), respectively, in 2050s; and 13% (4% -26%), 13% (5%-27%), and 16% (4%-33%), respectively in 2080s.

Major portion (about 91%) of the crops in the MVID belong to forages category (e.g., Alfaalfa) which has the highest crop water requirement for optimum production (638 mm annually) in the SSRB and is expected to increase more under the impact of climate change. Eventually, IDM simulated future water demands for MVID (Figure 4.3g) are expected to increase by 12% (2%-22%), 20% (7%-29%), and 23% (7%-52%) in 2020s, 2050s and in 2080s, respectively.

4.5.1.2 Private Irrigation Blocks

Figure 4.4 shows the IDM simulated water demand for the private irrigation blocks in the Red Deer, Bow, Oldman, and the South Saskatchewan River sub-basin of the SSRB in response to the climate scenarios projected by the four GCMs forced by SRES emissions of IPCC considered in three future periods (2020s, 2050s, and 2080s) with reference to the base case scenario (black square) and plotted against projected temperature change (ΔT °C).

Similar to the irrigation districts, simulated water demands for the base case scenario for private irrigation blocks vary among the sub-basins of SSRB. Private irrigation blocks that withdrawal water from the South Saskatchewan River sub-basin show the maximum average annual irrigation demand (Figure 4.4d) as they are located at the eastern region of SSRB where the net growing season moisture deficit is the highest. As most of the private irrigation blocks in the Bow River sub-basin are located in the western region of the SSRB, they show relatively lower average annual irrigation demand (Figure 4.4b).

As expected, the projected irrigation demands for private irrigation blocks show a gradual increase in the 21st century. Like the irrigation districts, projected irrigation demands for the private irrigation blocks are also strongly related to temperature changes which depend on the selected GCMs and SRES emission scenarios of IPCC. Table 4.3 shows percentage changes in irrigation demands for the private irrigation blocks located in Red Deer, Bow, Oldman and South Saskatchewan River sub-basins in 2020s, 2050s, and in 2080s with reference to the base case scenario.

Water demands for private irrigation blocks in Red Deer River sub-basin (Figure 4.4a) are expected to increase by 24% in 2020s, but they could range 18%-31%. Similarly, average water demands for private irrigation blocks in the Red Deer River sub-basin will be 30% (22%-36%) in 2050s and 33% (22% -52%) in 2080s. Private irrigation blocks located in the Bow river basin (Figure 4.4b) show an increase in the irrigation water demand by 10% (5%-16%), 16% (8%-23%), and 18% (6%-35%) in 2020s, 2050s, and in 2080s, respectively. Private irrigation blocks in Oldman (Figure 4.4c) and South Saskatchewan (Figure 4.4d) River sub-basins show similar changes in future irrigation demands over the 21st century with projected increase in irrigation water demands by 5% (1%-10%) and 7% (3%-13%) in 2020s, 9% (2%-13%) and 12% (6%-17%) in 2050s, and 11% (2%-23%) and 14% (5%-26%) in 2080s, respectively.

Again, similar to the irrigation district, the projected SRES scenarios of ECHAM4 and HadCM3 predicted the highest increase in future water demands of private irrigation blocks of SSRB, while that of CGCM2 lead to a minimal predicted increase in the water demands and that of CCSRNIES falls in between.

4.5.1.3 Sensitivity of Changes in Irrigation Demand

Since compare to the base case scenario all of the climate change scenario runs show a increase in the mean annual irrigation demand for irrigation district and private irrigation blocks in SSRB, an analysis has been done to assess the amount of increase in irrigation demand per °C rise of temperature in the 21st century and are listed in Table 4.4. It was found that, the % increase in mean annual irrigation demand per °C rise in temperature for most of the irrigation districts are range from about 4% to 5.5% (average of 4.4%). The MVID shows about 7.33% increase in irrigation demand per °C rise of temperature. Higher increase in irrigation demand per °C rise of temperature is related to the major crops category of MVID (forages) which has the highest crop water requirement for optimum production. Private irrigation blocks located at the Red Deer River basin show largest % increase in irrigation demand per °C rise of temperature (about 12.9%). Private irrigation blocks located at Bow, Oldman and South Saskatchewan River sub-basins projects about 6.05%, 3.27%, and 4.41% increase in annual irrigation demand per °C rise of temperature in the 21st century.

4.5.2 Simulated Irrigation Demand under the Combined Impacts of Climate Change and Climate Anomalies

4.5.2.1 Irrigation Districts

The percentage changes in the average annual water demand of the irrigation districts simulated by IDM for the SRES climate scenarios of 2050s combined with ENSO ('2050s+El Niño' and '2050s+La Niña'), with respect to that of 2050s climate scenarios alone are plotted against the precipitation and temperature changes in 2050s in Figure 4.5 and also shown in Table 4.2. It was found that water demands for the irrigation districts that are expected to increase by 12% under the climate change scenarios of 2050s, could subject to less increase by 2050s under the potential combined impact of climate change and climate anomalies, if the climate anomaly considered is El Niño (Figure 4.5). In contrast, if the climate anomaly considered is La Niña, then the combined impact of climate change and La Niña would only lead to a marginally higher projected irrigation demand for most of irrigation districts (e.g., AID, EID, MID, RID, SMRID, TID, WID) by 2050s, and a marginally lower projected irrigation demand for other irrigation districts (e.g., BRID, LID, LNID, and UID) by 2050s, than only if the impact of climate change is considered (Figure 4.5).

While comparing to the climate change scenario of 2050s, most of the irrigation districts located in the western regions (e.g., LID, MID, MVID, and UID) of SSRB show a modest increase (about 12.4% lower than that of 2050s) in irrigation

water demands under the combined case if the climate anomaly considered is El Niño (Figure 4.5d, Figure 4.5f, Figure 4.5g, and Figure 4.5k). Irrigation districts that located in the eastern region (e.g., BRID, EID, SMRID, and RID) show a moderate increase (about 5% lower than that of 2050s) in irrigation demands in the combined case if the climate anomaly considered is El Niño (Figure 4.5b, Figure 4.5c, Figure 4.5i, and Figure 4.5h). The averaged minimum (about 3%) and maximum (about 22%) decrease in irrigation demands under the '2050s+El Niño' scenario with reference to the 2050s climate change scenario is projected for WID (Figure 4.5l) and MVID (Figure 4.5g) located in the north-central and western region of SSRB, respectively.

In general El Niño events have overall drying effect on SSRB which can be explained from composites of 500-hPa geopotential height anomalies associated with El Niño. In an El Niño event there is a deeper than normal Aleutian low, an amplification, and eastward displacement of the western Canadian ridge. This upper-atmospheric flow pattern is likely associated with a split in the jet stream over North America: a weaker branch diverted northward and a lower subtropical branch shifted southward. The southern Canadian region as the SSRB lies in between the two jets and receive lower than normal precipitation resulting overall drying impacts (Shabbar et al. 1996; Shabbar and Khandekar 1996; Gan et al. 2007). However, despite of this general drying effect, there will be a decrease in irrigation water demands for irrigation districts under the '2050s+El Niño' combined scenario than that of the climate scenarios of 2050s

only. This is because during the irrigation period of SSRB (early May to mid October), the average precipitation is 3.81% higher and the average potential evaporation is 0.45% higher when the climate change scenarios are also affected by El Niño episodes than only if the impact of climate change is considered.

If climate anomaly considered is La Niña, irrigation districts that located in the eastern region of SSRB show marginal increase or no change in irrigation water demands from that of 2050s climate change scenarios alone, e.g., projected annual irrigation demand for EID (Figure 4.5c) and RID (Figure 4.5h) will be about 3% higher in '2050s+La Niña' scenarios than that of 2050s alone, but projected annual demand for TID (Figure 4.5j) and SMRID (Figure 4.5i) almost remain the same as that of 2050s alone. In contrast, projected water demands for irrigation districts located in the western region (e.g., LID, LNID, MVID, and UID) will be about 2% lower in the '2050s+La Niña' scenarios than in the 2050s climate change scenarios (Figure 4.5d, Figure 4.5e, Figure 4.5g, and Figure 4.5k). The maximum increase (about 5%) in average irrigation water demands in the '2050s+La Niña' scenarios with respect to the 2050s scenarios are projected for the RID (Figure 4.5h).

In general La Niña events have wetting effects on SSRB which can be explained from composites of 500-hPa geopotential height anomalies associated with La Niña. In a La Niña event there is a weaker than normal Aleutian low, an erosion, and westward displacement of the western Canadian ridge. The upper-

atmospheric flow associated with this circulation pattern includes stronger westerlies moving across the eastern Pacific and into southern Canada. As a result, the moist air originating from the Pacific result in positive precipitation anomalies over southern Canada (Shabbar et al. 1996; Shabbar and Khandekar 1996; Gan et al. 2007). However, during early May to mid October, the average precipitation and potential evaporation are projected to be 1.84% and 0.73% lower, respectively, than that of 2050s which lead to a marginal increase in the irrigation water demands for these irrigation districts.

4.5.2.2 Private Irrigation Blocks

The percentage changes in the IDM simulated average annual water demand for the private irrigation blocks of SSRB located in Red Deer, Bow, Oldman, and South Saskatchewan River sub-basins for the SRES climate scenarios of 2050s combined with ENSO, with respect to that of 2050s climate change scenarios alone are plotted against the precipitation and temperature changes in 2050s in Figure 4.6. It was found that, even though water demands for the private irrigation blocks are expected to increase by 17% in 2050s, while considering the potential combined impact of climate change and climate anomalies, a less increase in irrigation demands by 2050s are projected for all private irrigation blocks if the climate anomaly considered is El Niño (Figure 4.6). In contrast, if the climate anomaly considered is La Niña, then the combined impact of climate change and La Niña would lead to higher projected irrigation demands for most

private irrigation blocks located in Red Deer, Bow, and Oldman River sub-basins by 2050s, and a marginally lower projected irrigation demands for private irrigation blocks in the South Saskatchewan River sub-basin by 2050s, than only if the impact of climate change alone is considered.

Table 4.3 shows the percentage changes in irrigation demands for combined scenarios (2050s+El Niño and 2050s+La Niña) over that of the 2050s climate change scenarios for private irrigation blocks located in Red Deer, Bow, Oldman and South Saskatchewan River sub-basins. While comparing to the climate change scenario of 2050s, projected water demands in the combined scenarios for private irrigation blocks located in Red Deer, Bow, and Oldman and South Saskatchewan River sub-basins are 5%, 3%, 6%, and 7% lower, respectively, than that of 2050s if the climate anomaly considered is El Niño (Figure 4.6a, Figure 4.6b, Figure 4.6c, and Figure 4.6d). If the climate anomaly considered is La Niña, private irrigation blocks located in Red Deer, Bow, and Oldman River basin show a respective 6%, 4%, and 1% higher projected irrigation demands under the combined scenarios than that under the 2050s climate change scenarios alone. In contrast, projected irrigation demands for private irrigation blocks in the South Saskatchewan River sub-basin under 2050s+ La Niña episodes is about 2% lower than that of 2050s climate change scenarios.

Again, similar to the irrigation districts, irrigation water demands for private irrigation blocks under 2050s+El Niño combined scenarios are projected to be

higher than that of the climate change scenarios of 2050s alone because of higher projected precipitation and evaporation by about 3.81% and 0.45%, respectively in early May to mid October. In contrast, for the same period the average precipitation and potential evaporation under 2050s+ La Niña scenarios are projected to be 1.84% and 0.73% lower, respectively, than that of climate change scenarios of 2050s alone, which lead to a marginal increase in irrigation water demands for private irrigation blocks.

4.6 Summary and Conclusions

In this study, potential impacts of climate change on the future irrigation demand of SSRB are simulated by IDM of AAFRD on the basis of climate change scenarios projected by four GCMs forced by three SRES emission scenarios of IPCC (2001) for 2020s, 2050s, and 2080s of the 21st century. Furthermore, the combined impacts of climate change and climate anomalies (ENSO) for the 2050s are simulated by driving IDM with the meteorological dataset re-sampled from selected years of the SSRB agro-climatic dataset within the base case period (1928-1995) affected by El Niño and La Niña episodes.

IDM's simulations show that irrigation demand in the base case scenarios varies with the location of irrigation districts and location of private irrigation blocks. Irrigation districts located in the western region of SSRB show lower water demand in the base case scenario than those located in the eastern region.

Private irrigation blocks that are located in the South Saskatchewan River sub-basin, which is the eastern region of the SSRB, has the maximum mean annual irrigation demand. In contrast, most of the private irrigation blocks in the Bow River sub-basin, that are located in the western region of the SSRB, show a lower mean annual irrigation demand than others. These variations in irrigation demand between sub-basins of SSRB for the base case scenario are partly caused by variations in the net growing season moisture deficits over the SSRB, and partly because of the variations of crop mix categories within the irrigation districts and private irrigation blocks.

IDM's simulations for 2020s, 2050s, and 2080s only under the potential impact of climate change show a general increasing trend in the irrigation demand in the 21st century for both the irrigation districts and the private irrigation blocks. On an average, water demands for the irrigation districts and private irrigation blocks are expected to increase by 7% and 11% in the 2020s, but they could range from 2% to 13% and from 6% to 17%, respectively. Similarly, the average water demands for the irrigation districts and private irrigation blocks were 12% (4%-17%) and 17% (9%-22%), respectively, in the 2050s; and 13% (4% -26%) and 18% (8%-33%), respectively in the 2080s.

While considering the combined impact of climate change and climate anomalies (ENSO) for the 2050s, on an average, the projected water demand for irrigation district will be 8% lower in the combined '2050s+El Niño' scenarios but only be

1% higher in the combined '2050s+La Niña' scenarios than that of climate change scenarios of 2050s only. For the private irrigation blocks, on an average, the projected irrigation water demand will be 6% lower in the '2050s+El Niño' scenarios but still 1% higher in the combined '2050s+La Niña' scenarios than that of climate change scenarios of 2050s only.

4.7 References

Alberta Environment (1990) South Saskatchewan River Basin Water Management Policy, Planning Division. Alberta Environment.

Alberta Environment (1991) South Saskatchewan River Basin Water Allocation Regulation. Alberta Environment.

Alberta Environment (2003). "South Saskatchewan River Basin Water Management Plan Phase 2: Scenario Modelling Results Part 1." Alberta Environment.

Alberta Environment (2005). " South Saskatchewan River Basin Water Allocation." Alberta Environment.

Alberta Environment (2006) Approved Water Management Plan for the South Saskatchewan River Basin (Alberta). Alberta Environment.

Barrow, E., and Yu, G. (2005). "Climate Scenarios for Alberta." *A Report Prepared for the Prairie Adaptation Research Collaborative (PARC) in co-operation with Alberta Environment.*

Bates, B.C., Kundzewicz, Z.W., Wu, S. and Palutikof, J.P. (2008). " Climate Change and Water." Technical Paper of the Intergovernmental Panel on Climate Change, IPCC Secretariat, Geneva.

- Boyer, C., Chaumont, D., Chartier, I., and Roy, A.G. (2010). "Impact of climate change on the hydrology of St. Lawrence tributaries." *J. Hydrol.*, 384 (1-2), 65–83.
- Fischer, G., Tubiello, F. N., Velthuisen, H., and Wiberg, D. A. (2007). "Climate change impact on irrigation water requirement: Effect of mitigation, 1990-2080." *Technological Forecasting & Social Change*, 74, 1083-1107.
- Fowler, H. J., Blenkinsop, S., and Tebaldi, C. (2007). "Linking climate change modelling to impacts studies: Recent advances in downscaling techniques for hydrological modelling." *Int. J. Climatol.*, 27(12), 1547-1578.
- Gan, T.Y. (2000). "Reducing vulnerability of water resources of Canadian Prairies to potential droughts and possible climatic warming." *Water Resour. Manage.*, 14(2),111–135.
- Gan, T. Y., Gobena, A. K., and Wang, Q. (2007). "Precipitation of southwestern Canada - Wavelet, Scaling, Multifractal Analysis, and Teleconnection to Climate Anomalies." *J. of Geophysical Research*, 112, D10110.
- Graham, L.P., Hagemann, S., Jaun, S., and Beniston, M. (2007). "On interpreting hydrological change from regional climate models." *Climatic Change*, 81, 97–122.
- Hansen, J. W., Hodges, A.W., and Jones, J.W. (1998). "ENSO influences on Agriculture in the South-eastern United States." *J Climate*, 11, 404-411.

IPCC (2000). "Summary for Policymakers: Emissions Scenarios, A Special Report of Working Group III of the Intergovernmental Panel on Climate Change." *Cambridge University Press, UK.*

IPCC (2001) "Climate Change 2001: The Scientific Basis. Contribution of Working Group I to the Third Assessment Report of the Intergovernmental Panel on Climate Change." *Cambridge University Press, Cambridge, United Kingdom and New York, NY, USA.*

Irrigation Branch, Alberta Agriculture, Food and Rural Development (2000). "Irrigation in Alberta". Agdex 560 – 1.

Irrigation Water Management Study Committee (2002a). "South Saskatchewan River Basin: Irrigation in the 21st Century. Volume 1: Summary Report." *Alberta Irrigation Projects Association. Lethbridge, Alberta.*

Irrigation Water Management Study Committee (2002b). "South Saskatchewan River Basin: Irrigation in the 21st Century. Volume 2: On-Farm Irrigation Water Demand." *Alberta Irrigation Projects Association. Lethbridge, Alberta.*

Irrigation Water Management Study Committee (2002c). "South Saskatchewan River Basin: Irrigation in the 21st Century. Volume 3: Conveyance Water Management." *Alberta Irrigation Projects Association. Lethbridge, Alberta.*

Irrigation Water Management Study Committee (2002d). "South Saskatchewan River Basin: Irrigation in the 21st Century. Volume 4: Modeling Irrigation Water Management." *Alberta Irrigation Projects Association. Lethbridge, Alberta.*

Irrigation Water Management Study Committee (2002e). "South Saskatchewan River Basin: Irrigation in the 21st Century. Volume 5: Economic Opportunities and Impacts." *Alberta Irrigation Projects Association. Lethbridge, Alberta.*

Islam, Z. and Gan, T. (2012). "Effects of Climate Change on the Surface Water Management of South Saskatchewan River Basin." *J. Water Resour. Plann. Manage.* doi: 10.1061/(ASCE)WR.1943-5452.0000326 .

Jacob, J.M., Satti, S.R., Duke, M.D., and Jones, J.W. (2006). "Climate variability and impact on irrigation water demand in Northeast Florida." *In Garbecht, J.D. and Piechota, T.C. (Eds.), Climate Variation, climate change, and water resources engineering. 143-155.*

Jansen, M.E., Burman, R.D., and Allen, R.G. (1990). "Evapotranspiration and Irrigation Water Requirements." *ASCE Manuals and Reports on Engineering Practice No. 70. American Society of Civil Engineers. New York, NY.*

Kerkhoven, E. and Gan, T.Y. (2010). "Differences and sensitivities in potential hydrologic impact of climate change to regional-scale Athabasca and

Fraser River basins of the leeward and windward sides of the Canadian Rocky Mountains respectively." *Climatic Change*, 106(4), 583-607.

Lettenmaier, D.P. and Gan, T.Y. (1990). "Hydrologic sensitivity of the Sacramento-San Joaquin River Basin, California, to global warming." *Water Resour. Res.*, 26(1), 69–86.

McGinn, S.M., Akinremi, O.O., and Barr, A.G. (1994). "Description of the Grided Prairie Climate Database(GRIPCD) for years 1960-1989." *Agriculture and Agri-Food Canada. Publication No. 1522. Ottawa, ON.*

Meza, F.J. (2005). "Variability of reference evapotranspiration and water demands: Association to ENSO in the Mapio River Basin, Chile." *Global and Planetary Change*, 47(2-4), 212-220.

Miller, N.L., Bashford, K.E., and Strem, E. (2003). "Potential impacts of climate change on California hydrology." *J. American Water Resour. Assoc.*, 39(4), 771–784.

Royce, F.S., Fraisse, C.W., and Baigorria, G.A. (2011). "ENSO classification indices and summer crop yields in the Southeastern USA." *Agricultural and Forest Meteorology*, 151, 817–826.

Ryu, J. H., Palmer, R. N., Wiley, M. W., and Jeong, S. (2009). "Mid-Range Streamflow Forecasts Based on Climate Modeling-Statistical Correction and Evaluation." *J American Water Resour Assoc.*, 45(2), 355-368.

- Shabbar, A. and Khandekar, M. (1996). "The impact of El Nino-Southern Oscillation on the temperature field over Canada." *Atmosphere-Ocean*, 34, 401–416.
- Shabbar, A., Bonsal, B. and Khandekar, M. (1997). "Canadian precipitation patterns associated with the Southern Oscillation." *Journal of Climate*, 10, 3016–3027.
- Shen, S.S.P., Yin, H., Canon, K., Howard, A., Chenter, S., and Karl, T.R. (2005). "Temporal and Spatial Changes of the Agroclimate in Alberta, Canada, from 1901 to 2002." *Journal of Applied Meteorology*, 44, 1090-1105
- Thomas, A. (2008). "Agricultural irrigation demand under present and future climate scenarios in China." *Global and Planetary Change*, 60, 306-326.
- Wilby, R. L., Troni, J., Biot, Y., Tedd, L., Hewitson, B. C., Smithe, D. M. and Suttonf, R. T. (2009). "A review of climate risk information for adaptation and development planning." *Int. J. Climatol.*, 29, 1193–1215.
- Wilks, D. S. (2011). "Statistical methods in the atmospheric sciences (Vol. 100)". Academic press.
- Wolter, K. (Klaus.Wolter@noaa.gov) (2011a). "Multivariate ENSO Index (MEI)." (<http://www.esrl.noaa.gov/psd/enso/mei/>). *National Oceanic and Atmospheric Administration, Earth System Research Laboratory, Physical Sciences Division*.

- Wolter, K. (Klaus.Wolter@noaa.gov) (2011b). "Extended Multivariate ENSO Index (MEI.ext)." (<http://www.esrl.noaa.gov/psd/enso/mei.ext/>). *National Oceanic and Atmospheric Administration, Earth System Research Laboratory, Physical Sciences Division.*
- Wolter, K. and Timlin, M. (1993). "Monitoring ENSO in COADS with a seasonally adjusted principal component index." *In: Proceedings of the 17th Climate Diagnostics Workshop, Univ. of Oklahoma, Norman, OK*, pp. 52–57.
- Wolter, K. and Timlin, M. (1998). "Measuring the strength of ENSO—how does 1997/98 rank?" *Weather*, 53 (9), 315–324.
- Wolter, K. and Timlin, M. (2008). "An improved multivariate ENSO index (MEI)—a progress report." *In: Session 11: Technical Issues. Climate Prediction Applications Science Workshop, Chapel Hill, North Carolina (March 4–7).*
- Wolter, K. and Timlin, M. (2011). "El Niño/Southern Oscillation behaviour since 1871 as diagnosed in an extended multivariate ENSO index (MEI.ext)." *Int. J. Climatol.* 31, 1074–1087.
- Wood, A. W., Maurer, E. P., Kumar, A., and Lettenmaier, D. P. (2002). "Long-range experimental hydrologic forecasting for the eastern United States." *J Geophysical Res*, 107(D20), ACL 6-1-ACL 6-15.
- Xu, C.-Y., and Singh, V.P., (2004). "Review on Regional Water Resources Assessment Models under Stationary and Changing Climate." *Water Resour. Manage.*, 18, 591–612.

Zhou, Y., Zwahlen, F., Wang, Y, and Li, Y (2010). "Impact of climate change on irrigation requirement in terms of groundwater resources."
Hydrogeology Journal. 18, 1571-1582

Table 4.1 Characteristics of South Saskatchewan River Basin (SSRB) Irrigation Districts (Irrigation Water Management Study Committee 2002a; Irrigation Branch, Alberta Agriculture Food and Rural Development, 2000)

Irrigation District (ID)	Total Area (million m ²)	Irrigation Area (million m ²)	Length of Distribution System (km)	License Water Volume (million m ³)	Crop Mix (%)			
					Cereal	Forages	Oilseeds	Specialty Crops
Aetna (AID)	146	78	27	11.1	19.3	79.6	1.1	0
Bow River (BRID)	8,545	8,021	1,058	619.2	43.7	27.5	13.3	15.5
Eastern (EID)	11,376	11,127	1,784	919.0	29.6	52.4	8	10
Leavitt (LID)	193	186	56	14.8	20.5	79.5	0	0
Lethbridge Northern (LNID)	6,268	4,953	650	391.0	26.5	56.8	7.4	9.3
Magrath (MID)	741	453	106	41.9	49.8	40.5	9.3	0.4
Mountain View (MVID)	151	43	35	9.9	8.4	91	0.6	0
Ross Creek (RCID)	49	43	20	3.7	0	100	0	0
Raymond (RID)	1,852	1,306	247	99.9	35.9	54.3	9.7	0.1
St. Mary River (SMRID)	14,859	13,871	1,719	890.6	40.3	28.7	12.4	18.6
Taber (TID)	3,318	3,111	364	194.9	27.9	33.4	3	35.7
United (UID)	1,390	699	227	83.9	47.2	46.2	6.3	0.3
Western (WID)	3,567	2,738	1,077	342.9	38	46.2	12.4	3.4

Table 4.2 The percentage changes in irrigation demand for the 12 irrigation districts in 2020s, 2050s, 2080s, and combined scenarios (2050s+ El Niño and 2050s+ La Niña) from the base case scenario with respect to climate change scenarios projected by four General Circulations Models (CCSRNIES, CGCM2, ECHAM4, HadCM3) forced by three Special Report on Emissions Scenarios (SRES) emissions (A1FI, A21 and B21) of Intergovernmental Panel on Climate Change (IPCC) for the South Saskatchewan River Basin (SSRB)

Irrigation District ¹	% Change in average annual demand from base scenario									% Change in average annual demand from 2050s					
	2020s			2050s			2080s			El Niño+2050s			La Niña+2050s		
	Min	Ave	Max	Min	Ave	Max	Min	Ave	Max	Min	Ave	Max	Min	Ave	Max
AID	0	7	15	4	13	18	3	14	29	-7	-6	-1	-9	0	2
BRID	3	6	12	3	11	16	4	13	26	-9	-6	-5	-4	-1	2
EID	3	7	12	3	11	15	4	13	24	-5	-4	-2	0	1	3
LID	0	7	17	3	14	22	4	16	32	-14	-12	-3	-9	-2	0
LNID	2	7	13	4	12	17	4	13	26	-9	-7	-6	-3	-2	0
MID	3	9	16	4	12	17	5	13	27	-10	-8	-7	-7	0	1
MVID	2	12	22	7	20	29	7	23	52	-24	-22	-21	-9	-1	2
RID	2	7	13	3	11	15	3	12	23	-6	-4	-3	-7	5	8
SMRID	2	7	12	4	11	15	4	12	23	-8	-6	-5	-6	0	1
TID	3	7	12	5	12	16	5	13	26	-10	-9	-7	-7	0	2
UID	0	8	17	2	14	21	4	16	33	-12	-11	-10	-9	-2	2
WID	3	7	13	5	12	17	5	14	28	-6	-3	-2	2	3	4

Table 4.3 The percentage changes in irrigation demand for the private irrigation blocks in 2020s, 2050s, 2080s, and combined scenarios (2050s+ El Niño and 2050s+ La Niña) from the base case scenario with respect to climate change scenarios projected by four General Circulations Models (CCSRNIES, CGCM2, ECHAM4, HadCM3) forced by three Special Report on Emissions Scenarios (SRES) emissions (A1FI, A21 and B21) of Intergovernmental Panel on Climate Change (IPCC) for the South Saskatchewan River Basin (SSRB).

River Basin	% Change in average annual demand from base case scenario									% Change in average annual demand from 2050s					
	2020s			2050s			2080s			El Niño+2050s			La Niña+2050s		
	Min	Ave	Max	Min	Ave	Max	Min	Ave	Max	Min	Ave	Max	Min	Ave	Max
Red Deer	18	24	31	22	30	36	22	33	52	-7	-5	-2	2	6	9
Bow	5	10	16	8	16	23	6	18	35	-4	-3	-2	-1	4	7
Oldman	1	5	10	2	9	13	2	11	23	-6	-6	-4	-1	1	4
S. Saskatchewan	3	7	13	6	12	17	5	14	26	-8	-7	-5	-3	-2	0

Table 4.4 Percentage Changes in Future Irrigation Demand Per °C Rise in Temperature in the 21st Century for Irrigation districts and Private Irrigation Blocks for Different sub-basins of the South Saskatchewan River Basin (SSRB) considered in this study

Irrigation Districts or Private Irrigation Blocks	% Increase in Irrigation Demand Per °C Rise in Temperature
<i>Irrigation Districts</i>	
Aetna (AID)	3.93
Bow River (BRID)	4.09
Eastern (EID)	4.17
Leavitt (LID)	4.38
Lethbridge Northern (LNID)	4.50
Magrath (MID)	5.48
Mountain View (MVID)	7.33
Ross Creek (RCID)	4.03
Raymond (RID)	4.08
St.Mary River (SMRID)	4.37
Taber (TID)	4.57
United (UID)	4.53
Western (WID)	3.93
<i>Private Irrigation Blocks</i>	
Red Deer Sub-Basin	12.90
Bow Sub-Basin	6.05
Oldman Sub-Basin	3.27
S. Saskatchewan Sub-Basin	4.41

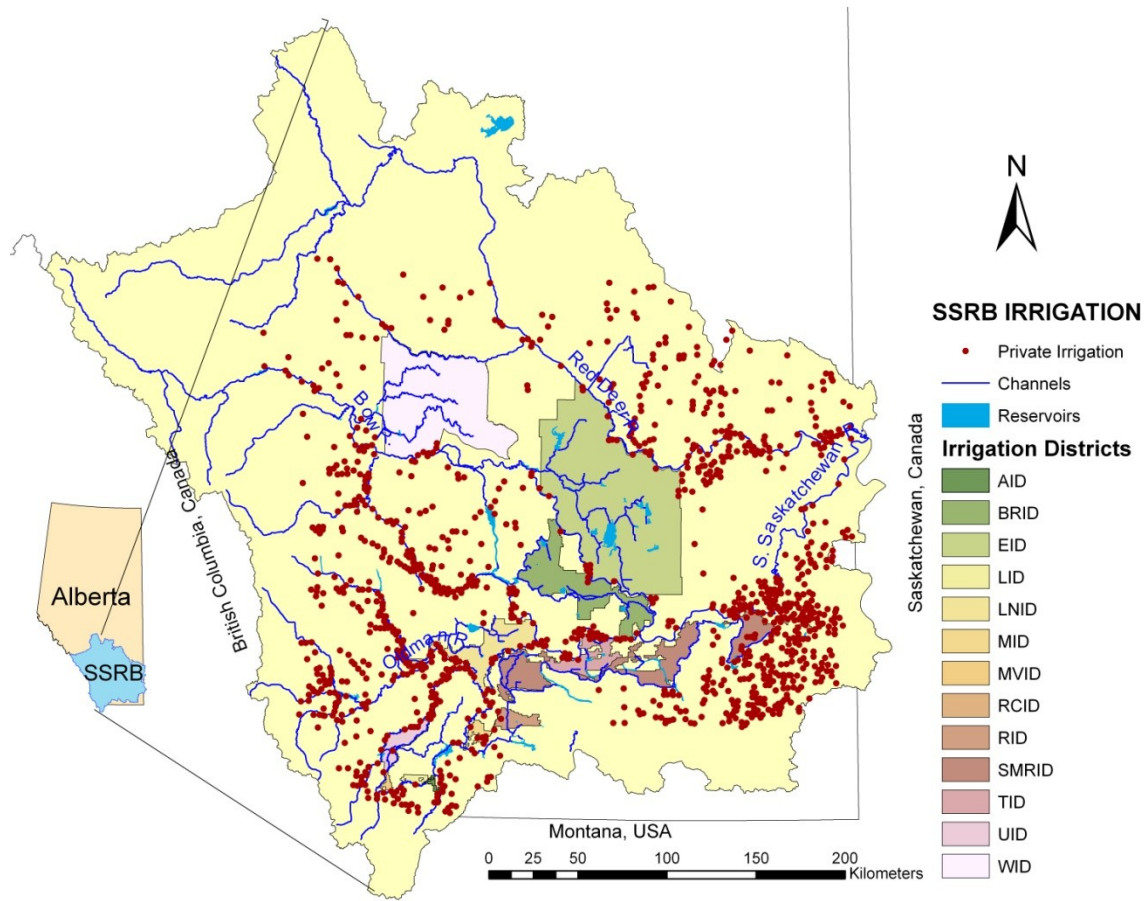


Figure 4.1 Irrigation districts and private irrigation in the South Saskatchewan River Basin (SSRB).

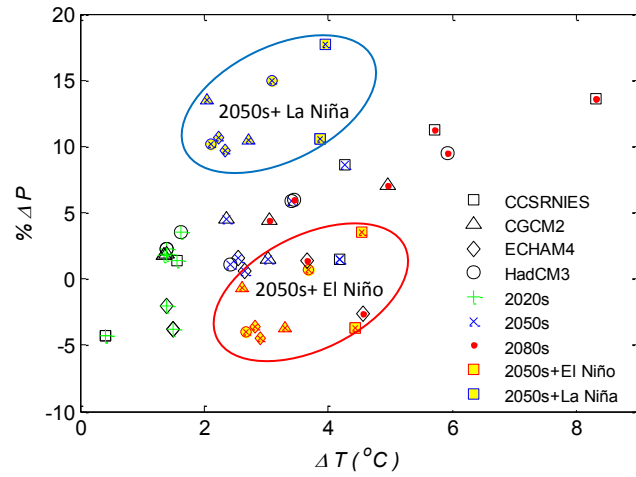


Figure 4.2 Percentage changes in the mean annual precipitation ($\% \Delta P$) and changes in the mean annual temperature (ΔT) for 2020s, 2050s, and 2080s climate scenario projected by four General Circulations Models (CCSRNIES, CGCM2, ECHAM4, HadCM3) forced by three Special Report on Emissions Scenarios (SRES) emissions (A1FI, A21 and B21) of Intergovernmental Panel on Climate Change (IPCC), and for climate scenarios of 2050s combined with El Niño and La Niña episodes for the South Saskatchewan River Basin (SSRB) as compared to the climate normal (1960-1991).

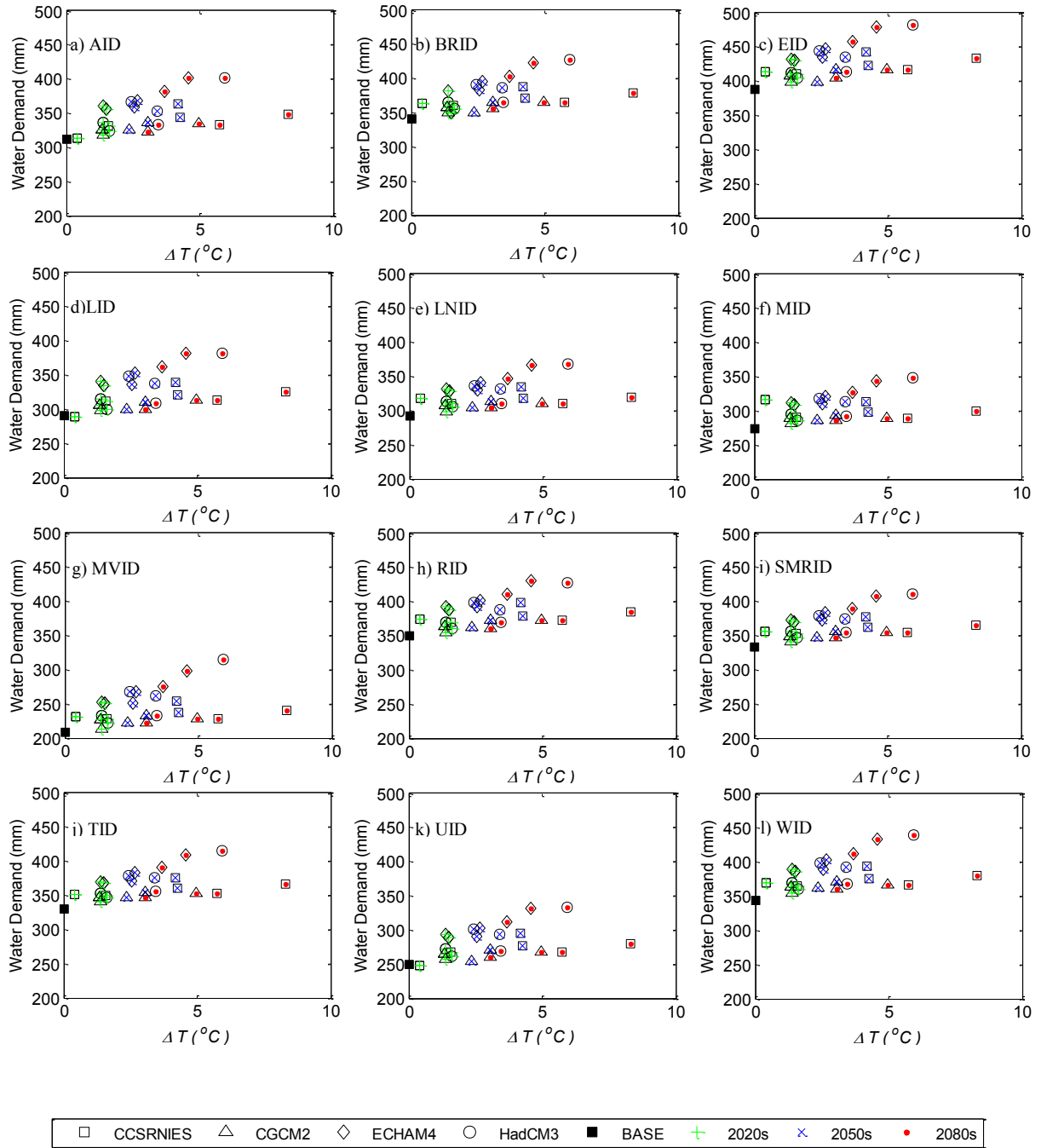


Figure 4.3 Irrigation District Model (IDM) simulated annual average irrigation demand for 12 irrigation districts of SSRB in comparison to that of the base case scenario (black square) with respect to the climate change scenarios projected by four GCMs (CCSRNIES, CGCM2, ECHAM4, and HadCM3) forced by three SRES emissions (A1FI, A21, and B21) of IPCC for 2020s, 2050s, and 2080s.

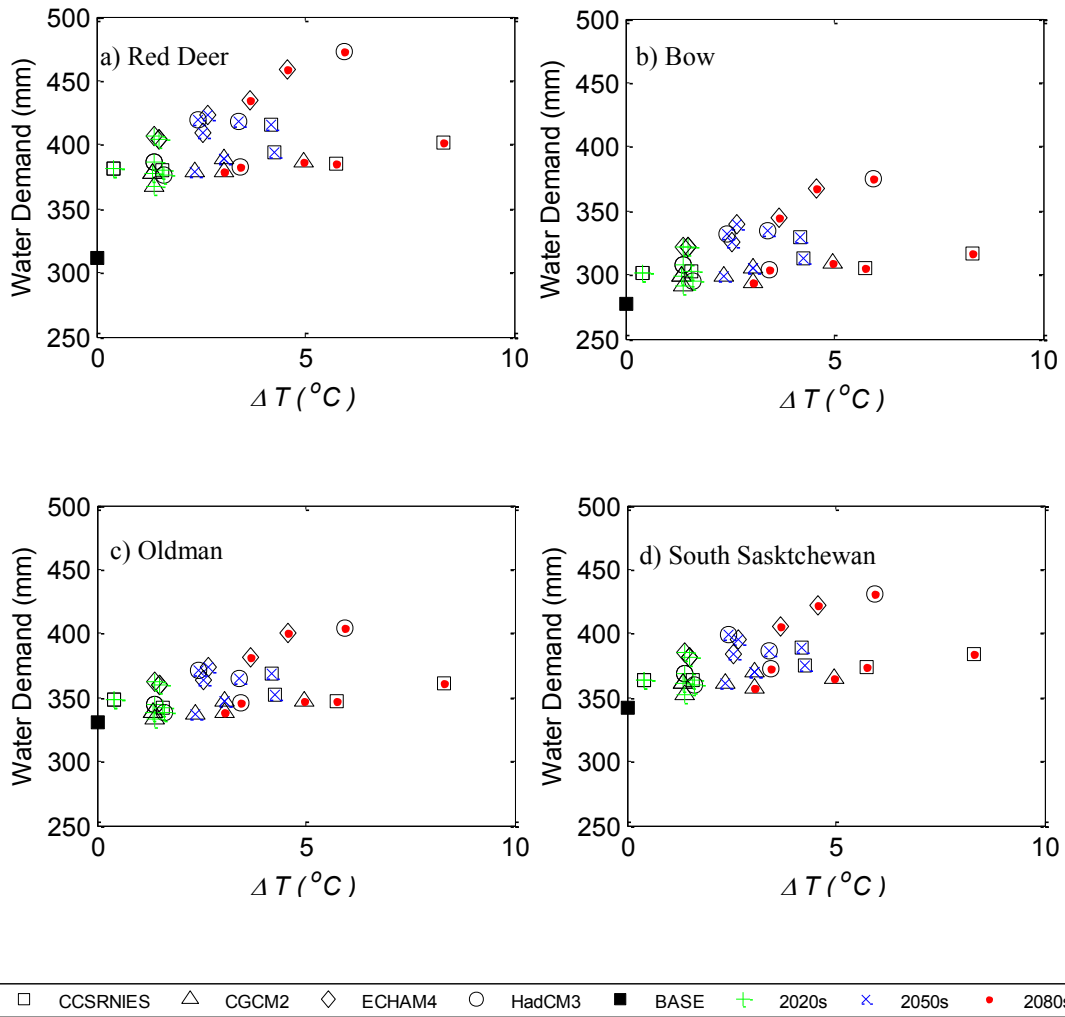


Figure 4.4 Irrigation District Model (IDM) simulated annual average irrigation demand for private irrigation blocks in Red Deer (a), Bow (b), Oldman (c), and South Saskatchewan River (d) sub-basins of SSRB in comparison to that of the base scenario (black square) with respect to the climate change scenarios projected by four GCMs (CCSRNIES, CGCM2, ECHAM4, and HadCM3) forced by three SRES emissions (A1FI, A21, and B21) of IPCC for 2020s, 2050s, and 2080s.

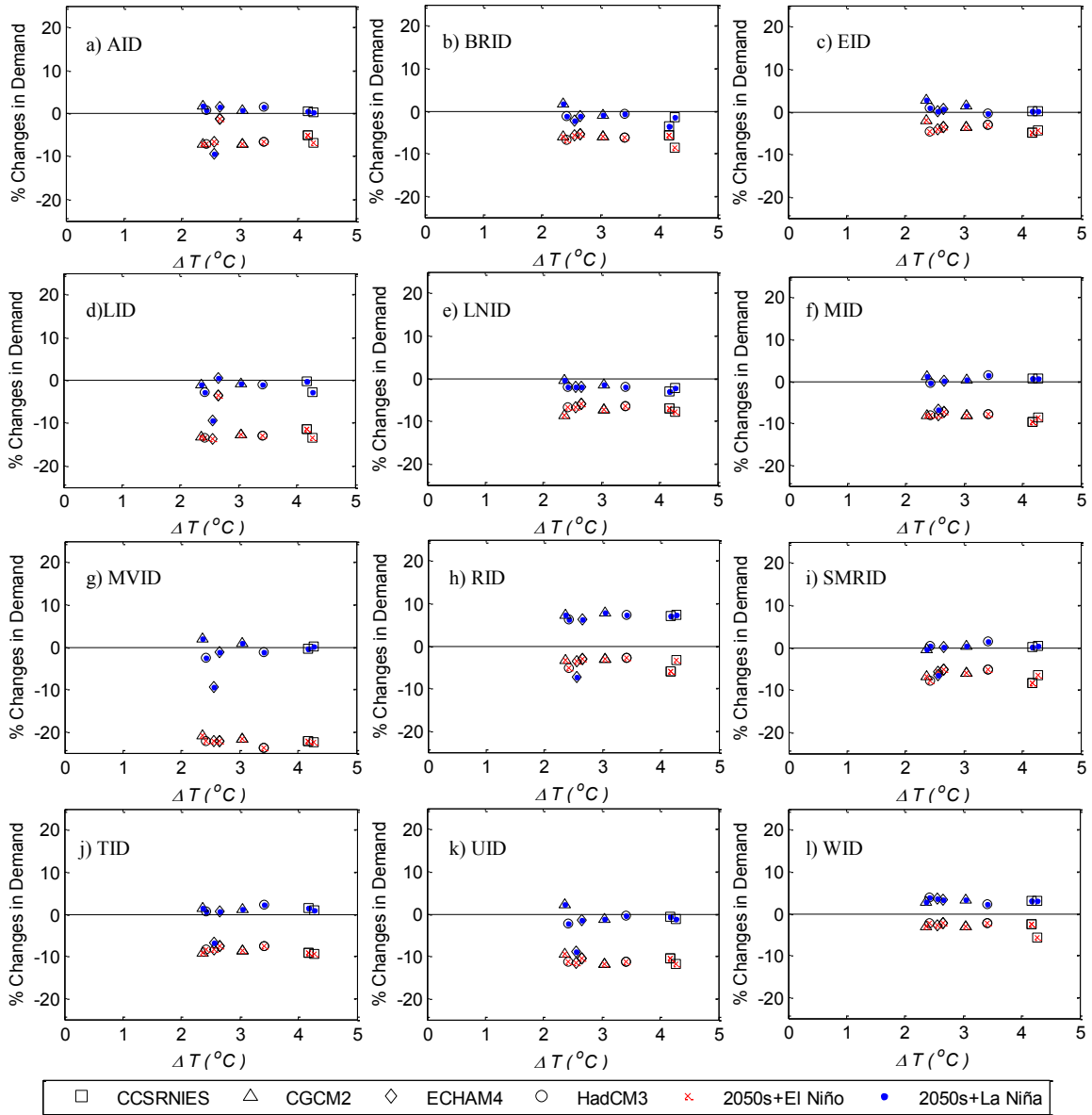


Figure 4.5 Irrigation District Model (IDM) simulated percentage changes in average annual irrigation demand for 12 irrigation districts of South Saskatchewan River Basin (SSRB) versus ΔT as compared to the climate scenarios of 2050s with respect to the combined scenarios projected by four General Circulations Models (CCSRNIES, CGCM2, ECHAM4, and HadCM3) forced by three Special Report on Emissions Scenarios (SRES) emissions (A1FI, A21, and B21) of Intergovernmental Panel on Climate Change (IPCC) combined with El Niño and La Niña episodes.

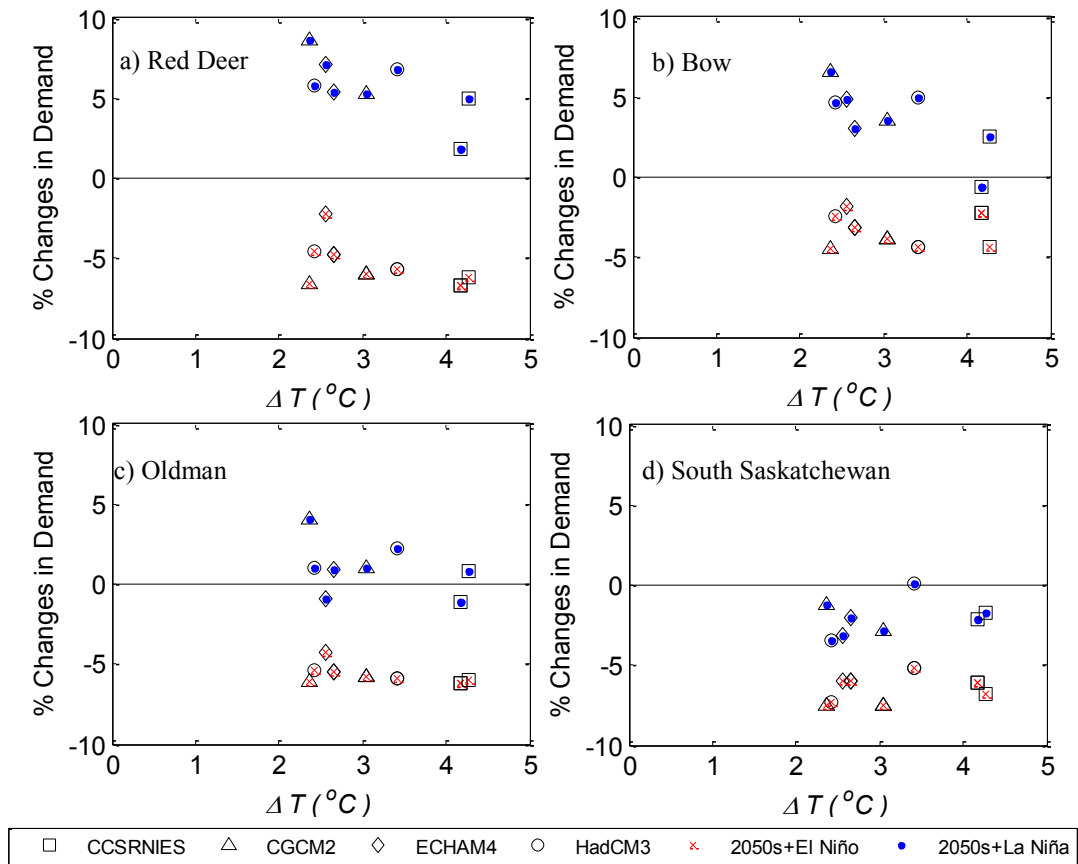


Figure 4.6 Irrigation District Model (IDM) simulated percentage changes in average annual irrigation demand for the private irrigation blocks of South Saskatchewan River Basin (SSRB) versus ΔT as compared to the climate scenarios of 2050s with respect to the combined scenarios projected by four General Circulations Models (CCSRNIES, CGCM2, ECHAM4, and HadCM3) forced by three Special Report on Emissions Scenarios (SRES) emissions (A1FI, A21, and B21) of Intergovernmental Panel on Climate Change (IPCC) combined with El Niño and La Niña episodes.

CHAPTER 5

Effects of Climate Change on the Surface Water Management of South Saskatchewan River Basin²

5.1 Introduction

A river basin system is made up of three basic components: water sources, in-stream and off-stream demands, and intermediate components. Water sources are rivers, canals, reservoirs, and aquifers; off-stream demands are irrigation fields, industrial plants, and cities; in-stream demands are hydropower, recreation, environment; and intermediate components are treatment plants, water reuse and recycling facilities. Water management involves development, control, protection, regulation, and beneficial use of water sources by meeting various water demands efficiently.

Climate change will affect basin hydrology in many ways because the hydrological cycle is intimately linked with changes in atmospheric temperature

² A version of this chapter has been published. **Islam, Z. and Gan, T. (2012). Effects of Climate Change on the Surface Water Management of South Saskatchewan River Basin. J. Water Resour. Plann. Manage. doi: 10.1061/(ASCE)WR.1943-5452.0000326**

and radiative fluxes. As a result, the economy and the livelihood of people will be affected. In recent decades there have been unequivocal, observational evidences of the climate system warming such as increases in the global average air and ocean temperatures (Bates et al. 2008). These changes in the global climate can affect the hydrological cycle such as precipitation, snowmelt, evaporation, soil moisture, and runoff. Such changes in the hydrologic system will affect agricultural productivity, flood control, municipal and industrial water supply, and fishery and wildlife management (Xu and Singh 2004). As we witness hydrologic extremes occurring more frequently and in greater severity worldwide, the potential impact of climate change is of great concern in the semi-arid Canadian Prairies that suffer from recurrent droughts (Gan 2000; Johnson et al. 2005; Fang and Pomeroy 2008; Withey and van Kooten 2011). Given that about 88% of the water supply of Canadian municipalities comes from surface sources (Environment Canada 2007), an assessment of the impact of climate change to the future water supply of Canada and strategies for reducing such vulnerability will be of national priority.

The Phase 1 of the South Saskatchewan River Basin (SSRB) management plan that ended in June 2002 issued a recommendation that any future transfer of water allocation between users within the SSRB would require the approval of Alberta Environment (Alberta Environment 2003a). Phase 2 started shortly thereafter in 2003 in which the Alberta Government launched the 'Water for Life Action Plan' for managing Alberta's water resources so that the water of SSRB

will be used in a sustainable, environmentally responsible way since its water resources have been under stress (Alberta Environment 2003b). On the basis of these studies, the water management plan for SSRB was approved in 2006 with a recommendation that Alberta Environment should not accept any further application for new water licenses for the Bow, Oldman and South Saskatchewan River sub-basins of SSRB (Alberta Environment 2006).

Climate change is expected to affect the spring snowmelt process of the Canadian Rockies, which constitutes a major component of the overall runoff of SSRB. However, in the above studies on the water management of the SSRB, the possible effects of climatic change on its future water supply over the 21st Century had not been considered. Tanzeeba and Gan (2012) simulated the potential impacts of climate change on three of the four sub-basins of SSRB and their results showed that SSRB will generally experience a decrease in the mean annual maximum flow in the 21st century, and all three sub-basins will experience an approximately 2 weeks earlier onset of the spring snow melt but a decrease in the summer flow. In another study, it was found that climate change could change the streamflows of SSRB from +5% to -30% in 2040-2069, and climate variability would further decrease its streamflows by 25% or more during dry years (Alberta Environment 2010).

About 75% of the licensed water use in the SSRB belongs to irrigation consumptive use (Alberta Environment 2005) which is expected to change

because of projected diminishing water supply of SSRB based on projected Special Report on Emissions Scenarios (SRES) climate scenarios of Intergovernmental Panel on Climate Change (IPCC). The future instream flow requirement is also expected to change. Even though the future non-irrigation water demand (e.g., municipal, industrial, stock watering, flood control, and lake stabilization) with respect to future population has been taken into consideration by Alberta Environment (Alberta Environment 2002a) in implementing Phase 2 of the SSRB water management plan (Alberta Environment 2003c), the government has not considered the possible effects of climate change on SSRB's future water resources management.

Based on the above statements of problems, the objectives of this study are: (a) with reference to climate change scenarios projected by General Circulation Models (GCMs) forced by certain SRES emissions of IPCC (2001) for the SSRB, investigate possible changes to future SSRB water demands and supplies under the effects of climate change, and (b) from the results of (a), investigate possible changes to the management of the SSRB water resources and adaptation strategies to enhance its resiliency against possible future water shortages.

5.2 Review of Water Resources Management Subjected to Climate Change

This section provides an overview of the Water Resources Management Model (WRMM) (Alberta Environment 2002b), various water resources uses applicable to SSRB, and the general approaches to account for the possible impact of climate change to basin-scale water resources.

5.2.1 Water Resources Management Modeling

There are different approaches to optimize the management of water resources, which can essentially be grouped under economic-driven optimization models (e.g. Cai et al. 2006; Draper et al. 2003; Letcher et al. 2004; Ward et al. 2006) and priority-driven optimization models (e.g. CALSIM of Draper et al. 2004; WEAP of Stockholm Environment Institute 2001; WRMM of Alberta Environment 2002b). In the former, the objective is to allocate water to maximize the accumulated net benefit over the planning period, while in the latter the objective is to minimize the total penalty (cost). The former generally consists of hydrologic and economic components, institutional rules and economic incentives (Ringler et al. 2006), and the latter consists of various water user groups, and priority of supplies. For both types of models, the basin is mostly presented as a node-link network representing the spatial relationships between various physical entities in a river basin. Optimization of a problem in

maximizing a net benefit or in minimizing a total penalty (cost) can be done by techniques such as Linear Programming, Non Linear Programming, Network Flow Programming, Dynamic Programming, Genetic Algorithm, and others.

Alberta Environment (2002b) developed the Water Resources Management Model (WRMM) as a planning tool for the water resources utilization of a river basin. WRMM is a deterministic surface water allocation model designed to handle a multipurpose, multi reservoir simulation problem. It has a nested optimization subprogram. In WRMM, water allocation priorities are defined by a penalty point system and the Network Flow Programming (NFP) optimization technique is used to minimize the overall system penalty.

Consider a network of ordered pairs (i, j) of arcs A and a total of N nodes. The minimum cost flow (or penalty) problem is formulated as the following:

Minimize an Objective function:

$$\text{Eq. 5.1} \quad \min Z = \sum_{(i,j) \in A} c_{ij} x_{ij} \quad \forall i, j \in N$$

subject to

$$\text{Eq. 5.2} \quad \sum_i x_{ij} - \sum_i x_{ji} = 0 \quad \forall j \in N$$

$$\text{Eq. 5.3} \quad 0 \leq l_{ij} \leq x_{ij} \leq u_{ij} \quad \forall (i, j) \in A$$

where c_{ij} , l_{ij} , x_{ij} , and u_{ij} are the cost (or penalty) per unit flow, lower bound on flow, flow, and the upper bound on flow along an arc (i, j) , respectively.

WRMM is set up to facilitate easy repeated analysis of responses of a river basin to different natural conditions and planning alternatives. The model can consider water supply from headwaters, local runoff from a sub-basin to the network, reservoir storage, release, precipitation and evaporation. Water demands considered in WRMM are instream flow in natural streams, flow in diversion channels, irrigation consumption, and hydropower production. The principal inputs of WRMM are natural flow data, consumptive irrigation demands, non-irrigation withdrawals, instream objectives, reservoir and canal structure capacities, and license priorities. Principal outputs are time series of reservoir levels, regulated channel flows, and irrigation or industrial consumptions.

Each WRMM run can be considered as an operational policy or structural alternative and the model outputs for various components are compared to assess the effects of alternative policies or design proposals. Each river is divided into a set of reaches and for each reach the flow is kept constant during a time period, and the runoff contribution along the reach is treated as a local inflow at the downstream end of the reach. A major withdrawal can represent industrial withdrawal or irrigation and non-irrigation consumptive use that may or may not be met, depending on the penalty assigned to it and the availability of water. Return flow channels are also included in WRMM to model any return flow

diverted back into the main watercourse from irrigation and industrial uses (Ilich 1993).

WRMM has been used as a planning tool in managing surface water resources in the SSRB of Western Canada (Alberta Environment 2003b, 2003c, 2010; Cutlac and Horbulyk 2011). It consists of a main module known as the SSRB-WRMM, and several relatively smaller modules. The SSRB-WRMM module iteratively passes flow data back and forth between the Highwood Interim Diversion Project (HIDP) module, Trans Alta Utilities (TAU) module, Southern Tributaries (STRIBS) module, Special Areas Water Supply Project (SAWSP) module, and the Acadia Valley Irrigation Project (ACADIA) module in search of optimal allocations of water among various users.

5.2.2 Water supply and demand in SSRB

The SSRB has a watershed area of 121,095 km², of which 41% is from the Red Deer, 22% from the Oldman, 21% from the Bow and 16% from the South Saskatchewan River sub-basin (Figure 5.1). Even though it occupies about a quarter of the surface area of Alberta, it provides nearly 57% of the water allocated in Alberta. However, ironically it only possesses less than 6% of Alberta's total water resources because southern Alberta has a semi-arid climate. Water supply for SSRB comes from the natural streamflow of the Red Deer, Bow, and Oldman Rivers and the apportioned water of the St. Mary River

between Canada and United States (Alberta Environment 2003c). Water demands in SSRB are categorized as described in the following three sections.

5.2.2.1 Instream Flow Requirement

There are two types of instream flow requirements considered in WRMM, the existing instream objectives, and flows for environmental protection or Instream Flow Needs (IFN) in terms of water quality (temperature, dissolved oxygen, ammonia), fish habitat, riparian vegetation and channel maintenance (Clipperton et al. 2003). Existing instream objectives are flows included as conditions attached to licenses that have been issued such that users are not permitted to withdraw water when the river flows fall below the specified instream objectives. In an approved water management plan for SSRB, Alberta Environment established water conservation objectives for Red Deer, Bow, Oldman, and South Saskatchewan River (SSR) sub-basins. Any licenses issued for applications received after May 1, 2005 in the Bow, Oldman and SSR would be subjected to the instream requirement which is 45% of the natural flow, or the existing instream objectives plus 10%, whichever is greater at any point in time. In the Red Deer River, from Dickson Dam to the confluence with the Blindman River, the instream requirement is 45% of the natural flow rate or $16 \text{ m}^3/\text{s}$, whichever is greater at any point in time. Downstream of the confluence, future licenses that withdraw water from November to March have the same instream requirement as the upstream. However, for future licenses that withdraw water

from April to October and for all existing licenses of the Red Deer River, the instream requirement is 45% of the natural flow or 10 m³/s, whichever is bigger.

5.2.2.2 Consumptive Demands

Water consumption by the current and future licenses issued by Alberta Environment for irrigation districts, private irrigation blocks, and non-irrigation consumptive uses are included in this demand. In SSRB, the largest water consumptive demand is that of irrigation. SSRB has 13 irrigation districts of which 3 are in the Bow River, 9 in the Oldman River, and 1 in the SSR sub-basins. Besides, there are more than 2,500 private irrigation projects in Alberta and about 80% of which are in the SSRB (Irrigation Water Management Study Committee 2002). The irrigation demands depend on the climatic condition and thus vary year to year, while the non-irrigation demands are kept unchanged from year to year (Alberta Environment 2003c).

5.2.2.3 Apportionment of the South Saskatchewan River Flow

According to the 1969 Master Agreement on Apportionment for the South Saskatchewan River between Alberta and Saskatchewan, annually one half of the natural flow of the SSRB shall be passed onto Saskatchewan. However, if the natural flow falls below 5.2 billion m³, Alberta can still keep more than half of the natural flow to a maximum of 2.6 billion m³ provided that the instantaneous flow does not fall below 42.5 m³/s (Alberta Environment 2003c).

5.2.3 Allocated Licenses

Licenses for the private irrigation and non-irrigation consumptive use have been divided into senior, junior and future licenses. Different penalty values are assigned to differentiate these licenses in WRMM. Senior licenses are not subjected to instream objectives. In the Red Deer sub-basin, senior licenses were licenses that either have been allocated before the Dickson Dam began operation in 1977; or for the Oldman and South Saskatchewan sub-basins, licenses issued before the Oldman Dam began operation in 1988; and for the Bow River sub-basin, licenses issued before the instream objectives operation based on the 80% Fish Rule Curve which became effective in 1992. All licenses in the SSRB allocated after Dickson Dam and Oldman Dam began operation, and after the instream objective based on 80% Fish Rule Curve became effective, are considered as junior licenses. Essentially, the amount of water allocated to junior licenses will depend on whether instream objectives are met or not, and they can be further subdivided into two categories: Junior License and Junior License Subjected to water conservation objectives. Any future license to be issued will be subjected to the same conditions of the current junior license holders.

5.2.4 Projection of Future Climate Scenarios

To generate future climate scenarios subjected to the effects of climate change for water resources management impact studies, we can either use the synthetic, analogue, Regional Climate Models (RCMs), or GCM based

approaches. In a synthetic approach, the future climatic variables are changed incrementally by arbitrary amounts in annual, seasonal or monthly time scales. In an analogue approach, climate change scenarios are constructed by identifying recorded climate regimes expected to resemble the future climate. A spatial analogue approach, which attempts to identify regions that have a climate similar to that projected for the study region in the future, or a temporal analogue approach in which past climate for a given location is assumed to resemble the projected future climate for that location, can be used. Climate scenarios based on the projections of GCMs have been used increasingly in climatic change impact studies. However, because of their relatively coarse spatial and temporal resolutions, they should be downscaled to subgrid scales before they are adequate for basin scale hydrologic modeling. Downscaling of GCM output can either be done statistically, in which empirical relationships are established between GCM-scale climate variables (predictors) and local-scale meteorological variables (predictands) using statistical methods, or it can be done dynamically, where a RCM is used to produce higher resolution outputs. Statistical downscaling techniques include a simple delta change method, or more sophisticated, regression models, weather typing schemes and weather generators. In this study, climate change scenarios are statistically downscaled from GCM outputs using a delta change approach, as

$$\text{Eq. 5.4} \quad T_2 = T_1 + (T_2' - T_1')$$

$$\text{Eq. 5.5} \quad P_2 = P_1 \times \frac{P_2'}{P_1'}$$

where T_1 and P_1 are the baseline observed temperature and precipitation; T_2 and P_2 are the future temperature and precipitation of climate scenarios; T_1' and P_1' are the GCM simulated mean temperature and precipitation for climate normal period (1961-1990); and T_2' and P_2' are the GCM simulated mean temperature and precipitation for future periods, respectively. This approach has been used in many past climate change studies on water resources (e.g. Lettenmaier and Gan 1990; Wood et al. 2002; Miller et al. 2003; Ryu et al. 2009; Boyer et al. 2010; Kerkhoven and Gan 2010; Tanzeeba and Gan 2012). The Delta change approach incorporates GCM-projected changes in key climatic variables such as temperature and precipitation by a simple calculation. Partly because it avoids tedious computation, it has been a popular approach in many climate change studies. It is considered a stable and robust method (Fowler et al. 2007; Graham et al. 2007). However, there are disadvantages to this simplistic approach: it assumes a constant bias; it only accounts for changes to the mean, maxima or minima of climate variables and it ignores possible changes to the variance of these climate variables; and in the case of precipitation, properties such as the temporal sequence of wet days or dry days are assumed to remain unchanged (Fowler et al., 2007, Wilby et al., 2009; Boyer et al., 2010).

5.3 Research Methodology

To account for uncertainties associated with GCMs' projected climate scenarios, climate scenarios based on four GCMs forced by multiple SRES emission scenarios for the SSRB are considered. Among the four GCMs selected are Japan's CCSRNIES which projected the warmest climate for the SSRB, Germany's ECHAM4 which projected the driest climate, UK's HadCM3 which projected the wettest climate, and Canada's CGCM2 which projected changes that are in between the other three GCMs' projections. The three SRES emission scenarios selected are the fossil fuel intensive, A1FI, and the mid-range emission, A21 and B21 scenarios (IPCC 2000). The change fields of the mean monthly precipitation (% change) and the mean monthly temperature (absolute change) centered on 2010-2039, 2040-2069 and 2070-2099, and is collected from the Canadian Climate Change Scenarios Network. To assess the effects of climate change on the SSRB, WRMM was driven by input data representing the base case scenario for SSRB and then by data that represent changes to the base case scenario according to climate projections of four GCMs forced by three SRES emissions (CCSRNIES A1FI, CCSRNIES B21, ECHAM4 A21, ECHAM4 B21, HadCM3 A1FI, HadCM3 B21, CGCM2 A21 and CGCM2 B21) for the 2010-2039, 2040-2069 and 2070-2099 periods.

5.3.1 Base Case Scenario

The base case scenario used in this study is based on the approved SSRB Water Management Plan Model (Alberta Environment 2006). In this scenario, provisions are simulated that expand irrigation districts in the Bow and Oldman River basins by 20% and 10 %, respectively. However, private irrigation water uses are limited at their current areas. Water allocations for the SAWSP and for the ACADIA project to be implemented in the future have also been applied in the base case scenario. At the base case scenario, water demands for the non-irrigation consumptive uses are projected to their fully licensed volume allocations. Due to projected population increase and economic development in SSRB, demand for non-irrigation water withdrawals is projected to increase between 29% to 66% by 2021, and 52% to 136% by 2046 (Alberta Environment 2002a). However, in the approved water management plan, non-irrigation water uses are limited at their current levels. In the base case scenario, releases from the Bearspaw Dam provided by TAU are included to reflect their current operations. Future water conservation and current instream objectives are also included in the base case scenario (Tom Tang, Environmental Modeling, Alberta Environment and Sustainable Resource Development, personal communication). As the base case scenario is based on the historical datasets of 1928-1995, in order to investigate the possible impact of climate change on the approved SSRB Water Management Plan upon which various water allocation policies have been

implemented, the base case period chosen for in this study is also 1928-1995, instead of the standard climate normal of 1961-1990.

5.3.2 Climate Change Scenarios

In various climate scenario simulations, the base case scenario (1928-1995) datasets of this study will be adjusted with respect to selected SRES climate scenarios of IPCC (2001) as explained below:

Step1: Adjusting Natural Flows, Apportionment and Instream Flow Requirement

Input data for WRMM includes natural flow data at a number of nodes that link the network of the SSRB water management plan (See **Appendix C** for detail schematic), which comes from the Bow, Red Deer, Oldman, and South Saskatchewan River sub-basins. Further, the apportionment flow and instream flow requirements are also estimated on the basis of these natural flows. To generate future natural flows at these nodes, the fully distributed land surface scheme, Modified Interaction Soil Biosphere Atmosphere (MISBA) of Kerkhoven and Gan (2006) was calibrated for these sub-basins using 20 years (1961-1980) of re-analysis data of the European Centre for Mid-range Weather Forecasts (ERA-40). After calibration, keeping all the parameters unchanged, MISBA was validated against 10 years (1981-1990) of data independent of the calibration experience. The goodness-of-fit statistics obtained for the calibration and validation runs of MISBA on these sub-basins of Bow, Red Deer, Oldman and

South Saskatchewan River are listed in Table 5.1. In general, coefficient of determination (R^2) and Nash-Sutcliffe coefficient of efficiency (E_f) range from 0.63 to 0.80 and 0.46 to 0.79, respectively, in calibration runs, and 0.62 to 0.82 and 0.34 to 0.74, respectively, in validation runs. After validation, MISBA was set to simulate the streamflow of the sub-basins for the climate normal (1961-1990) and after that the monthly mean flows for the sub-basins were computed.

A two-step process was adopted to downscale climate projections at GCM scale to local scale input for MISBA to simulate the streamflow of the sub-basins. First, using the Adaptive Gaussian Window Interpolation method (Agüi and Jiménez 1987), the change fields of mean monthly precipitation (% change) and mean monthly temperature (absolute change) at selected grids of the four GCMs for 2010-2039, 2040-2069 and 2070-2099 were interpolated to the ERA-40 grids selected for the sub-basins of SSRB. Second, these interpolated change fields of GCMs were used to adjust the 1961-1990 climate normal of ERA-40 at grids selected for the sub-basins of SSRB to derive the projected climate scenarios for these sub-basins for 2010-2039, 2040-2069, and 2070-2099 (Tanzeeba and Gan 2012). It is noted that in applying this simple, interpolation approach to change fields derived from GCM projections, we assume that such GCM scale change fields generally do not exhibit unsmooth or sharp gradient of changes between neighboring grid cells. We acknowledge that this assumption may not hold true in highly heterogeneous landscapes, where topography could cause considerable spatial climatic variations (i.e. the Andes); however, the assumption is useful for

relatively homogeneous areas such as the Amazon, and other global areas with relatively homogeneous landscapes, such as the Canadian Prairies. Therefore the approach of Tanzeeba and Gan (2012), e.g., the Adaptive Gaussian Window Interpolation method, should be generally applicable to estimate change fields of SSRB sub-basins. However, this approach is likely limited by the assumption that relationships between climate variables in the baseline ('current climates') will be maintained towards the future (Ramirez and Jarvis 2010), under possible climate change impacts projected by GCMs. It is possible that climate change may alter local weather patterns at small scales (Fowler et al. 2007), and such changes are obviously not accounted for with the delta approach or other statistical downscaling/ interpolation methods (Wang .et al. 2012).

The above adjusted ERA-40 data was then used to drive MISBA for each sub-basin, and the monthly ratios of these simulated streamflows were computed from the streamflow simulated for the sub-basins that corresponded to the SRES scenarios and that correspond to the climate normal. The weekly natural flow data selected for WRMM (1928-1995) for each month was adjusted according to these simulated monthly ratios. The apportionment flow and instream flow requirements were also recomputed using these adjusted natural flows.

Step 2: Adjusting Irrigation Consumptive Demand

For each IPCC SRES climate scenario, the Irrigation District Model (IDM) of Alberta Agriculture Food and Rural Development (AAFRD) was used to generate the irrigation consumptive demands for all irrigation blocks and return flows from district irrigation blocks. IDM contains two integrated modules: the Irrigation Requirements Module (IRM), which contains meteorological and field-based data needed to determine farm delivery requirements, and the Network Management Module (NMM), which represents the physical characteristics of each district or private irrigation block, including pipelines, canals, reservoirs and return flow channels, and their respective operating characteristics and losses. Integration and joint use of the IDM and WRMM were tested in calibration runs simulating the St. Mary Project for 1988 and the Eastern Irrigation District (EID) for 1994 to 1999. Adjustments were made to variable parameter settings until modelled gross diversions and return flows for the EID matched recorded data reasonably well. Insufficient historical data from other irrigation blocks precluded calibration in other districts (Irrigation Water Management Study Committee 2002). For each IPCC SRES climate scenario, the maximum/minimum temperature, precipitation and the potential evaporation of IRM weather data files for various irrigation blocks were adjusted to determine the farm delivery requirement of the blocks. NMM then was used to combine the irrigation consumptive demands from the IRM and convert them to canal flows and diversions required to meet the water demands (Irrigation Water Management

Study Committee 2002). For irrigation districts, the average annual irrigation demands from each irrigation block are estimated as the total areally weighted demand divided by the total area of that irrigation district. Similarly for private irrigation water uses, the average annual water demands for senior, junior and future licenses are estimated by dividing the total areally weighted demand for each category by the total area of that category.

Step 3: Adjusting Station Precipitation

For each of the three climate change periods considered (2010-2039, 2040-2069, and 2070-2099), precipitation input to reservoirs of SSRB, e.g., as input to WRMM, were adjusted from the base case period (1928-1995) precipitation dataset of all meteorological stations of the SSRB, e.g., P_1 was adjusted to P_2 according to Equation 5. This delta change adjustment is different from interpolating precipitation of the ERA-40 reanalysis data described in Step 1 to be used as input to the MISBA land surface scheme.

Step 4: Adjusting Station Lake Evaporation Data

Station lake evaporation data are used in WRMM to calculate evaporation from the reservoirs. First, monthly mean temperature data from GCMs grid for the climate normal (1961-1990) period was used to compute the lake evaporation using a simplified form of the Penman's Equation of Linacre (1977):

Eq. 5.6

$$E_0 = \frac{700 \frac{T + 0.006h}{100 - L} + 15(0.0023h + 0.37T + 0.53T_R + 0.35R_{ann} - 10.9)}{80 - T}$$

where, E_0 is the daily lake evaporation (mm/day) of a particular month, T is the mean monthly temperature ($^{\circ}\text{C}$), h is the station elevation (m), L is the latitude (degrees) of the station, T_R is the monthly mean range of temperature ($^{\circ}\text{C}$) and R_{ann} is the difference between the mean monthly temperatures of the hottest and the coldest months ($^{\circ}\text{C}$). Next, the monthly T data from the nearest GCM grid for the future 30-years periods (2010-2039, 2040-2069, and 2070-2099) were used to compute the lake evaporation subjected to the effect of climate change periods, and the monthly ratios of lake evaporation between SRES climate scenarios and the climate normal period were computed. Finally, the weekly lake evaporation data of the base case scenario of this study (1928-1995) selected for WRMM were adjusted according to these monthly ratios.

Step 5: WRMM Simulation Using Updated Hydrometeorologic Base Data

From all the above datasets, the Hydrometeorologic Base Data File (HBDF) of SSRB and its sub components, e.g., STRIBS, HIDP, ACADIA, SAWSP, were updated for various IPCC SRES climate scenarios, and used to drive WRMM to simulate possible changes in water management due to changes in irrigation demand, instream flow requirements and the apportionment agreement between Alberta and Saskatchewan. However, water allocations to non-irrigation consumptive

users such as industry, municipalities, etc., were still based on their licensed allocations under the approved SSRB management plan, assuming that these water demands will not be affected by the impact of climate change (Tom Tang, Team Lead, Environmental Modeling, Alberta Environment and Sustainable Resource Development, personal communication).

5.4 Discussions of Results

5.4.1 Projected Changes to Future Water Supply

The primary controlling factors for the water availability of a basin under climatic changes are changes to precipitation and temperature. Figure 5.2 shows percentage changes from climate normal of 1961-1990 in the mean annual precipitation ($\% \Delta P$) and changes in the mean annual temperature (ΔT) predicted by four GCMs (CCSRNIES, CGCM2, ECHAM4, HadCM3) forced by three SRES emission scenarios (A1FI, A21 and B21) of IPCC for the study periods (2010-2039, 2040-2069, and 2070-2099) in the SSRB. Predicted changes in the temperature and precipitation vary between the GCMs and the selected SRES scenarios. In general, for SSRB, most GCMs project an increase in the precipitation while all GCMs project an increase in temperature with respect to the climate normal of 1961-1990. Compared to the climate normal, the temperature of the SSRB is projected to increase by 0.5-1.5 °C by 2010-2039, 2.5-4.25 °C by 2040-2069 and 3-8°C by 2070-2099. On the average, temperature is expected to increase by 1.3°C, 3.1°C and 5.0 °C in 2010-2039, 2040-2069 and

2070-2099, respectively while precipitation is projected to change between -4.25% to 3.5 % by 2010-2039, 1% to 8.0% by 2040-2069 and -2.5% to 13.5 % by 2070-2099.

Next, MISBA was driven by these projected changes in the precipitation and temperature of GCMs to simulate the future natural streamflow at selected nodes within SSRB. A summary of the locations and projected streamflow for SSRB are listed in Table 5.1. It was found that even though precipitation is projected to increase by about 13.5% over the 21st century, except for a few cases, most of the scenario runs show a decrease in the mean annual average streamflow for most sub-basins located in Oldman, Bow and Red Deer River basins. The mean annual average flow is projected to decrease due to an enhanced evaporation caused by rising temperature that offsets the increase in precipitation (Tanzeeba and Gan 2012). The simulated percentage changes in the mean annual average streamflows and the mean annual maximum streamflows averaged over the SSRB are shown in Figure 5.3. It was found that in the 2010-2039 scenario, except for the cases of CGCM2 B21 and HadCM3 B21, all other GCMs projected a decrease in the average and maximum annual streamflows. In 2040-2069, based on the climate scenario of CCSRNIES B21, MISBA projected a 9% increase in the annual maximum streamflows, but based on CGCM2 B21's climate scenario, MISBA only projected a slight increase (1%) in the annual average and maximum streamflows. However, based on other GCMs and SRES scenarios, MISBA projected a significant decrease in the annual average and

maximum streamflows over SSRB. In 2070-2099, except for A1FI and B21 of CCSRNIES, for all other cases of GCMs and SRES scenarios, MISBA projected a significant decrease in the streamflows of SSRB. Overall, based on ECHAM4's climate projections, MISBA simulated the largest decrease in the mean annual average streamflow of 14%, 12% and 18%, and mean annual maximum streamflow of 18%, 16% and 19% for the 2010-2039, 2040-2069 and 2070-2099, respectively.

The seasonal changes of streamflow in future periods were also analyzed. In general, most of the scenario runs projected an increase in streamflow in winter (December-February) and spring (March-May), at the expense of decreased streamflow in the summer (Jun-August) and autumn (September-November). Under a warmer climate, we expect an earlier onset of the spring snowmelt and an increase in the rainfall over snowfall ratio. This study results for SSRB show that on the average, winter streamflow is expected to increase significantly (114%) while spring streamflow will only increase by about 7% in 2070-2099. In contrast, summer streamflow is expected to decrease by about 16% while autumn streamflow will decrease marginally (about 2%) in 2070-2099.

5.4.2 Projected Changes to Future Water Demand

The projected percentage changes in the average annual irrigation water demand for 13 irrigation districts, and private irrigation blocks, for the 2010-2039, 2040-2069 and 2070-2099, with respect to that of the base case scenario,

are plotted in Figure 5.4. It was found that changes in the projected irrigation demands are strongly related to temperature changes, and dependent on the selected GCMs and SRES emission scenarios of IPCC. On average, water demands for the irrigation districts are expected to increase by 7% in 2010-2039, but they could range 2%-13%. Similarly, average water demands for the irrigation districts were 12% (4%-17%) in 2040-2069 and 13% (4% -26%) in 2070-2099. The water demand for private irrigation blocks are expected to increase by an average of about 11% (6%-17%), 17% (9%-22%) and 18% (8%-33%) in 2010-2039, 2040-2069 and 2070-2099, respectively. In general, ECHAM4 and HadCM3 projections lead to the highest increases in future water demand in SSRB, whereas that of CGCM2 leads to the least increase in water demand, and that of CCSRNIES falls in between.

5.4.3 Simulated Deficits under Climate Change

On the basis of future water supply and demands projected in response to all the SRES climate scenarios considered, WRMM simulated changes to the number of deficit years out of 68 years (1928-1995) to specific water sectors of SSRB, such as irrigation districts, private irrigation, non-irrigation consumptive use and instream flow requirements. According to the instream requirement, a deficit year is defined as a year when the flow is less than the instream objectives for two or more weeks. For the irrigation consumptive use, a deficit is defined as when the amount of water delivered is less than the lesser of the demand or the

amount allocated to that group, and a deficit year is defined as a year when the annual irrigation water deficit exceeds 100 mm. For the non-irrigation consumptive use, a deficit is when the amount of water delivered to a group is less than its demand, and a deficit year is a year when the annual deficit exceeds 10% of the demand (Alberta Environment 2003c).

Out of 68 years (1928-1995), the number of deficit years (percent) expected for different water user groups in Red Deer River, Oldman River, Bow River and South Saskatchewan River sub-basins of SSRB under the impact of climate change were estimated. The rivers in each sub-basin were divided into reaches and the percent deficit years for all the licenses of each user group present in each reach were first estimated for the base case and the climate change scenarios (2010-2039, 2040-2069, and 2070-2099) individually. Then the weighted average percent deficit years of all user groups in all the four sub-basins of SSRB were estimated on the basis of the total number of licenses present in each user group of the four sub-basins.

The estimated percent deficit years for each user group for SSRB in response to the climate scenarios projected by the four GCMs forced by SRES emissions of IPCC considered, in comparison to that of the base case scenario (black square), are plotted with respect to projected temperature change (ΔT °C) in Figure 5.5. For some user groups, the percent deficit years seem not to be affected by the effects of climate change (Figure 5.5: a, c and h) while some user groups (Figure

5.5:b, d, e, f, g) could expect an increase in the percent deficit years and the projected percent increase is sensitive to ΔT , SRES emission scenarios and GCMs chosen but the relationships are quite scattered without a distinct pattern. As expected, the variability increases from 2010-2039 to 2040-2069 and 2070-2099 given that uncertainties are expected to grow as we project to the more distant future. Furthermore, we expect the uncertainty associated with infrastructure planning for future water management to grow even more with time because the latter will be affected by more unknowns than just the future climate. Other than uncertainties associated with the future climate, there are also uncertainties associated with future technology, economy and society and other unknown or unforeseeable factors for the latter.

Overall, the instream flow requirement will either not, or only marginally, be affected by the impact of climate change (Figure 5.5a), given that the deficit years had been about 48% in the base case scenario and about 48%-52% in 2010-2039 and 47%-51% in 2040-2069. In 2070-2099, under the climate projections of CGCM2 and ECHAM4, WRMM's projected percent deficit years will be 51%-57% while under that of CCSRNIES and HadCM3, WRMM's projected percent deficit years will be 44%-47%. Since instream flow requirements are essential to protect the ecological well being of aquatic life (Clipperton et al., 2003), they have priority over irrigation water demands and so they are not expected to be much affected by the climate change impact.

The irrigation districts are predicted to be progressively affected by climate change (Figure 5.5b) given that the percent deficit years increase from about 3% in the base case scenario to about 10% (5%-18%) in 2010-2039, 14% (6%-27%) in 2040-2069 and 18% (5%-47%) in 2070-2099, respectively. Among the SRES climate scenarios considered, ECHAM4 A21 and CCSRNIES 21 predicted the largest and the least future increase in percent deficit years respectively, while the SRES emission scenarios of HadCM3 and CGCM2 fall in-between these extremes.

Because they have the privilege of getting water over their junior counterparts, senior private irrigation users will not be affected by the impact of climate change in 2010-2039, and are only marginally affected in 2040-2069 and 2070-2099 (Figure 5.5c), e.g., the percent deficit years were about 3% in the base case scenario, 3%-6% in 2040-2069 and 3%-7% in 2070-2099. In contrast, as junior license holders, junior private irrigation blocks are projected to be progressively affected by the potential impact of climate change over the 21st century, e.g., the percent deficit years that were about 11% in the base case scenario are projected to increase to 16%-24% in 2010-2039, 19%-30% in 2040-2069 and 19%-43% in 2070-2099 (Figure 5.5d). However, predicted changes in the percent deficit years are not very sensitive to the selected GCMs and SRES emission scenarios. Overall, compared to other GCMs, ECHAM4 predicted the largest increase in the percent deficit years for the junior private irrigation users.

Similar to the junior private irrigation blocks, significant effects of climate change are also projected to future private irrigation blocks of SSRB, given that the percent deficit years of about 12% in the base case scenario is projected to increase to about 16%-24% in 2010-2039, 16%-28% in 2040-2069 and 15%-39% in 2070-2099 (Figure 5.5e). Further, similar to the junior licenses, predicted changes in the percent deficit years for future private irrigation blocks are also found to be not sensitive to GCMs and the selected SRES climate scenarios. Again, the climate scenarios of ECHAM4 lead to the largest projected increase in the percent deficit years.

Unlike senior private irrigation users, other than a few cases (CCSRNIES A1FI, CCSRNIES B21 and CGCM2 A21), senior non-irrigation consumptive uses could be significantly affected by climate change (Figure 5.5f). The deficit years in the base case scenario of 13% change to 6%-40% by 2010-2039, 3%-47% by 2040-2069 and 1%-63% by 2070-2099, of which the maximum projected increase was again the SRES climate scenarios of ECHAM4.

Similarly, junior license holders under the non-irrigation consumptive use group are expected to be progressively affected by the impact of climate change over the 21st century. The percent deficit years of about 29% in the base case scenario is projected to increase to 62% (43%-53%) in 2010-2039, 74% (45%-58%) in 2040-2069, and 79% (43%-67%) in 2070-2099 (Figure 5.5g), and again, the largest projected increase in the percent deficit years are that of ECHAM4's

SRES climate scenarios. Given that the future non-irrigation consumptive user group has low priority to water supply, WRMM model simulations show that this group is expected to suffer with high percent deficit years (about 48%) even under the base case scenario. However, this high percent in deficit years is only projected to increase marginally to 53% by 2010-2039, 55% by 2040-2069 and 57% by 2070-2099 (Figure 5.5h).

5.5 Conclusions

In this study, potential impacts of climate change on the water resources management of SSRB are simulated by MISBA, IDM, and WRMM on the basis of climate change scenarios projected by four GCMs (CCSRNIES, ECHAM4, HadCM3, and CGCM2) forced by three SRES emissions (A1FI, A21, B21) of IPCC (2001) for three future periods (2010-2039, 2040-2069, and 2070-2099). Under these SRES climate projections, the maximum decrease in the mean annual average streamflow of SSRB simulated by MISBA was 14%, 12% and 18% in 2010-2039, 2040-2069 and 2070-2099, respectively. In contrast, IDM's simulations show an increase in the irrigation water demand by 7%, 12%, and 13% for the irrigation districts, and by 11%, 17%, and 18% for the private irrigation blocks, for 2010-2039, 2040-2069 and 2070-2099, respectively.

On the basis of WRMM's simulations for the three future periods, the instream flow requirement will only be marginally affected, but the irrigation districts are

predicted to be progressively affected by climate change as the percent deficit years increase from about 3% in the base case scenario to about 10% in 2010-39, 14% in 2040-2069, and 18% in 2070-2099. Senior private irrigation users will not be affected in 2010-2039, and only marginally affected in 2040-2069 and 2070-2099. In contrast, the percent deficit years for junior and future private irrigation users which were about 11% and 12% in the base case scenario, are projected to increase to 19% and 18% in 2010-2039, 24% and 22% in 2040-2069, and 27% and 24% in 2070-2099, respectively. The percent deficit years of senior and junior licenses under the non-irrigation water use category are expected to increase from 13% and 29% in the base case scenario to 23% and 47% in 2010-2039, 23% and 50% in 2040-2069, and 28% and 52% in 2070-2099, respectively. WRMM's simulations also show that the future non-irrigation water user group is expected to suffer with high percent deficit years in the three future periods considered. Overall, on the basis of this climate change impact study for SSRB, it seems that license holders categorized under district irrigation, junior and future private irrigation, and senior, junior and future non-irrigation consumptive user groups, will be progressively and most significantly affected in the 21st century.

5.6 References

Agüí, J.C., and Jiménez, J. (1987). "On the performance of particle tracking." *J. Fluid. Mech.*, 185, 447-468.

Alberta Environment (2002a). "South Saskatchewan River Basin non-irrigation water use forecasts." *Alberta Environment*.

Alberta Environment (2002b). "Water Resources Management Model Computer Program Description." *Southern Region, Resource Management Branch. Alberta Environment*.

Alberta Environment (2003a). "Terms of Reference: Phase Two Water Management Plan for the South Saskatchewan River Basin." *Alberta Environment*.

Alberta Environment (2003b). "South Saskatchewan River Basin Water Management Plan Phase 2: background Studies". *Alberta Environment*.

Alberta Environment (2003c). "South Saskatchewan River Basin Water Management Plan Phase 2: Scenario Modelling Results Part 1." *Alberta Environment*.

Alberta Environment (2005). " South Saskatchewan River Basin Water Allocation." *Alberta Environment*.

Alberta Environment (2006). "Approved Water Management Plan for the South Saskatchewan River Basin (Alberta)." *Albeta Environment*.

- Alberta Environment (2010). "South Saskatchewan Regional Plan: Water Quantity and Quality Modeling Results." *Alberta Environment*.
- Bates, B.C., Kundzewicz, Z.W., Wu, S. and Palutikof, J.P. (2008). "Climate Change and Water." *Technical Paper of the Intergovernmental Panel on Climate Change, IPCC Secretariat, Geneva*.
- Boyer, C., Chaumont, D., Chartier, I., and Roy, A.G. (2010). "Impact of climate change on the hydrology of St. Lawrence tributaries." *J. Hydrol.*, 384 (1-2), 65–83.
- Cai, X., Ringler, C., and Rosegrant, M.W. (2006). "Modeling water resources management at the basin level, methodology and application to the Maipo River Basin." *Research report 149, International Food Policy Research Institute, Washington, DC*.
- Clipperton, G.K., Koning, C.W., Allan, G.H., Locke, J.M., and Mahoney, B.Q. (2003). "Instream Flow Needs Determinations for the South Saskatchewan River Basin, Alberta, Canada." *Alberta Environment*.
- Cutlac, I.M., and Horbulyk, T.M. (2011). "Optimal water allocation under short-run water scarcity in the South Saskatchewan River Basin." *J. Water Resour. Plann. Manage.*, 137(1), 92-100.
- Draper, A.J., Jenkins, M.W., Kirby, K.W., Lund, J.R., and Howitt, R.E. (2003). "Economic-engineering optimization for California water management." *J. Water Resour. Plann. Manage.*, 129(3), 155–164.

- Draper, A.J., Munévar, A., Arora, S.K., Reyes, E., Parker, N., Chung, F.I., and Peterson, L.E. (2004). "CalSim: generalized model for reservoir system analysis." *J. Water Resour. Plann. Manage.*, 136(6), 480–489.
- Environment Canada (2007). "Municipal Water Use Report, 2004 Statistics." *Environment Canada*.
- Fang, X., and Pomeroy, J.W. (2008). "Drought impacts on Canadian prairie wetland snow hydrology." *Hydrol. Process.*, 22(15), 2858–2873.
- Fowler, H. J., Blenkinsop, S., and Tebaldi, C. (2007). "Linking climate change modelling to impacts studies: Recent advances in downscaling techniques for hydrological modelling." *Int. J. Climatol.*, 27(12), 1547-1578.
- Gan, T.Y. (2000). "Reducing vulnerability of water resources of Canadian Prairies to potential droughts and possible climatic warming." *Water Resour. Manage.*, 14(2),111–135.
- Graham, L.P., Hagemann, S., Jaun, S., and Beniston, M. (2007). "On interpreting hydrological change from regional climate models." *Climatic Change*, 81, 97–122.
- Ilich, N. (1993). "Improvement of the return flow allocation in the water resources management model (WRMM) of Alberta environment." *Can. J. Civ. Eng.*, 20(4),613–621.

IPCC (2000). "Summary for Policymakers: Emissions Scenarios, A Special Report of Working Group III of the Intergovernmental Panel on Climate Change." *Cambridge University Press, UK.*

IPCC (2001) "Climate Change 2001: The Scientific Basis. Contribution of Working Group I to the Third Assessment Report of the Intergovernmental Panel on Climate Change." *Cambridge University Press, Cambridge, United Kingdom and New York, NY, USA.*

Irrigation Water Management Study Committee (2002). "South Saskatchewan River Basin: Irrigation in the 21st Century, Volume 1: Summary Report." *Alberta Irrigation Projects Association, Lethbridge, Alberta.*

Johnson, W.C., Millett, B.V., Gilmanov, T., Voldseth, R.A., Guntenspergen, G.R., and Naugle, D.E. (2005). "Vulnerability of northern prairie wetlands to climate Change." *BioScience*, 55(10), 863-872.

Kerkhoven, E. and Gan, T.Y. (2006). "A modified ISBA surface scheme for modeling the hydrology of Athabasca River Basin with GCM-scale data." *Advanced in Water Resour.*, 29(6), 808-826.

Kerkhoven, E. and Gan, T.Y. (2010). "Differences and sensitivities in potential hydrologic impact of climate change to regional-scale Athabasca and Fraser River basins of the leeward and windward sides of the Canadian Rocky Mountains respectively." *Climatic Change*, 106(4), 583-607.

- Letcher, R.A., Jakeman, A.J., and Croke, B.F.W. (2004). "Model development for integrated assessment of water allocation options." *Water Resour. Res.*, 40, W05502.
- Lettenmaier, D.P. and Gan, T.Y. (1990). "Hydrologic sensitivity of the Sacramento-San Joaquin River Basin, California, to global warming." *Water Resour. Res.*, 26(1), 69–86.
- Lincare, E.T. (1977). "A simple formula for estimating evaporation rates in various climates, using temperature data alone." *Agricultural Meteorology*, 18, 409-424.
- Miller, N.L., Bashford, K.E., and Strem, E. (2003). "Potential impacts of climate change on California hydrology." *J. American Water Resour. Assoc.*, 39(4), 771–784.
- Ramirez, J. and Jarvis, A. (2010) "Downscaling Global Circulation Model Outputs: The Delta Method." *CIAT Decision and Policy Analysis Working Paper*, no. 1.
- Ringler, C., Vu Huy, N., and Msangi, S. (2006). "Water allocation policy modeling for the Dong Nai river basin: an integrated perspective." *J. American Water Resour. Assoc.*, 42(6), 1465–1482.
- Ryu, J. H., Palmer, R. N., Wiley, M. W., and Jeong, S. (2009). "Mid-Range Streamflow Forecasts Based on Climate Modeling-Statistical Correction and Evaluation." *J American Water Resour Assoc.*, 45(2), 355-368.

- Stockholm Environment Institute (2001). "WEAP (Water Evaluation and Planning): User Guide for WEAP21". *Stockholm Environment Institute, Boston USA*.
- Tanzeeba, S. and Gan, T.Y. (2012). "Potential impact of climate change on the water availability of South Saskatchewan River Basin." *Climatic Change*, 112, 355-386.
- Wang, T., Hamann, A., Spittlehouse, D.L., and Murdock, T.Q. (2012) "ClimateWNA—High-Resolution Spatial Climate Data for Western North America." *J. Applied Meteorology and Climatology*.51, 16-29.
- Ward, F.A., Booker, J.F., and Michelsen, A.M. (2006). "Integrated economic, hydrologic and institutional analysis of alternative policy responses to mitigate impacts of severe drought in the Rio Grande Basin." *J. Water Resour. Plann. Manage.*, 132(6), 488–502.
- Wilby, R. L., Troni, J., Biot, Y., Tedd, L., Hewitson, B. C., Smithe, D. M. and Suttonf, R. T. (2009). "A review of climate risk information for adaptation and development planning." *Int. J. Climatol.*, 29, 1193–1215.
- Withey, P. and van Kooten, G.C. (2011). "The effect of climate change on optimal wetlands and waterfowl management in Western Canada." *Ecological Economics*, 70(4), 798–805.

Wood, A. W., Maurer, E. P., Kumar, A., and Lettenmaier, D. P. (2002). "Long-range experimental hydrologic forecasting for the eastern United States." *J Geophysical Res*, 107(D20), ACL 6-1-ACL 6-15.

Xu, C.-Y., and Singh, V.P. (2004). "Review on Regional Water Resources Assessment Models under Stationary and Changing Climate." *Water Resour. Manage.* 18, 591–612.

Table 5.1 Statistics of calibration and validation runs using Modified Interaction Soil Biosphere Atmosphere (MISBA), and MISBA simulated percentage changes in mean annual runoff from the climate normal (1961-1990) with respect to climate change scenarios projected by four General Circulations Models (CCSRNIES, CGCM2, ECHAM4, HadCM3) forced by three Special Report on Emissions Scenarios (SRES) emissions (A1FI, A21 and B21) of Intergovernmental Panel on Climate Change (IPCC) for the South Saskatchewan River Basin (SSRB)

Basin	Calibration (1961-1980)		Validation (1981-1990)		% Change in Mean Annual Runoff from Climate Normal (1961-1990)								
	R^2	E_f	R^2	E_f	2010-2039			2040-2069			2070-2099		
					Min	Max	Ave	Min	Max	Ave	Min	Max	Ave
Red Deer at Dickson Dam	0.68	0.58	0.69	0.44	-10	3	-3	-9	20	2	-9	38	8
Red Deer at Red Deer	0.67	0.64	0.67	0.47	-15	1	-5	-10	19	0	-13	38	6
Red Deer Near Nevis	0.72	0.67	0.70	0.52	-14	2	-6	-12	12	-3	-17	21	2
Red Deer at Big Valley	0.73	0.68	0.75	0.63	-14	1	-6	-12	12	-3	-17	21	1
Red Deer at Drumheller	0.74	0.72	0.78	0.64	-16	1	-8	-15	10	-4	-22	20	-2
Red Deer Near Jenner	0.63	0.57	0.82	0.74	-24	0	-12	-26	9	-12	-42	17	-13
Red Deer at Bindloss	0.70	0.67	0.77	0.69	-24	-2	-12	-27	7	-13	-43	12	-14
Oldman near Waldron Corner	0.80	0.76	0.63	0.53	-23	-2	-14	-22	0	-14	-32	21	-12
Oldman near Brocket	0.68	0.63	0.77	0.69	-14	2	-7	-16	8	-6	-23	28	-3
Oldman near Fort Macleod	0.74	0.74	0.70	0.62	-14	4	-5	-15	13	-3	-24	33	1
Oldman near Lethbridge	0.80	0.79	0.74	0.68	-13	3	-5	-10	-1	-5	-19	6	-4
Crowsnest near Lundbreck	0.69	0.46	0.62	0.36	-18	-3	-11	-19	4	-10	-23	22	-8
Castle near Beaver Mines	0.78	0.69	0.68	0.56	-16	7	-6	-15	2	-7	-24	7	-7
Pincher at Pincher Creek	0.77	0.76	0.70	0.66	-15	5	-4	-13	10	-3	-23	28	-2
Belly below Waterton Confluence	0.73	0.71	0.69	0.58	-16	9	-3	-15	15	-2	-25	41	2
St. Mary at St. Mary Dam	0.72	0.64	0.63	0.54	-16	2	-7	-19	-2	-9	-31	8	-7
Willow above Chain Lakes	0.72	0.69	0.74	0.73	-18	3	-7	-25	28	-6	-33	60	0
Willow near Claresholm	0.77	0.76	0.81	0.66	-16	7	-5	-14	4	-4	-29	23	-2
Willow near Nolan	0.76	0.75	0.77	0.44	-20	6	-7	-20	2	-8	-39	21	-6
Elbow below Glenmore Dam	0.71	0.57	0.63	0.36	-12	1	-4	-12	10	-3	-22	14	-4
Bow at Calgary	0.70	0.50	0.69	0.34	-12	1	-6	-15	12	-3	-21	24	-1

R^2 - coefficient of determination, E_f - Nash-Sutcliffe coefficient of efficiency

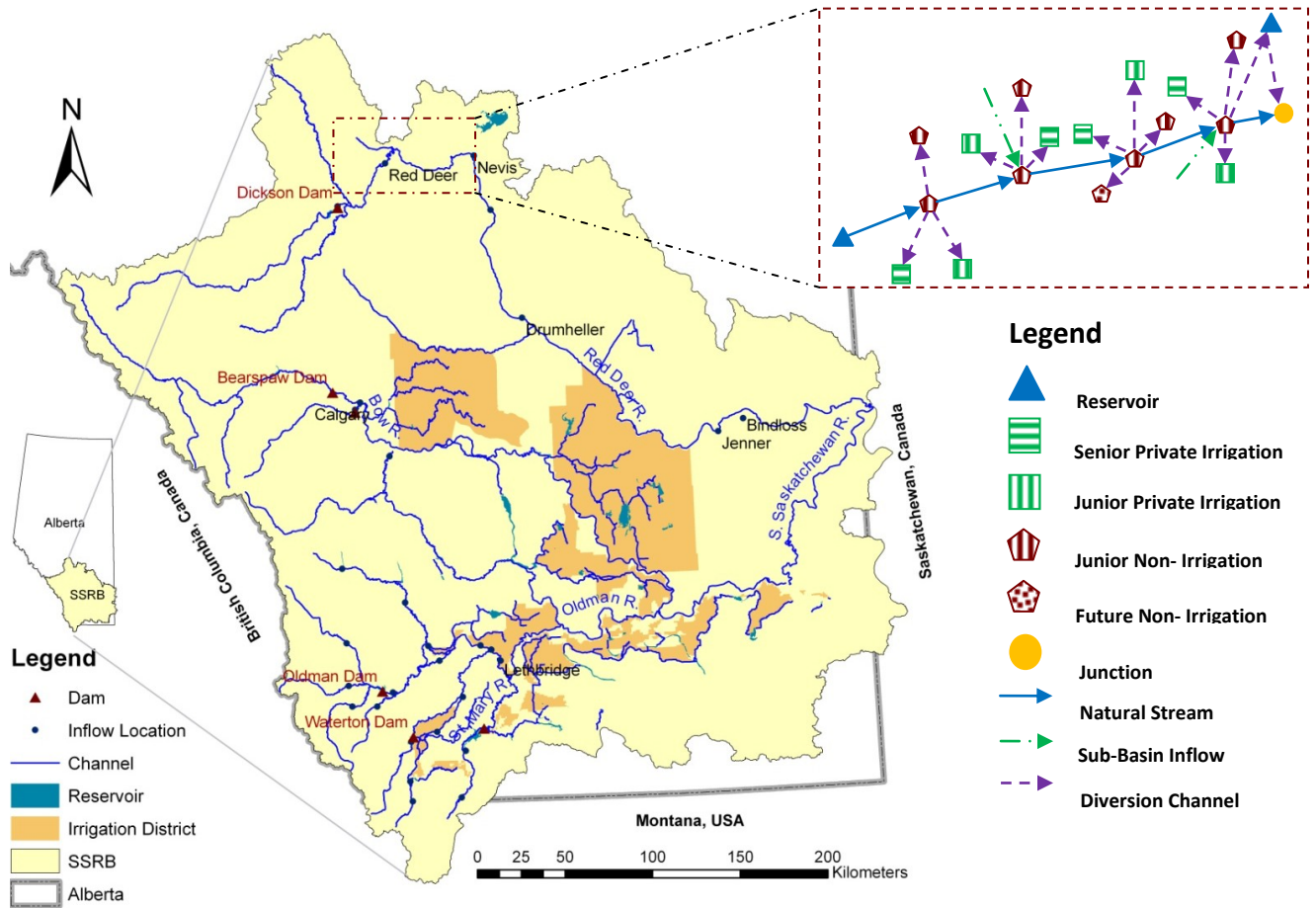


Figure 5.1 The South Saskatchewan River Basin (SSRB) (left) and a part of the SSRB water management node-link network schematic (right). See Appendix C for detail schematic.

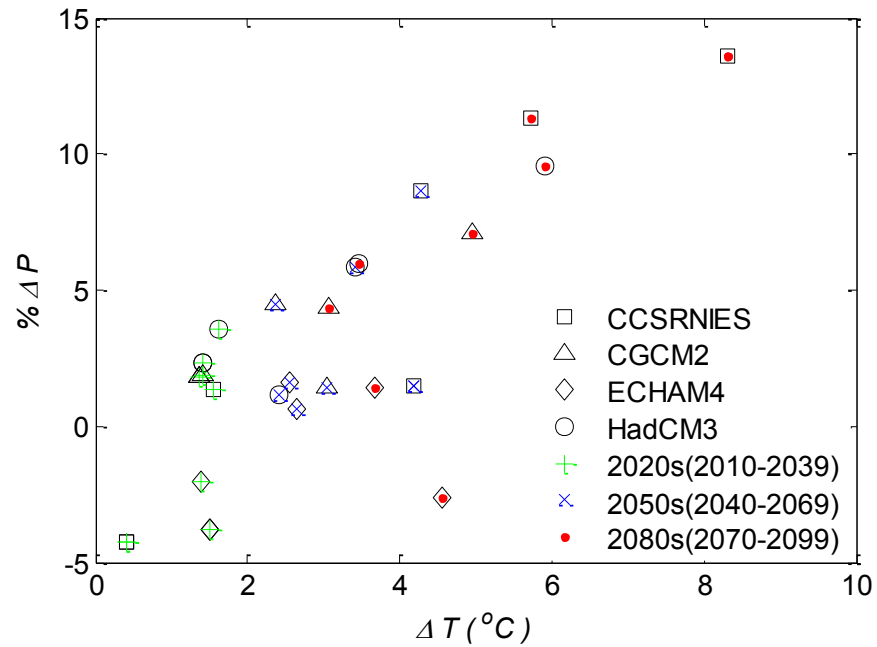


Figure 5.2 Percentage changes in the mean annual precipitation ($\% \Delta P$) and changes in the mean annual temperature (ΔT) projected by four General Circulations Models (CCSRNIES, CGCM2, ECHAM4, HadCM3) forced by three Special Report on Emissions Scenarios (SRES) emissions (A1FI, A21 and B21) of Intergovernmental Panel on Climate Change (IPCC) for the South Saskatchewan River Basin (SSRB) as compared to the climate normal (1960-1991).

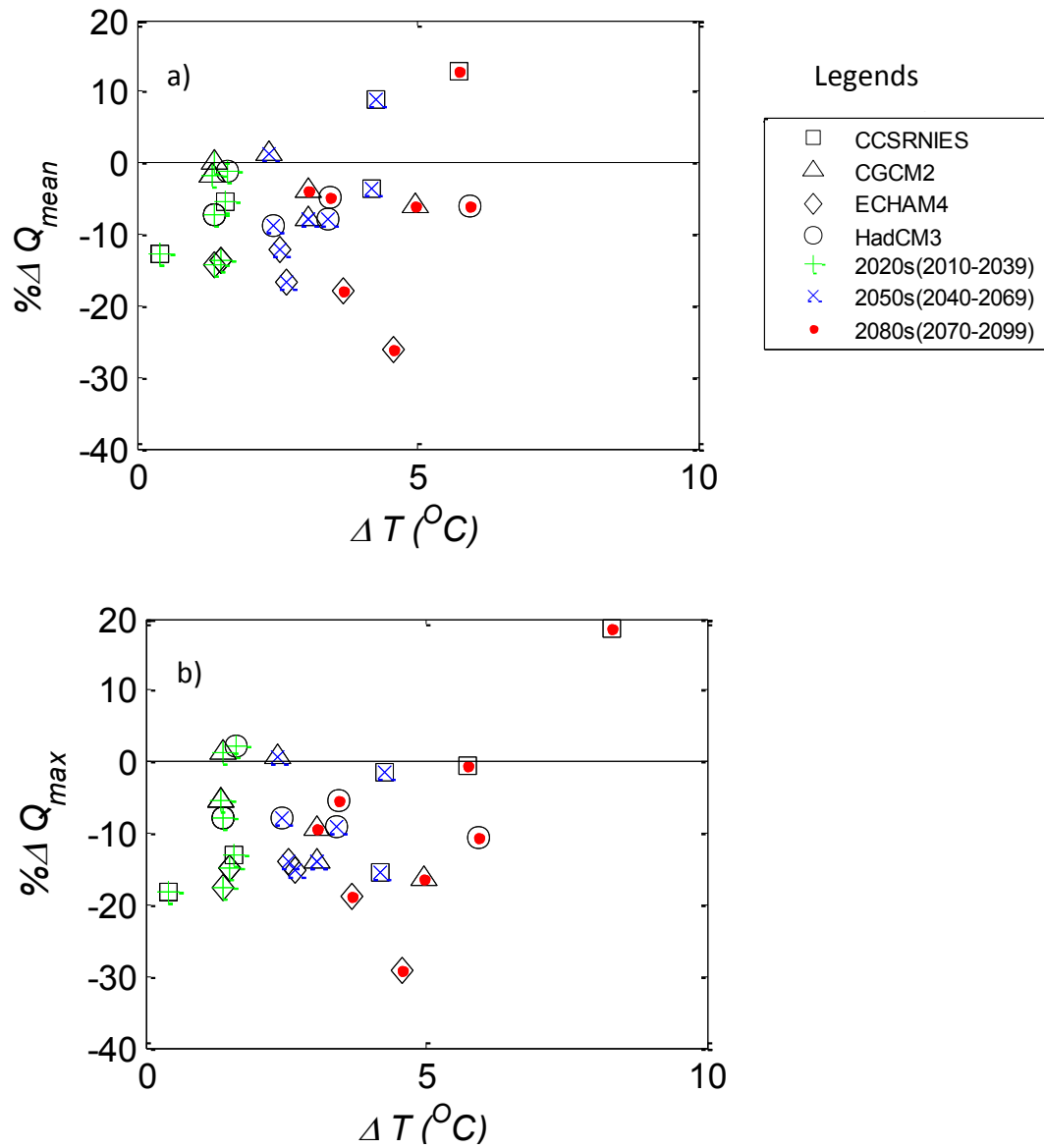


Figure 5.3 Modified Interaction Soil Biosphere Atmosphere (MISBA) simulated a) percentage changes in mean annual average streamflow ($\% \Delta Q_{mean}$), and b) percentage changes in mean annual maximum streamflow ($\% \Delta Q_{max}$) for the South Saskatchewan River Basin (SSRB) versus ΔT as compared to the climate normal (1960-1991) with respect to the climate change scenarios projected by four General Circulations Models (CCSRNIES, CGCM2, ECHAM4, and HadCM3) forced by three Special Report on Emissions Scenarios (SRES) emissions (A1FI, A21, and B21) of Intergovernmental Panel on Climate Change (IPCC) for 2010-2039, 2040-2069, and 2070-2099.

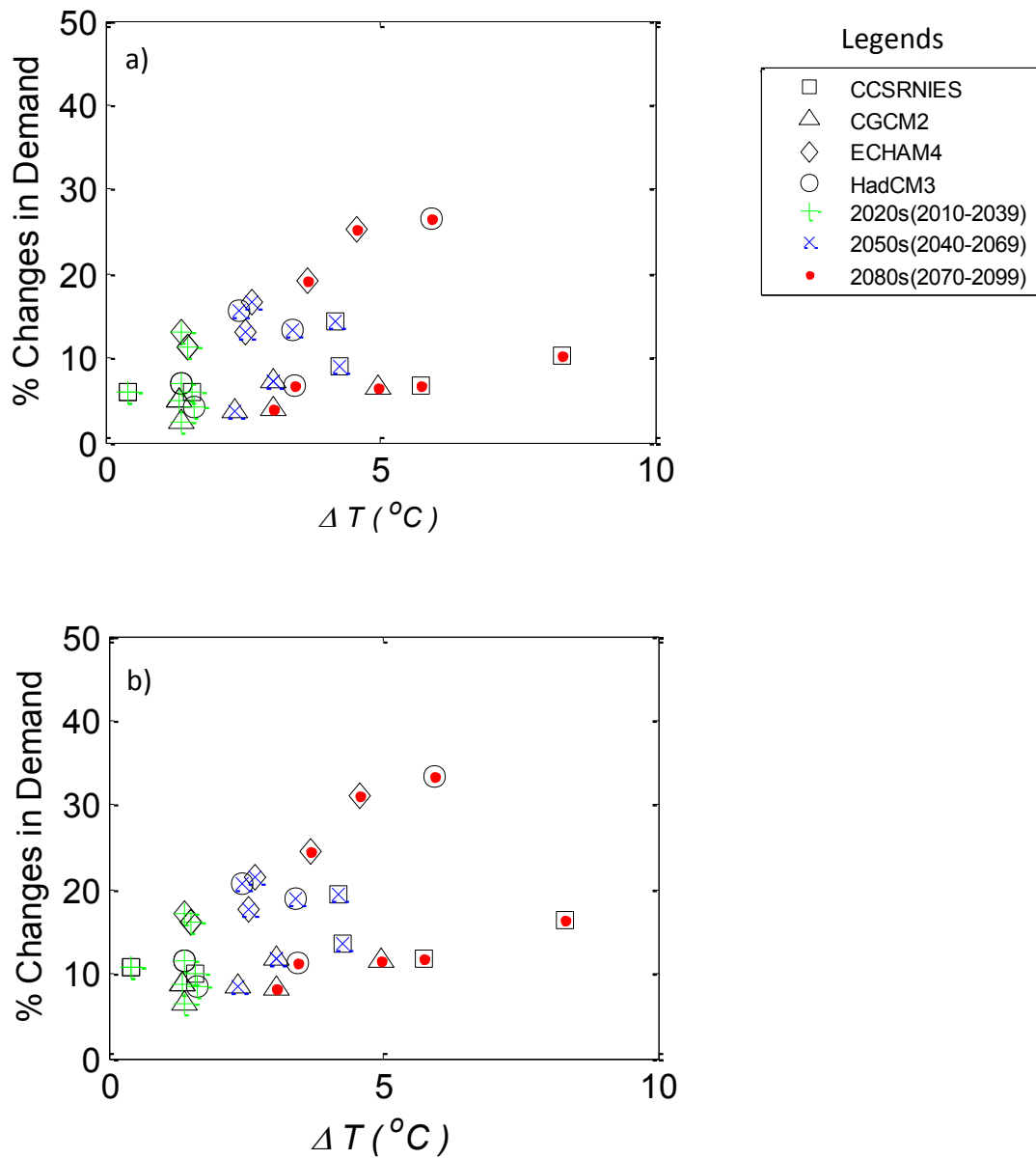


Figure 5.4 Irrigation District Model (IDM) simulated percentage changes in average annual irrigation demand for the South Saskatchewan River Basin (SSRB) versus ΔT as compared to the base case scenario with respect to the climate change scenarios projected by four General Circulations Models (CCSRNIES, CGCM2, ECHAM4, and HadCM3) forced by three Special Report on Emissions Scenarios (SRES) emissions (A1FI, A21, and B21) of Intergovernmental Panel on Climate Change (IPCC) for 2010-2039, 2040-2069, and 2070-2099 for Irrigation Districts (a), and Private Irrigation blocks (b).

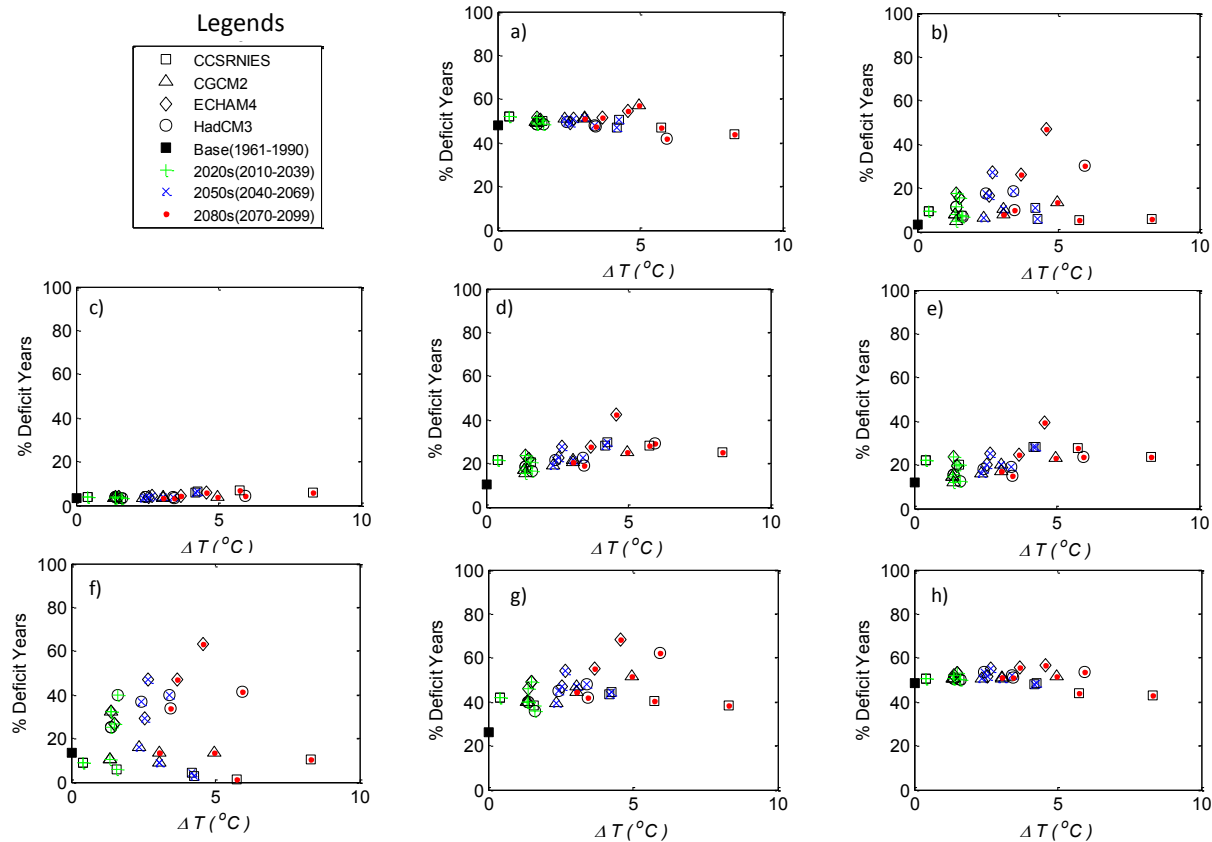


Figure 5.5 Water Resources Management Model (WRMM) simulated % Deficit Years versus ΔT for base case scenario and climate change periods with respect to the climate change scenarios projected by four GCMs (CCSRNIES, CGCM2, ECHAM4, and HadCM3) forced by three SRES emissions (A1FI, A21, and B21) of IPCC for 2010-2039, 2040-2069, and 2070-2099 for different water sectors of the SSRB: a) Instream flow requirement b) District irrigation c) Senior private irrigation d) Junior private irrigation e) Future private irrigation f) Senior non-irrigation consumptive uses g) Junior non-irrigation consumptive uses h) Future non-irrigation consumptive uses.

CHAPTER 6

Combined Effects of Climate Change and Climate Anomalies on Surface Water Management of South Saskatchewan River Basin

6.1 Introduction

Surface water management involves the development, control, protection, regulation, and beneficial use of surface water resources by meeting various off-streams (i.e., irrigation fields, industrial plants, and cities) and in-stream water demands (i.e., hydropower, recreation, and environment) efficiently. However, surface water management could be affected by the possible impact of climate change which could change basin hydrologic processes in many ways because the hydrological cycle is intimately linked with changes in atmospheric processes such as temperature and radiative fluxes. Such changes in the hydrologic system would affect agricultural productivity, flood control, municipal and industrial water supply, and fishery and wildlife management (Xu and Singh 2004). Other than the potential impact of climate change, climate anomalies as El Niño

Southern Oscillation or ENSO may lead to significant changes in streamflow (Gobena and Gan 2006). The ENSO-streamflow relationship also appears to be modulated by interdecadal oscillations of the North Pacific called the Pacific Decadal Oscillation (PDO). The interactions between ENSO and PDO are constructive when they are in phase and destructive otherwise. Therefore, the impact of climate change on the streamflow could be quite significantly modified by some climate anomalies individually and collectively, when such climate anomalies are active. Given that about 88% of the water supply of Canadian municipalities comes from surface sources (Environment Canada 2007), the combined effects of climate change and climate anomalies on surface water management is of great concern in the semi-arid Canadian Prairies that suffer from recurrent droughts (Gan 2000; Johnson et al. 2005; Fang and Pomeroy 2008; Withey and van Kooten 2011).

The South Saskatchewan River Basin (SSRB), having a total watershed area of 121,095 km², consist of Oldman (22%), Bow (21%), Red Deer (41%), and South Saskatchewan (16%) river sub-basins (Figure 6.1). Even though it occupies about a quarter of the surface area of Alberta, it provides nearly 57% of the water allocated in Alberta. However, ironically it only possesses less than 6% of Alberta's total water resources because southern Alberta has a semi-arid climate.

Water supplies for SSRB come from the natural streamflow of Red Deer, Bow, and Oldman River and the apportioned water (between Canada and United States) of the St. Mary River (Alberta Environment 2003a), while water demands in SSRB are instream flow requirements, consumptive demands (i.e., water consumption by the current and future licenses issued by Alberta Environment for irrigation districts, private irrigation blocks, and non-irrigation consumptive use), and apportionment of the South Saskatchewan River flow between Alberta and Saskatchewan. The water withdrawals in SSRB are regulated by Alberta Government's issued licenses. Licenses for the private irrigation and non-irrigation consumptive use have been divided into senior, junior and future licenses. Senior licenses are not subjected to instream objectives. In the Red Deer sub-basin, senior licenses were licenses that either have been issued before the Dickson Dam began operation in 1977; or for the Oldman and South Saskatchewan sub-basins, licenses issued before the Oldman Dam began operation in 1988; and for the Bow River sub-basin, licenses issued before the instream objectives operation based on the 80% Fish Rule Curve which became effective in 1992. All licenses in the SSRB issued after the Dickson and Oldman dams had begun operation, and after the instream objective based on a 80% Fish Rule Curve had become effective, are considered as junior licenses. Any future license to be issued will be subjected to the same conditions of the current junior license holders (Islam and Gan 2012).

The Phases 1 and 2 of the SSRB management plan that ended in 2006 issued a water management plan for this basin with a recommendation that Alberta Environment should not accept any further application for new water licenses for the Bow, Oldman and South Saskatchewan River sub-basins of SSRB (Alberta Environment 2003a; 2003b; 2005; 2006). However, the possible effects of climatic change, and possible combined impacts of climate change and climate anomalies on its future water supply over the 21st century had not been considered in aforementioned water management study for the SSRB.

Tanzeeba and Gan (2012) simulated the potential impacts of climate change on three of the four sub-basins of SSRB and their results showed that SSRB is projected to experience a decrease in the mean annual maximum flow in the 21st century, and all three sub-basins could experience an approximately 2-week earlier onset of the spring snow melt but at the expense of decreased summer flow. In another study, it was found that climate change could change the streamflows of SSRB from +5% to -30% in 2040-2069, and climate variability would further decrease its streamflows by 25% or more during dry years (Alberta Environment 2010). Gobena and Gan (2006) showed that past El Niño (La Niña) episodes had lead to significantly negative (positive) streamflow anomalies in south western Canada, and Gan et al. (2007) also found statistically significant negative correlation between winter precipitation of south western Canada and the ENSO index 'Niño3' (about -0.41 to -0.42), Pacific/North American index, PNA (about -0.44 to -0.52) and PDO (about -0.44 to -0.54). In addition, the irrigation

consumptive uses which comprises about 75% of the licensed water use in the SSRB (Alberta Environment 2005) are also expected to change because the water supply of SSRB is expected to decrease under future climate projected by General Circulation Models (GCMs) driven by Special Report on Emissions Scenarios (SRES) climate scenarios of the Intergovernmental Panel on Climate Change (IPCC), and the combined effect of climate change and climate anomalies.

Islam and Gan (2012) applied the Modified Interaction Soil Biosphere Atmosphere (MISBA) model, the Water Resources Management Model (WRMM) of Alberta Environment, and the Irrigation District Model (IDM) of Alberta Agriculture Food and Rural Development (AAFRD) to assess the future water resources management outlook for SSRB under the potential impacts of climate change. They showed that, under climate scenarios projected by four GCMs forced by SRES emissions of IPCC, MISBA simulated a significant decrease in the mean annual average and mean annual maximum streamflows over selected nodes within the SSRB; however, the irrigation water demand is projected by IDM to increase progressively over the 21st century; and WRMM simulated significant changes to the number of deficit years out of 68 years (1928-1995) to specific water sectors of the SSRB. Overall, according to this study, the instream flow requirement of SSRB will either not or only marginally affected, but irrigation districts will be progressively affected by climate change. The senior private irrigation users will not be affected by climate change in 2010-2039

(2020s), and only marginally affected in 2040-2069 (2050s) and 2070-2099 (2080s). In contrast, junior and future private irrigation users are projected to be progressively affected by climate change. On the other hand, for non-irrigation consumptive uses, all senior, junior and future licenses could be significantly affected by climate change. However, Islam and Gan (2012) did not consider how the impact of climate change could be altered or modified by El Niño and La Niña episodes.

Based on the above statements of problems, the objectives of this research study are: (a) to investigate possible changes to future SSRB water demands and supplies under the impact of climate change projected by GCMs forced by selected SRES emissions of IPCC (2001) for 2050s combined with the possible impacts of El Niño and La Niña episodes; and (b) from the results of (a), investigate possible changes to the management of SSRB's water resources under the combined impact of climate change and ENSO episodes.

6.2 Model Descriptions

6.2.1 Modified Interaction Soil Biosphere Atmosphere (MISBA)

MISBA (Kerkhoven and Gan 2006), a modified version of the Interaction Soil Biosphere Atmosphere or ISBA (Nolihan and Planton 1989; Nolihan and Mahfouf 1996) is a soil vegetation atmosphere transfer scheme selected to model the

hydrologic processes of the SSRB. MISBA is designed to simulate the exchange of heat, mass and momentum between the land or water surface and the overlying atmosphere (Tanzeeba 2009). MISBA uses the relationship of Deardorff (1978) to model the canopy interception of precipitation; MISBA assumes a three-layer soil, where evaporation from soil and vegetation is based on energy balance and aerodynamics. MISBA uses a sub-grid runoff scheme that considers sub-grid variation of soil moisture by the Xinanjiang distribution (Habets et al. 1999). In ISBA, sub-surface runoff is represented by a gravity drainage scheme following a linear reservoir. However, in MISBA the sub-surface runoff equation is converted from a linear function to a nonlinear function of soil water to account for interflow more accurately. MISBA has a three-layer snow model where the upper snow layer serves as the interface between snow pack and the atmosphere and the lower layer acts as an interface between snow pack and the soil surface. The simulated runoff of MISBA was routed by a Muskingum-Cunge routing model (Cunge 1969) to obtain the total basin stream flow.

6.2.2 Irrigation District Model (IDM)

IDM (Irrigation Water Management Study Committee 2002) has been selected to compute the irrigation consumptive demands for all irrigation blocks and return flows from district irrigation blocks. IDM contains two integrated modules: the Irrigation Requirements Module (IRM), which contains meteorological and field-based data needed to determine farm delivery requirements, and the Network

Management Module (NMM), which represents the physical characteristics of each district or private irrigation block, including pipelines, canals, reservoirs and return flow channels, and their respective operating characteristics and losses (Irrigation Water Management Study Committee 2002).

6.2.3 Water Resources Management Model (WRMM)

Water resources management optimization models can generally be classified under economic-driven and priority-driven, optimization models. In the former, the objective is to allocate water to maximize the cumulative net benefit over the planning period, while in the latter the objective is to minimize the total penalty (cost). Based on the later approach, Alberta Environment (2002) developed WRMM as a planning tool for the utilization of water resources of a river basin. WRMM is a deterministic surface water allocation model designed to handle a multipurpose, multi reservoir simulation problem with a nested optimization subprogram. In WRMM, water allocation priorities are defined by a penalty point system whereby the overall system penalty is minimized by the Network Flow Programming optimization technique (Islam and Gan 2012; Straatman et al. 2011).

Consider a network of ordered pairs (i, j) of arcs A and a total of N nodes. The minimum cost flow (or penalty) problem is formulated as:

Minimize an Objective function:

Eq. 6.1

$$\min Z = \sum_{(i,j) \in A} c_{ij} x_{ij} \quad \forall i, j \in N$$

subject to

Eq. 6.2

$$\sum_i x_{ij} - \sum_i x_{ji} = 0 \quad \forall j \in N$$

Eq. 6.3

$$0 \leq l_{ij} \leq x_{ij} \leq u_{ij} \quad \forall (i, j) \in A$$

where c_{ij} , l_{ij} , x_{ij} , and u_{ij} are the cost (or penalty) per unit flow, flow lower bound, flow value, and the flow upper bound along an arc (i, j) , respectively.

WRMM is set up to allow easy, repeated analysis of responses of a river basin to different natural conditions and planning alternatives. WRMM can consider various form of water supply (e.g., from headwaters, local runoff from a sub-basin to the network, reservoir storage, release, precipitation and evaporation) and water demands (e.g., instream flow in natural streams, flow in diversion channels, irrigation consumption, and hydropower production).

6.3 Research Methodology

To assess the combined effects of climate change and climate anomalies on the water resources management of SSRB, WRMM has been driven by three sets of input data: the first is the SSRB hydrometeorologic base case dataset (1928-

1995); the second is the base case dataset adjusted for the SRES climate projections of four GCMs for 2050s; and the third dataset represents selected years of the base case dataset affected by El Niño and La Niña episodes, re-sampled and adjusted for the SRES climate projections of four GCMs for 2050s.

6.3.1 Base Case Scenario and Climate Change Scenarios

The base case scenario used in this study is based on the historical datasets of 1928-1995 approved in the SSRB Water Management Plan Model of Alberta Environment (2006). In order to investigate the possible combined impacts of climate change and climate anomalies on the approved SSRB Water Management Plan upon which various water allocation policies have been implemented, the base case period chosen for in this study (1928-1995) is not that of the standard climate normal of 1961-1990.

The climate change scenarios used in this study is the same as that of Islam and Gan (2012), based on multiple climate change scenarios projected by four GCMs forced by several SRES emission scenarios for the SSRB. Considering many climate change scenarios is one practical way to account for uncertainties associated with GCMs' projected climate scenarios. The four GCMs selected are Japan's CCSRNIES which projected the warmest climate for the SSRB, Germany's ECHAM4 which projected the driest climate, UK's HadCM3 which projected the wettest climate, and Canada's CGCM2 which projected changes that are in between the other three GCMs' projections. The three SRES emission scenarios

selected are the fossil fuel intensive, A1FI, and the mid-range emission, A21 and B21 scenarios (IPCC 2000).

Climate change scenarios are statistically downscaled from GCM outputs using a delta change approach. The Delta change approach incorporates GCM-projected changes in key climatic variables such as temperature and precipitation by a simple calculation (e.g., the percentage change fields of the mean monthly precipitation, and the absolute change in mean monthly temperature). Even though it is considered a stable and robust method (Fowler et al. 2007; Graham et al. 2007), there are disadvantages to this simplistic approach: it assumes a constant bias; it only accounts for changes to the mean, maxima or minima of climate variables and it ignores possible changes to the variance of these climate variables; and in the case of precipitation, properties such as the temporal sequence of wet days or dry days are assumed to remain unchanged (Fowler et al., 2007, Wilby et al., 2009; Boyer et al., 2010).

6.3.2 Climate Subjected to Combined Climate Change and ENSO Impact

Step 1: Classification of El Niño and La Niña years

El Niño and La Niña years can be classified by the onset year of occurrence, strength, duration, or timing (Hanley et al., 2003). In this study, El Niño and La Niña years have been classified based on the extended Multivariate ENSO Index

(MEI), namely, MEI.ext (Wolter and Timlin 2011). MEI.ext is a simplified version of MEI based on reconstructed sea level pressure and sea surface temperature fields and is computed for four overlapping 4-month seasons, Nov–Feb, Feb–May, May–Aug, and Aug–Nov, from Dec1870/Jan1871 through Nov/Dec 2005 (135 full years).

First, the 135 years of MEI.ext values are ranked from the smallest value (e.g., 1), which denote the strongest La Niña case for that season, to the largest value (e.g., 135), which denotes the strongest El Niño case. Then, using pre-defined percentiles, the ranked, seasonal indices are classified to indicate warm, cold, or neutral conditions, e.g., the top 25 percentiles (ranks 102 or above) as warm episodes, the bottom 25 percentile (ranks 34 or lower) as cold episodes and in between (ranks 35-101) as neutral episodes. Finally, a year is classified as an El Niño or a La Niña year if out of four overlapping 4-month seasons at least three indicates warm or cold episodes, respectively (please see **Appendix B** for details). This classification leads to 14 El Nino years between 1928 and 1995 (1930, 1940, 1941, 1958, 1959, 1969, 1977, 1980, 1983, 1987, 1991, 1992, 1993, and 1994) and 7 La Niña years (1950, 1955, 1956, 1971, 1974, 1975, 1989).

Step2: Adjusting Natural Flows

Input data for WRMM includes natural flow data at a number of nodes that link up the network of the SSRB water management plan (See **Appendix C** for a

detailed schematic). To generate future natural flows at these nodes, MISBA was first calibrated and validated for these sub-basins using 20 years (1961-1980) and 10 years (1981-1990) of the ERA-40 re-analysis data of the European Centre for Mid-range Weather Forecasts (ECMWF), respectively. In general, the coefficient of determination (R^2) and Nash-Sutcliffe coefficient of efficiency (E_f) of streamflow data simulated by MISBA range from 0.63 to 0.80 and 0.46 to 0.79, respectively, in calibration runs, and 0.62 to 0.82 and 0.34 to 0.74, respectively, in validation runs. Then, MISBA was set to simulate the streamflow of the sub-basins for the climate normal (1961-1990) period and after that the monthly mean flows for the sub-basins were computed. Next, from the ERA-40 dataset, data that correspond to El Niño (e.g., 1969, 1977, 1980, 1983, and 1987) and La Niña (1971, 1974, 1975, and 1989) years were re-sampled using the standard bootstrap method with replacement to replace the 30-year climate normal (1961-1990) data.

Next, a two-step process was adopted to downscale climate projections at GCM scale to local scale data as input for MISBA. First, using the Adaptive Gaussian Window Interpolation method (Agüi and Jiménez 1987), the change fields of mean monthly precipitation (% change) and mean monthly temperature (absolute change) at selected grids of the four GCMs for 2050s were interpolated to the ERA-40 grids selected for the sub-basins of SSRB. Second, these interpolated change fields of GCMs were used to adjust the re-sampled ERA-40

data at grids selected for the sub-basins of SSRB (Tanzeeba and Gan 2012; Islam and Gan 2012).

Finally, MISBA was driven by these re-sampled and adjusted ERA-40 reanalysis data to simulate the streamflow of SSRB that reflect the combined effects of climate change and El Niño and La Niña episodes for each sub-basins for the 2050s, and the monthly ratios of these simulated streamflows were computed from the streamflow simulated for the sub-basins that corresponded to the combined scenarios and that correspond to the climate normal. The weekly natural flow data selected for WRMM (1928-1995) for each month was adjusted according to these simulated monthly ratios. The apportionment flow and instream flow requirements were also re-computed using these adjusted natural flows.

Step 2: Adjusting Irrigation Consumptive Demand

First, from the agro-climatic dataset of SSRB, data that correspond to El Niño (e.g., 1930, 1940, 1941, 1958, 1959, 1969, 1977, 1980, 1983, 1987, 1991, 1992, 1993, and 1994) and La Niña (1950, 1955, 1956, 1971, 1974, 1975, 1989) years were re-sampled using the standard bootstrap method with replacement to replace the 68-year (1928-1995) base case data. Then the re-sampled agro-climatic dataset (e.g., maximum/minimum temperature, precipitation, and the potential evaporation) were adjusted according to the projections of selected

IPCC SRES climate scenarios of 2050s. Finally, IDM was driven by these re-sampled and adjusted climate data to generate the irrigation consumptive demands for all irrigation blocks of SSRB that reflect the combined effects of climate change, El Niño and La Niña episodes for 2050s. For irrigation districts, the average annual irrigation demands from each irrigation block are estimated as the total, areally weighted demand divided by the total area of that irrigation district. Similarly for private irrigation water uses, the average annual water demands for senior, junior and future licenses are estimated by dividing the total areally weighted demand for each category by the total area of that category.

Step 3: Adjusting Meteorological Stations' Precipitation

Precipitation data of selected climate stations are used in WRMM to calculate precipitation input to reservoirs. First, from the precipitation dataset of all meteorological stations of the SSRB, data that correspond to El Niño and La Niña years were re-sampled using the standard bootstrap method with replacement to replace the 68-year (1928-1995) base case data. Then, for each IPCC SRES climate scenarios of 2050s, re-sampled precipitation data were adjusted to reflect the combined effects of climate change and El Niño and La Niña episodes.

Step 4: Adjusting Lake Evaporation Data

Lake evaporation data collected for climate stations are used in WRMM to calculate evaporation from the reservoirs. First, from the lake evaporation

dataset of all meteorological stations of the SSRB, data that correspond to El Niño and La Niña years were resampled using the standard bootstrap method with replacement to replace the 68-year (1928-1995) base case data. Then, for each IPCC SRES climate scenarios of 2050s, resampled lake evaporation dataset data were adjusted using a simplified form of the Penman's Equation of Linacre (1977) to reflect the combined effects of climate change and El Niño and La Niña episodes (Islam and Gan 2012).

Step 5: WRMM's Simulation based on Updated Hydrometeorologic Base Data

From all the above datasets, the Hydrometeorologic Base Data File of SSRB were updated for various IPCC SRES climate scenarios of 2050s affected by El Niño and La Niña episodes, and used to drive WRMM to simulate possible changes in water management due to changes in water supply and demands under the potential impact of climate change, and the combined impacts of climate change and climate anomalies, respectively.

6.4 Discussions of Results

6.4.1 Projected Changes to Future Water Supply

The water availability of a basin under climatic changes primarily depends on projected changes to precipitation and temperature. Figure 6.2 shows percentage changes in the mean annual precipitation ($\% \Delta P$) and changes in the

mean annual temperature (ΔT) in the SSRB predicted by four GCMs (CCSRNIES, CGCM2, ECHAM4, HadCM3) which were forced by three SRES emission scenarios (A1FI, A21 and B21) of IPCC for the 2050s, and climate scenarios of 2050s combined with ENSO (2050s+El Niño and 2050s+La Niña) episodes. Predicted changes in the temperature and precipitation vary between the GCMs and the selected SRES scenarios. Compared to the climate normal, the temperature of SSRB is projected to increase by 2.5-4.25 °C by 2050s while precipitation is projected to change between 1% to 8.0%. When considering potential combined impacts of both climate change and climate anomalies such as El Niño, it seems on the average that precipitation could decrease by 5.15% while temperature could marginally increase by about 0.3°C beyond that of the SRES climate scenarios of 2050s. In contrast, for La Niña years, on the average precipitation could increase by about 9% while temperature decreases by about 0.3° C beyond that of SRES climate scenarios of 2050s. In general drying (wetting) effect of El Niño (La Niña) events on SSRB can be explained from composites of 500-hPa geopotential height anomalies associated with El Niño (La Niña). In an El Niño (La Niña) event there is a deeper (weaker) than normal Aleutian low, amplification (erosion), and eastward (westward) displacement of the western Canadian ridge. In El Niño events, this upper-atmospheric flow pattern is likely associated with a split in the jet stream over North America: a weaker branch diverted northward and a lower subtropical branch shifted southward. The southern Canadian region as the SSRB lies in between the two jets and receive lower than normal

precipitation resulting overall drying impacts (Shabbar et al. 1996; Shabbar and Khandekar 1996; Gan et al. 2007). In contrast, in La Niña events, the upper-atmospheric flow associated with the aforementioned circulation pattern includes stronger westerlies moving across the eastern Pacific and into southern Canada. As a result, the moist air originating from the Pacific result in positive precipitation anomalies over southern Canada (Shabbar et al. 1996; Shabbar and Khandekar 1996; Gan et al. 2007).

A summary of the locations and streamflow projected by MISBA for SSRB under the SRES climate scenarios of 2050s and climate scenarios combined with ENSO (2050s+El Niño and 2050s+La Niña) are listed in Table 6.1. It was found that even though precipitation is projected to increase by about 3% by 2050s, except for a few cases, most of the scenario runs show a decrease in the mean annual average streamflow for most sub-basins located in Oldman, Bow and Red Deer River basins. While considering the potential combined impact of climate change and climate anomalies, a further decrease in streamflow by 2050s is projected if the climate anomaly considered is El Niño since El Niño has the tendency to result in drier climate in Alberta (Gan et al., 2007). In contrast, if the climate anomaly considered is La Niña, then considering the combined impact of climate change and La Niña would lead to a higher projected streamflow in SSRB by 2050s, than only if the impact of climate change is considered. The mean annual average flow is projected to decrease due to an enhanced evaporation caused by rising temperature that offsets the increase in precipitation (Tanzeeba and Gan

2012; Islam and Gan 2012). The projected percentage changes in the mean annual average and the mean annual maximum streamflows averaged over the SSRB for the 2050s scenario and combined scenarios are plotted against the precipitation and temperature changes in 2050s in Figure 6.3.

It was found that in 2050s, based on the B21 SRES climate scenario projected by CCSRNIES, MISBA projected a 9% increase in the annual maximum streamflows, but based on CGCM2`'s SRES B21 climate scenario, MISBA only projected a slight increase (1%) in the annual average and maximum streamflows. However, based on other GCMs and SRES scenarios, MISBA projected a significant decrease in the annual average and maximum streamflows over SSRB by 2050s. While considering the potential combined impact of climate change and climate anomalies, a further decrease in the streamflow of SSRB by 2050s was simulated if the climate anomaly considered was El Niño. In contrast, if the climate anomaly considered was La Niña, the combined impact would lead to a higher projected streamflow in SSRB by 2050s, than only if the impact of climate change was considered for SSRB. With reference to the 1961-1990 climate normal, on an average, the % change in the mean annual average streamflow of SSRB under the potential combined impact of climate change and El Niño are projected as -18%, as compared to -6% by 2050s, if only climate change impact is considered. On the other hand, if the potential combined impact of climate change and La Niña is considered, the corresponding projected % change in the mean annual

streamflow by 2050s will be 2%. Similar results are also found for the mean annual maximum streamflows.

With reference to the 1961-1990 climate normal, on average, the % change in the mean annual maximum streamflow of SSRB under the potential combined impact of climate change and El Niño are projected as -17%, as compared to -10% by 2050s, if only climate change impact is considered. On the other hand, if the potential combined impact of climate change and La Niña is considered, the corresponding projected % change in the mean annual maximum streamflow by 2050s will be 9%. Overall, the largest decrease in the mean annual average streamflow (-29%) and mean annual maximum (-23%) streamflows were projected under the 2050s climate scenario of ECHAM4 combined with El Niño episode. The largest increase in the mean annual average streamflows (+18%) and mean annual maximum streamflows (+22%) were projected under the 2050s climate projection of CCSRNIES and HadCM3, respectively, combined with La Niña episode.

At seasonal time scale, most of the climate scenarios of 2050s considered lead to a projected increase in winter and spring streamflow, but a significant decrease in the summer streamflow, and a decrease in the autumn streamflow. These seasonal changes are projected to be more severe in winter, summer and autumn; and modest in spring when the combined impact of climate change and El Niño are considered. In contrast, if the climate anomaly considered is La Niña,

the projected change to the winter streamflow by 2050s is either severe, or similar to only if climate change impact is considered.

6.4.2 Projected Changes to Future Water Demand

Figure 6.4 (a and b) show the projected percentage changes in the average annual irrigation water demand in SSRB for 13 irrigation districts, and private irrigation blocks for the 2050s scenario and combined scenarios, with respect to that of the base case. Further, the percentage changes in the average annual water demand for the combined scenario, with respect to that of 2050s climate scenarios, are plotted against the precipitation and temperature changes in 2050s in Figure 6.5 (a & b).

On the average, water demands for the irrigation districts are expected to increase by 12% (4%-17% range) in 2050s. While considering the potential combined impact of climate change and climate anomalies, a more modest increase in irrigation demand by 2050s is projected if the climate anomaly considered is El Niño. In contrast, considering the combined impact of climate change and La Niña would lead to a marginally higher projected irrigation demand by 2050s, than only if the impact of climate change is considered (Figure 6.4a). For irrigation district, on the average, an 8% decrease in annual water demand was projected for the '2050s+El Niño' combined scenario than that of climate scenarios of 2050s only (Figure 6.5a). In contrast, a further 1% increase in

water demand by 2050s is projected if the climate anomaly considered is La Niña (Figure 6.5a).

Similar results are observed for private irrigation blocks (Figure 6.4b and Figure 6.5b). Water demands for the private irrigation blocks are expected to increase by 17% (9%-22% range) in 2050s. While comparing to the impact of climate scenarios of 2050s only, a 6% decrease in the annual water demand for private irrigation blocks was projected for the '2050s+El Niño' combined scenarios (Figure 6.5b). In contrast, a further 1% increase in the water demand by 2050s is projected if the climate anomaly considered is La Niña (Figure 6.5b).

Even though El Niño (La Niña) has a overall drying (wetting) effect on SSRB (see Section 6.4.1 for details), there is a further decrease in the projected irrigation water demand for district and private irrigation blocks for the 2050s+El Niño combined scenario than that of the climate scenarios of 2050s only because during the irrigation period of early May to mid October, the average precipitation is projected to be 3.81% higher while the average potential evaporation is projected to be 0.45% higher when the climate scenarios affected by El Niño episodes than only if the impact of climate change is considered. In contrast, for early May to mid October, the average precipitation and potential evaporation are 1.84% and 0.73% lower, respectively, when the 2050s+La Niña combined scenario than only that of the climate scenarios of 2050s are

considered, which lead to a marginal increase in the irrigation water demand for district and private irrigation.

6.4.3 Deficits under Combined Climate Change and Anomaly

Impact

On the basis of future projected changes in water supply and demand under the combined impacts of climate change and climate anomalies for 2050s, percentage changes to the number of deficit years (Islam and Gan 2012) out of 68 years (1928-1995) simulated by WRMM to specific water sectors of SSRB (e.g., irrigation districts, private irrigation, non-irrigation consumptive use and instream flow requirements), in comparison to that of the base case scenario (black square), are plotted with respect to projected temperature change (ΔT °C) in Figure 6.6.

The instream flow requirement that was marginally affected by the impact of climate change in 2050s (Islam and Gan 2012), is expected to be affected slightly more under the combined scenarios, given that the deficit years for the instream flow requirements of about 50% in 2050s scenario, are projected to be about 57% and 53% when the 2050s scenario combined with El Niño and La Niña episodes, respectively (Figure 6.6a). A further increase in deficits years for instream flow requirements in the 2050s scenario affected by El Niño episodes is due to a further decrease in streamflows in combined scenario than that of climate change alone in 2050s. However, a further increase in the number of

deficit years for instream flow requirements in the climate change scenario for 2050s affected by La Niña episodes is because the average autumnal (September-November) streamflows of Bow and Oldman sub-basins, which were used to calculate instream flow requirement based on the Fish Rule Curve for those sub-basins, have been projected to significantly decrease for both El Niño (about 15%) and La Niña (about 11%) episodes.

The irrigation districts, that are predicted to be progressively affected by climate change over the 21st century (Islam and Gan 2012), is expected to be more severely affected under the combined impact of climate change and El Niño, given that the percent deficit years increase from about 14% in the 2050s scenarios to about 18% in 2050s scenario combined with El Niño episodes (Figure 6.6b). In contrast, the combined impact of climate change, SRES scenarios of 2050s, and La Niña as the climate anomaly on the irrigation district will be more moderate than that of 2050s only, given that the percent deficit years decrease from about 14% in the 2050s scenarios to about 8% in the 2050s scenario combined with La Niña episodes (Figure 6.6b). Among the SRES climate scenarios of 2050s combined with ENSO episodes considered, ECHAM4 A21 SRES scenario combined with El Niño episodes and CCSRNIES B21 SRES scenario combined with La Niña scenario predicted the largest and the least future increase in percent deficit years of irrigation districts, respectively.

The percent deficit years for the senior, junior, and future private irrigation blocks are projected to increase from about 4%, 24%, and 22%, under the SRES climate change scenarios of 2050s, to about 8%, 31%, and 31%, respectively, under the SRES scenarios of 2050s combined with El Niño episodes. However, under the SRES scenarios of 2050s combined with La Niña episodes, WRMM projected a more modest increase in the percent deficit years for the senior, junior and future private irrigation blocks, e.g., 3%, 20%, and 18%, respectively (Figure 6.6c, Figure 6.6d, and Figure 6.6e). It should be noted that, the projected impacts are much less for senior private irrigation users because they have the priority of getting water over their junior counterparts. Among the SRES climate scenarios of 2050s combined with ENSO episodes considered, CCSRNIES B21, CCSRNIES B21, and ECHAM4 A21 scenario combined with El Niño episodes predicted the largest increase in percent deficit years for the senior, junior and future private irrigation blocks, e.g., 12%, 37%, and 40%, respectively. However, WRMM predicted the least increase in percent deficit years for the senior, junior and future private irrigation blocks, e.g., 2%, 16%, and 10%, under the 2050s SRES scenarios of CCSRNIES A1FI, CCSRNIES A1FI, and CGCM2 B21 combined with La Niña episodes, respectively.

With reference to the 2050s climate change scenarios, the water demand for irrigation districts and private irrigation blocks in the '2050s+El Niño' scenarios are projected to decrease by 8%, and 6%, respectively, but the percent deficit years are expected to increase due to the significant decrease in streamflows of

SSRB for these '2050s+El Niño' combined scenarios. On the other hand, the percent deficit years of irrigation districts and private irrigation blocks for the '2050s+La Niña' combined scenarios are projected to decrease, even under a projected marginal increase (about 1%) in the irrigation demand than that of 2050s climate change scenarios only because the streamflows of SSRB is projected to increase marginally in the '2050s+La Niña' scenarios.

The senior, junior, and future non-irrigation consumptive users could be significantly affected by the combined impacts of climate change and climate anomalies (Figure 6.6f, Figure 6.6g, and Figure 6.6h). The percent deficit years for the senior, junior, and future non-irrigation users are projected to increase from about 61%, 51%, and 51%, under the SRES climate scenarios of 2050s, to about 67%, 56%, and 53%, respectively, under the SRES scenarios of 2050s combined with El Niño episodes. Under the SRES scenarios of 2050s combined with La Niña episodes, WRMM projected virtually no change to the increase in the percent deficit years for the senior, junior, and future non-irrigation water users, e.g., 68%, 51%, and 52%, respectively. Among the SRES climate scenarios of 2050s combined with ENSO episodes considered, again, ECHAM4 A21 scenario combined with El Niño episodes and CCSRNIES B21 scenario combined with La Niña scenario predicted the largest and the least future increase in the percent of deficit years, respectively, for all senior, junior and future licenses under non-irrigation consumptive uses.

6.5 Summary and Conclusions

In this study, potential combined impacts of climate change and climate anomalies (El Niño Southern Oscillation or ENSO) on the water resources management of SSRB are simulated by MISBA, IDM, and WRMM on the basis of climate change scenarios projected by four GCMs (CCSRNIES, ECHAM4, HadCM3, and CGCM2) forced by three SRES emission scenarios (A1FI, A21, B21) of IPCC (2001) for the 2050s combined with El Niño and La Niña episodes.

Under these climate change projections combined with El Niño and La Niña episode, the largest decrease and increase in the mean annual streamflow predicted for SSRB in the 2050s were -29% and +18%, respectively. Under the combined impact of climate change projections for 2050s and El Niño, IDM's simulations show a further decrease in the irrigation water demand by 7% than that projected for the climate change impacts of the 2050s only. In contrast, the irrigation water demand is projected to only marginally increase by about 1% in the 2050s if the climate anomaly considered is La Niña, instead of El Niño.

On the basis of WRMM's simulations, for the climate change scenarios of the 2050s combined with El Niño or La Niña episodes, the instream flow requirement is projected to be affected slightly more than WRMM's simulation for the climate change scenarios of 2050s only. The irrigation districts, senior private irrigation, junior private irrigation, and future private irrigation blocks are projected to be

more (less) severely affected under the combined impact of climate change and El Niño (climate change and La Niña) than under the impacts of climate change alone. The projected impacts in terms of the mean % deficit years in the 2050s for these licenses are 14%, 4%, 24%, and 22% for climate change scenarios alone; 18%, 8%, 31%, and 31% for 'climate change + El Niño' scenarios; and 8%, 3%, 20%, and 18% for 'climate change + La Niña' scenarios, respectively. In contrast, WRMM's simulations for the 2050s in terms of % deficit years show a marginal increase for the senior, junior and future licenses of non-irrigation water users under both 'climate change + El Niño' scenarios and 'climate change + La Niña' scenarios, than that under climate change scenarios only.

Overall, on the basis of results obtained for this study on the combined impact of climate change and climate anomaly (when El Niño or La Niña is active), license holders of SSRB categorized under district irrigation, junior and future private irrigation, and senior, junior and future non-irrigation consumptive user groups could be more, or less, significantly affected, depending on whether the climate anomaly considered is El Niño or La Niña, than the impact of climate change alone.

6.6 References

- Agüí, J.C., and Jiménez, J. (1987). "On the performance of particle tracking." *J. Fluid. Mech.*, 185, 447-468.
- Alberta Environment (2002). "Water Resources Management Model Computer Program Description." *Southern Region, Resource Management Branch*. Alberta Environment.
- Alberta Environment (2003a). "South Saskatchewan River Basin Water Management Plan Phase 2: Scenario Modelling Results Part 1." *Alberta Environment*.
- Alberta Environment (2003b). "South Saskatchewan River Basin Water Management Plan Phase 2: background Studies". *Alberta Environment*.
- Alberta Environment (2005). "South Saskatchewan River Basin Water Allocation." *Alberta Environment*.
- Alberta Environment (2006). "Approved Water Management Plan for the South Saskatchewan River Basin (Alberta)." *Albeta Environment*.
- Alberta Environment (2010). "South Saskatchewan Regional Plan: Water Quantity and Quality Modeling Results." *Alberta Environment*.
- Boyer, C., Chaumont, D., Chartier, I., and Roy, A.G. (2010). "Impact of climate change on the hydrology of St. Lawrence tributaries." *J. Hydrol.*, 384 (1-2), 65–83.

- Cunge, J. A. (1969). "On the Subject of a Flood Propagation Method (Muskingum Method)." *Journal of Hydraulic Research*, 7 (2), 205-230.
- Deardorff, J. W. (1978). "Prediction of Ground Surface Temperature and Moisture, With Inclusion of a Layer of Vegetation." *Journal of Geophysical Research*, 83 (C4), 1889-1903.
- Environment Canada (2007). "Municipal Water Use Report, 2004 Statistics." Environment Canada.
- Fang, X., and Pomeroy, J.W. (2008). "Drought impacts on Canadian prairie wetland snow hydrology." *Hydrol. Process.*, 22(15), 2858–2873.
- Fowler, H. J., Blenkinsop, S., and Tebaldi, C. (2007). "Linking climate change modelling to impacts studies: Recent advances in downscaling techniques for hydrological modelling." *Int. J. Climatol.*, 27(12), 1547-1578.
- Gan, T. Y., Gobena, A. K., and Wang, Q. (2007). "Precipitation of southwestern Canada - Wavelet, Scaling, Multifractal Analysis, and Teleconnection to Climate Anomalies." *J. of Geophysical Research*, 112, D10110.
- Gan, T.Y. (2000). "Reducing vulnerability of water resources of Canadian Prairies to potential droughts and possible climatic warming." *Water Resour. Manage.*, 14(2), 111–135.
- Gobena, A. K., and Gan, T. Y. (2006). "Low-frequency variability in southwestern Canadian streamflow: links to large-scale climate anomalies." *Int. J. Climatol.*, 26 (13), 1843-1869.

- Graham, L.P., Hagemann, S., Jaun, S., and Beniston, M. (2007). "On interpreting hydrological change from regional climate models." *Climatic Change*, 81, 97–122.
- Habets, F, J Nolihan, C Golaz, J. P. Goutorbe, P. Lacarrère, and E Leblois (1999). "The ISBA surface scheme in a macroscale hydrological model applied to the Hapex–Mobilhy area. Part 1. Model and database." *Journal of Hydrology*, 75-96.
- Hanley, D.E., Bourassa, M.A, O’Brien, J.J., Smith, S.R. and Spade, E.R. (2003). "A Quantitative Evaluation of ENSO Indices, Notes and Correspondence." *J.Climate*, 16, 1249-1258.
- IPCC (2000). "Summary for Policymakers: Emissions Scenarios, A Special Report of Working Group III of the Intergovernmental Panel on Climate Change." *Cambridge University Press, UK*.
- IPCC (2001) "Climate Change 2001: The Scientific Basis. Contribution of Working Group I to the Third Assessment Report of the Intergovernmental Panel on Climate Change." *Cambridge University Press, Cambridge, United Kingdom and New York, NY, USA*.
- Irrigation Water Management Study Committee (2002). "South Saskatchewan River Basin: Irrigation in the 21st Century, Volume 1: Summary Report." *Alberta Irrigation Projects Association, Lethbridge, Alberta*.

- Islam, Z. and Gan, T. (2012). "Effects of Climate Change on the Surface Water Management of South Saskatchewan River Basin." *J. Water Resour. Plann. Manage.* doi: 10.1061/(ASCE)WR.1943-5452.0000326 .
- Johnson, W.C., Millett, B.V., Gilmanov, T., Voldseth, R.A., Guntenspergen, G.R., and Naugle, D.E. (2005). "Vulnerability of northern prairie wetlands to climate Change." *BioScience*, 55(10), 863-872.
- Kerkhoven, E. and Gan, T.Y. (2006). "A modified ISBA surface scheme for modeling the hydrology of Athabasca River Basin with GCM-scale data." *Advanced in Water Resour.*, 29(6), 808-826.
- Lincare, E.T. (1977). "A simple formula for estimating evaporation rates in various climates, using temperature data alone." *Agricultural Meteorology*, 18, 409-424.
- Mishra. V., Cherkauer. K.A., Niyogi, D. et al (2010). "A regional scale assessment of land use/land cover and climatic changes on water and energy cycle in the upper Midwest United States." *Int. J. Climatol.*, 30(13), 2025–2044.
- Shabbar, A. and Khandekar, M. (1996). "The impact of El Nino-Southern Oscillation on the temperature field over Canada." *Atmosphere-Ocean*, 34, 401–416.
- Shabbar, A., Bonsal, B. and Khandekar, M. (1997). "Canadian precipitation patterns associated with the Southern Oscillation." *Journal of Climate*, 10, 3016–3027.

- Straatman, B., Hasbani, J. G., Tang, T., Berg, K., Moreno, N., & Marceau, D. (2011). "Linking a Land-Use Cellular Automata with a Water Allocation Model to Simulate Land Development Constrained by Water Availability in the Elbow River Watershed in Southern Alberta." *GEOMATICA*, 65(4), 365-374.
- Tanzeeba, S. and Gan, T.Y. (2012). "Potential impact of climate change on the water availability of South Saskatchewan River Basin." *Climatic Change*, 112, 355-386.
- Wilby, R. L., Troni, J., Biot, Y., Tedd, L., Hewitson, B. C., Smithe, D. M. and Suttonf, R. T. (2009). "A review of climate risk information for adaptation and development planning." *Int. J. Climatol.*, 29, 1193–1215.
- Withey, P. and van Kooten, G.C. (2011). "The effect of climate change on optimal wetlands and waterfowl management in Western Canada." *Ecological Economics*, 70(4), 798–805.
- Wolter, K. and Timlin, M. (2011). "El Niño/Southern Oscillation behaviour since 1871 as diagnosed in an extended multivariate ENSO index (MEI.ext)." *Int. J. Climatol.* 31, 1074–1087.
- Xu, C.-Y., and Singh, V.P., (2004). "Review on Regional Water Resources Assessment Models under Stationary and Changing Climate." *Water Resour. Manage.*, 18, 591–612.

Table 6.1 Modified Interaction Soil Biosphere Atmosphere (MISBA) simulated percentage changes in mean annual runoff from the climate normal (1961-1990) with respect to climate change scenarios projected by four General Circulations Models (CCSRNIES, CGCM2, ECHAM4, HadCM3) forced by three Special Report on Emissions Scenarios (SRES) emissions (A1FI, A21 and B21) of Intergovernmental Panel on Climate Change (IPCC) in 2050s, and 2050s scenario combined with El Niño and La Niña Episodes.

Basin	% Change in Mean Annual Runoff from Climate Normal (1961-1990)								
	2050s			2050s+El Niño			2050s+La Niña		
	Min	Max	Ave	Min	Max	Ave	Min	Max	Ave
Red Deer at Dickson Dam (REDEERDD)	-9	20	2	-15	18	-3	-12	19	0
Red Deer at Red Deer (REDEERRD)	-10	19	0	-13	19	-3	-20	5	-11
Red Deer Near Nevis(REDEERNN)	-12	12	-3	-3	25	9	-16	9	-5
Red Deer at Big Valley (REDEERBV)	-12	12	-3	-19	10	-8	-15	10	-5
Red Deer at Drumheller (REDEERDH)	-15	10	-4	-12	15	0	-21	0	-11
Red Deer Near Jenner(REDEERNJ)	-26	9	-12	-30	7	-16	-12	20	2
Red Deer at Bindloss(REDEERBL)	-27	7	-13	-32	2	-18	-19	13	-5
Oldman near Waldron Cor.(OLDMANWC)	-22	0	-14	-36	-17	-30	-30	4	-19
Oldman near Brocket(OLDMANBR)	-16	8	-6	-30	-5	-19	-3	24	8
Oldman near Fort Macleod(OLDMANFM)	-15	13	-3	-27	0	-16	-2	29	11
Oldman near Lethbridge(OLDMANLT)	-10	-1	-5	-25	-17	-21	7	20	14
Crowsnest near Lundbreck(CROWSTLB)	-19	4	-10	-32	-9	-21	-4	26	8
Castle near Beaver Mines(CASTLEBM)	-15	2	-7	-30	-11	-23	-8	21	3
Pincher at Pincher Creek(PINCHRPC)	-13	10	-3	-28	-5	-18	-3	25	8
Belly below Waterton Confl.(BELLYBWC)	-15	15	-2	-28	2	-15	-4	26	9
St. Mary at St. Mary Dam(STMARYSD)	-19	-2	-9	-25	-4	-14	2	22	11
Willow above Chain Lakes(WILLOWCL)	-25	28	-6	-39	1	-25	-17	51	5
Willow near Claresholm(WILLOWCS)	-14	4	-4	-48	-33	-41	1	22	11
Willow near Nolan(WILLOWNN)	-20	2	-8	-60	-42	-51	-3	23	10
Elbow below Glenmore Dam(ELBOWGLD)	-12	10	-3	-24	4	-13	-5	20	4
Bow at Calgary(BOWCLGRY)	-15	12	-3	-24	12	-10	-12	17	0
Highwood near the Mouth(HOGHMOU)	-31	12	-12	-51	-5	-30	-27	19	-7

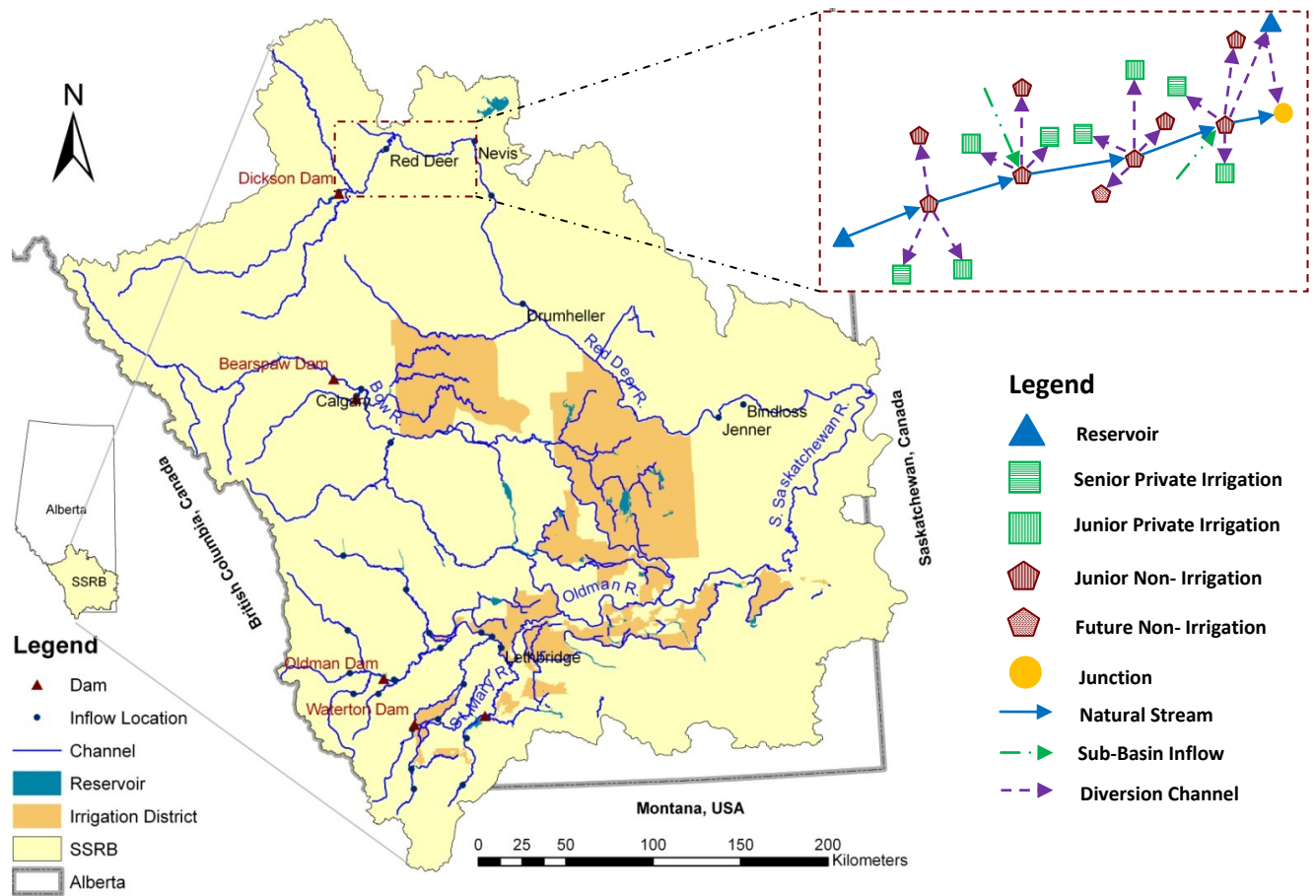


Figure 6.1 The South Saskatchewan River Basin (SSRB) (left) and a part of the SSRB water management node-link network schematic (right). See Appendix C for detail schematic.

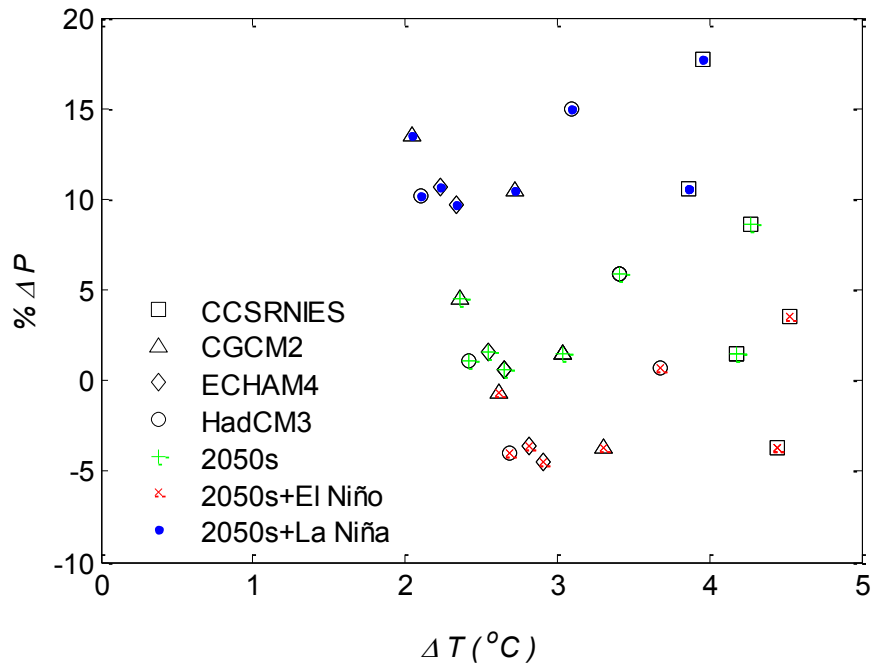


Figure 6.2 Percentage changes in the mean annual precipitation ($\% \Delta P$) and changes in the mean annual temperature (ΔT) for 2050s climate scenario projected by four General Circulations Models (CCSRNIES, CGCM2, ECHAM4, HadCM3) forced by three Special Report on Emissions Scenarios (SRES) emissions (A1FI, A21 and B21) of Intergovernmental Panel on Climate Change (IPCC), and for climate scenarios of 2050s combined with El Niño and La Niña episodes for the South Saskatchewan River Basin (SSRB) as compared to the climate normal (1960-1991).

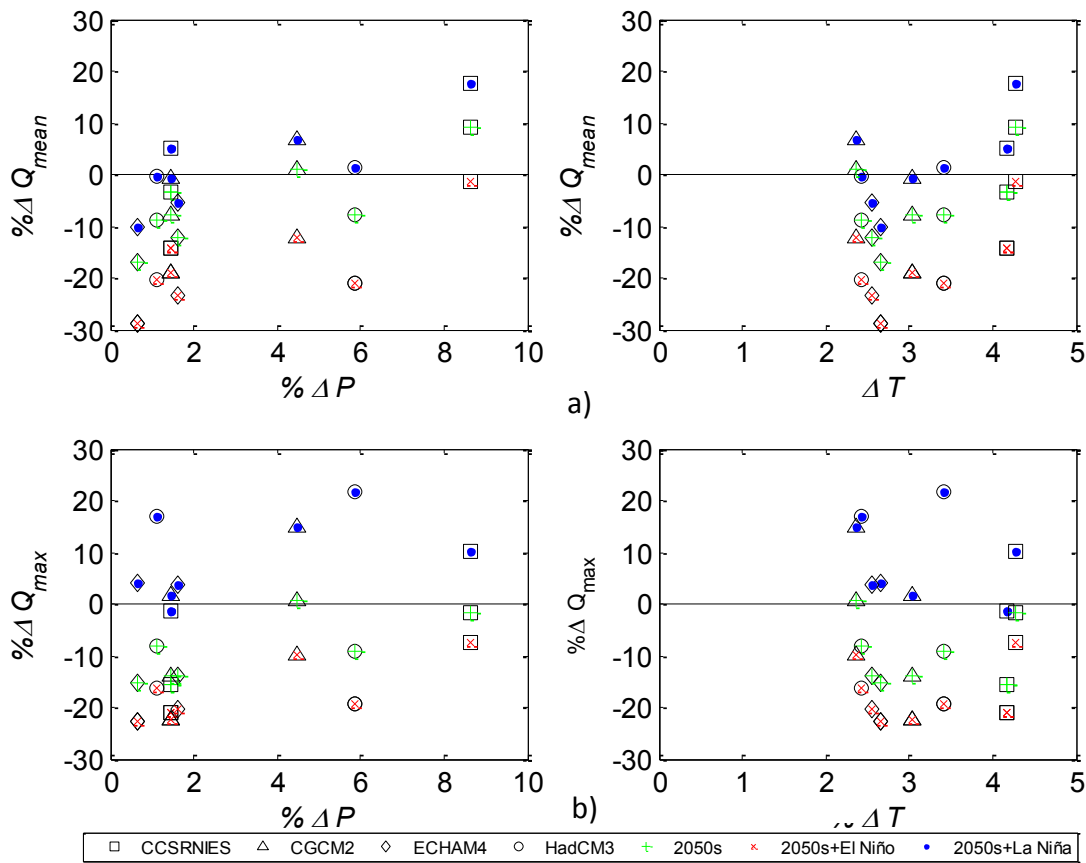


Figure 6.3 Modified Interaction Soil Biosphere Atmosphere (MISBA) simulated a) percentage changes in mean annual average streamflow ($\% \Delta Q_{mean}$), and b) percentage changes in mean annual maximum streamflow ($\% \Delta Q_{max}$) for the South Saskatchewan River Basin (SSRB) versus ΔT and $\% \Delta P$ as compared to the climate normal (1960-1991) with respect to the climate change scenarios projected by four General Circulations Models (CCSRNIES, CGCM2, ECHAM4, and HadCM3) forced by three Special Report on Emissions Scenarios (SRES) emissions (A1FI, A21, and B21) of Intergovernmental Panel on Climate Change (IPCC) for 2050s, and for climate scenarios of 2050s combined with El Niño and La Niña episodes.

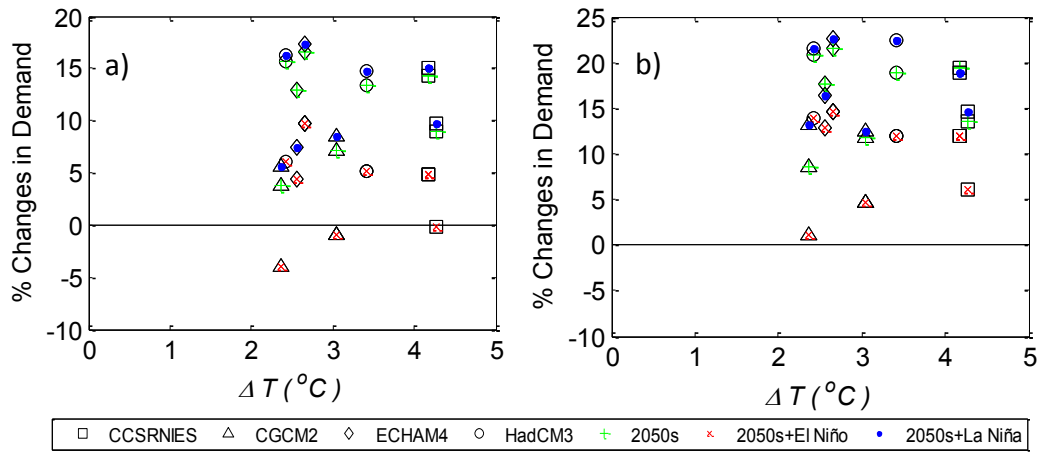


Figure 6.4 Irrigation District Model (IDM) simulated percentage changes in average annual irrigation demand for the South Saskatchewan River Basin (SSRB) versus ΔT as compared to the base case scenario with respect to the climate change scenarios projected by four General Circulations Models (CCSRNIES, CGCM2, ECHAM4, and HadCM3) forced by three Special Report on Emissions Scenarios (SRES) emissions (A1FI, A21, and B21) of Intergovernmental Panel on Climate Change (IPCC) for 2050s, and for climate scenarios of 2050s combined with El Niño and La Niña episodes for Irrigation Districts (a), and Private Irrigation blocks (b).

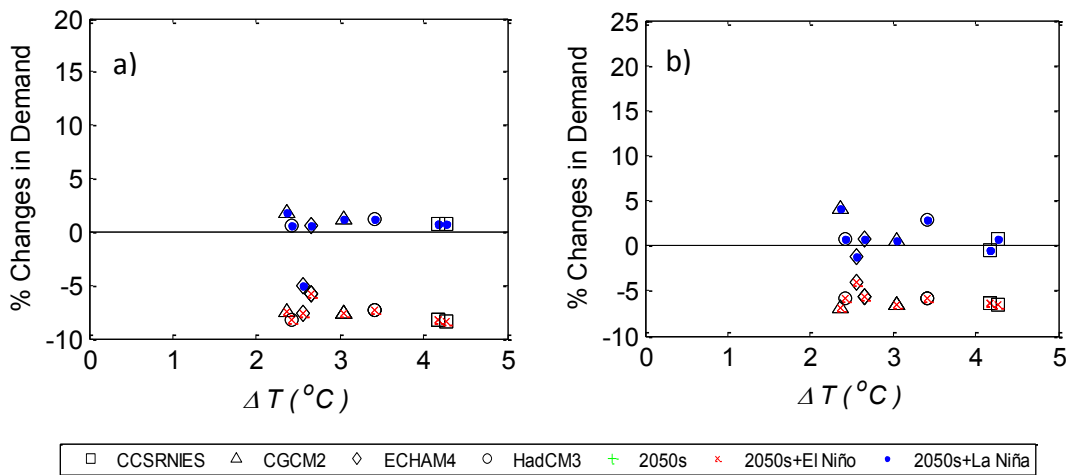


Figure 6.5 Irrigation District Model (IDM) simulated percentage changes in average annual irrigation demand for the South Saskatchewan River Basin (SSRB) versus ΔT as compared to the climate scenarios of 2050s with respect to the combined scenarios projected by four General Circulations Models (CCSRNIES, CGCM2, ECHAM4, and HadCM3) forced by three Special Report on Emissions Scenarios (SRES) emissions (A1FI, A21, and B21) of Intergovernmental Panel on Climate Change (IPCC) combined with El Niño and La Niña episodes for Irrigation Districts (a), and Private Irrigation blocks (b).

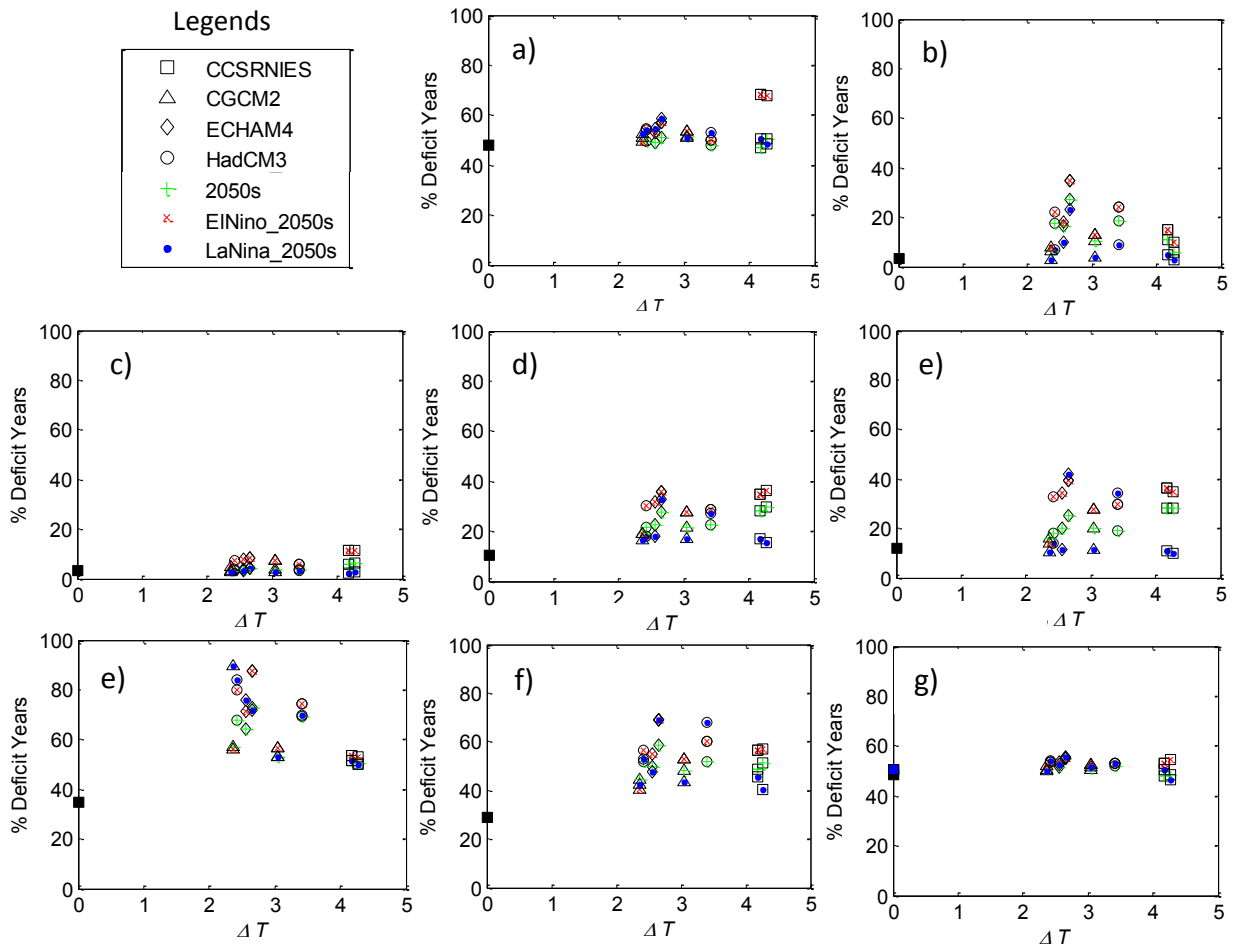


Figure 6.6 Water Resources Management Model (WRMM) simulated % Deficit Years versus ΔT for base case scenario and combined scenarios (2050s+El Niño, 2050s+La Niña) with respect to the climate change scenarios projected by four GCMs(CCSRNIES, CGCM2, ECHAM4, and HadCM3) forced by three SRES emissions (A1FI, A21, and B21) of IPCC for 2050s combined with El Niño and La Niña episodes for different water sectors of the SSRB: a) Instream flow requirement b) District irrigation c) Senior private irrigation d) Junior private irrigation e) Future private irrigation f) Senior non-irrigation consumptive uses g) Junior non-irrigation consumptive uses h) Future non-irrigation consumptive uses.

CHAPTER 7

Conclusions and Recommendations

7.1 Summary and Conclusions

This research study is focused on investigating the potential impact of climate change, and the combined impacts of climate change and El Niño Southern Oscillation or ENSO on the hydrology and water resources management for the South Saskatchewan River Basin (SSRB) of Alberta for the 21st century. The potential impact of climate change to SSRB was simulated by a hydrologic, an irrigation demand, and a water resources management model by adjusting the base case observed climate of SSRB with Special Report on Emission Scenario (SRES) climate change scenarios projected by four General Circulation Models (GCMs) of the Intergovernmental Panel on Climate Change (IPCC) for 2010-2039 (2020s), 2040-2069 (2050s), and 2070-2099 (2080s). The combined impacts of climate change and climate anomalies for 2050s were also simulated by driving these models with re-sampled climate data of SSRB observed during El Niño and La Niña years within the base case period and adjusted with the SRES climate scenarios of the aforementioned GCMs. The entire study can be divided into five different phases:

In the first phase (Chapter 2), a semi-distributed (DPHM-RS) and a fully-distributed (MISBA) physically based hydrologic model were applied to a small unregulated river basin, the Blue River Basin (BRB) of Oklahoma, to explore the effect of basin discretization in basin-scale hydrologic modeling. It was found that, for a given climatic regime and river basin characteristics (topography, vegetation and geology), there might be an optimum level of discretization in modeling basin hydrology in a semi-distributed manner and for BRB it turned out to be 7 sub-basins (170 km² per sub-basin). While comparing the results of DPHM-RS to the fully distributed model MISBA, the calibration and validation period statistics demonstrate generally well performance of MISBA in both stages over the semi-distributed DPHM-RS.

In the second phase (Chapter 3), fully distributed hydrologic model, the Modified Interaction Soil Biosphere Atmosphere (MISBA) was selected to simulate the future streamflow of SSRB under the potential impact of climate change, and the combined impacts of climate change and climate anomalies. It was found that under these SRES climate projections, the maximum decrease in the mean annual average streamflow of SSRB simulated by MISBA was 14%, 12% and 18% in 2020s, 2050s and 2080s, respectively. On average, at the end of 21st century, the mean winter and spring streamflow of sub-basins of SSRB are projected to increase by about 8% and 10% of their mean annual streamflow, respectively. In contrast, the mean summer and autumn streamflow of the sub-basins of the SSRB are projected to decrease by 31% and 7% of their mean annual streamflow,

respectively. While considering the potential combined impact of climate change and climate anomalies, a further decrease in streamflow by 2050s is projected if the climate anomaly considered is El Niño. In contrast, if the climate anomaly considered is La Niña, then considering the combined impact of climate change and La Niña would lead to a higher projected streamflow in SSRB by 2050s, than only if the impact of climate change is considered. On the average, under these climate change projections combined with El Niño and La Niña episode, the largest decrease and increase in the mean annual streamflow predicted for SSRB in the 2050s were -29% and +18%, respectively.

In the third phase (Chapter 4), the Irrigation District Model (IDM) of Alberta Agriculture Food and Rural Development was used to assess the future irrigation water demand of the SSRB under the potential impact of climate change, and the combined impacts of climate change and climate anomalies. IDM's simulations show an increase in the irrigation water demand by 7%, 12%, and 13% for the irrigation districts, and by 11%, 17%, and 18% for the private irrigation blocks, for 2020s, 2050s, and 2080s, respectively. Under the combined impact of climate change and El Niño, IDM's simulations show a decrease in irrigation water demand by 8% and 6% than that of 2050s climate scenario only for irrigation districts and private irrigation blocks, respectively. In contrast, a further increase in irrigation water demand by 1% is projected by 2050s if the climate anomaly considered is La Niña.

In the fourth phase (Chapter 5), the Water Resources Management Model (WRMM) of Alberta Environment was used to assess the future outlook of water resources management of SSRB under these projected changes in water supply and demand in response to the potential impacts of climate change. On the basis of WRMM's simulations for the three future periods, it seems that SSRB water license holders categorized under district irrigation, junior and future private irrigation, and senior, junior and future non-irrigation consumptive user groups will be progressively and most significantly affected in the 21st century. The percent deficit years of irrigation districts, junior private irrigation blocks, future private irrigation blocks increase from about 3%, 11% and 12% in the base case scenario to about 10%, 19% and 18% in 2020s; 14%, 22% and 24% in 2050s; and 18%, 27% and 24% in 2080s, respectively. The percent deficit years of senior and junior licenses under the non-irrigation water use category are expected to increase from 13% and 29% in the base case scenario to 23% and 47% in 2020s, 23% and 50% in 2050s, and 28% and 52% in 2080s, respectively.

In the fifth phase (Chapter 6), the WRMM was used to assess the future outlook of water resources management of SSRB under the potential combined impacts of climate change and climate anomalies. On the basis of WRMM's simulations on the combined impact of climate change and climate anomaly, license holders of SSRB categorized under district irrigation, junior and future private irrigation, and senior, junior and future non-irrigation consumptive user groups could be more, or less, significantly affected, depending on whether the climate anomaly

considered is El Niño or La Niña, than the impact of climate change alone. The percent deficit years for irrigation districts, senior private irrigation, junior private irrigation, and future private irrigation blocks were changed from about 14%, 4%, 24%, and 22% in the 2050s climate scenario to about 18%, 8%, 31%, and 31% in '2050s+El Niño' scenario, and 8%, 3%, 20%, and 18% in '2050s+La Niña' scenario, respectively. A marginal increase in percent deficit years for the senior, junior and future licenses under the category of non-irrigation water users is also expected under these combined scenarios.

In view of these findings, it will be crucial to slowly implement adaptation strategies to the future water resources management of SSRB to reduce its vulnerability and to enhance its resiliency against the potential impact of climate change and climate anomalies.

7.2 Recommendations

7.2.1 Adaptation

Adaptation to climate change and climate variability is required to minimize the impacts of unavoidable changes to be explained below (Huggel et al. 2012). As agriculture plays a vital role in Alberta's economy, indicators regarding the adaptive capacity of SSRB for agriculture under the possible impacts of climate change and climate variability are discussed below. Swanson et al. (2007) developed a geographic information system (GIS)-based indicator of the adaptive

capacity to climate change of agriculturally-based communities in the Prairie region. They derived twenty indicators representative of adaptive capacity for Census Divisions across the Prairies and organized them into six determinants: economic resources, technology, infrastructure, information, skills and management, institutions and networks, and equity. Their study shows that SSRB has a higher adaptive capacity than the northern neighbour of the Prairies' agricultural region.

In SSRB, climate change is expected to impact its surface water resources management in two ways: by decreasing the future supply of water, but increasing the future irrigation water demand, which amounts to about 75% of the total water allocated to various users in the basin. Therefore any adaptation strategy for SSRB to combat the possible impact of climate change and climate anomalies will only be effective if both factors are taken into consideration. A survey by Wheaton et al. (2007) regarding past print media on adaptation to possible impacts of climate change over the Prairie Provinces (e.g., drought) for the 1999-2006 periods' shows that four areas of greatest emphasis on adaptation for SSRB based on number of articles written had been "crops", followed by "livestock", "water", and "economics". Nevertheless, in all these areas, key elements essential to achieve robust climate change adaptation for SSRB require a close integration between strategic planning, standardized processes, continuity and stakeholder involvement (Alberta SRD 2010).

Firstly, changing reservoir operation rules in headwaters of SSRB under possible diminished future water supply will be a key adaptation strategy to climate change impact. A report by the Bow River Project Research Consortium (2010) for the Bow river system recommended an integrated adaptive management that addresses the economic, environmental and social impacts associated with water allocations to all water users from headwaters to the confluence at the Oldman River. Their study shows that if the Bow River and its controlled tributaries will be managed as an integrated system, it should attempt to meet the in-stream flow requirements during low flow seasons necessary to maintain a healthy fish and riparian habitat, provide recreation opportunities, and potentially improve the water quality of major parts of the river. Similar studies to follow for other sub-basins of SSRB are given under the South Saskatchewan River Basin Adaptation to Climate Variability Project (Alberta Water Portal 2012).

Given that irrigation is the major water user in SSRB, the following adaptation measures have been recommended to minimize the biophysical, social and economic vulnerabilities of SSRB to possible future climate change impact: (1) promote drought-resistant crop varieties or crops suitable for a changed climate, (2) alternatives to high water demand crops such as alfalfa, (3) breed crop seeds that could use water more efficiently in times of drought, and (4) explore ways to reduce water use in agriculture by introducing efficient irrigation systems (Alberta Environment 2008). Furthermore, high resolution satellite data (e.g., Landsat-TM5 or Landsat-ETM) may be used to map vegetation indices such as

Normalized Difference Vegetation Index (NDVI) of agricultural land which is an indication of biomass and land productivity. The NDVI map can be used to digitally divide the field into zones of low, median and high productivity. To promote farming that maximizes crop yield and sustainability, the application of fertilizer, pesticides, and water are adjusted according to the productivity zones given in the NDVI (or other vegetation indices) map. Ideally, more precise fertilizer and water usage will maximize crop yield, and satellite images that map crop residues after harvest can also be used to promote soil health which is related to crop residues.

Moreover, exploring ways of reducing water use in key industries (e.g., energy industry), preserving wetlands and natural areas by putting land use policies in place, and review standards for buildings, roads and highways to ensure they will withstand challenges caused by a changing climate and climate extremes, are possible potential adaptation measures to increase SSRB's resiliency against the potential impact of climate change and climate anomalies (Alberta Environment 2008).

7.2.2 Future Study

In current study the combined impacts of climate change and climate anomalies on the surface water management of SSRB has been investigated. However, in addition to climate anomalies and climate change, landuse changes can be another possible significant cause to future changes to the hydrology of SSRB.

Landuse changes can occur either by land development for the municipal expansion, or the expansion of industries within SSRB, or a gradual shift of vegetation patterns because of the prolonged effect of a warmer climate as has been demonstrated by various studies (Lawler et al. 2006; Malcolm et al. 2002). It is anticipated that the grassland of southern Alberta would gradually expand northward, if the climate of southern Alberta slowly becomes warmer and also drier projected by some GCMs (IPCC 2007). Both the aforementioned modes of landuse changes are likely and their effects can be incorporated into hydrologic model MISBA of Kerkhoven and Gan (2006). Then, differences to the potential hydrologic impact of climate change and anomalies to the SSRB with and without considering the effects of changes to vegetation patterns caused by climate warming and by land development for agriculture, municipal and industrial purposes could be investigated in future studies.

Climate scenarios based on GCMs simulations have been using increasingly to predict future climatic change impact studies. However, they are not designed to assess the hydrological impacts, and to do so some of their limitations need to be resolved: GCMs remain coarse in spatial resolution and are unable to resolve various subgrid scale features required for impact studies (Fowler et al. 2007); GCMs simulated climatic variables used for hydrologic impact studies are more reliable in seasonal or monthly scales while hydrological models typically use daily time step (Schulze 1997; Xu 1999); GCMs simulations are more accurate for calculating the free troposphere variables than the surface variables, while

the ground surface variables directly affect the surface processes (Xu 1999); and GCMs can predict climate related variables (e.g. wind speed, temperature, humidity, air pressure etc.) more accurately than the variables important for hydrologic impact assessment, such as, precipitation, runoff, soil moisture, and evapotranspiration (Xu, 1999). In current study, these gaps between GCMs and hydrological model have been resolved by incorporating statistical downscaling of GCM data to basin scale hydrologic modeling. Future studies can consider the dynamic downscaling, in which a higher resolution Regional Climate Model (RCM) can be used to produce higher resolution outputs of GCM data either by nesting the RCM within a GCM or, by using the large-scale and lateral boundary conditions from GCMs to run RCMs in offline mode to produce downscaled meteorological variables required to drive hydrological models.

So far studies conducted on the impacts of climate change on Albertan river basins are based on hydrologic models driven in a stand-alone mode without considering the possible effect of feedback or interactions between land and the atmosphere (Alberta Environment 2010; Kerkhoven and Gan 2011a; Tanzeeba and Gan 2012; Islam and Gan 2012). However, our climate may be sensitive to the state and spatial variations of the land surface fluxes, and the planetary boundary layer. The land-atmosphere interaction may strengthen the influence of land surfaces in middle to high latitude areas through a positive feedback (in warm climate) or the snow-atmosphere-cloud feedback (in cold climate). With higher resolution atmospheric and hydrologic data becoming more readily

available, future studies can conduct climate change studies on basin hydrology using a coupled, atmospheric-hydrologic modeling framework instead of off-line framework as what has been done in the past. Accounting for the feedback between the atmosphere and the land surface should enhance our capability to predict the hydrologic impact of climate change and climate anomalies, and to reduce uncertainties associated with such long-term predictions of basin hydrology.

Major sources of uncertainty in predicting the hydrologic response of a river basin to future climate change are: uncertainty associated with the climate change scenario, especially the global political and economic decisions made in the future which triggered the future greenhouse gas emissions; uncertainty associated with the GCMs; uncertainty added by the downscaling technique used to translate the coarse scale GCM output to a regional spatial scale; sample uncertainty associated with the natural variability; uncertainty associated with the hydrological model structure; and uncertainty associated with hydrological model parameters (Kerkhoven and Gan 2011b; Maurer 2007; Kay et al. 2009). In current study, to account for uncertainties associated with GCMs and climate change emission scenarios, climate scenarios based on four GCMs forced by multiple SRES emission scenarios for the SSRB are considered. Future studies can examine the uncertainty involved in downscaling techniques by considering multiple statistical and dynamic downscaling methodologies.

7.3 References

Alberta Environment (2008). "Albertans and Climate Change: Moving Forward."

Alberta Environment

Alberta Environment (2010). "South Saskatchewan Regional Plan: Water

Quantity and Quality Modeling Results." *Alberta Environment*.

Alberta SRD (2010). "Climate Change Adaptation Framework: Manual." *Alberta*

Sustainable Resource Development.

Alberta Water Portal (2012). "South Saskatchewan River Basin Adaptation to

Climate Variability Project," Available through website:

<http://www.albertawater.com/index.php/projects-research/ssrb-adaptation-project> , accessed on December 21, 2012.

Bow River Project Research Consortium (2010). "Bow River Project: Final

Report." *The Bow River Project Research Consortium*.

Fowler, H. J., Blenkinsop, S., and Tebaldi, C. (2007). "Linking climate change

modelling to impacts studies: Recent advances in downscaling techniques for hydrological modelling." *Int. J. Climatol.*, 27(12), 1547-1578.

Huggel, C., Rohrer, M., Calanca, P., Salzmann, N., Vergara, W., Quispe, N., &

Ceballos, J. L. (2012). "Early warning systems: The last mile of adaptation." *Eos, Transactions American Geophysical Union*, 93(22), 209.

IPCC (2007). "Climate Change 2007, Intergovernmental Panel on Climate Change Fourth Assessment Report."

Islam, Z. and Gan, T. (2012). "Effects of Climate Change on the Surface Water Management of South Saskatchewan River Basin." *J. Water Resour. Plann. Manage.* doi: 10.1061/(ASCE)WR.1943-5452.0000326 .

Kay, A. L., Davies, H. N., Bell, V. A. and Jones, R. G. (2009). "Comparison of uncertainty sources for climate change impacts: flood frequency in England." *Climatic Change*, 92, 41–63.

Kerkhoven, E. and Gan, T.Y. (2006). "A modified ISBA surface scheme for modeling the hydrology of Athabasca River Basin with GCM-scale data." *Advanced in Water Resour.*, 29(6), 808-826.

Kerkhoven, E. and Gan, T.Y. (2011a). "Differences and sensitivities in potential hydrologic impact of climate change to regional-scale Athabasca and Fraser River basins of the leeward and windward sides of the Canadian Rocky Mountains respectively." *Climatic Change*, 106(4), 583-607.

Kerkhoven, E. and Gan T.Y. (2011b). "Unconditional Uncertainties of Historical and Simulated River Flows Subjected to Climate Change." *Journal of Hydrology*, 396 (1-2), 113-127.

Lawler, J.J., D. White, R.P. Neilson, and A.R. Blaustein (2006). "Predicting climate-induced range shifts: model differences and model reliability." *Global Change Biology*, 12, 1568-1584.

- Malcolm, J.R., A. Markham, R.P. Neilson, and M. Garaci (2002). "Estimated migration rates under scenarios of global climate change." *Journal of Biogeography*, 29, 835-849.
- Maurer, E.P. (2007). "Uncertainty in hydrologic impacts of climate change in the Sierra Nevada, California, under two emissions scenarios." *Climatic Change*, 82:309–325.
- Schulze, R. E. (1997). "Impacts of global climate change in a hydrologically vulnerable region: challenges to South African hydrologists." *Progress in Physical Geography*, 21, 113.
- Swanson, D.A., J.C. Hiley, H.D. Venema and R. Grosshans. (2007). "Indicators of Adaptive Capacity to Climate Change for Agriculture in the Prairie Region of Canada: An analysis based on Statistics Canada's Census of Agriculture." *Working Paper for the Prairie Climate Resilience Project*, Winnipeg: International Institute for Sustainable Development.
- Tanzeeba, S. and Gan, T.Y. (2012). "Potential impact of climate change on the water availability of South Saskatchewan River Basin." *Climatic Change*, 112, 355-386.
- Wheaton, E., Koshida, G., Bonsal, B., Johnston, T., Richards, W. and Wittrock, V. (2007). "Agricultural Adaptation to Drought (ADA) in Canada: The case of 2001 to 2002." *Saskatchewan Research Council, SRC Publication No. 11927-1E07*

Xu, C. (1999). "Climate Change and Hydrologic Models: A Review of Existing Gaps and Recent Research Development." *Water Resources Management*, 13, 369-382.

Appendix A

MISBA Parameters

Primary Parameters	% Sand % Clay Vegetation Type Land Water Ratio
Secondary Parameters	Saturated Volumetric Moisture Content Wilting Point Volumetric Water Content Saturated Matric Potential Saturated Hydraulic Conductivity Slope of the Retention Curve Soil Thermal Coefficient at Saturation Two Force Restore Coefficients for Soil Moisture Two Coefficients of Surface Volumetric moisture at the balance of gravity and Capillary Forces. The Superficial or Top Soil Depth The Depth of the Rooting Layer The Total Modeled Soil Depth Fraction of Vegetation Minimum Surface Resistance Maximum Surface Resistance Leaf Area Index Roughness Length for Momentum Roughness Length for Heat Transfer Albedo Emissivity Time Constant of the Day

Appendix B

Four-month seasonal table (NDJF, FMAM, MJJA, ASON) for Extended MEI rankings (1871 to 2005) are classified to indicate warm (W), cold (C), or neutral (N) conditions. Bold (Bold Italic) record indicate an El Niño (La Niña) year (after Wolter and Timlin 2011³)

Year	Ranks				Episodes				Year	Ranks				Episodes			
	NDJF	FMAM	MJJA	ASON	NDJF	FMAM	MJJA	ASON		NDJF	FMAM	MJJA	ASON	NDJF	FMAM	MJJA	ASON
1871	63	79	36	71	N	N	N	N	1939	28	34	83	99	C	C	N	N
1872	42	39	34	36	N	N	C	N	1940	100	124	123	110	N	W	W	W
1873	24	12	35	58	C	C	N	N	1941	120	131	128	126	W	W	W	W
1874	38	15	20	24	N	C	C	C	1942	122	108	37	21.5	W	W	N	C
1875	36	21	3	20	N	C	C	C	1943	15	48	86	49	C	N	N	N
1876	25	4	10	64	C	C	C	N	1944	58	81	76	55	N	N	N	N
1877	86	87	120	133	N	N	W	W	1945	54	52	52	69	N	N	N	N
1878	133	130	92	35	W	W	N	N	1946	62	59	65	87	N	N	N	N
1879	27	43	27	38	C	N	C	N	1947	82	54	54	37	N	N	N	N
1880	23	23	70	68	C	C	N	N	1948	71	93	75	63	N	N	N	N
1881	83	70	56	43	N	N	N	N	1949	70	64	48	32	N	N	N	C
1882	41	32	33	50	N	C	C	N	1950	20	10	6	13	C	C	C	C
1883	45	36	45	66	N	N	N	N	1951	12	40	107	115	C	N	W	W
1884	79	89	95	94	N	N	N	N	1952	101	91	61	76	N	N	N	N
1885	98	86	79	108	N	N	N	W	1953	81	107	91	93	N	W	N	N
1886	92	57	11	12	N	N	C	C	1954	75	67	30	21.5	N	N	C	C
1887	9	14	55	65	C	C	N	N	1955	21	11	4	3	C	C	C	C
1888	80	113	117	130	N	W	W	W	1956	3	9	14.5	26	C	C	C	C
1889	130	120	38	9	W	W	N	C	1957	37	88	126	122	N	N	W	W
1890	6	7	9	18	C	C	C	C	1958	125	126	124	92	W	W	W	N
1891	47	76	82	74	N	N	N	N	1959	102	112	102	79	W	W	W	N
1892	61	13	19	6	N	C	C	C	1960	72	74	64	53.5	N	N	N	N
1893	5	5	1	2	C	C	C	C	1961	69	73	77	51	N	N	N	N

³ Wolter, K. and Timlin, M. (2011). "El Niño/Southern Oscillation behaviour since 1871 as diagnosed in an extended multivariate ENSO index (MEI.ext)." *Int. J. Climatol.* 31, 1074–1087.

Year	Ranks				Episodes				Year	Ranks				Episodes			
	NDJF	FMAM	MJJA	ASON	NDJF	FMAM	MJJA	ASON		NDJF	FMAM	MJJA	ASON	NDJF	FMAM	MJJA	ASON
1894	11	8	24	29	C	C	C	C	1962	29	44	40	40	C	N	N	N
1895	34	33	62	86	C	C	N	N	1963	52	58	100	118	N	N	N	W
1896	65	65	111	123	N	N	W	W	1964	109	53	18	14	W	N	C	C
1897	124	118	74	46	W	W	N	N	1965	40	75	125	127	N	N	W	W
1898	46	30	47	33	N	C	N	C	1966	128	115	90	73	W	W	N	N
1899	44	56	96	112	N	N	N	W	1967	57	41	32	34	N	N	C	C
1900	115	125	121	91	W	W	W	N	1968	48	37	46	97	N	N	N	N
1901	96	69	69	47	N	N	N	N	1969	108	117	116	106	W	W	W	W
1902	55	97	129	129	N	N	W	W	1970	103	82	21	15	W	N	C	C
1903	116	96	41	39	W	N	N	N	1971	10	1	12	11	C	C	C	C
1904	17	27	80	103	C	C	N	W	1972	39	80	133	132	N	N	W	W
1905	107	121	131	125	W	W	W	W	1973	132	109	22	7	W	W	C	C
1906	114	92	60	25	W	N	N	C	1974	1	3	25	31	C	C	C	C
1907	30	28	44	70	C	C	N	N	1975	31	25	8	1	C	C	C	C
1908	49	22	23	23	N	C	C	C	1976	4	16	94	117	C	C	N	W
1909	22	29	7	8	C	C	C	C	1977	105	99	103	109	W	N	W	W
1910	8	2	2	10	C	C	C	C	1978	113	94	67	77	W	N	N	N
1911	19	20	29	96	C	C	C	N	1979	97	83	99	107	N	N	N	W
1912	110	100	43	67	W	N	N	N	1980	112	119	108	88	W	W	W	N
1913	76	47	72	98	N	N	N	N	1981	67	77	68	80	N	N	N	N
1914	106	102	105	119	W	W	W	W	1982	77	95	130	134	N	N	W	W
1915	118	122	114	53.5	W	W	W	N	1983	135	135	132	81	W	W	W	N
1916	43	24	5	4	N	C	C	C	1984	73	66	49	59	N	N	N	N
1917	2	6	14.5	16	C	C	C	C	1985	32	31	51	52	C	C	N	N
1918	14	35	109	113	C	N	W	W	1986	60	68	93	120	N	N	N	W
1919	127	123	119	104	W	W	W	W	1987	123	132	134	131	W	W	W	W
1920	89	98	66	62	N	N	N	N	1988	121	85	13	5	W	N	C	C
1921	74	26	39	41	N	C	N	N	1989	7	17	26	48	C	C	C	N
1922	50	62	50	44	N	N	N	N	1990	85	105	84	89	N	W	N	N
1923	33	45	89	111	C	N	N	W	1991	90	111	113	105	N	W	W	W
1924	104	55	16	17	W	N	C	C	1992	129	133	127	100	W	W	W	N

Year	Ranks				Episodes				Year	Ranks				Episodes			
	NDJF	FMAM	MJJA	ASON	NDJF	FMAM	MJJA	ASON		NDJF	FMAM	MJJA	ASON	NDJF	FMAM	MJJA	ASON
1925	26	60	87	124	C	N	N	W	1993	111	127	122	114	W	W	W	W
1926	126	128	112	75	W	W	W	N	1994	99	103	110	121	N	W	W	W
1927	78	61	53	85	N	N	N	N	1995	119	114	97	56	W	W	N	N
1928	91	72	78	45	N	N	N	N	1996	51	50	57	57	N	N	N	N
1929	66	63	101	101	N	N	N	N	1997	53	101	135	135	N	N	W	W
1930	95	116	118	128	N	W	W	W	1998	134	134	81	30	W	W	N	C
1931	131	129	98	82	W	W	N	N	1999	18	19	28	27	C	C	C	C
1932	84	110	115	78	N	W	W	N	2000	13	18	42	61	C	C	N	N
1933	68	49	31	19	N	N	C	C	2001	35	46	59	60	N	N	N	N
1934	16	42	63	72	C	N	N	N	2002	64	84	106	116	N	N	W	W
1935	59	51	73	90	N	N	N	N	2003	117	106	71	95	W	W	N	N
1936	87	90	85	83	N	N	N	N	2004	94	78	88	102	N	N	N	W
1937	88	71	58	84	N	N	N	N	2005	93	104	104	42	N	W	W	N
1938	56	38	17	28	N	N	C	C									

Appendix C

South Saskatchewan River Basin (SSRB) Water Resources Management Model Schematic (Used with Permission from Tom Tang, Environmental Modeling, Alberta Environment and Sustainable Resource Development, personal communication)

